UCRL 10119

University of California

Ernest O. Lawrence Radiation Laboratory

TWO-WEEK LOAN COPY

This is a Library Circulating Copy which may be borrowed for two weeks. For a personal retention copy, call Tech. Info. Division, Ext. 5545

INORGANIC MATERIALS RESEARCH DIVISION ANNUAL REPORT, 1961

Berkeley, California

DISCLAIMER

This document was prepared as an account of work sponsored by the United States Government. While this document is believed to contain correct information, neither the United States Government nor any agency thereof, nor the Regents of the University of California, nor any of their employees, makes any warranty, express or implied, or assumes any legal responsibility for the accuracy, completeness, or usefulness of any information, apparatus, product, or process disclosed, or represents that its use would not infringe privately owned rights. Reference herein to any specific commercial product, process, or service by its trade name, trademark, manufacturer, or otherwise, does not necessarily constitute or imply its endorsement, recommendation, or favoring by the United States Government or any agency thereof, or the Regents of the University of California. The views and opinions of authors expressed herein do not necessarily state or reflect those of the United States Government or any agency thereof or the Regents of the University of California.

Research and Development

UCRL-10119
UC-2 General, Miscellaneous,
and Progress Reports
TID-4500 (17th Ed.)

UNIVERSITY OF CALIFORNIA
Lawrence Radiation Laboratory
Berkeley, California

Contract No. W-7405-eng-48

INORGANIC MATERIALS RESEARCH DIVISION ANNUAL REPORT, 1961

March 12, 1962

Printed in USA. Price $2.75. Available from the
Office of Technical Services
U. S. Department of Commerce
Washington 25, D.C.

INORGANIC MATERIALS RESEARCH DIVISION ANNUAL REPORT, 1961

Contents

General Introduction 1

I. CHEMISTRY

A. THERMODYNAMICS AND HIGH-TEMPERATURE CHEMISTRY

1. Application of the Sideband Technique to Wide-Line NMR Spectra (Acrivos) 2

2. Analysis of the $A_3(X_3)_3$ Nuclear Spin System and π-Electron Coupled Hyperfine Splitting Constants in Aromatic Hydrocarbons (Acrivos) 3

3. Hyperfine Splitting in Aromatic Free Radicals (Acrivos) 6

4. Nonstoichiometry in Nonmetallic Compounds (Brewer). 6

5. The Dissociation Energies of Gaseous Alkali Halides (Brewer and Brackett) 7

6. Dissociation Energies of Gaseous Metal Dioxides (Brewer and Rosenblatt) 7

7. The Ultraviolet Spectra of MgOH and MgO (Brewer and Trajmar) 7

8. The Heat of Formation of CF_2 (Brewer, Margrave, Porter, and Wieland) 9

9. The Heat of Sublimation and Dissociation Energy of Gaseous C_2 (Brewer, Hicks, and Krikorian) . . . 9

10. A Vapor-Phase Equilibrator for Activity Coefficient Determinations (Brewer, Simonson, and Tong) . . 9

11. Apparatus for the Determination of Radiative Lifetimes (Brewer, Berg, and Rosenblatt) 10

12. The $^1\Sigma$ - $^1\Pi$ Bands of MgO (Brewer, Trajmar, and Berg) 11

13. Thermodynamic Properties of Gaseous Metal Dihalides (Brewer, Somayajulu, and Brackett) 12

*Preceding Annual Report: UCRL-9579

14. The Relationship Between Absorption Intensity and Fluorescence Lifetime of Molecules (Strickler and Berg) 13

15. Radiative Lifetime of Gaseous Iodine (Brewer, Berg, and Rosenblatt) 16

16. Research in Progress--Brewer 16

17. The Microwave Spectrum and Quadrupole Interaction in Cis 1, 2-Dichloroethylene (Flygare and Howe) 17

18. Strong-Field Stark Effect (Howe and Flygare) 18

19. Simple Molecular Orbital Theory of The Dichloroethylenes (Howe, Muirhead, and Goldstein) 18

20. The Near Ultraviolet Absorption Spectrum of Tetrolaldehyde (Muirhead and Howe) 19

21. Research in Progress--Howe 20

22. Temperature Dependence of the Knight Shift in $Na-NH_3$ Solutions (Acrivos and Pitzer) 20

23. Transmission Probabilities for Isotopic Reactions of the Type $H + H_2$ (Mortensen and Pitzer) 23

24. Temperature Dependence of the Knight Shift in $Ca-NH_3$ Solutions (Acrivos, Brown, and Pitzer) . . . 24

25. Silver Oxide: The Effects of Particle Size on Heat Capacity from 2 to 80°K and on Entropy (Gregor and Pitzer) 24

26. The Silver–Silver Oxide Electrode, and the Entropy of Mercuric Oxide (Gregor and Pitzer) 29

27. Orbital Radii, Bond Length, and Resonance (Somayajulu) 31

28. Bond Energies, Valence-State Energies, and Resonance (Somayajulu) 31

B. SOLID-STATE PHYSICS AND CHEMISTRY

1. Apparatus for Drawing 0.003-Inch Wires (Jura and Newhart) 33

2. Static Pressures Approaching a Megabar (Jura and Nicol) 33

3. Size Effects on Metallic Conductivity (Jura and Nicol) 33

4. Rare Earth Metals: Electrical and Magnetic Properties at High Pressures (Jura and Souers) 34

5. Multiple Samples in Bridgman Anvils (Jura and Stromberg) 35

6. Mossbauer Experiments (Jura, Rasmussen, Stone, and Nicol) 36

7. The Low-Temperature Heat Capacities of Anti-Ferromagnetic MnF_2 and CoF_2 (Phillips) 37

8. Heat Capacity of Indium Below $1^{o}K$ (Phillips and O'Neal) 40

9. Apparatus for Calorimetry Below 0.1 ^{o}K (Phillips and O'Neal) 42

10. Calorimetric Studies of the Superconducting Transition (Phillips and Zainal) 43

11. Research in Progress--Phillips 43

C. REACTION KINETICS

1. The Kingdon Cage as a Molecular Beam Detector (Brooks and Herschbach) 44

2. Influence of Vibrations on Molecular Structure Determinations (Herschbach and Laurie) 48

3. Anharmonic Potential Constants and Their Dependence upon Bond Length (Herschbach and Laurie) 48

4. Reactive Scattering in Crossed Molecular Beams. Reactions of Rubidium and Cesium Atoms with Alkyl Iodides (Kinsey, Kwei, and Herschbach) 49

5. Reactive Scattering in Crossed Molecular Beams. Reactions of Potassium Atoms with Alkyl Iodides (Norris, Kwei, and Herschbach) 52

6. Research in Progress--Herschbach 54

7. The Photoionization of Nitric Oxide (Doering and Mahan) 56

8. Research in Progress--Mahan 57

9. The Analysis of Hydrogen Atom Concentrations in a Chemically Reacting System by Means of Paramagnetic Resonance Absorption (Edelstein and Myers) 57

10. Research in Progress--Myers 59

D. INORGANIC CHEMISTRY

1. The NMR Relaxation Mechanisms of O^{17} in Aqueous Solutions of Paramagnetic Cations, and the Lifetime of Water Molecules in the First Coordination Sphere (Connick and Swift). 60

2. Hydrolysis and Polymerization in Solutions of Chromic Ion (Thompson and Connick) 62

3. Rates of Interconversion of the Chloride Complexes of Ruthenium (III) (Mercer, Hasty, and Connick) 63

4. Research in Progress--Connick 64

5. Digermanium Hexachloride Obtained by Electric Discharge Methods (Jolly and Kopp) 64

6. Germanium Hydrides (Jolly and Drake) 65

7. Infrared Spectra of Metal-Ammonia Solutions (Gold and Jolly) 67

8. Diphosphorus Tetrachloride (Lindahl and Jolly) 73

9. Research in Progress--Jolly 76

10. A Study of the Mechanism of Electro-Oxidation of Chromous Ion in Chloride Media (Mathews and Orlemann) 76

11. Research in Progress--Orlemann 77

12. Temperature-Dependent Chemical Shifts in the NMR Spectra of Gases (Petrakis and Sederholm). 77

13. NMR Fluorine-Fluorine Coupling Constants in Saturated Organic Compounds (Petrakis and Sederholm) 77

14. NMR Investigation of the Potential Energy Function in Halogen-Substituted Ethanes (Sederholm, Thompson, and Newmark) 78

15. Research in Progress--Sederholm 84

II. METALLURGY AND CERAMICS

A. INFLUENCE OF MICROSTRUCTURE ON PHYSICAL PROPERTIES

1. The Influence of Dispersed Oxide Phases on the Mechanism of Deformation of Silver (Fetta and Himmel) 85

2. Dislocation Damping Phenomena in High-Purity Silver and Dilute Silver Alloys (Guinan and Himmel) . 86

3. The Nucleation of Porosity During Diffusion Processes in Metals (Maher and Himmel) 88

4. Research in Progress -- Himmel. 89

5. Internal Stresses in Ceramic Systems (Jacobson and Fulrath) 89

6. Mechanical Properties and Chemical Reactivity in Mullite - Glass Systems (Studt and Fulrath) 90

7. Stress-Enhanced Gaseous Permeability of Ceramic Materials (Studt and Fulrath). 92

8. Research in Progress--Fulrath 93

9. Investigation of Structure and Properties of Martensite (Parker) 93

10. Ductile Ceramics (Parker) 94

11. Research in Progress -- Parker 95

B. INFLUENCE OF SUBMICROSCOPIC STRUCTURE ON PHYSICAL PROPERTIES: ELECTRON MICROSCOPY

1. The Structure of Precipitation-Hardened Alloys (Thomas) 96

2. Helical Dislocations in Quenched and Aged Al-5% Mg (Eikum and Thomas). 96

3. The Interaction Between Vacancies and Zones and the the Kinetics of Preprecipitation in Al-Rich Alloys (Federighi and Thomas). 102

4. Direct Observations of Solid-State Phase Transformations (Hren and Thomas) 103

5. Mechanism of Yielding in Niobium (Van Torne and Thomas) 107

6. Research in Progress -- Thomas 112

7. Growth Faults in Silicon (Thomas and Washburn) 114

8. Dislocation Substructures in Deformed and Recovered Molybdenum (Benson, Thomas, and Washburn) 121

9. Factors Affecting the Dislocation Substructure in Deformed MgO (Elkington, Washburn, and Thomas). . 125

10. Plastic Behavior at Large Strain (Murty and Washburn). 127

11. Deformation Substructures in Copper (Price and Washburn) 131

12. Fatigue Damage in MgO (Subramanian and Washburn) . 134

13. Research in Progress -- Washburn 137

C. KINETICS OF DISLOCATION MECHANISMS

1. Determination of the Short-Range Order in the Intermetallic Compound Ag_2Al (Dorn and Neumann) . . 138

2. On the Nature of Dispersed-Particle Strengthening at Low Temperatures (Dorn and Mitchell) 143

3. On the Rate-Controlling Mechanism of Deformation in Aluminum-Magnesium Alloys (Dorn and Mitra) . . 143

4. Theory of Creep Based on Fluctuations of Short-Range Order (Dorn and Mitra) 144

5. On the Low-Temperature Rate-Controlling Mechanism of Deformation for Prismatic Slip in Single Crystals of the Hexagonal Ag-Al Intermetallic Phase (Dorn and Mote) 145

6. Deformation Mechanisms of Mg-Li Alloys (Dorn, Mote, and Ahmadieh) 146

7. Mechanism of High-Temperature Deformation in Ag-Al-Zn Alloys (Dorn, Mote, and Howard) 147

8. The Effect of Temperature on the Yield Strength of the Polycrystalline Hexagonal Ag-Al Intermetallic Phase (Tanaka, Mote, and Dorn) 147

9. The Effect of Strain Rate on Diffusion (Dorn, Mote, and Wazzan) 149

10. Mechanisms of Deformation in Pure Polycrystalline Aluminum (Dorn and Osborne) 150

11. Geometric Foundations of Continuum Mechanics (Simmons and Dorn) 150

12. Research in Progress -- Dorn 151

D. HIGH-TEMPERATURE REACTIONS

1. Glass-Metal Interactions: Nature of Wetting and Adherence (Pask and Fulrath). 152

2. Wettability of Iron by Molten Sodium Disilicate (Cline, Fulrath, and Pask) 152

3. Effect of Composition on the Glass-Iron Interface (Gaidos and Pask) 153

4. The Vapor Pressure of Magnesium Fluoride (Hammer and Pask) 154

5. The Effect of Crystal Orientation on the Plastic Flow of Magnesium Oxide (Hulse, Copley, and Pask) . 154

6. Kinetics of the Oxidation of Magnesium Fluoride (Messier and Pask) 157

7. Purification of MgF_2 and Growth of Single Crystals (Scott and Pask) 157

8. Deformation and Fracture of Polycrystalline Lithium Fluoride (Scott and Pask). 158

9. Kinetics of the Oxidation of Magnesium Fluoride (Messier and Pask) 159

10. The Anatase-Rutile Transformation (Shannon and Pask). 160

11. Research in Progress -- Pask 161

12. Termination of ONR-ARPA Contract (Searcy) 162

13. The Composition and Properties of the Solid Produced by Reaction of Thorium with Hydrochloric Acid (Newbury and Searcy) 162

14. Effect of Channel Length on the Force Exerted by Effusing Vapors (Schulz and Searcy) 164

15. The Vapor Pressure and Heat of Sublimation of Calcium Fluoride (Schulz and Searcy) 165

16. An Experimental Evaluation of the Torsion-Effusion Method for Determination of Vapor Pressures with Tin, Germanium, and Silver (Schulz and Searcy). . . . 167

17. Research in Progress -- Searcy 171

III. REACTOR MATERIALS ENGINEERING

1. Liquid Metal Extraction (Olander) 173

2. Kinectics of the Chlorination of UCl_4 in UCl_4-LiCl-KCl Melts with Elemental Chlorine (Olander) 174

3. Diffusion of Fission Gases in Ceramic Fuel Bodies (Pigford, Olander, Jaffe, Rufeh, and Shaked) . . . 175

4. Particle-Voltaic Effect in Semiconductors (Pigford and Posey) 175

5. Thermionic Emission by Refractory Materials (Pigford, Koenig, and Wichner) 177

IV. MISCELLANEOUS

1. The Tides: A Dynamic Explanation (Pratt). 178

2. Research in Progress -- Pratt 181

V. PUBLICATIONS, 1961 182

INORGANIC MATERIALS RESEARCH DIVISION ANNUAL REPORT, 1961

Leo Brewer, Division Head
Alan W. Searcy, Associate Division Head

Lawrence Radiation Laboratory, Department of Chemistry,
Department of Mineral Technology, and Department of Nuclear Engineering
University of California, Berkeley, California

March 12, 1962

GENERAL INTRODUCTION

The Inorganic Materials Research Division Program is now in its second year of operation as a concerted interdisciplinary effort. Primary concern is the investigation of fundamental physical and chemical characteristics, knowledge of which will permit a reasonable prediction of possible new materials and reactions in extreme environments. In addition to the actual research accomplishments, this Division has a responsibility for training competent scientists on a broad interdisciplinary basis. These scientists will be able to help develop fundamental programs of significance to the AEC and to other agencies supporting the national interest. Interdisciplinary contacts are being promoted within the Laboratory through development of joint research programs involving principal investigators from different fields, and by establishment of seminars and symposia involving participants from different fields.

This past year an international conference, "The Impact of Transmission Electron Microscopy on Theories of the Strength of Crystals," was sponsored under this Division. The conference involved nearly twenty speakers and more than 100 participants -- it was considered highly successful. The manuscripts and discussion transcripts are scheduled for publication in book form early in 1962.

The following report is organized into three primary sections -- Chemistry, Metallurgy and Ceramics, and Reactor Materials -- to be consistent with the AEC organizational branches from which funds are budgeted. Each of the primary sections is further divided into a number of general research areas, with all the work of a particular investigator listed under what seems the most appropriate area.

I. CHEMISTRY

A. THERMODYNAMICS AND HIGH-TEMPERATURE CHEMISTRY

1. APPLICATION OF THE SIDEBAND TECHNIQUE TO WIDE-LINE NMR SPECTRA*

Juana Vivó Acrivos

The solution of the Bloch macroscopic equations of motion[1] for a magnetic dipole subject to a sinusoidally modulated magnetic field has been applied successfully to record directly the NMR absorption. Here the only conditions on the system are

$$\omega_M T_1,\ \omega_M T_2 \gg 1,$$

where ω_M is the modulation frequency and T_1, T_2 are respectively the spin lattice and cross relaxation times for the paramagnetic species. The time-dependent resonance signal is of the form

$$F(t) = \sum_{n,k=-\infty}^{+\infty} \phi_n J_k(\beta) J_n(\beta) \exp i(n-k)\omega_M t, \qquad (1)$$

where

$$\phi_n = \frac{[-|\gamma| H_1 M_0 T_2 (1 - i T_2 \Delta_n w)]}{[1 + T_2^2 (\Delta_n w)^2 + \gamma^2 T_1 T_2 J_n^2(\beta) H_1^2]},$$

J_n = Bessel functions of the first kind,

$$\Delta_n w = (|\gamma| H_0 - w + n\omega_M),$$

$\beta = |\gamma| H_M/\omega_M$, and $F = \nu + iu$ in the notation of (1); ϕ_n is of the same form as the resonance signal in the static case, except for the saturation parameter which is now reduced by the factor $J_n^2(\beta)$ for the nth harmonic. This affects only the saturation experiments, since ordinarily, in order to avoid undesirable distortion effects, H_1 is set so small that $\gamma^2 H_1^2 T_1 T_2 \ll 1$.

In the lock-in detector,[2] $F(t)$ is mixed with a reference signal $S(t) = \cos(\omega_M t - \phi)$ in such a way that the integral over a cycle ($t = 0,\ 2\pi/\omega_M$) gives the dc output. This means that in Eq. (1) only the terms with $(n-k) = \pm 1$ will contribute to the dc signal which is a function of the reference phase angle ϕ and is given by

---

*Résumé of a paper published in J. Chem. Phys. 36, 1097 (1962).

[1] F. Bloch, Phys. Rev. 70, 460 (1946); 120, 104 (1956).

[2] R. H. Dicke, Rev. Sci. Instr. 17, 273 (1946).

$$F(\phi) = \oint F(t)S(t)dt = \sum_{n=-\infty}^{+\infty} \phi_n J_n(\beta) \left[\frac{2n}{\beta} J_n(\beta) e^{-i\phi} + 2iJ_{n-1}(\beta) \sin\phi \right]. \qquad (2)$$

The real and imaginary components of ϕ_n, the absorption and dispersion modes respectively, are isolated by setting $\phi = 0$ or 90°:

$$F(0) = \sum_{n=-\infty}^{+\infty} a_n(\beta)\phi n, \quad [\text{for } a_n(\beta) = 2n/\beta\, J_n^{\,2}(\beta)],$$

$$F(90^o) = \sum_{n=\infty}^{+\infty} b_n(\beta)\phi n,$$

$$\{b_n(\beta) = 2i[-n/\beta\, J_n^{\,2}(\beta) + J_{n-1}(\beta)]\}. \qquad (3)$$

The measurement of the NMR spectra with the natural line widths is carried out with $\gamma^2 H_1^{\,2} T_1 T_2 << 1$. Therefore in this case the optimum conditions are obtained when $\phi = 0$ and $|a_1|_{max} = 0.42$ for $\beta = 1.5\,[J_1(\beta)/J_0(\beta)] = 1.35$ and when $\phi = 90$ with $|b_0|_{max} = 0.68$ for $\beta = [(\beta^2 + \frac{1}{2})^{1/2} - \frac{1}{2}]\, J_0(\beta)/J_1(\beta) = 1.08$. The value of β is determined directly from the spectra when the saturation parameter is negligible by comparing the amplitude of the different sidebands, $a_n(\beta)$ or $b_n(\beta)$.

2. ANALYSIS OF THE $A_3(X_3)_3$ NUCLEAR SPIN SYSTEM AND π-ELECTRON COUPLED HYPERFINE SPLITTING CONSTANTS IN AROMATIC HYDROCARBONS*

Juana Vivó Acrivos

The exact analysis of the NMR spectra of the substituted benzenes s-$(CH_3)_3C_6H_3$ and s-$(CH_3)_3C_6H_3$ was undertaken in order to verify that the long-range coupling in aromatic hydrocarbons can arise only from π-electron-coupled interactions. The nuclear spin functions for the $A_3(X_3)_3$ system were derived and used to analyze the NMR spectra of mesitylene and its fluorocarbon derivative. The measured coupling constants, together with the NMR parameters shown in Fig. IA. 2-1, are given in Table I. Also, the Ramsey theory,[1] together with the simple Huckel mo's for the hydrocarbons, was used to calculate the π-electron-coupled hyperfine constants. Here the virtual processes that give rise to the interaction are singlet-triplet transitions in which the perturbation Hamiltonian is the electron–nuclear spin Fermi contact term. The agreement of theory and experiment is evident from Table II.

---

* Résumé of a paper to be published in J. Mol. Phys. (UCRL-9531, May 1961).

[1] N. F. Ramsey, Phys. Rev. 91, 303 (1953).

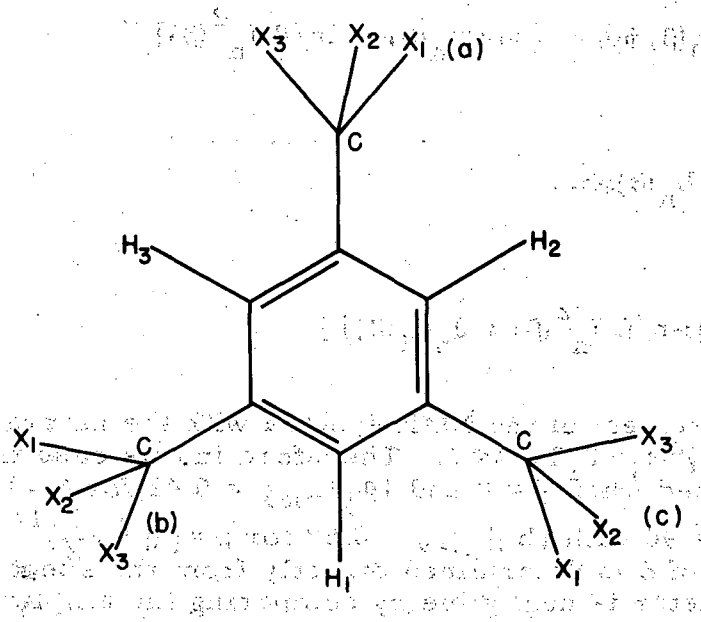

Chemical shifts

$\delta_0 = \delta(H_1)\ldots$

$\delta_1 = \delta(X_a)\ldots, X = F, H$

Coupling constants

$J_0 = J(H_1 - H_2),\ldots$ $\quad J' = J(H_1 - X_a),\ldots$

$J_1 = J(X_a - X_b),\ldots$ $\quad J = J(H_1 - X_b),\ldots$

$J_1' = J(X_{ia} - X_{ja}),\ldots$

MU-23417

Fig. IA. 2-1. Parameters of the NMR spectrum of the $A_3(X_3)_3$ system.

Table I. Parameters of the NMR spectra.

	$(CH_3)_3C_6H_3$	$(CF_3)_3C_6H_3$	C_6H_6
δ_0	-6.63±.02 ppm from TMS	-8.07±.02 ppm from TMS	-7.30 ppm from TMS
δ_1	-2.23±.02 ppm from TMS		
$2J+J'$	±(2.24±.10 cps)	±2.1±.5 cps	
J_0	±(2.2±.5 cps)	±1.9±.5 cps	
J/J'	+(2.0±.5)		
J_1	$\|J_1\| < 0.35$ cps		

Table II. Comparison of the calculated and experimental values of the J^{π} coupling constants.

	Experimental results		M. O.	V. B.
	$(CH_3)_3C_6H_3$	$(CF_3)_3C_6H_3$	(this work)	(Ref. 2)
J	±(0.89±.10)cps		-0.87 cps	-0.50
J'	±(0.45±.10)cps		-0.37	-0.24
$2J+J'$	±(2.24±.10)cps	±(2.1±.5) (2.2)	-2.27	-1.24
$\|J_1\|$	< 0.35		-0.32	-0.29

[2] H. M. McConnell, J. Mol. Spectroscopy 1, 11 (1957).

3. HYPERFINE SPLITTING IN AROMATIC FREE RADICALS*

Juana Vivó Acrivos

The theory of hyperfine splitting in aromatic free radicals first developed by Weissman[1] and McConnell et al.[2] has been derived from the point of view of the density matrix formalism of Löwdin[3] and McWeeny.[4] The new method clarifies many obscure points of the theory and also makes the student realize the precise physical significance of the virtual processes that give rise to the electron-nuclear spin Fermi contact terms in aromatic free radicals in solution.

*Abstract of a chapter on the theory of hyperfine splitting in aromatic free radicals to be printed in a book co-authored by Professor John E. Wertz of the University of Minnesota by the Ronald Publishing Co. (UCRL-9998, Dec. 1961).

[1] S. I. Weissman, J. Chem. Phys. 22, 1135 (1954); 25, 890 (1956).

[2] H. M. McConnell, J. Chem. Phys. 24, 764 (1956); 28, 1188 (1958), and H. M. McConnell and D. B. Chesnut, J. Chem. Phys. 28, 167 (1958).

[3] P. O. Löwdin, Advances in Chemical Physics, Vol. II (Interscience Publishers, Inc., New York, 1959).

[4] R. McWeeny, Revs. Modern Phys. 32, 335 (1960).

4. NONSTOICHIOMETRY IN NONMETALLIC COMPOUNDS*

Leo Brewer

The law of definite proportion as ordinarily understood cannot be applied to solid and liquid phases. The ratio of chlorine atoms to sodium atoms in sodium chloride, for example, can be changed continuously. The variation in ratio is very small, but changes drastically those properties that depend on the fugacities of the components or on the crystal order. Examples are cited of oxide and sulfide phases whose compositions are demonstrably variable. Examples are presented of big changes in electrical conductivity, color, thermal shock resistance, vapor pressures, and certain kinds of chemical reactivity that accompany small compositional changes.

*Abstract of a paper published in J. Chem. Ed. 38, 90 (1961).

5. THE DISSOCIATION ENERGIES OF GASEOUS ALKALI HALIDES*

Leo Brewer and Elizabeth Brackett†

The equilibrium vapor pressures of the alkali halides have been subjected to a rigorous thermodynamic treatment to obtain dissociation energies of the diatomic molecules. The data have been treated for deviation from perfect gas behavior and have been evaluated by a third-law method using spectroscopic data for the gases and heat-capacity measurements for the condensed phases. The experimental dissociation energies have been compared with theoretical calculations. Thermodynamic data for calculation of equilibrium behavior of alkali halides under various high temperature conditions have been tabulated.

*Abstract of two papers:
Leo Brewer and Elizabeth Brackett, The Dissociation Energies of Gaseous Alkali Halides, Chem. Revs. 61, 425-432 (1961), and
Leo Brewer, Thermodynamic Properties of the Alkali Halides, UCRL-9952, Nov. 1961.

†Now at Department of Chemistry, Rice University, Houston, Texas.

6. DISSOCIATION ENERGIES OF GASEOUS METAL DIOXIDES*

Leo Brewer and Gerd M. Rosenblatt

High-temperature equilibria data for the gaseous metal dioxides have been evaluated by second-law and third-law methods. A procedure for prediction of gaseous free energy functions has been devised. Enthalpies of dissociation are tabulated for 32 gaseous dioxides.

*Abstract of paper published in Chem. Revs. 61, 257-263 (1961).

7. THE ULTRAVIOLET SPECTRA OF MgOH AND MgO*

Leo Brewer and Sandor Trajmar†

The complex ultraviolet band system around 3800 A emitted by high-temperature systems containing magnesium has been studied by a number of

*J. Chem. Phys. (to be published, 1962).

†Now at Jet Propulsion Laboratory, California Institute of Technology, Pasadena, California.

workers but has not been analyzed.[1,2,3,4] Previous work had established that the bands are due to both hydroxide and oxide species, but neither formula was unambiguously fixed, and in particular the question whether the oxide species is diatomic or more complex has remained unsettled.

Examination of the spectrum from a King furnace and from a vacuum arc with varying hydrogen pressures, with varying activities of MgO, and with deuterium substitution has shown that the hydroxide species is MgOH and that the oxide species is MgO with no detectable contribution from other species.

A molecular orbital correlation of the electronic levels of the alkaline earth oxides with the levels of other eight-valence electron molecules such as BN, CN^+, and C_2 has provided a prediction of the low-lying electronic levels of MgO. These results indicate that the most important contributor to the partition function and to thermodynamic functions of MgO gas at high temperatures is the (still unobserved) $^3\Pi$ state rather than the commonly assumed $^1\Sigma$ ground state. Thus thermodynamic calculations based on the $^1\Sigma$ state yield concentrations of MgO gas which are in error by almost an order of magnitude.

---

[1] A. G. Gaydon and D. Pesic, Proc. Phys. Soc. (London) A73, 244 (1959).

[2] E. M. Bulewicz, and P. M. Sugden, Trans. Faraday Soc. 55, 720 (1959).

[3] D. Pesic, Proc. Phys. Soc. (London) A76, 844 (1960).

[4] R. F. Barrow and D. V. Crawford, Proc. Phys. Soc. A57, 12 (1945).

8. THE HEAT OF FORMATION OF CF_2*

Leo Brewer, John L. Margrave,† Richard F. Porter,‡ and Karl Wieland§

Observation of the CF_2 spectrum in a graphite King furnace containing CF_4 provides an estimate of the heat formation of CF_2 gas.

*Abstract of paper in J. Chem. Phys. 65, 1913 (1961).

†Now at Department of Chemistry, University of Wisconsin, Madison, Wisconsin.

‡Now at Department of Chemistry, Cornell University, Ithaca, New York.

§Now at Physihalisches Institut för Universitat, Basel, Switzerland.

9. THE HEAT OF SUBLIMATION AND DISSOCIATION ENERGY OF GASEOUS C_2*

Leo Brewer, William Hicks,† and Oscar H. Krikorian‡

The triplet Swan bands and singlet Phillips bands of C_2 have been studied in emission between 2600 and 3000 °K in a graphite King furnace. The temperature coefficients allow fixing of the dissociation products at the convergence limit of the Deslandres-d'Azambuja bands. A discrepancy between the spectroscopic limit and that obtained from thermal measurements is attributed to a positive deviation of the Birge-Sponer plot of vibrational levels due to interaction of $^1\Pi$ states. All available data are evaluated to obtain the best values for the heat of sublimation and dissociation energy of C_2.

*Abstract of paper published in J. Chem. Phys. 36, 182 (1962).

†Now at E. I. de Nemours and Co., Pigments Department, Experimental Station, Wilmington, Delaware.

‡Now at Lawrence Radiation Laboratory, Livermore.

10. A VAPOR-PHASE EQUILIBRATOR FOR ACTIVITY COEFFICIENT DETERMINATIONS*

Leo Brewer, Thomas R. Simonson, and Lee Karl J. Tong

A vapor-phase distributor has been designed that allows rapid and accurate determinations of activity coefficients of volatile solutes. It has

*Abstract of a paper in J. Phys. Chem., 65, 420 (1961).

been used to determine the activity coefficient of mesityl oxide in a variety of aqueous salt solutions, but it can be applied to many types of solutions. A deviation from Henry's Law of 20% has been found for saturated mesityl oxide solutions. The distribution of iodine between water and carbon tetrachloride has been studied. It has been confirmed that the variation of distribution ratio with iodine concentration is entirely consistent with expected regular solution behavior and is not due to new species such as I^+ or I_4.

11. APPARATUS FOR THE DETERMINATION OF RADIATIVE LIFETIMES

Leo Brewer, Robert A. Berg, and Gerd M. Rosenblatt

Preliminary reports on an apparatus to determine the radiative lifetimes of excited electronic states of molecules have appeared in two theses based on work in this Laboratory.[1, 2] The apparatus utilizes the method of phase displacement:[3] the upper molecular electronic state is continually populated by light modulated at frequency f. The fluorescence from the excited state displays the excitation modulation but is delayed in phase by an angle $\Delta\phi$, which is related to the radiative lifetime, τ, by the equation

$$\tan \Delta\phi = 2\pi f \tau.$$

The frequency of modulation, f, must be chosen so that its reciprocal is somewhat greater than the lifetime to be measured. Two modulator systems are now in use. A double-grating arrangement of original design with a fixed-speed rotating wheel modulates light at 60 kc for investigation of the lifetime range 10^{-5} to 10^{-7} sec. Modulation at higher speed is accomplished by periodic dispersion of light traversing a water tank. Ultrasonic waves produced in the water tank cause modulation at 5.2 Mc for investigation of the lifetime range 10^{-9} to 10^{-7} sec. Light signals are converted to electronic signals in photomultiplier tubes, and phase measurements are made electronically with a phase meter.

In addition to being limited by the precision of the phase meter, the accuracy of measurements may be greatly reduced by systematic errors. A comprehensive investigation of optical and electronic sources of phase-measurement error has led to procedures for determining lifetimes with satisfactory accuracy.

Measurements have been successfully made of the fluorescence lifetime of a solid phosphor ($BaPt[Cn]_4 \cdot 4H_2O$), of a series of strongly fluorescent organic molecules in solution (see IA. 14), and of iodine vapor. The work on iodine is discussed in a separate report.

---

[1] Richard G. Brewer, A Method for Determining Radiative Lifetimes of High-Temperature Molecules (Part I of thesis), UCRL-8387, July 1958.

[2] Fred E. Stafford, Measurement of Radiative Lifetimes (thesis), UCRL-8854, Sept. 1959.

[3] E. A. Bailey and G. K. Rollefson, J. Chem. Phys. 21, 1315 (1953).

12. THE $^1\Sigma$ - $^1\Pi$ BANDS OF MgO*

Leo Brewer, Sandor Trajmar,† and Robert Berg‡

The demonstration by Brewer and Trajmar[1] that the ultraviolet bands of magnesium are due to a single species, diatomic MgO, when hydrogen is rigorously excluded has prompted a new attempt at analysis of these bands. The isotopic shifts measured by Pesic[2] indicated that the spectral bands from 3672 to 3820 A were due to 0-0 sequences although possibly from several overlapping band systems. The bands emitted in the region 3766 to 3785 A by a magnesium arc in low-pressure oxygen have been successfully analyzed and shown to be due to a $^1\Sigma$ - $^1\Pi$ transition with the lower $^1\Pi$ state the same as the upper state of the $A^1\Pi$ - $X^1\Sigma$ transition previously analyzed by Lagerqvist and Uhler.[3] The agreement of combination differences for the $^1\Pi$ state with those reported by Lagerqvist and Uhler proves the correctness of the analysis and the assignment of vibrational and rotational numbering.

The analyzed bands constitute only a portion of the ultraviolet bands of MgO. The remainder of the bands are due to possibly two additional band systems. Molecular orbital correlations would suggest that these additional band systems are a $^1\Pi$ - $^1\Pi$ system, to the red side of the $^1\Sigma$ - $^1\Pi$ system, analogous to the Deslandres-d'Azumbuza bands to C_2, and a $^3\Pi$ - $^3\Pi$ system with a strong progression analogous to the Fox-Herzberg bands of C_2. There is also the possibility that the triplet band system may be a $^3\Pi$ - $^3\Sigma$ transition, also with a strong progression.

---

*Astrophysical J. (to be published, 1962).

†Now at Jet Propulsion Laboratory, California Institute of Technology, Pasadena, California.

‡Now at Department of Chemistry, Harvard University, Cambridge, Massachusetts.

[1] L. Brewer and S. Trajmar, J. Chem. Phys. (in press).

[2] D. Pesic, Proc. Phys. Soc. (London) A 76, 844 (1960).

[3] A. Lagerqvist and U. Uhler, Arkiv Fysik 1, 459 (1949).

13. THERMODYNAMIC PROPERTIES OF GASEOUS METAL DIHALIDES*

Leo Brewer, Gollakota R. Somayajulu, † and Elizabeth Brackett‡

The thermodynamic properties of the gaseous dihalides of Be, Mg, Ca, Sr, Ba; Zn, Cd, Hg; Sn, Pb; and Ti, V, Cr, Mu, Fe, Co, Ni, Cu are reviewed for three particular purposes.

1. Evaluation of entropies of gaseous metal dihalides through the treatment of vapor pressure data by the second law of thermodynamics.

The available vapor pressure measurements are treated by the Σ plot method[1] using tabulated heat capacities[2] for the condensed halides when available. The heat capacities of the gaseous molecules are calculated by use of estimated molecular constants. As the rotational and vibrational contributions to the heat capacity are very close to the chemical values these heat capacities are insensitive to the choice of molecular constants.

2. Use of these experimental entropies to aid in the estimation of entropies and free-energy functions that can be used for third-law calculations.

Free-energy functions are calculated by assuming these molecules to be linear harmonic oscillators. The translational contribution can be calculated accurately. The rotational contribution is calculated from observed[3,4] or estimated internuclear distances. The electronic contribution is estimated from the partition function of the dipositive gaseous metal ion. The vibrational contribution is determined mainly by the doubly degenerate bending frequency which is lower than the stretching frequencies. As one cannot estimate the contribution of the bending frequency accurately, the bending frequency has been used as a parameter to yield agreement between the experimental and calculated free-energy functions. Bending frequencies obtained in this manner are used to calculate an average value of the ratio (bending force constant)/(stretching force constant), which is then used to predict unknown values.

---

*Abstract of paper to be published in Chem. Revs. (UCRL-9840, Sept. 1961).

†Now at Osmania University, India

‡Now at Department of Chemistry, Rice University, Houston, Texas.

[1] G. N. Lewis, M. Randall, K. S. Pitzer, and L. Brewer, Thermodynamics, 2nd Ed. (McGraw-Hill Book Company, Inc., New York, 1961).

[2] K. K. Kelley, U. S. Bur. Mines Bull. 584, (1960)

[3] O. Bastiansen and E. W. Lund, Ann. Rev. Phys. Chem. 10, 31 (1959).

[4] H. Bloom, J. O. Bockris, N. E. Richards, and R. G. Taylor, J. Am. Chem. Soc. 80, 2044 (1958).

3. Evaluation of enthalpies of formation of gaseous metal dihalides by both the second and third law of thermodynamics.

In addition to tables of free-energy functions for 72 condensed and gaseous dihalides, values of the molecular constants used, and a companion of the experimental and calculated free-energy functions, extensive tables are also presented of the enthalpies of sublimation and formation of the solid halides and the enthalpies of formation and atomization of the gaseous halides. Experimental heats of ionization are calculated and compared with those calculated from empirical potential functions.[5] In addition, melting point and fusion data, and the constants for the equations

$$\Delta C_p^{\,o} = \Delta a + \Delta b\, T + \Delta c\, T^2,$$

$$\Delta F^o = \Delta H_I - \Delta a\, T \ln T - \frac{1}{2}\Delta b\, T^2 - \frac{1}{2}\Delta c\, T^{-1} - I\, T$$

are presented.

Polymerization in the vapor and the nature of the bonding in the molecules are briefly discussed.

[5] D. Cubicciotti, Stanford Research Institute Technical Note No. 7 (1960).

14. THE RELATIONSHIP BETWEEN ABSORPTION INTENSITY AND FLUORESCENCE LIFETIME OF MOLECULES

Stewart J. Strickler† and Robert A. Berg‡

The equations usually given relating fluorescence lifetimes to absorption intensity are strictly applicable only to narrow-line atomic transitions.[1, 2, 3, 4] It is often desirable, however, to be able to correctly calculate from absorption data the mean lifetimes of excited states of molecules.

† Now at Department of Chemistry, Rice University, Houston, Texas.

‡ Now at Department of Chemistry, Harvard University, Cambridge, Massachusetts.

[1] A. Einstein, Physik. Z. 18, 121 (1917).

[2] R. Ladenburg, Z. Physik 4, 451 (1921).

[3] R. C. Tolman, Phys. Rev. 23, 693 (1934).

[4] G. N. Lewis and M. Kasha, J. Am. Chem. Soc. 67, 994 (1945).

The relation between absorption and emission probabilities is based on Planck's blackbody radiation law and the Boltzmann distribution law. The absorption probability is easily related to experimentally measured quantities; the emission probability corresponds to the reciprocal of the lifetime τ_0. When account is taken of the usual wavelength shift of the fluorescence emission away from the absorption band, the following relation applicable to molecular transitions, is obtained:

$$\frac{1}{\tau_0} = \frac{8 \times 2303\pi\, c\, n^2}{N} \left\langle \tilde{\nu}_f^{-3} \right\rangle_{av}^{-1} \frac{g_\ell}{g_u} \int \epsilon \; d \ln \tilde{\nu} \qquad (1)$$

$$= 2.880 + 10^{-9}\, n^2 \left\langle \nu_f^{-3} \right\rangle_{av}^{-1} \frac{g_\ell}{g_u} \int \epsilon \; d \ln \tilde{\nu} ,$$

where n is the refractive index of the medium in which measurements are made; N is Avogadro's number; c is the speed of light in vacuum; g_ℓ and g_u are the degeneracies of the lower and upper electronic states of the transition, respectively; $\tilde{\nu}_f$ is the frequency of the fluorescence, measured in cm^{-1}; and ϵ is the molar extinction coefficient. The integration extends over the entire absorption band of the electronic transition; absorption frequency is measured in cm^{-1}.

Equation (1) was tested on eleven π-π transitions in strongly absorbing molecules. Lifetimes were calculated by use of (a) the extinction data obtained with a Cary model 14 spectrophotometer, (b) the mean fluorescence frequency determined spectrographically.

Calculated lifetimes were compared with directly observed lifetimes measured with a phase fluorometer that had been constructed in the laboratory of Professor Leo Brewer. The results are given in Table I and indicate that equation (1) is correct at least to within a few percent.

The principal assumptions made in deriving Eq. (1) are that the absorption band is strong and that there is no large change in configuration in the excited state. However, it is likely to be correct as to order of magnitude even for weak transitions or for "symmetry-forbidden" transitions, which can be seen in absorption because of distortion of the molecule in an excited state.

Table I. Comparison of observed and calculated lifetimes (nanoseconds).

Compound	Solvent	Observed	Calculated	Error
Perylene	benzene	4.79	4.29	-10%
Acridone	EtOH	11.80	12.06	+ 2%
9-aminoacridine	EtOH	13.87	15.43	+11%
	EtOH-HCl	14.07	14.19	+ 1%
	H_2O	16.04	16.40	+ 2%
	H_2O-HCl	15.45	16.67	+ 8%
N-methylacridinium chloride	H_2O	34.78	44.37	+28%
Fluorescein	H_2O-NaOH	4.02	4.37	+ 9%
Rhodamine B	EtOH	6.16	6.01	- 2%
	EtOH-HCl	4.65	5.55	+19%
Rubrene	benzene	16.42	22.42	+37%

15. RADIATIVE LIFETIME OF GASEOUS IODINE

Leo Brewer, Robert Berg, and Gerd Rosenblatt

The radiative lifetime of the B O_u^+ state of I_2 has been measured by the phase-shift method.[1, 2, 3] The iodine was excited by the mercury green line, which results in mainly population of the v' = 26 vibrational level of iodine. The lifetime is found to decrease with iodine pressure between 10^{-5} and 10^{-3} atm owing to quenching of the excited electronic state of iodine by other iodine molecules. The lifetime of the excited state of iodine was also studied in a molecular beam in an effort to find ways to reduce quenching. The true radiative lifetime of the B O_u^+ state of I_2 was found to be 7×10^{-7} sec.

A previous determination[4] of 1×10^{-8} has been shown to be in error owing to the effect of scattering of the exciting light from the mercury lamp. In this study, it was found that phase shifts corresponding to lifetimes as short as 10^{-8} sec were obtained unless care was taken to minimize scattered light. Even with elaborate precautions to minimize scattered light, lifetime measurements taken at iodine pressures from 10^{-7} atm to almost 10^{-5} atm were considerably shorter than the true lifetime, owing to the shift introduced by dilution of the fluorescent light by scattered exciting light.

---

[1] E. A. Bailey and G. K. Rollefson, J. Chem. Phys. 21, 1315 (1953).

[2] R. G. Brewer, I. A Method for Determining Radiative Lifetimes of High-Temperature Molecules II. The Probability of Spontaneous Nuclear Reactions in Molecular Hydrogen, (thesis) UCRL-8387, Sept. 1958.

[3] Fred E. Stafford, Measurement of Radiative Lifetimes (thesis), UCRL-8854, Sept. 1959.

[4] H. H. Hupfeld, Z. Physik 54, 484 (1929).

16. RESEARCH IN PROGRESS--BREWER

1. Measurements of values of the radiation transition probabilities of C_2 and CN. (With Lucy Hagan.)

2. The Deslandres-d'Azambuja bands of C_2 are being examined under high dispersion in an effort to obtain the energies of additional excited vibrational levels of the $c^1\Pi_g$ state and thus obtain a precise dissociation energy for C_2. (With Martin Shetlar.)

3. Study of the ultraviolet bands of MgO and MgOH is being continued in an effort to analyze additional portions of the spectrum. New methods of excitation are being sought. Infrared spectra studies of the alkaline earth oxides are also being initiated in a continuing effort to fix the low-lying electronic states of these molecules and thus to allow the calculation of reliable high-temperature thermodynamic functions. (With Robert Hauge.)

4. Molecular beams of high-temperature molecules are being produced in an effort to adapt molecular beam techniques to novel methods of spectroscopic study that may allow much more rapid analysis of band systems and identification of low-lying electronic states. The beams are also to be used for radiative-lifetime studies. (With Robert Walsh and Beat Myer.)

5. Work is being continued on thermodynamic evaluation of high-temperature vaporization data for the gaseous diatomic oxides of the elements and tabulation of thermodynamic constants for these molecules. (With Gerd M. Rosenblatt.)

6. Papers are in preparation which discuss some of the fundamental problems of the field of kinetics of vaporization of solids at high temperatures. (With Gerd M. Rosenblatt.)

7. Vapor species ($CdCl_2$ and LiFl) and the reaction products of gas discharges (in nitrogen and sulfur vapors) are trapped at low temperatures in different matrix materials. Spectral studies are planed to characterize the species and their concentrations, recombination rates, and general matrix properties. (With Beat Myer, Alan Snelson, and Ray McNamee.)

17. THE MICROWAVE SPECTRUM AND QUADRUPOLE INTERACTION IN CIS 1, 2-DICHLOROETHYLENE*

Willis H. Flygare and John A. Howe

As a result of their study of the microwave spectrum of cis 1, 2-dichloroethylene, Shimizu and Takuma report a value of -46 Mc for the component of the quadrupole coupling tensor lying in the C-Cl bond direction.[1] Since this result, if correct, requires an unusually large degree of "ionic character" in the C-Cl bond, and since Livingston reports a solid-state value of 70 Mc,[2] the microwave spectrum was re-examined. This examination shows that the above authors incorrectly assigned various rotational transitions and that in consequence their results are without significance.

As demonstrated by the internal consistency of our results, we have correctly assigned the spectrum, and find for cis $CHCl^{35}CHCl^{35}$ that the rotational constants are A = 11, 518. 3 Mc, B = 2, 545. 1 Mc, and C = 2, 082. 6 Mc. Measurements of the hyperfine splittings yield quadrupole coupling constants of X_{aa} = 3.7 Mc and X_{bb} = -35.7 Mc. These values, when used in conjunction with reasonable structural parameters, give a value $X_{zz} \approx 70$ Mc and show that the electron distribution in the C-Cl bond does not differ greatly from that found in CH_2CHCl or in CH_2CCL_2.

---

*Abstract of paper published in J. Chem. Phys. 36, 440 (1962).

[1] T. Shimizu, and H. Takuma, J. Phys. Soc. Japan 15, 646 (1960).

[2] R. Livingston, J. Phys. Chem. 57, 496 (1953).

18. STRONG-FIELD STARK EFFECT*

John A. Howe and Willis H. Flygare

Although a formal solution to the quantum-mechanical problem of a rigid asymmetric rotor containing one or more quadrupolar nuclei and subject to a space-fixed electric field has been discussed by various authors, cf. Mizushima,[1] no mention has been made of the great simplifications in computational and experimental procedure that occur in certain cases. In particular, we have given solutions appropriate to the case of a molecule containing two identically situated Cl nuclei and in the situation where the Stark perturbation is considerably greater than the quadrupole coupling energy. The results show that in this case the Stark effect of a $0_{00} \rightarrow 1_{11}$ transition consists of a triplet whose frequency varies quadratically with the electric field. It further shows that if attention is restricted to the center component of this triplet, then it is unnecessary to consider quadrupole coupling terms, and the dipole moment may be determined from the measurements in the usual fashion.[2]

The dipole moments of $CH_2CCl_2^{35}$ and $COCl_2^{35}$ have been determined by this method to have the values 1.34 D and 1.117 D respectively.

*Abstract of paper published in J. Chem. Phys., 36, 650 (1962).

[1] M. Mizushima, J. Chem. Phys. 21, 539 (1953).

[2] S. Golden and E. B. Wilson, Jr., J. Chem. Phys. 16, 669 (1948).

19. SIMPLE MOLECULAR ORBITAL THEORY OF THE DICHLOROETHYLENES*

John A. Howe, James S. Muirhead, and Jacob H. Goldstein

Although the concept of conjugation has been much employed to explain certain molecular properties, Dewar and Schmeising have recently raised the possibility that such effects are in reality due to changes in hybridization.[1] However, as Goldstein has shown,[2] the field-gradient asymmetry along the C-Cl bond in the vinyl and phenyl halides affords quantitative evidence for conjugation of the lone-pair electrons with the carbon π electrons.

*Abstract of a paper published in J. Chem. Phys. 36, 841 (1962).

[1] M. J. S. Dewar and H. N. Shmeising, Tetrahedron 5, 166 (1959).

[2] J. H. Goldstein, J. Chem. Phys. 24, 106 (1956).

In this paper we have further strenthened this contention by performing a simple MO calculation with no adjustable parameters and showing that first, the calculated ionization potentials and π moments are in satisfactory agreement with experiment, and that secondly, a lone-pair defect of approx .05 electron is correctly predicted for $CH_2C\ Cl_2$.[3] The calculated values are as follows.

	IP (ev)	Lone-pair defect	u_π, Δ
$CH_2\ C\ Cl_2$	9.78	0.060	1.39
CH Cl CH Cl	9.66	0.051	0.60[a]

[a]cis isomer only

[3]S. Sekino and T. Nishikawa, J. Phys. Soc. Japan 12, 43 (1957).

20. THE NEAR ULTRAVIOLET ABSORPTION SPECTRUM OF TETROLALDEHYDE*

James S. Muirhead and John A. Howe

Historically, much of the progress in chemical bonding theory has resulted from intensive study of various "prototype" molecules such as ethylene, butadiene, acrolein, etc. Of current interest in this Laboratory is another such system, C≡C–C=O.

Since the near-ultraviolet absorption spectrum of H–C≡C–CHO has been previously reported[1] we have attempted, by a similar study, to assess the effect on the C≡C–C=O system that results from replacing H by CH_3. The results are in accord with the usual picture in which the CH_3 group is said to be electron-donating via both the inductive and hyperconjugative effects: the $n \rightarrow \pi^*$ transition shows a 460 cm^{-1} blue shift, the C=O stretch frequency in the π^* state is lowered to 1035 cm^{-1}, and the transition tentatively identified as $N \rightarrow V$ is shifted red some 1300 cm^{-1}. Lastly, it should be added that the effect of methyl substitution on the $n \rightarrow \pi^*$ transition is comparable in magnitude to that attendant on replacing C=L adjacent to the C=O group by a C≡L group in the same position.

*Brief summary of paper to be published in J. Chem. Phys., April 1962.

[1]J. A. Howe and J. H. Goldstein, J. Am. Chem. Soc. 80, 4846 (1958).

21. RESEARCH IN PROGRESS--HOWE

Current research efforts are being devoted exclusively to the project in high-temperature microwave spectroscopy. Because of difficulties in procurement and in fabrication techniques, the high-temperature spectrometer is only now nearing completion. The electronics have been designed, assembled, and thoroughly tested (and in some cases, modified). The high-temperature cell has been assembled, vacuum-checked, and subjected to initial heating tests. The parallel-plate wave guide assembly is the only unit not at hand, and tests to ascertain how the required platinum-alumina bonds are to be made are in progress. It is expected, and hoped, that initial searches for K-band absorptions in 1 b halide vapors will commence in April.

22. TEMPERATURE DEPENDENCE OF THE KNIGHT SHIFT IN $Na-NH_3$ SOLUTIONS*

Juana Vivó Acrivos and Kenneth S. Pitzer†

The temperature dependence of the Knight shift of the NMR spectra for $Na-NH_3$ solutions in the concentration range of mole ratio R = 5 to 700 has been measured for the Na^{23} and N^{14} resonances. Figure IA-22-1 shows the NMR shifts. These data allow one to extend the chemical equilibrium data known at -33°C[1, 2] throughout the temperature interval 22° to -33°C. For $R \geqslant 150$ these solutions obey the following chemical equilibria:[3, 4]

$$Na_{(am)} = Na^{+}_{(am)} + e^{-}_{(am)}, \text{ with equilibrium constant } K_1, \quad (1)$$

$$Na_{(am)} = 1/2\ Na_{2(am)}, \text{ with equilibrium constant } K_2, \quad (2)$$

or

$$1/2\ Na_2 = Na^{+}_{(am)} + e^{-}_{(am)}, \text{ with equilibrium constant } K_3 = \frac{K_1}{K_2}. \quad (3)$$

The standard heats of reaction for the chemical equilibria 1, 2 and 3 are obtained from the temperature dependence of the respective equilibrium constant, thus, from Fig. IA-22-2,

*Summary of a manuscript to be submitted to J. Chem. Phys.

†Now President of Rice University, Houston, Texas.

[1] J. L. Dye, G. E. Smith, and R. F. Sankauer, J. Am. Chem. Soc. 82, 4803, 4797 (1960).

[2] E. C. Evers and P. W. Frank, J. Chem. Phys. 30, 61 (1959).

[3] E. Huster, Ann. Physik 33, 477 (1938).

[4] E. Becker, E. R. H. Lindquist, and B. Alder, J. Chem. Phys. 25, 971 (1956).

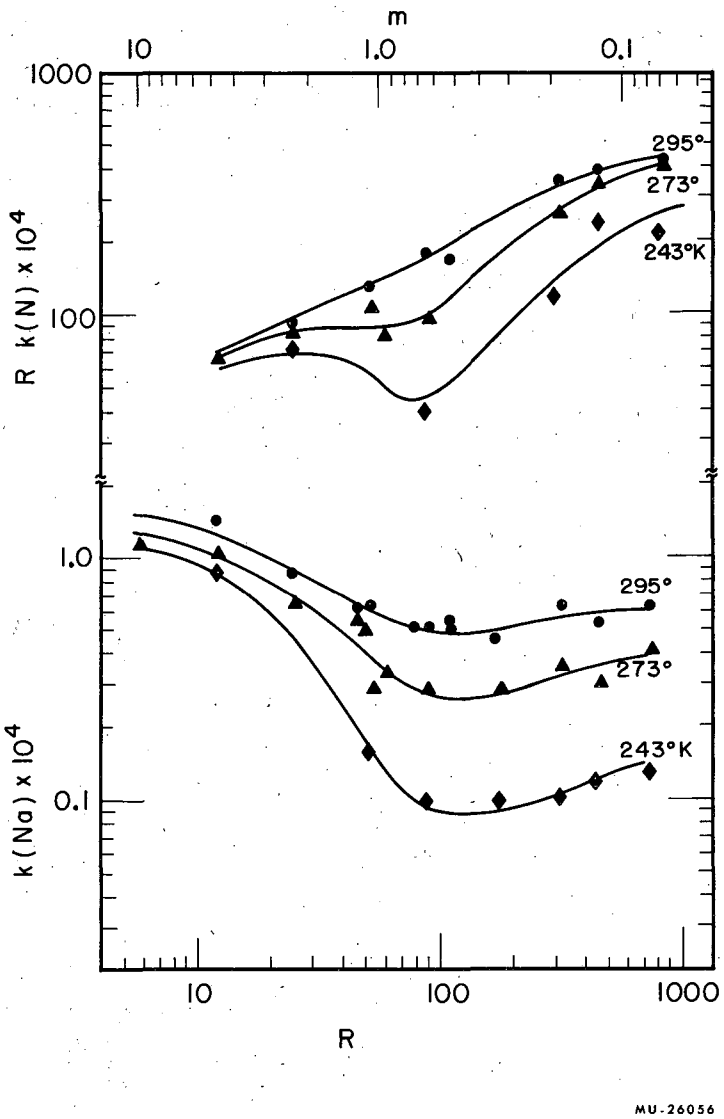

Fig. IA. 22-1. Isothermal concentration dependence of the KS in Na-NH_3 solutions.

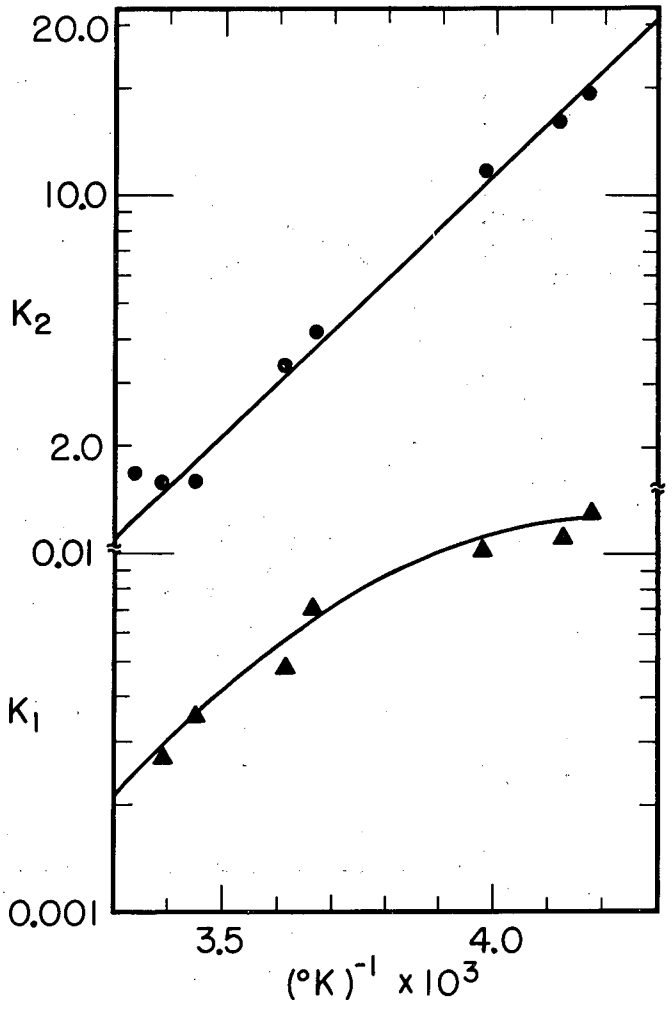

Fig. IA. 22-2. Inverse temperature dependence of the dissociation and dimerization equilibrium constants for $Na_{(am)}$ in the $Na\text{-}NH_3$ solutions for R = 150.

$$\Delta H_1^o\ (298) = -6.6 \pm .5 \text{ kcal/mole},$$

$$\Delta H_2^o = -7.3 \pm .5 \text{ kcal/mole},$$

$$\Delta H_3^o\ (298) = \Delta H_1\ (298) - \Delta H_2 = 0.7 \text{ kcal/mole}. \quad (4)$$

Here ΔH_2^o is found to be constant throughout the temperature interval whereas ΔH_1^o and consequently ΔH_3^o are not. Also, the value of ΔH_3^o at room temperature is in agreement with the heat of dilution determined by Stuart R. Gunn and Leroy G. Green (LRL Livermore, private communication), $\Delta H_3 = 0.7$ kcal/mole.

In the more concentrated region $R < 100$, these solutions show a metallic nature. The sharp minimum in the curves for k(N) at the lower temperatures indicates this boundary region between metallic and nonmetallic electron systems.

23. TRANSMISSION PROBABILITIES FOR ISOTOPIC REACTIONS OF THE TYPE $H + H_2$

Earl Mortensen and Kenneth Pitzer†

A theory is developed for calculating the wave function and thus the transmission and reflection coefficients for the reaction $H + H_2 \rightarrow H_2 + H$ by solving a two-dimensional time-independent Schrödinger equation for the relative motion of three particles on a straight line. It is shown that the vibrational bending energy in the activated state may be taken as an addition to the effective potential for the longitudinal motion. Transmission coefficients have been calculated at a few selected energies for the above reaction by use of a Sato potential surface. A manuscript describing this work, under the title "Theoretical Transmission Probabilities for Various Isotopic Reactions of the Type $H + H_2$," has been submitted to the Journal of the Chemical Society and is being presented at a symposium of the Chemical Society of London.

A new IBM 7090 program for making these calculations is presently being written. A more complete study of the transmission coefficients or permeabilities at a number of energies for the above reaction and for those reactions in which hydrogen is replaced by one of its isotopes is being planned.

---

†Now President of Rice University, Houston, Texas.

24. TEMPERATURE DEPENDENCE OF THE KNIGHT SHIFT IN Ca-NH_3 SOLUTIONS

Juana Vivó Acrivos, Judith C. Brown,† and Kenneth S. Pitzer‡

The temperature dependence of the N^{14} Knight Shift in the Ca-NH_3 solutions is being studied. Results have been obtained which differ from those in the NH_3-Na system, in which the fast exchange mechanism narrows the absorption line.[1] When there is fast exchange between the NH_3 associated with the species $e^-_{(am)}$ and the bulk ammonia, the proton hyperfine structure of the N^{14}-NMR absorption is not observed; this is the case for the Na-NH_3 solutions. In the Ca-NH_3 solutions, the hyperfine structure is not resolved at room temperature, but at 0°C it is clearly resolved. (See Fig. IA. 24-1.) A calibrated ESR-MNR experiment is being set up to detect the absolute number of spins in solution for both the Na-NH_3 and Ca-NH_3 systems by direct comparison of the ESR absorption at 16 Mc/sec and 5.7 oe, with the H^1 NMR absorption at the same frequency and a field of 3,757.8 oe.

---

†Now at Centre d'Etudes Nucléaires de Saclay, Seine Oise, France.

‡Now President of Rice University, Houston, Texas.

[1] J. Vivó Acrivos and K. S. Pitzer, Temperature Dependence of the Knight Shift of the Na^{23}-$N^{14}H_3$ System, (UCRL-9997, March 1962) submitted to J. Chem. Phys.

25. SILVER OXIDE: THE EFFECTS OF PARTICLE SIZE ON HEAT CAPACITY FROM 2 TO 80°K AND ON ENTROPY

Lawrence V. Gregor† and Kenneth S. Pitzer‡

In 1937 Pitzer and Smith measured the heat capacity of silver oxide (Ag_2O) over the range 13 to 300°K and found anomalously high values in the range 20 to 40°K.[1] Hysteresis effects were noted with respect to the excess heat capacity. The entropy associated with the anomaly was approximately 0.5 cal/°C mole. Kobayashi[2] measured the heat capacity of silver oxide at higher temperatures and observed a heat evolution of approximately 315 cal/mole in the range 100 to 200°C the first time that a given sample was heated through this region.[2] Repeated heating gave no further heat evolution.

---

*Brief version of a paper to be published in J. Am. Chem. Soc.

†Now at I. B. M. Research Center, Yorktown Heights, New York.

‡Now President of Rice University, Houston, Texas.

[1] K. S. Pitzer and W. V. Smith, J. Am. Chem. Soc. 59, 2633 (1937).

[2] K. Kobayashi, Sci. Repts. Tôhoku Imp. Univ. I 35, 173 (1951)

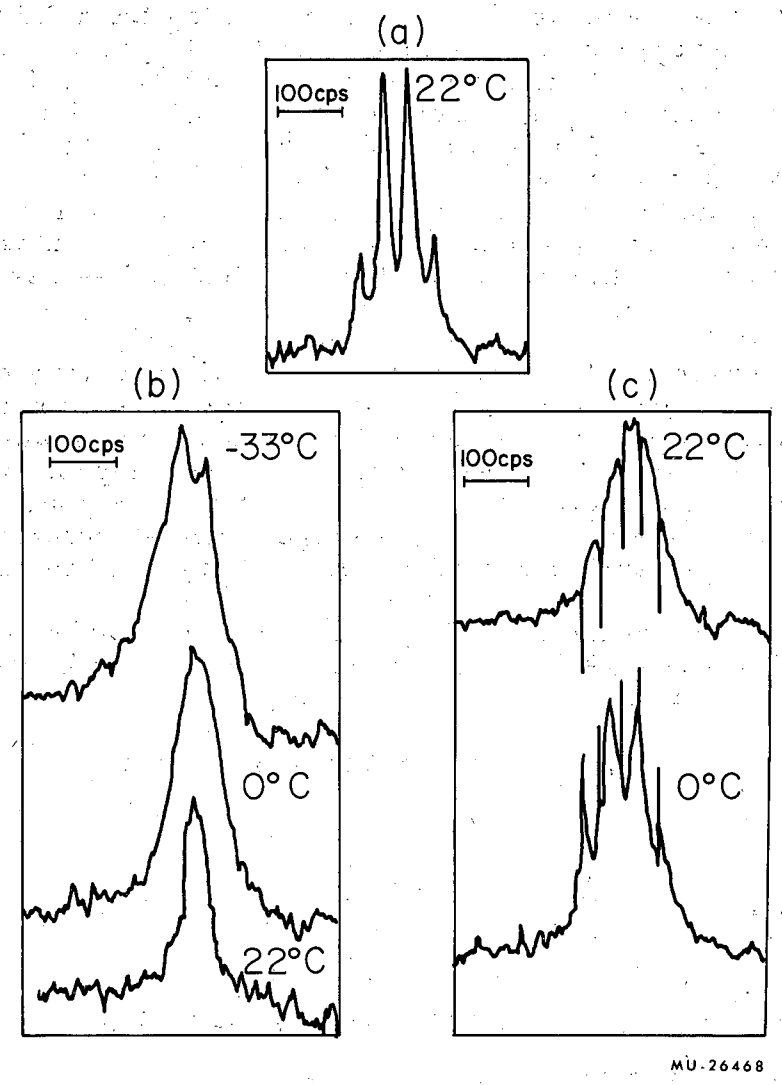

Fig. IA. 24-1. N^{14} NMR absorption: (a) 0.5 molal NaCl in NH_3(22°C), (b) Na-NH_3, R = 740 (22°C; 0°C and -33°C), and (c) Ca-NH_3, R = 79 (22°C and 0°C). [Solutions (b) and (c) have KS of the same order of magnitude.]

In each case the sample was precipitated from aqueous solution and was dried at temperatures not exceeding 115°C. Recently Gerkin prepared relatively large crystals of silver oxide which had been annealed above 200°C and found no anomaly in the low-temperature heat capacity in the range 14 to 300°K.[3] The investigation reported here was designed to yield further information about these peculiar effects.

The heat capacity of Ag_2O has been measured from 2.2 to 80°K for a finely divided annealed sample, and from 3.3 to 24°K for a macrocrystalline annealed sample (a portion of the sample prepared by Gerkin). The anomalously high heat capacity originally observed in unannealed Ag_2O between 20 and 50°K is also found in the finely divided sample, though the anomalous region is smaller and narrower, and its maximum occurs at a lower temperature. No anomalous peak in the heat capacity of macrocrystalline Ag_2O is observed down to 3.3°K, but the heat capacity of this material is higher below 14°K than that of the finely divided sample. These results are shown in Figs. IA. 25-1 and IA. 25-2.

The heat capacity of the various samples of Ag_2O may be discussed in terms of its unusual crystal structure, and a mechanism proposed to correlate the anomalous behavior of Ag_2O below 15°K and between 20 and 40°K. The mechanism involves the interaction of the two independent sublattices of the structure of Ag_2O, and it is proposed that for very small particles there is a transition from a symmetric high-temperature structure to a slightly distorted low-temperature structure in the vicinity of 20 to 30°K.

Revised values of the thermodynamic properties of macrocrystalline Ag_2O at 298.15°K are given, based on the observed heat-capacity data below 15°K. The results are:

$$S^{o}_{298.15} = 28.91 \pm .07 \text{ cal/deg mole},$$

$$H^{o}_{298.15} - H^{o}_{0} = 3387 \pm 5 \text{ cal/mole},$$

$$\left(-\frac{F^{o} - H^{o}_{0}}{T}\right)_{298.15} = 17.55 \pm .07 \text{ cal/deg mole}.$$

[3] R. E. Gerkin, Ph. D. Dissertation, University of California, 1960; see also Pitzer, Gerkin, Gregor, and Rao, Pure and Appl. Chem. 2, 211 (1961).

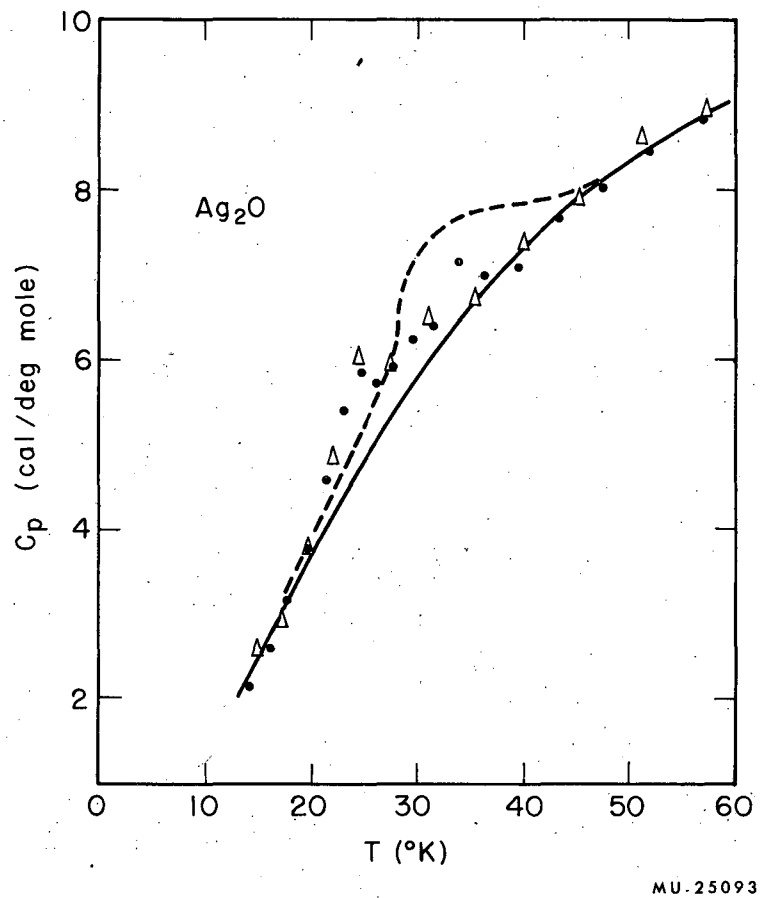

Fig. IA. 25-1. Heat capacity of annealed finely divided silver oxide.

△ Series 1

● Series 2

— Macrocrystalline sample, Gerkin and Pitzer.

--- Fine-particle unannealed sample, Pitzer and Smith.

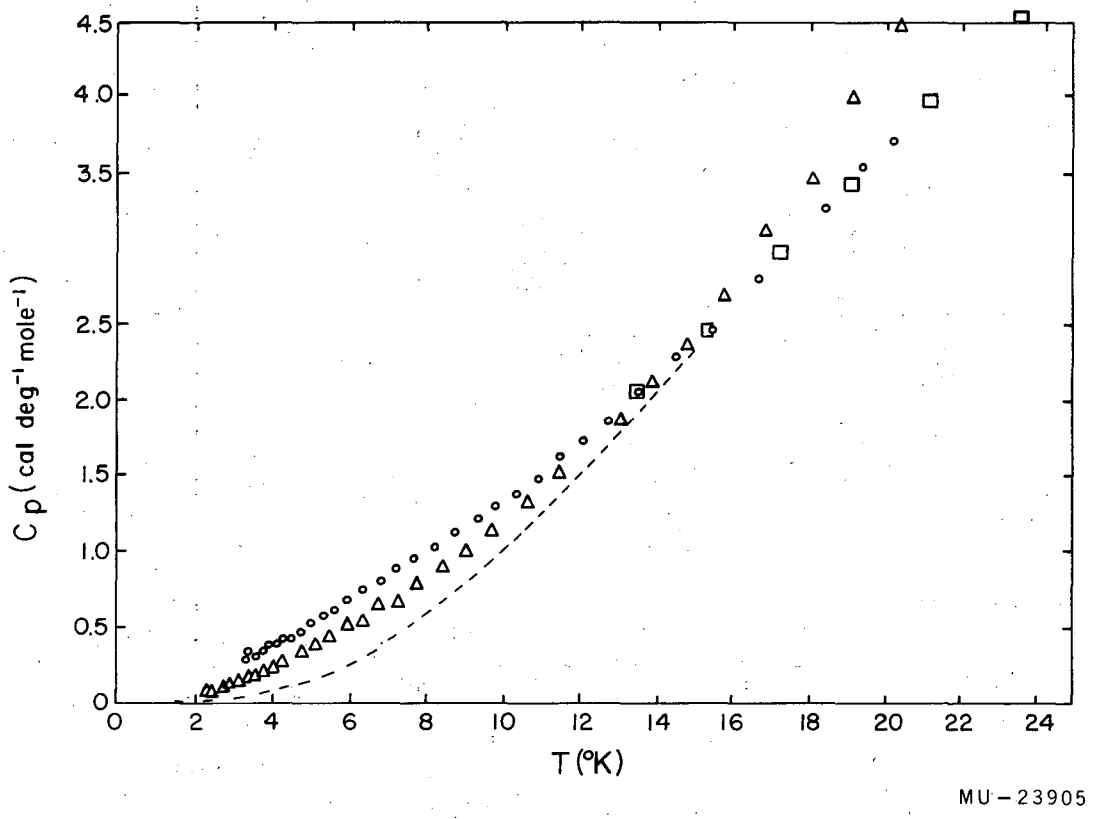

Fig. IA. 25-2. Heat capacity of silver oxide at lower temperatures.
○ Macrocrystalline sample, this research.
□ Macrocrystalline sample, Gerkin and Pitzer.
△ Small-particle annealed sample.

26. THE SILVER-SILVER OXIDE ELECTRODE, AND THE ENTROPY OF MERCURIC OXIDE*

Lawrence V. Gregor† and Kenneth S. Pitzer‡

Attempts have been made by many workers to measure the equilibrium potential of the $Ag-Ag_2O$ electrode. Cells composed of this electrode, a stable reference half-cell (such as Hg-HgO), and an electrolyte (e.g., aqueous NaOH) quite generally gave emf values that were unstable, decreased with time, and were lower by several millivolts than the value calculated for the cell reaction

$$2Ag + HgO \rightarrow Hg + Ag_2O \qquad (1)$$

from the standard free energies of formation of HgO and Ag_2O.

The failure to measure the equilibrium potential of the electrode was inconclusively attributed to a variety of reasons such as suboxide formation, surface films, etc. Hamer and Craig were finally able to prepare and study stable $Ag-Ag_2O$ half-cells,[1] and their emf measurements were in reasonable agreement with the calculated value. The method of electrode preparation utilized by these authors involved partial reduction of Ag_2O to Ag at 60° by H_2. Since the reduction is exothermic, it is possible that the samples of Ag_2O were heated to well above 60°C.

It has been known for some time that the previous thermal history of Ag_2O has a marked effect on the heat capacity and consequently the thermodynamic properties of this substance. Pitzer and Smith noticed an anomalously high heat capacity between 20° and 40°K in Ag_2O that had been dried at 110°C.[2] Kobayashi observed an irreversible evolution of heat at about 150°C amounting to 315 cal/mole for Ag_2O.[3] Recent measurements have shown that the low-temperature heat capacity anomaly can be modified or removed altogether depending on the crystal size and the extent of annealing above the Kobayashi temperature.[4, 5]

---

*Brief version of a paper to be published in J. Am. Chem. Soc.

†Now at E. I. Du Pont de Nemours and Co., Gibbstown, N. Jersey.

‡Now President of Rice University, Houston, Texas.

[1] W. J. Hamer and D. N. Craig, J. Electrochem. Soc. 104, 206 (1956).

[2] K. S. Pitzer and W. V. Smith, J. Am. Chem. Soc. 59, 2633 (1937).

[3] K. Kobayashi, Sci. Repts. Tôhoku Imp. Univ. I 35, 173 (1951).

[4] K. S. Pitzer, R. E. Gerkin, L. V. Gregor, and C. N. R. Rao, Pure and Appl. Chem. (IUPAC) 2, 211 (1961).

[5] L. V. Gregor and K. S. Pitzer, IA. 25.

This investigation was undertaken to explore methods of preparing stable $Ag-Ag_2O$ electrodes which did not involve heating the electrode material, and to study the behavior of such electrodes when prepared from samples of Ag_2O subjected to various annealing treatments.

Stable, reversible $Ag-Ag_2O$ electrodes have been prepared by partial electrolytic reduction of Ag_2O mixed with finely divided Ag in contact with a platinum wire. There is no apparent difference in the equilibrium electrode potential for annealed and unannealed Ag_2O, provided that there is no great change in particle size. The average potential for the cell reaction

$$2\ Ag + HgO \longrightarrow Ag_2O + Hg$$

is $-0.2447 \pm .001$ v at 25°C. The free energy of formation of Ag_2O at 25°C is -2691 ± 10 cal/mole. Limited measurements of dE^o/dT were made, and the value of $-0.000201 \pm .00001$ v/deg used to calculate $\Delta S^o = -9.27 \pm .5$ cal/deg mole for the cell reaction. This value, together with the entropies of Ag, Hg, and Ag_2O,[6] yields $17.4 \pm .6$ cal/deg mole for the entropy of HgO at 298°K. This result is compared in Table I with values from other sources.

Table I. Molal entropy of mercuric oxide (cal/deg)

Low temp. C_p (B. and J., Ref. 7)	$16.80 \pm .1$
Ag_2O cell (H. and C., Ref. 1)	$17.56 \pm .5$
Ag_2O cell (this research)	$17.4 \pm .6$
H_2 cell, various authors (Refs. 1, 6, 7)	$17.3 \pm .3$

Also shown in Table I is the entropy value for HgO calculated from the heat capacity measurements by Bauer and Johnston[7] from 15 to 300°K with a Debye function extrapolation to 0°K. In addition, several workers have studied the galvanic cell with the reaction

$$H_2(g) + HgO(s) = H_2O(\ell) + Hg(\ell),$$

and the results have been reviewed recently by several authors[1, 6, 7] and combined with other data to yield the final value in Table I.

The entropy values from the two types of cell are quite concordant, but the presumably more precise value based on the low-temperature heat capacity data is slightly outside the estimated limits of error on the low side. The structure of red or yellow orthorhombic HgO was shown by Aurivillius to involve long chains -O-Hg-O-Hg-O-Hg- with 180° angles at Hg and 109° angles at oxygen.[8] Such a structure might lead to an abnormal heat-capacity

[6] K. K. Kelley, U. S. Bur. Mines Bull. 592 (1961).

[7] T. W. Bauer and H. L. Johnston, J. Am. Chem. Soc. 75, 2217 (1953).

[8] K. Aurivillius, Acta Chem. Scand. 10, 852 (1956).

curve at temperatures below 15°K, where Bauer and Johnston's measurements began. The results of our measurements below 15°K on macrocrystalline Ag_2O indicate that substantial deviation from the Debye curve is possible for heavy metal oxides.[7]

27. ORBITAL RADII, BOND LENGTH, AND RESONANCE*

G. R. Somayajulu†

The radius of a s-p hybrid orbital has been found to be given by the expression: $r = A - B/(1 + \lambda^2)$ where A is the radius of the pure p orbital, B, a universal constant equal to 0.336 A and λ, the coefficient of mixing in the hybrid $s + \lambda p$. When radii appropriate for the orbitals that are paired together are used, the bond length is additive of the orbital radii and no Schomaker-Stevenson correction is necessary. This correlation shows that most bonds can be treated as covalent, single, and localized.

*Abstract of paper submitted to J. Chem. Phys. (UCRL-9568, Feb. 1961).

†Now at Osmania University, India.

28. BOND ENERGIES, VALENCE-STATE ENERGIES, AND RESONANCE*

G. R. Somayajulu†

In order to evaluate the effects of resonance (both π-electron and ionic-covalent) on the heats of atomization of molecules, bond energies have been estimated on the basis of the relation

$$k_e r_e^2/E = \text{constant},$$

applicable for bonds of any type and of any order between two given atoms, and on the basis of the valence-state energies of the atoms. The valence-state energy of an atom is defined as that part of the heat of atomization of the molecule that can be attributed to the atom in a state corresponding to the state of hybridization in the molecule. For the formation of the molecule from the atoms in their valence states (not necessarily spectroscopic states) the energy given off is the sum of the valence-state energies, which is equal to the total heat of atomization. An assumption is made that the valence-state energy of hydrogen in homologous compounds is constant, being equal to its standard heat of formation; this has facilitated the derivation of the

*Abstract of UCRL-9590, Feb. 1961

†Now at Osmania University, India.

valence-state energies of the other atoms in the homologous compounds. On the basis of the valence-state energies of certain standard atoms--viz., primary, secondary, tertiary, quaternary, trigonal, and digonal carbon atoms, hydrogen, etc.--the expected heats of atomization of several conjugated and hyperconjugated molecules have been determined. If resonance were to be important, the observed heat of atomization of a molecule would be higher than its expected value by an amount called the stabilization energy. Thus the stabilization energy of benzene is 19.56 kcal/mole at $0^{o}K$. However, for a number of classical hydrocarbon molecules, the stabilization energies are all negative, indicating no resonance. Alkylation has been found to lower the stabilization energies of ethylene, benzene, and acetylene, but increases those of formaldehyde, formic acid, formamide, etc. Thus in classical hydrocarbon molecules containing nonhydrocarbon groups, there seems to be evidence in favor of resonance.

It has been suggested that the strengths of heteropolar bonds, explained by Pauling on the basis of ionic-covalent resonance, may be explained in terms of the strengths of the hybrid orbitals.

B. SOLID-STATE PHYSICS AND CHEMISTRY

1. APPARATUS FOR DRAWING 0.003-INCH WIRES

George Jura and Duane Newhart

An apparatus has been built for the back extrusion of metals to form the 0.003-in. diameter wires needed for resistance work. So far wires have been made of Yb, Ce, Pb, Bi, Cd, and Pr. Suitable wire of these metals is not commercially available.

2. STATIC PRESSURES APPROACHING A MEGABAR

George Jura and Malcolm Nicol

The development of a new ring technique for Bridgman anvils opens the possibility of reaching pressures higher than ever reached before. As an example of the change in load to obtain a given pressure, we cite the results using anvils whose face diameter is 1/4 in. In the old standard method, a pressure of 88 kbars is reached when the load is 80 kbars. With the new ring, the same pressure is attained at a load of 15 kbars. With Bi wire, several experiments have been performed such that if this simple relationship between pressure and load were maintained, a pressure of 2.8 Mbars would have been reached. Actually, a permanent deformation of carbides occurs. If the maximum pressure is determined on the basis of the maximum permanent deformation, the pressure reached is about 1 Mbar.

To determine the pressure that has been reached, further calibration work on the pressure scale is in progress. It is believed that the pressure scale can be extended with relatively little effort from the present 125 kbars to about three or four times this value in the systems now available.

This technique is such that it can be applied to measure the electrical conductivity of any metal, or a semiconductor with a gap on the order of 1 v.

3. SIZE EFFECTS ON METALLIC CONDUCTIVITY

George Jura and Malcolm Nicol

An investigation almost completed is concerned with the dimensions of the sample whose resistance is being measured. One effect of high pressure is to increase the Debye temperature, which perforce means an increase in the mean free path of the electrons. It is known that at 1 atmosphere and at room temperature there is no noticeable decrease in the conductivity of a metal until one of the dimensions is decreased to about 1000 A. This

figure will be larger at higher pressures. The purpose of these experiments is twofold, first to find the minimum sample size that will give data that correspond to bulk measurements, and second to have an approximate method of determining the mean free path of the electrons at a given pressure. When the mean free path approaches the dimensions of the sample an increase in resistivity is noted. The experiments have been done with aluminum to date.

Hoops and strips of metal varying in thickness from 0.003 to 0.00025 in. have been used in these experiments. The width of the sample has been of the order of 0.01 in.

The available data indicate that up to 100 kbars there is no noticeable change in resistivity as long as the dimension of the sample is greater than 0.001 in. There is a slight increase in resistivity when the thickness is decreased to 0.0005 in., but the difference is hardly beyond the experimental error. At 0.0025 in., the resistivity is greater than that observed with the heavier samples. This would indicate that the mean free path is of the order of 1/4 the thickness of the sample when this quantity is calculated from the theory of Sondheim. At 100 kbars there is an increase of about 10% in the resistivity over the thicker samples. These experiments are to be repeated with the new techniques whereby a thin and a standard sample will be measured simultaneously to remove the variation in results that is due to the inherent geometrical difficulties in reproducing the position of the sample in the system.

4. RARE EARTH METALS: ELECTRICAL AND MAGNETIC PROPERTIES AT HIGH PRESSURES

George Jura and Clark Souers

A program has been undertaken to study the electrical and magnetic properties of the rare earth metals. There is no doubt of the ultimate success of the electrical resistance measurements, and there is reasonable hope that at least the Curie temperature of gadolinium can be determined reasonably accurately.

The work was started on ytterbium because the data of Bridgman showed a very large rise with increased pressure, and a subsequent decrease in the specific resistance. Our work has shown that this is a phase transition. In the present work the Yb is at constant pressure, instead of the pressure gradient existent in the work of Bridgman. At 20°C the transition pressure is 40 ± 2 kbars. At 175°C the transition pressure is 32 kbars. From this and intermediate points, one would assume that this is the transition that occurs in Yb at around 800 °C at 1 atm.

This transition can be used as a fixed point on the pressure scale, since the specific resistance falls by a factor of 14 at the transition.

It is hoped to extend this work up to temperatures of about 450°C, and to as low temperatures as possible.

5. MULTIPLE SAMPLES IN BRIDGMAN ANVILS

George Jura and Harold Stromberg

The work recently reported by Montgomery and others[1] has led to some very interesting modifications of the loading and the geometry used in the anvils. The full extent of the possibilities of the new techniques have not yet been fully explored, but already a number of very important results have been obtained. In all earlier work with the anvils it has been necessary to make the resistance measurements through the anvils. Any attempts at placing leads through the pyrophyllite ring failed because the wire was pinched, owing to the large pressure gradient in the ring.

The pressure gradient in the ring can be decreased by increasing the width and height of the ring. So far, the best results have been obtained with a ring thickness of 3/32 in. and height of 0.020 in. Actually, the ring height is usually obtained by the use of two 0.010-in. rings. Leads then can be run into the sample through the two rings, obviating a drilling through the wall.

The metal leads used are platinum and tungsten. It has been found that the wires must be 0.005 in. in diameter to hold. When the wires are of this dimension, platinum will hold without pinching up to pressures of about 125 kbars, and tungsten to at least 150 kbars.

Three different metal samples have been loaded at one time, and the leads so set that true four-lead measurements could be made independently on each sample. However, we have not yet succeeded in obtaining results on more than two. The spatial requirements when three wires are used are quite severe. The probability of success with two samples is very high.

There is another advantage in this technique. The effective face diameter of the anvils is decreased by an amount corresponding to the increase in distance over which the pressure varies, consequently higher pressures are obtained with smaller loads.

---

[1] Peter W. Montgomery, Harold Stromberg, George H. Lura, and George Jura, Calibration of Bridgman Anvils, a Pressure Scale to 125 kbars, UCRL-9807, Aug. 1961.

6. MOSSBAUER EXPERIMENTS

George Jura, John O. Rasmussen, John A. Stone, and Malcolm Nicol

The nucleus under investigation is Dy^{161}, which has an excited state 25 kv above the ground state. It has been shown that it is possible to determine the Mossbauer effect for this system to pressures of 100 kbars. The only spectrum that is completed is that at 35 kbars. Most of the spectrum has been determined at 56 kbars.

The Dy^{161} is obtained in the following manner. A disc of Gd metal is irradiated in a high neutron flux. The n, β reaction of Gd^{160} yields Tb, which β-decays to the excited Dy^{161}. The disc is mounted in the anvils in the usual manner. The radiation measured is that which passes through the pyrophyllite ring. The absorber is dysprosium metal deposited on aluminum foil. The aluminum foil is mounted on a canted wheel, which is driven at various velocities by an appropriate oscillator and power supply.

At 1 atm, a single absorption is observed whose width is about 9 cm/sec. There is no resolution of fine structure down to liquid nitrogen temperatures. A preliminary experiment at 20 kbars yields a similar result. At 35 kbars, the width of the band has increased to about 25 cm/sec, and a number of features of the spectrum are resolved. The minimum number of features is 14, and if statistics of 100 to 1 are accepted, there are 22.

The width of the absorption at 56 kbars has been determined, and the measurable effect extends over about 65 cm/sec. The number of features is about double that found at 35 kbars. There are still regions of this spectrum that have not been fully determined. It is doubtful that any attempt will be made to determine the spectrum at 100 kbars, because of the long time that would be needed. It is planned to determine the spectrum at several pressures below 35 kbars to determine whether the onset of fine structure is sudden or gradual.

To the present, no real progress has been made in elucidating the observed fine structure. It is known that the gadolinium matrix does not become ferromagnetic up to the highest pressures we have used. Qualitatively, the crystal field appears to be increasing sufficiently rapidly to separate the levels in the emitter to the extent that the fine structure becomes observable. If this explanation is correct, it appears that pressure could be used to increase the resolution.

7. THE LOW-TEMPERATURE HEAT CAPACITIES OF ANTIFERROMAGNETIC MnF_2 AND CoF_2*

Norman E. Phillips

At low temperatures, the heat capacity of a nonmetallic antiferromagnet can be expected to be the sum of three contributions: a lattice term proportional to T^3; a nuclear hyperfine-interaction term proportional to T^{-2}; and any heat capacity arising from magnetic interactions. In the absence of anisotropy, spin wave theory predicts a T^3 dependence for the latter term. The inclusion of anisotropy modifies this result, giving a heat capacity that varies exponentially with temperature. If the anisotropy field is large enough, one can expect a temperature interval in which only the lattice and hyperfine heat capacities are appreciable.

The experimental data for MnF_2 and CoF_2 have been analyzed into the three components by plotting CT^2 versus T^5 as shown in Fig. IB.7-1. For CoF_2, the experimental points follow a straight line from 4.2° to 1.5°K. Below 1.5°K, the points fall below the line. This behavior is apparently related to a thermal relaxation time observed in this salt. This thermal relaxation time increased rapidly with decreasing temperature, reaching a maximum of approximately 10 minutes at 1.5°K and decreasing again at lower temperatures. Both observations are consistent with a nuclear relaxation time which increased with decreasing temperature so that at the lowest temperatures the corresponding hyperfine heat capacity contribution was not observed. The linear relation between CT^2 and T^5 for CoF_2 suggests that there is no significant magnetic contribution to the heat capacity in this temperature region. For MnF_2, the linear region extends only to approx 1.8°K. Positive deviations are observed above this temperature. These are assumed to represent the magnetic heat capacity. The hyperfine heat capacity and lattice heat capacity were obtained from the intercept and slope of the straight line for both salts. The T^3 lattice heat capacities obtained in this way are in excellent agreement with an extrapolation of the lattice heat capacity obtained by an analysis of the higher-temperature data by Stout and Catalano.[1] This is demonstrated in Fig. IB.7-2 as a plot of effective Debye temperature versus temperature.

Kubo has derived a dispersion relation for antiferromagnetic spin waves in which anisotropy is included in a molecular field approximation.[2] Eisele and Keffer have calculated the thermodynamic functions in the same approximation.[3] For the heat capacity, their result is presented as the ratio of the observed magnetic heat capacity to the T^3 heat capacity expected for an

---

*This work was carried out in collaboration with Edward Catalano (Lawrence Radiation Laboratory, Livermore) and reported at the International Conference on Magnetism, Kyoto, Oct. 1961. To be published in the Journal of the Physical Society of Japan.

[1] J. W. Stout and E. Catalano, J. Chem. Phys. 23, 2013 (1955).

[2] R. Kubo, Phys. Rev. 87, 568 (1952).

[3] J. A. Eisele and F. Keffer, Phys. Rev. 96, 929 (1954).

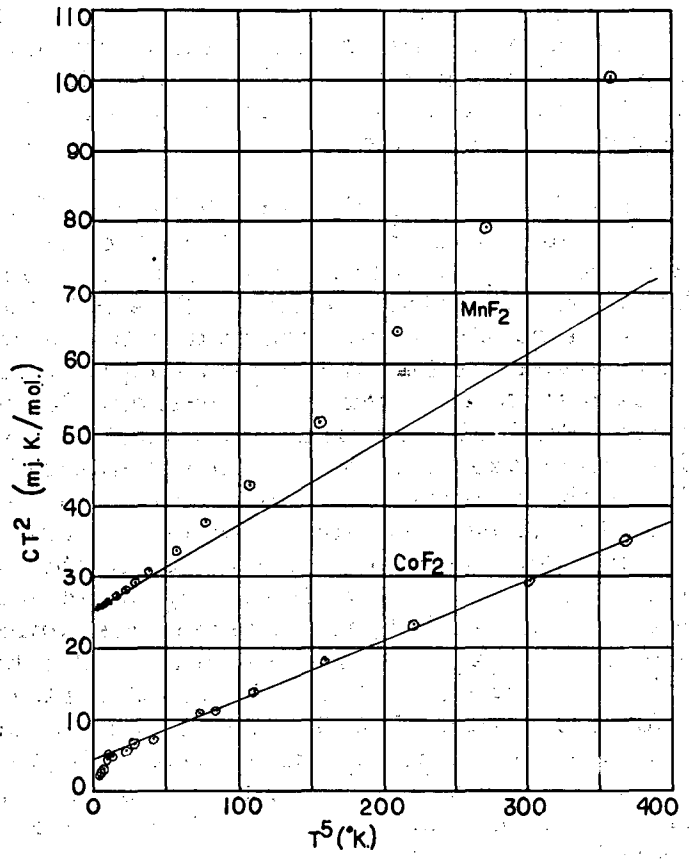

MU-26398

Fig. IB.7-1. Total heat capacity, C (mj/mol deg), of MnF_2 and CoF_2 shown as CT^2 versus T^5.

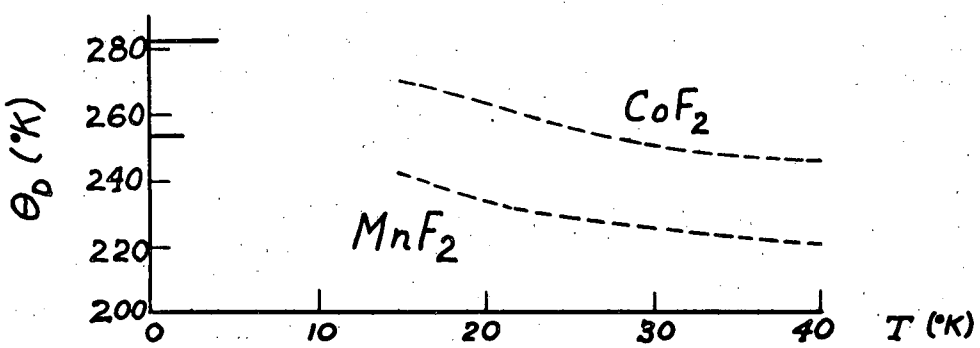

MU-26399

Fig. IB. 7-2. Apparent Debye temperature. The dashed curve is from the work of Stout and Catalano (Ref. 1); the solid lines represent the measurements in this experiment.

isotropic antiferromagnet, and is given as a function of T/T_{AE}. T_{AE}, a measure of the anisotropy, is given by

$$k\,T_{AE} = 2(zJK)^{1/2}\,S,$$

where $J/2$ is the exchange integral, K is the anisotropy constant, S is the spin, and z is the number of nearest-neighbor magnetic ions. The observed magnetic heat capacity for MnF_2, C_M, is compared with the result of Eisele and Keffer[3] in Fig. IB. 7-3. T_{AE} has been taken as 12.7°K in accord with critical-field and magnetic resonance experiments.[4-6] On the whole, the agreement must be considered as reasonable. The experimental and theoretical curves have the same general slope. The magnitude is very sensitive to the value of the exchange integral. This had been estimated from the Neel temperature, T_N, by use of the usual molecular field formula. At the low-temperature end, of course, the error in C_M is quite large, and the comparison should be made with this fact in mind.

The absence of magnetic heat capacity and the long nuclear relaxation times observed in CoF_2 are both indicative of a high anisotropy field for this salt.

---

[4] I. S. Jacobs, J. Appl. Phys. Suppl. 32, 615 (1961).

[5] S. Foner, Phys. Rev. 107, 683 (1957).

[6] F. M. Johnson and A. M. Nethercot, Phys. Rev. 104, 847 (1956); 114, 705 (1959).

8. HEAT CAPACITY OF INDIUM BELOW 1°K

Norman Phillips and H. Roger O'Neal

The heat capacity of indium has been measured in the normal and superconducting states between approximately 0.1°K and 1°K. The normal-state heat capacity is adequately represented by the sum of a nuclear quadrupole contribution proportional to T^{-2}, an electronic contribution proportional to T, and a lattice term proportional to T^3. The nuclear quadrupole and lattice heat capacities are in excellent agreement with values calculated from measurements of nuclear quadrupole resonance and sound velocity respectively. The electronic heat capacity in superconducting indium is a relatively small part of the total at low temperatures, and a direct comparison of the lattice heat capacity in the normal and superconducting states is possible. In fact, the total heat capacity in the superconducting state is less than the lattice heat capacity in the normal state at temperatures below approximately 0.4°K. The nuclear quadrupole heat capacity does not appear in the superconducting state, presumably because the spin-lattice relaxation time is very long. The discrepancy in lattice heat capacities is in qualitative but not quantitative agreement with that reported by Bryant and Keesom

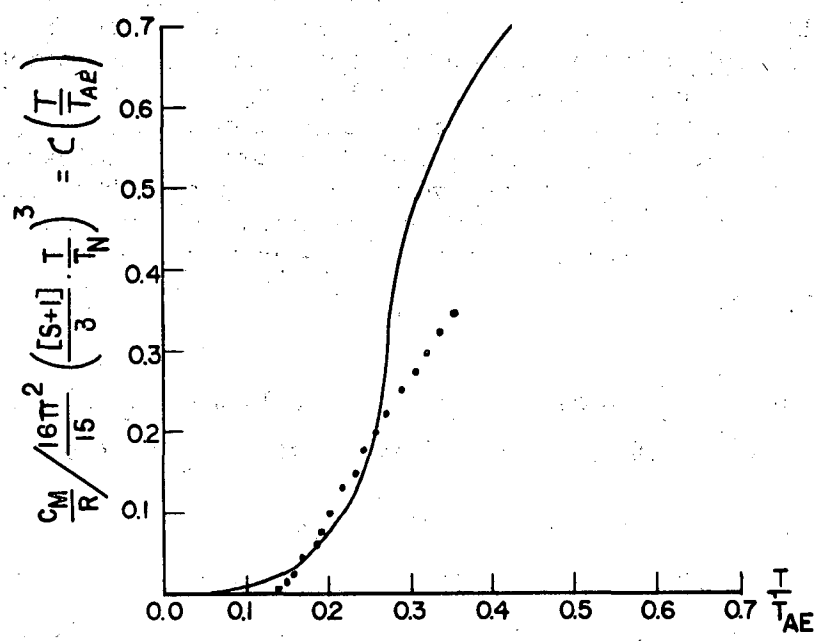

MU-26400

Fig. IB.7-3. Magnetic heat capacity, C_M, of MnF_2. The curve is from the calculation of Eisele and Keffer (Ref. 3). The points represent the experimental values.

from measurements above 0.3°K.[1] Part of the difference between these measurements and those reported by Bryant and Keesom is due to their assumption that the quadrupole heat capacity would appear in the superconducting state.

Daunt and Olsen have suggested that this effect is produced by a temperature dependence of the vibrational spectrum which gives a temperature-dependent zero-point energy.[2] They suggested that this temperature dependence was different in the normal and superconducting states and, further, that the whole frequency spectrum changed in the same way as the low-frequency modes observed in ultrasonic measurements. It seems reasonable that the effect is associated with changes in zero-point energy, but it must be associated entirely with the superconducting state, otherwise the normal-state lattice heat capacity would not agree with that calculated from elastic constants either in this work or any other. Furthermore, the whole frequency spectrum cannot shift in the same way or a large latent heat would be observed associated with the discontinuity in elastic constants at the zero-field transition.

---

[1] C. A. Bryant and P. H. Keesom, Phys. Rev. Letters 4, 460 (1960).

[2] J. G. Daunt and J. L. Olsen, Phys. Rev. Letters 6, 267 (1961).

9. APPARATUS FOR CALORIMETRY BELOW 0.1 °K

Norman E. Phillips and H. Roger O'Neal

Apparatus has been constructed in which a spherical single crystal of cerium magnesium nitrate is used as a thermometer and a different paramagnetic salt is used as a refrigerant. This makes possible accurate temperature measurements down at least to 0.01°K without imposing any restrictions on the choice of cooling salt except those relating to its efficiency. At present, measurements have been limited to above 0.08°K by the relatively low magnetic field available in the apparatus, but preliminary measurements suggest that it will be feasible to extend the measurements to appreciably lower temperatures. In particular, it has been possible to obtain thermal equilibrium between the carbon thermometer on the sample and the cerium magnesium nitrate crystal in less than a minute. Heat capacity measurements have been made on copper and on potassium bromide (chosen for the small magnitude and third-power temperature dependence of its heat capacity), and they agree to within 1% with the values obtained by extrapolation of measurements at higher temperatures. Heat capacity measurements have also been made on the material used in the heater wire.

10. CALORIMETRIC STUDIES OF THE SUPERCONDUCTING TRANSITION

Norman E. Phillips and Hanna Zainal

In order to put an upper limit to the width of the superconducting transition and to the latent heat at the zero-field transition, detailed calorimetric studies have been started in the immediate vicinity of T_c. At present the measurements are limited by the residual heat input to the sample and by incomplete compensation of stray magnetic fields. The transition in aluminum has been shown to be 95% complete within 10^{-4}°K.

11. RESEARCH IN PROGRESS--PHILLIPS

1. Apparatus for magnetic susceptibility measurements in the Low-Temperature Laboratory 100-kilo-oersted magnets has been partially completed. The apparatus will be used for studies on the critical field of antiferromagnets.

2. The critical field of indium isotopes is being investigated in connection with the relation between the isotopic similarity principle for superconductors and the lattice heat capacity.

3. Apparatus for heat capacity measurements at temperatures below 0.1°K is being developed. The present apparatus using two paramagnetic salts will be improved by increasing the magnetic field available and by more effective vibration isolation.

4. Work has been started on nuclear cooling experiments.

5. A number of low-temperature calorimetric studies are being continued: lattice and electronic heat capacity of superconductors, ferromagnetic superconductors, ferromagnets, antiferromagnets, and normal metals.

C. REACTION KINETICS

1. THE KINGDON CAGE AS A MOLECULAR BEAM DETECTOR

Philip R. Brooks and Dudley R. Herschbach

Studies of molecular beam scattering at thermal energies have mostly been confined to beams of alkali metals and their compounds, since these can be readily detected by surface ionization. In order to carry out measurements of collision cross sections for other molecules, we have constructed a space-charge detector,[1] or "Kingdon Cage," similar to that described by Estermann and Stern in 1933.[2] In principle this detector should be capable of detecting any ionizable species, although it has previously been used only to measure the ionization potentials of a few molecules.[3]

The operation of the detector is based on neutralizing part of the space charge in a diode by positive ions formed from the beam.[4] The design aims to maximize this effect. A closed nickel cylinder forms the anode. Coaxial with it is a tungsten cathode, a hot filament which passes through small holes in the ends of the cylinder. At the periphery of one circular end cap is a small hole to admit the beam. A second, identical diode, isolated from the beam, is used in order to balance out contributions from the background gas. The filaments of the two diodes are connected in parallel and heated from the same source to compensate for fluctuations in the heating current. The difference in the plate currents of the two diodes is the measured detector signal.

A molecular beam entering the detector is ionized if the anode potential is greater than a minimum "appearance potential." The positive ions formed from the beam must discharge to the very thin cathode some distance away. Since the initial velocity of these ions is almost parallel to the cathode, a much longer time is required for a positive ion to discharge to the cathode than for an electron to discharge to the anode. Another factor that prolongs the lifetime of the positive ions is that the point of minimum potential occurs some distance away from the cathode filament, so that the positive ions are trapped in a potential well and form a cylindrical sheath coaxial with the filament. When the diode is operated in the region of space-charge-limited emission, the partial neutralization of the electron space charge by the positive ions produces an increase in the plate current that is several orders of magnitude greater than that due to the positive ion current alone. The amplification factor is essentially just the ratio of the lifetime of a positive ion to that of an electron.

---

[1] P. R. Brooks and D. R. Herschbach, Bull. Am. Phys. Soc. 6, 513 (1961).

[2] I. Estermann and O. Stern, Z. Physik 85, 135 (1933).

[3] T. N. Jewitt, Phys. Rev. 46, 616 (1934).

[4] K. H. Kingdon, Phys. Rev. 21, 408 (1923).

A plot of the signal (difference in plate currents for the two diodes) versus anode bias is shown in Fig. IC. 1-1 for a methyl iodide beam. It is seen that above the appearance potential the beam begins to be ionized and produces an increase in the plate current, which increases with the bias voltage. At sufficiently high voltages, however, the diode begins to operate in the emission-limited region. Here the anode collects all the electrons emitted by the filament. As a result the positive ions are not able to increase the plate current, and the difference signal declines again.

The largest signal thus far observed, 400 μamp, was produced by a methyl iodide beam, with the bias at 13 v and the filament temperature about 2400°K. The intensity of the beam entering the detector, as calculated from the source pressure and slit geometry, was about 10^{11} molecules/sec; this beam would produce a positive ion current of 2×10^{-8} amp if every beam molecule were ionized. The amplification of the observed signal is therefore about 2×10^{4}, which is close to the estimate of the ratio of positive ion lifetime to electron lifetime given by Varney.[5]

For measurements of collision cross sections, it is necessary to determine the variation of detector signal with beam intensity. This has been studied by varying the pressure of the beam source. Figure IC. 1-2 shows typical results for methyl iodide, ethane, and n-heptane. The signal decreases roughly as the square of the beam intensity. Since the relationship appears to be quantitative for a given molecule, the detector will be suitable for scattering measurements.

A study of the sensitivity of the detector as a function of the molecular weight and ionization potential of the beam species is in progress. In addition to the three compounds shown in Fig. IC. 1-2, nitrogen and nitric oxide have been detected, but both these compounds exhibit an effect opposite to that expected from destruction of space charge: under certain conditions, they poison the emission. A possible explanation is suggested by other data, which show that bombardment of a tungsten filament with positive nitrogen or oxygen ions raises the effective work function of the filament.[6]

---

[5] R. N. Varney, Phys. Rev. 47, 483 (1935).

[6] S. Dushman, Revs. Modern Phys. 2, 381 (1930).

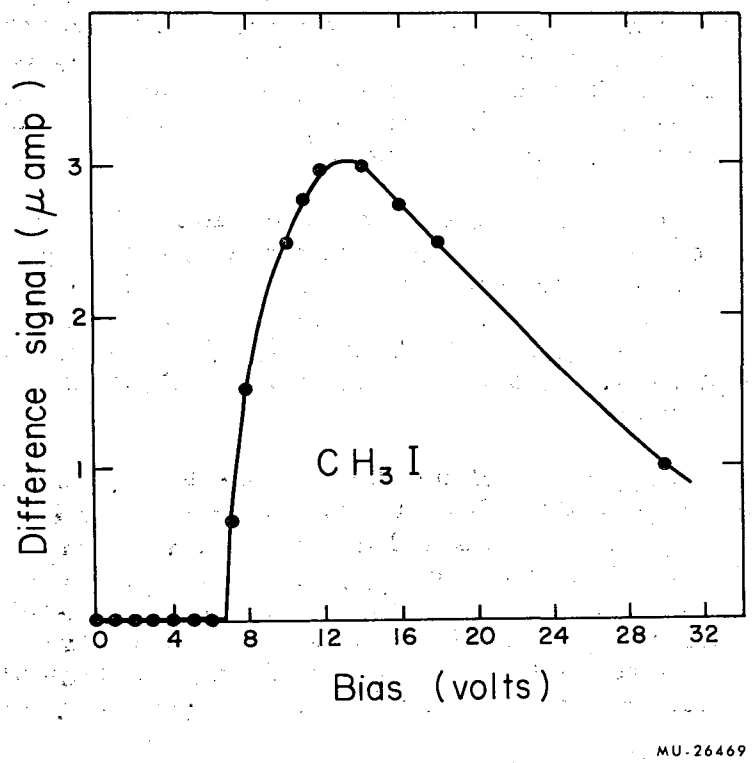

Fig. IC. 1-1. Signal as a function of anode bias for CH_3I beam.

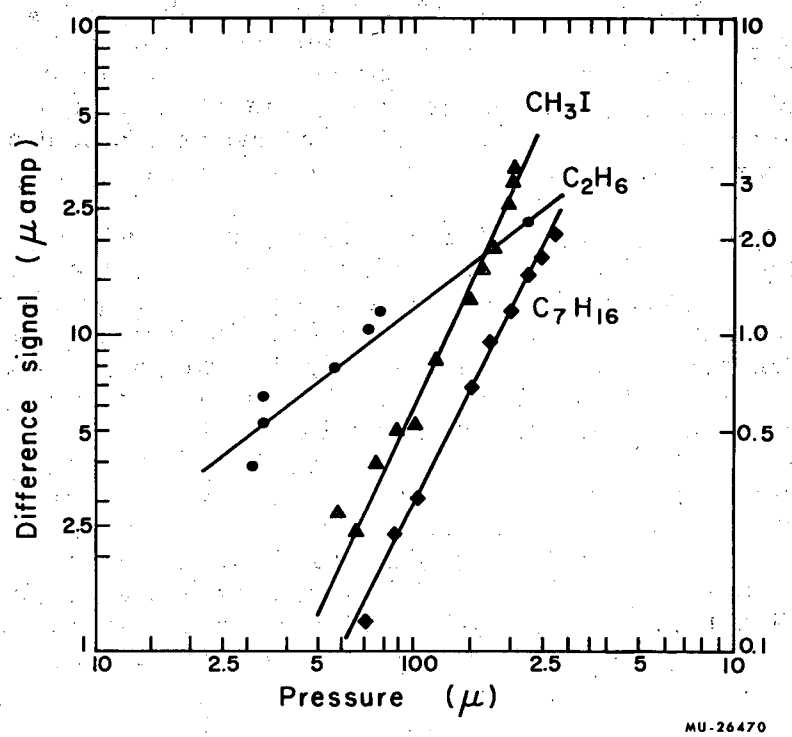

Fig. IC. 1-2. Signal as a function of beam intensity for CH_3I.

2. INFLUENCE OF VIBRATIONS ON MOLECULAR STRUCTURE DETERMINATIONS

Dudley R. Herschbach and Victor W. Laurie

Spectroscopic experiments yield effective moments of inertia which contain contributions from vibration-rotation interactions. For polyatomic molecules, the corrections rarely can be determined experimentally, and a molecular structure derived from the effective moments has no simple relation either to the equilibrium structure or to the average structure determined by diffraction methods. Previous theoretical treatments of vibration-rotation interaction have provided a perturbation expansion about the equilibrium configuration.[1] However, the most important correction terms involve the anharmonic part of the vibrational potential,[2] which seldom is known with sufficient accuracy to permit useful calculations.

A more general treatment has been derived in which the perturbation expansion may be referred to any arbitrarily chosen, fixed configuration of the atoms.[3] From this it is found that to a practical approximation the entire effect of anharmonicity is absorbed in displacing the average from the equilibrium configuration. Hence only the harmonic part of the vibraional potential is needed to correct observed effective moments of inertia to those for the average structure of a molecule.

This formulation has been used to calculate the average structural parameters for the ground vibrational state of several molecules, including CO_2, CS_2, H_2O, SO_2, O_3, NO_2, CH_4, and HCN. It is found that bond lengths involving H atoms are 0.003 to 0.005 Å longer than the corresponding D atom bond. For bonds involving heavier elements isotopic differences are smaller, but still have a significant effect on structure determinations.

---

[1] Extensive reviews have been given by H. H. Nielsen, Revs. Modern Phys. 23, 90 (1951); Hanbuch der Physik 37, 173 (Springer-Verlag, Berlin, 1959).

[2] D. R. Herschbach and V. W. Laurie, Bull. Am. Phys. Soc. 5, 500 (1960).

[3] Dudley R. Herschbach and Victor W. Laurie, Influence of Vibrations on Molecular Structure Determinations. I. General Formulation of Vibration-Rotation Interactions. (UCRL-10006, March 1962), to be submitted to J. Chem. Phys.

---

3. ANHARMONIC POTENTIAL CONSTANTS AND THEIR DEPENDENCE UPON BOND LENGTH

Dudley R. Herschbach and Victor W. Laurie

An empirical study of cubic and quartic vibrational force constants for diatomic molecules has shown them to be approximately exponential functions

of internuclear distance.[1] A family of curves has been obtained, determined by the location of the bonded atoms in rows of the periodic table. Displacements between successive curves correspond closely to those in Badger's rule for quadratic force constants (for which the parameters have been redetermined to accord with all data now available).[2] Constants for excited electronic and ionic states appear on practically the same curves as those for the ground states. Predictions based on the diatomic correlations agree with the available cubic constants for bond stretching in polyatomic molecules, regardless of the type of bonding involved.

In the course of this study an extensive table of vibrational force constants has been prepared.[3] This includes data for all well established electronic states for which vibrational and rotational parameters have been determined.

[1] D. R. Herschbach and V. W. Laurie, J. Chem. Phys. 35, 458 (1961).

[2] R. M. Badger, J. Chem. Phys. 2, 128 (1934); 3, 710 (1935).

[3] D. R. Herschbach and V. W. Laurie, Table of Vibrational Force Constants, UCRL-9694, July 1961.

4. REACTIVE SCATTERING IN CROSSED MOLECULAR BEAMS. REACTIONS OF RUBIDIUM AND CESIUM ATOMS WITH ALKYL IODIDES

James L. Kinsey, George H. Kwei, and Dudley R. Herschbach

From previous crossed-beam studies of the reactions of K atoms with alkyl iodides,[1] it was concluded that the angular distribution of products in the center-of-mass coordinate system is strongly peaked along the direction of the initial relative velocity vector, and that most of the energy of reaction appears as internal excitation of the products. Similar studies of the reactions of Rb and Cs atoms with CH_3I and C_2H_5I have now been carried out.[2, 3, 4] The same qualitative features are found to hold for these reactions, and the activation energies are again negligibly small. Figures IC. 4-1 and IC. 4-2 show results of typical runs for the reactions of Rb and Cs with

[1] D. R. Herschbach, G. H. Kwei, and J. A. Norris, J. Chem. Phys. 34, 1842 (1961).

[2] J. L. Kinsey, G. H. Kwei, and D. R. Herschbach, Bull. Am. Phys. Soc. 6, 152 (1961).

[3] G. H. Kwei, J. A. Norris, J. L. Kinsey, and D. R. Herschbach, in International Conference on the Physics of Electronic and Atomic Collisions (W. A. Benjamin, Inc., New York, 1961), Vol. 2, p. 98.

[4] A review of the crossed-beam work at Berkeley has been given by D. R. Herschbach, Chemical Reactions in Crossed Molecular Beams, The Vortex 22, 348 (1961) (UCRL-9801, July 1961).

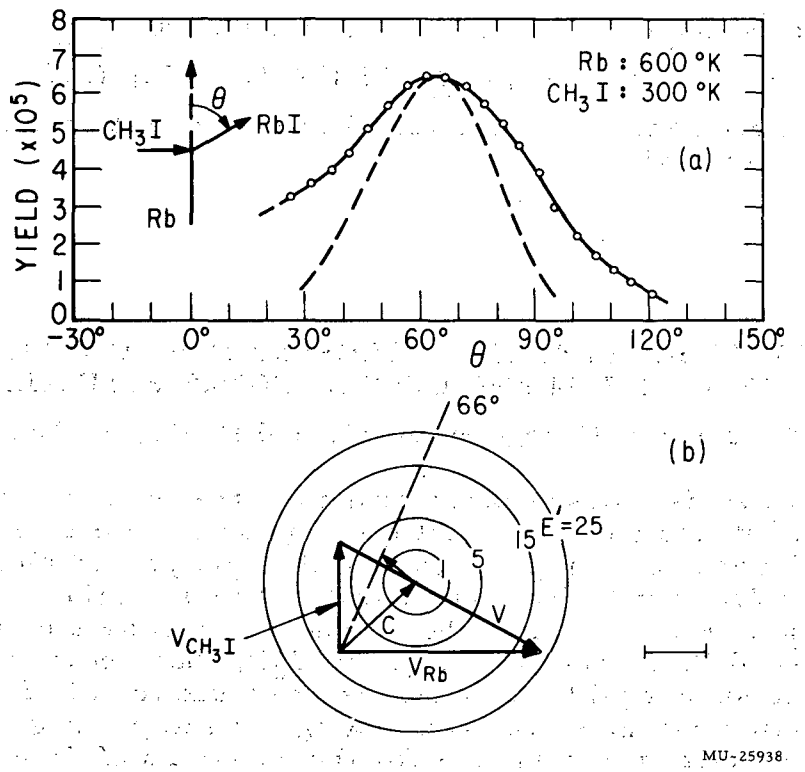

Fig. IC.4-1. Results from reaction of Rb atoms with CH_3I.

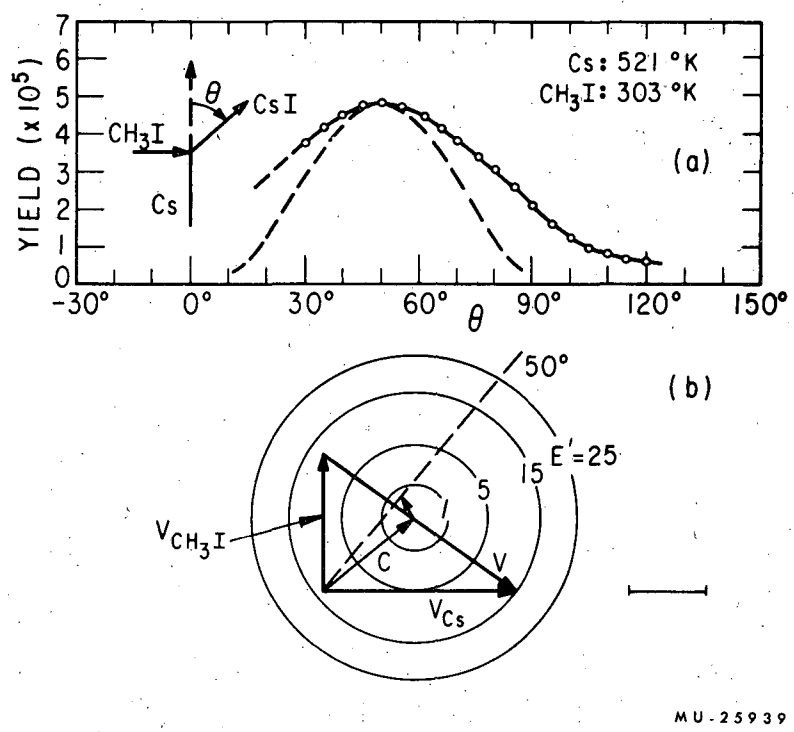

Fig. IC. 4-2. Results of reaction of Cs atoms with CH_3I.

with CH_3I. The dashed curves are calculated on the following basis: The recoil velocity vector of the alkali halide was assumed to come off "backwards" along the direction of the initial relative velocity vector $\vec{v}$. The magnitude of the recoil vector chosen was such that it would produce scattering at the peak of the observed laboratory-system angular distribution for the most probable velocities in the reactant beams (see vector diagrams in Figs. IC. 4-1 and IC. 4-2.) An average over the Maxwellian velocity distributions in the reactant beams was then carried out to estimate the width of the angular distribution.[5] The total energy available to the reaction products is about 25 kcal/mole (the initial energy of the reactants plus the difference in the M-I and C-I bond dissociation energies), but only about 2.0 kcal/mole goes into the translational energy of separation of the products in the Rb+CH_3I reaction, and only 0.7 kcal/mole in the Cs reaction (compared with 2.7 kcal/mole for the K reaction).

[5] S. Datz, D. R. Herschbach, and E. H. Taylor, J. Chem. Phys. 35, 1549 (1961).

5. REACTIVE SCATTERING IN CROSSED MOLECULAR BEAMS. REACTIONS OF POTASSIUM ATOMS WITH ALKYL IODIDES

James A. Norris, George H. Kwei, and Dudley R. Herschbach

The crossed-beam study of the reaction of K with CH_3I previously reported[1] has been extended to other alkyl iodides, and further details of the reactive scattering have been established.

The temperature dependence of the yield of KI has been measured for the CH_3I and C_2H_5I reactions. Typical results are shown in Fig. IC. 5-1. For both reactions, the yield is practically independent of temperature and indicates that the activation energy is negligible, less than 0.3 kcal/mole.

The analysis of the angular distribution of KI[1] has been confirmed by experiments in which the angle of intersection of the reactant beams is varied. It is found that the KI peak shifts to 68° and to 129° for intersection angles of 60° and 135°, respectively. This is in agreement with the predictions derived from the original analysis (based on data for a 90° intersection, as in Fig. IC. 5-1).

The data shown in Fig. IC. 5-2 have established that the product distribution is not symmetrical with respect to a plane perpendicular to the initial relative velocity vector. Such symmetry is a characteristic feature of any theoretical model which postulates that the collision complex persists

[1] D. R. Herschbach, G. H. Kwei, and J. A. Norris, J. Chem. Phys. 34, 1842 (1961).

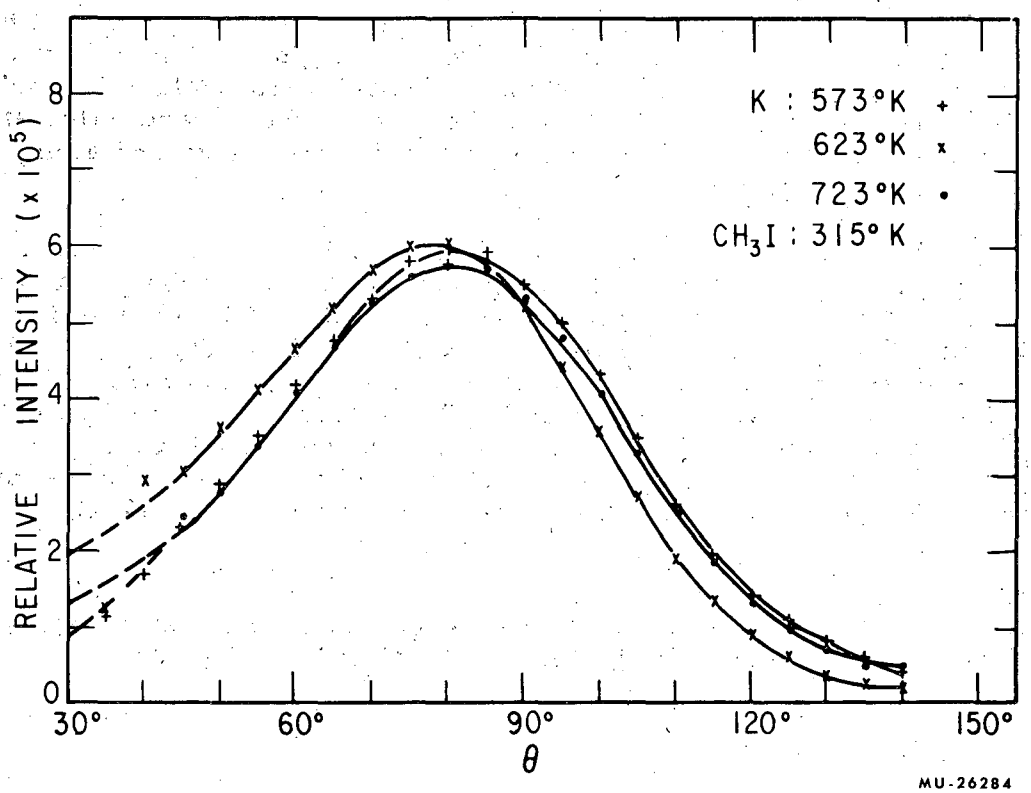

Fig. IC. 5-1. Results of reaction of K with CH_3I in crossed molecular beams.

long enough to ensure the decay of phase relations associated with the formation of the complex.[2] The vector diagrams at the bottom of Fig. IC. 5-2 show the most probable velocities in the colliding beams, the center-of-mass velocity vector c, and the relative velocity vector v. The spheres drawn about the tip of c indicate the possible spectrum of KI recoil vectors allowed by the conservation laws. As indicated, each sphere corresponds to a particular relative translational energy of the products, which can range up to a maximum of 25 kcal/mole (the difference in dissociation energies of the K-I and C-I bonds). The earlier work showed that most of the KI recoil velocity vectors which contribute to the observed wide angle peak are quite short, and oriented "backwards" along v.[1] However, the question of a possible peak at low angles, corresponding to recoil vectors "forward" along v, was left open; the large background of elastic scattering near the parent K beam makes difficult the observation of such a peak. Although we still cannot rule out a forward peak, Fig. IC. 5-2 shows that if present it must be considerably less intense than the backward peak. This is seen by comparison of the data with the dashed curves, which were calculated by assuming equal intensity of scattering forward and backward along v, as indicated in the vector diagrams.

Angular distributions have also been measured (at 90° intersection) for the reactions of K atoms with i-propyl, n-propyl, n-butyl, and n-amyl iodides. Under conditions similar to those of Fig. IC. 5-1 it is found that all these reactions have KI peaks in the neighborhood of 90°. This indicates that the average relative translational energy of the products decreases as the mass of the R group is increased. The decrease in energy is roughly linear, from 2.7 kcal/mole for CH_3 to 0.5 kcal/mole for C_5H_{11}. There is no noticeable effect from "steric interference" as the R group becomes larger; the collision yield remains about the same as for the CH_3I reaction.

[2] J. A. Norris, G. H. Kwei, J. L. Kinsey, and D. R. Herschbach, Bull. Am. Phys. Soc. 6, 339 (1961); Rev. mex. fis. 10, 19 (1961).

6. RESEARCH IN PROGRESS--HERSCHBACH

1. An inhomogeneous electric deflecting field has been constructed. It will be used in an attempt to measure the distribution of rotational states of the product KBr in the reaction

$$K + HBr \rightarrow H + KBr$$

and analogous reactions. If successful, the experiment should provide a critical test of theoretical models which predict the angular momentum distribution in reactions.

2. J. L. Kinsey is studying the reactions of hydrogen atoms with alkali halides,

$$H + MX \rightarrow M + HX.$$

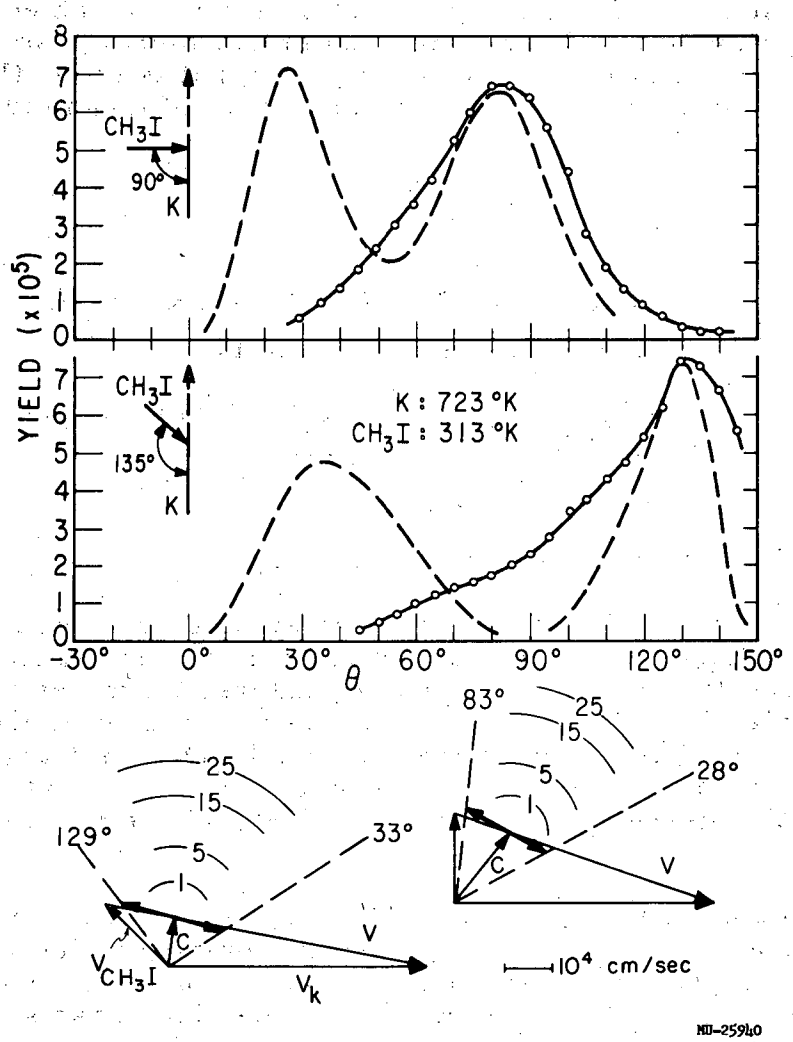

Fig. IC. 5-2. Product distribution from reaction of K with CH_3I.

Again, these reactions are of particular interest for a test of theoretical predictions concerning the role of angular momentum.

3. G. H. Kwei has completed a new crossed-beam apparatus which incorporates a toothed-wheel velocity selector. This will be used to measure the energy dependence of both elastic and reactive scattering.

4. K. R. Wilson is building a new detection system which employs phase-sensitive detection of a modulated molecular beam and mass analysis of the ions produced by surface ionization of the beam; it is hoped that this will improve the detection sensitivity by three orders of magnitude.

7. THE PHOTOIONIZATION OF NITRIC OXIDE*

John P. Doering and Bruce H. Mahan

Nitric oxide was photoionized with 1236-A (9.9-ev) photons, and the rate of the dissociative recombination reaction

$$NO^+ + e \rightarrow N + O \qquad (1)$$

was measured. Two methods were used.

In the first method, the rate of ionization, q, was measured by applying a high voltage to electrodes contained in the ionization cell. The maximum current drawn was limited by, and was therefore a measure of, the rate of ionization. The high voltage was then removed and the steady-state concentration of charges was measured by using a Langmuir-type probe. The value of α, the dissociative recombination rate constant, was then calculated from the steady-state relation $q = \alpha n^2$, where n is the charge concentration.

In the second method, the rate of decay of the charge concentration was measured as a function of time after the ionizing radiation had been extinguished. These measurements indicate that α is between 5×10^{-7} and 2×10^{-6} cc/ion sec. This corresponds to a reaction cross section of approximately 10^{-11} cm^2, which is very nearly the square of the de Broglie wave length of the electron. This indicates that there are few quantum restrictions on the dissociative recombination process.

*Short version of paper to be published in J. Chem. Phys.

8. RESEARCH IN PROGRESS--MAHAN

1. An apparatus which will measure the concentration of electrons in ionized gases by using microwave cavity resonance is being built. This, combined with our probe technique which measures only ion concentration, will allow us to study electron attachment processes such as

$$O_2 + e + M \rightarrow O_2^- + M.$$

2. The rates of charge exchange between ions are being measured. The reactions

$$NO^+ + NO^- \rightarrow 2\ NO,$$

$$NO^+ + O_2^- \rightarrow NO + O_2,$$

$$I^+ + I^- \rightarrow 2I$$

are currently being investigated. Although charge exchange appears to be a bimolecular process, the reaction is actually of third order. The role of the third body appears to be to remove angular momentum from the ion pair so that they may approach close enough to transfer an electron.

9. THE ANALYSIS OF HYDROGEN ATOM CONCENTRATIONS IN A CHEMICALLY REACTING SYSTEM BY MEANS OF PARAMAGNETIC RESONANCE ABSORPTION

Norman E. Edelstein and Rollie J. Myers

In many of the important high-temperature and free-radical systems hydrogen atoms play a key role in their reaction mechanisms. The most prominent of these systems is probably the gas-phase reaction of hydrogen and oxygen.

The paramagnetic resonance spectrum of hydrogen atoms falls outside the range of almost all other free radicals, and it is a strong enough absorption so that 0.01 mm of hydrogen atoms can be measured in a system with a total pressure of 1 mm. This method of analysis does not perturb the system and measurements can be easily made on a reaction mixture as it flows down a plain quartz tube. As the result of some previous microwave measurements,[1] we were particularly interested in the low-pressure reaction of hydrogen atoms with oxygen molecules, and we have followed the decay of the hydrogen atom concentration in such a system. We have also studied this decay in the presence of nearly pure hydrogen.

[1] For a review of previous work on this reaction see Richard T. Meyer, Free-Radical Microwave Spectroscopy. I. The Dipole Moment and Kinetics of Hydroxyl Radicals. II. Apparatus for Continuous Ultraviolet Photolysis (Ph. D. Thesis), University of California, Berkeley, 1961.

The reaction was studied in the pressure range of 0.1 mm Hg to 0.8 mm Hg. H atoms produced in a microwave discharge were pumped into a mixing section where O_2 or a third body could be added. Then this mixture was pumped through a cylindrical quartz tube which passed through the detection cavity of an electron spin resonance (ESR) spectrometer. The discharge in hydrogen, separated from the mixing section by a diaphragm with a 1-mm-diam hole, was produced by a 100-watt magnetron operating at 10 cm^2. Hydrogen saturated with water was used because the percentage dissociation of the H_2 increases with the addition of water. The amount of dissociation was approximately 10% to 20%. The quartz reaction tube was about 120 cm long. Runs were made with tubes of two different diameters, the larger one approximately 0.92 cm, the other approximately 0.72 cm. The discharge apparatus, the flow system, and the reaction tube were mounted on a movable cart which rode on rails. They could be moved a total distance of 80 cm. Measurements were usually made every 10 cm along the tube. The volume flow of H_2 down the tube was on the order of 5 to 10 cm^3/min at 1 atm pressure, and the linear flow of H_2 at the partial pressure of H_2 in the low-pressure section of the tube was on the order of 200 to 400 cm/sec.

A number of measurements were made on the recombination of H atoms in pure H_2. The reaction appeared to be zero-order with respect to H atoms. At very low H atom concentrations the reaction became first-order. If the recombination of H atoms were a homogeneous gas-phase reaction, the reaction would be second-order in H atoms. For a heterogeneous surface reaction the order would be less than two. Coating the quartz tube with phosphoric acid or dichloro-dimethyl silane did not affect this reaction.

The rate of decay of hydrogen atoms increased with the addition of O_2. Runs were made with the partial pressure of O_2 varying from 0.05 mm Hg to 0.3 mm Hg. At the higher O_2 concentrations the reaction appeared to be first-order with respect to H atoms. At the lower O_2 concentrations the order of the reaction was between first and zero. Some measurements were made with the tube of smaller diameter. The rate of reaction of H atoms plus O_2 was faster than in the larger tube. Qualitatively, the rate of decay of H atoms seems to be directly proportional to the concentration of H atoms and to the concentration of O_2, and inversely proportional to the total pressure. The half life of the H atoms for the first-order reaction is on the order of 0.1 sec. At low O_2 concentrations there are two competing reactions. One is the zero-order recombination of H atoms on the walls, the other is the first-order reaction of H atoms plus O_2. Then a combination of these two reactions would appear to be between first and zero order.

A possible mechanism to explain the observed dependence on total pressure, partial pressure of the H atoms, and partial pressure of O_2, and also the increase of the rate of decay of H atoms with an increase in the surface to volume ratio, is

$$H + O_2 \xrightarrow{k_1} HO_2^*,$$

$$HO_2^* \xrightarrow{k_2} H + O_2,$$

$$HO_2^* + \text{Wall} \xrightarrow{k_3} HO_2 + \text{Wall}.$$

Assuming steady-state conditions for HO_2^*, i.e.,

$$\frac{d(HO_2)^*}{dt} \approx 0, \text{ and } k_2 >> k_3, \text{ then}$$

$$\frac{-d(H)}{dt} = k_1 (H)(O_2) \left[\frac{k_3}{k_2} \right],$$

where at moderately low pressures, k_3 is proportional to the surface to volume ratio and inversely proportional to pressure. Other mechanisms can be written but the above is one of the simplest.

Further work is in progress to obtain more quantitative results and to learn more about the heterogeneous nature of these reactions.

[2] T. M. Shaw, J. Chem. Phys. 31, 1142 (1959).

10. RESEARCH IN PROGRESS--MYERS

a. Paramagnetic Relaxation of Transition-Metal Ions in Solution

The electron spin of some transition-metal ions is coupled very weakly with the solvent molecules in a solution. In these cases relatively sharp paramagnetic resonance absorption signals can be observed. By utilizing the saturation of the observed signals with high microwave power we plan to study spin relaxation. This can be applied to Mu^{++}, Cr^{+++}, and their complexes in aqueous solution. It might be also possible to study these ions in molten salt solutions.

b. Paramagnetic Resonance of Free Radicals

Many free radicals have been detected by paramagnetic resonance. The NF_2 radical can be found from the dissociation of N_2F_4, and we hope to detect the SF_3 radical by similar methods. We plan to measure the rates of some atomic reactions in the gas phase and in flow systems. We also plan to detect some new inorganic and organic free radicals.

D. INORGANIC CHEMISTRY

1. THE NMR RELAXATION MECHANISMS OF O^{17} IN AQUEOUS SOLUTIONS OF PARAMAGNETIC CATIONS, AND THE LIFETIME OF WATER MOLECULES IN THE FIRST COORDINATION SPHERE

Robert E. Connick and Terry J. Swift

The effect of paramagnetic cations on the transverse relaxation time of O^{17} in nuclear magnetic resonance studies of water has been reported previously.[1,2] Lower limits were obtained for the first-order rate constants which govern the water-exchange process between the bulk of the solution and the first coordination sphere of the cations.

In this work the temperature and frequency dependences of the relaxation were used to yield rate constants and activation energies for the exchange of water molecules between the bulk of the solutions and the first coordination sphere of Mn^{+2}, Fe^{+2}, Co^{+2}, Ni^{+2}, and Cu^{+2}. In some cases, electronic T_1's and coupling constants were also obtained.

The Bloch equations, modified by McConnell to include the possibility of chemical exchange,[3] were applied to the limiting conditions present in a dilute aqueous solution of paramagnetic ions. Virtually all of the temperature and frequency effects predicted by the modified Bloch equations for a two-species system were verified experimentally.

Evidence was found for a Co^{+2} species with coordination number less than 6 (perhaps tetrahedral) in aqueous solutions near 100°C. The data for Cu^{+2} were interpreted in terms of six coordinated water molecules in a distorted octahedron, with a ratio of about 10^5 for the axial water-exchange rate over that of the equatorial water.

The observed activation energies and rate constants for water exchange are given in Table I.

---

[1] R. E. Connick and R. E. Poulson, J. Chem. Phys. 30, 759, (1959).

[2] R. E. Connick and E. D. Stover, J. Phys. Chem. 65, 2075 (1961).

[3] H. M. McConnell, J. Chem. Phys. 28, 430 (1958).

Table I. Parameters for exchange of O between the first coodination sphere of Mn^{+2}, Fe^{+2}, Co^{+2}, Ni^{+2}, and Cu^{+2} and bulk water.

Ion	Quantity	Value
Mn^{+2}	A[a]	8.1
	B	3.1×10^7
Fe^{+2}	A	7.7
	B	3.2×10^6
Co^{+2}	A	8.0
	B	1.13×10^6
Ni^{+2}	A	11.6
	B	2.7×10^4
Cu^{+2} (axial)	A	5
	B	2×10^8
Cu^{+2} (equat.)	A	11
	B	1.0×10^4

a. $A = \Delta H^{\ddagger}$ (kcal),

$B = k_1$ (sec^{-1} at 298°K).

2. HYDROLYSIS AND POLYMERIZATION IN SOLUTIONS OF CHROMIC ION

Sister Gertrude Thompson and Robert E. Connick

Previous researchers have isolated three chromium species from refluxed chromic nitrate and perchlorate solutions by means of ion-exchange techniques.[1,2] These species have been tentatively identified as follows: a purple species as the monomer, Cr^{3+}; a blue species as the dimer, $Cr_2(OH)_2^{4+}$ or Cr_2O^{4+}; and a green species as the trimer, $Cr_3(OH)_4^{5+}$ or $Cr_3O_2^{5+}$. The spectra of these three species have been rechecked, and the values determined for the absorbance per mole of Cr at the maxima are:
purple species, 575 mμ, 13.1, and 408 mμ, 15.3;
blue species, 580 mμ, 17.3, and 416 mμ, 20.3;
green species, 582 mμ, 18.3, and 424 mμ, 29.4.
These values are in good agreement with those reported by Finholt[1] for the polynuclear species. The agreement indicates a possible error in chromium analysis as an explanation for the deviation of Laswick and Plane's values[2] from those reported here. The blue species was also prepared in larger quantities by rapidly passing a stream of oxygen through a chromous solution, as reported by Ardon and Plane,[3] and gave spectra identical with those for the species isolated from refluxed solutions.

Equilibrium studies of the hydrolysis of the monomeric species are now feasible using ion exchange for the analysis. The cation exchanger, Dowex AG 50W-X2, 200–400 mesh, is used to absorb the refluxed chromium. Calcium perchlorate has been found to displace the purple species and elute the blue and green species from this resin. The separation of the species is complete and can be accomplished in a short time. Establishment of the equilibrium constants will be used to verify the dimeric character of the blue species[1,4] and to establish whether the green species is a trimer.

Rate studies are being conducted on the decomposition of the green species in strongly acidic solutions. This species was isolated by displacement elution from a resin of the same cross linkage, but lower mesh size, by thorium perchlorate solutions. Rate studies will also be run on the decomposition of the blue species in acid solutions of varying concentrations.

---

[1] James E. Finhold, Chemistry of Some Hydrolyzed Cr(III) Polymers (Thesis), UCRL-8879, April 1960.

[2] J. A. Laswick and R. A. Plane, J. Am. Chem. Soc. 81, 3564 (1959).

[3] M. Ardon and R. A. Plane, J. Am. Chem. Soc. 81, 3197 (1959).

[4] M. Ardon and Linenberg, J. Phys. Chem. 65, 1443 (1961).

3. RATES OF INTERCONVERSION OF THE CHLORIDE COMPLEXES OF RUTHENIUM(III)

Edward E. Mercer,† Robert A. Hasty, and Robert E. Connick

The identification of the chloride complexes of ruthenium(III) was discussed in the preceding annual report, and an additional paper has been published.[1] Work has been begun on the measurement of the rates of interconversion of these species, and values of the rate constants have been obtained for certain cases.

The kinetics of the decomposition of the two neutral species, cis and trans $RuCl_3$, have been studied in detail. The reactions are first-order in the ruthenium species and independent of the hydrogen ion and chloride ion concentrations in approximately 0.1 M HCl. The first-order rate constants at 25°C are given below:

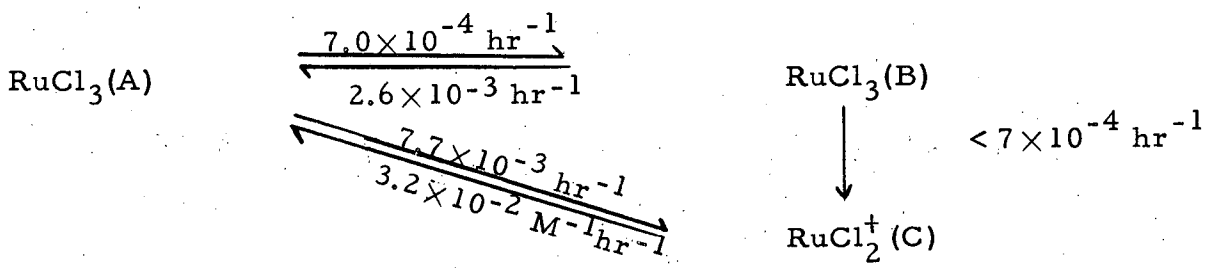

The isomerization reaction between the two neutral species is also acid- and chloride-independent. No decomposition of $RuCl_3(B)$ directly to $RuCl_2^+(C)$ was detected, and an upper limit to the rate constant is given. Also no decomposition to $RuCl_2^+(T)$ was observed. The second-order rate constants for the back reactions have been calculated from the forward rates and the equilibrium constants.

At present the rates of interconversion of $RuCl_6^{\equiv}$, $RuCl_5^{=}$, and the two $RuCl_4^-$ complexes are being examined. The $RuCl_4^-$ species are separated by using the chloride form of Dowex-1 resin. A modification of the "injection method" described by Below[2] is employed to mix the solutions and to follow the optical density at a selected wavelength of the reacting mixture with respect to time.

---

†Now at Chemistry Department, University of South Carolina, Columbia, South Carolina.

[1] R. E. Connick and D. A. Fine, J. Am. Chem. Soc. 83, 3414 (1961).

[2] John F. Below, Jr., Rapid Reactions: Kinetics of the Formation of the Ferric Thiocyanate Complex (Thesis), UCRL-3011, June 1955.

4. RESEARCH IN PROGRESS--CONNICK

1. Nuclear magnetic resonance studies of the lifetimes of water molecules in the first coordination spheres of metal ions will be extended to other cations. It is hoped that by modification of the apparatus the accessible temperature range can be expanded to include higher temperatures. Such measurements would hlep to clarify the reactions occurring with Cu^{++} and Co^{++}. The effect of complexing on the rates will be studied also.

2. Determination of the rates of interconversions of Ru(III) chloride complexes will be continued.

3. The equilibria between the various hydrolyzed and polymerized chromic species will be studied in order to fix the formulas of species and to ascertain stabilities. Attention will be focused on the green species, as it is not yet known whether it contains more than one component.

5. DIGERMANIUM HEXACHLORIDE OBTAINED BY ELECTRIC DISCHARGE METHODS

William L. Jolly and Richard W. Kopp

Only two reports concerning the synthesis of Ge_2Cl_6 appear in the literature. In the first, by Schwarz and Baronetsky in 1954, the synthesis was accomplished by passing $GeCl_4$ vapor over germanium metal at about 340°.[1] Yields of roughly 10 to 20 mg in 4 to 5 weeks are reported. The second mention of this compound was by Shriver and Jolly in 1958.[2] They succeeded in obtaining yields of 250 mg per hour by passing $GeCl_4$ vapor through a microwave discharge, resulting in the reaction

$$2\ GeCl_4 = Ge_2Cl_6 + Cl_2.$$

The work reported here was undertaken to extend this latter investigation, using other electric discharge methods, to improve the yields, and ultimately to study the chemistry of this new and interesting compound.

The apparatus used by Shriver and Jolly has been modified to allow a "semi-automatic" operation. The $GeCl_4$ may be recycled indefinitely through the discharge zone. Since only a small percentage of the $GeCl_4$ is decomposed per pass, this is a great advantage.

---

[1] R. Schwarz and E. Baronetsky, Z. anorg. allgem. Chem. 275, 1 (1954).

[2] D. Shriver and W. L. Jolly, J. Am. Chem. Soc. 80, 6692 (1958).

A solenoid discharge, which consisted of a copper coil around the cylindrical reaction tube, was used initially. The discharge source was a 50-Mc radio-frequency oscillator with a 2.5-kv 500-ma power supply. When a flow rate of about 0.6 g per minute was used, less than 1% of the $GeCl_4$ decomposed, with about 25 mole % of this forming Ge_2Cl_6, the remainder forming $GeCl_2$ and $(GeCl)_x$. This gave a yield of about 60 mg of Ge_2Cl_6 per hour.

A plug of copper wool was placed in the discharge tube just past the coil to act both as a reducing agent and as an obstruction to raise the pressure and reduce the flow rate. At a flow rate of about 0.1 g per minute, more than 6% of the $GeCl_4$ decomposed, with about 50% of this being converted to Ge_2Cl_6, giving yields of about 150 mg of Ge_2Cl_6 per hour. Although chlorine was collected, some of the copper wool was oxidized to CuCl.

Because of these disappointingly low yields, it was decided to try another form of discharge, suggested by the work of Wartik.[3] The reaction tube consists of a series of separated copper wool plugs. The end plugs are connected, by means of tungsten electrodes, to a 60-cycle high-voltage line, creating a discharge between the plugs. A water jacket around the discharge tube cools the reaction tube. Here again copper acts as a reducing agent, forming CuCl. No chlorine gas is recovered with this system. Work is currently under way to determine the conditions that give the best yields. To date, for short periods of time, yields equivalent to more than 500 mg per hour have been obtained. This corresponds to a flow rate of about 0.55 g per minute, about 6.5% of the $GeCl_4$ decomposing, with about 30 mole % of this forming Ge_2Cl_6. It is expected that even higher yields can be obtained.

[3] T. Wartik, paper presented at the 138th Meeting of the American Chemical Society, New York, September 1960, Paper 55.

6. GERMANIUM HYDRIDES

William L. Jolly and John E. Drake

We have made a further study of the preparation of germanium hydrides by the slow addition of an aqueous alkaline solution of hydroborate and germanate to acids.[1,2] The ratio of BH_4^-/Ge(IV) was varied from 0.55 to 6.15, and various acids were tried. The best results were obtained with glacial acetic acid and with a BH_4^-/Ge(IV) ratio of about 3. The yields, based on the amount of germanium dioxide, were as follows: monogermane 73%, digermane 9%, and trigermane 2.5%.

[1] W. L. Jolly, J. Am. Chem. Soc., 83, 335 (1961).

[2] John E. Drake, The Preparation of Some Germanium Hydrides, UCRL-9709, May 1961.

We have converted monogermane into higher germanes by circulating it through an ozonizer-type silent electric discharge both at low pressures (about 4 cm of dibutyl phthalate) and at high pressures (up to 0.5 atm). The best results were obtained from the high-pressure system in which voltages up to 15 kv were used.[3] The discharge tube was maintained at -78° so as to collect the products, and the monogermane was circulated through the system by a Toepler pump. Digermane and trigermane were separated by distillation under a vacuum, and the other hydrides were separated by gas-liquid chromatography on a column containing 10% silicone fluid on Celite; the separation of the two isomeric tetragermanes was good at 90°. At 95 to 195° thirteen additional peaks were clearly resolved, corresponding to species up to the octagermanes. A further unresolved band undoubtedly corresponded to the nonagermanes.

Digermane was identified by its infrared spectrum and vapor pressure. The infrared spectra of trigermane, the tetragermanes, and the pentagermanes are very similar in the sodium chloride region, and hence may be used only to identify these compounds as germanium hydrides. Trigermane was principally identified by its mass spectrum and its proton magnetic resonance spectrum. The latter spectrum, like those of propane and trisilane, is characterized by a small ratio of chemical shift to spin-spin coupling constant for the protons in $-MH_2-$ and $-MH_3$ (where M = C, Si, or Ge). By a comparison with the spectrum of trisilane,[4] the resonance fields in trigermane were found to be $-GeH_3$ = 3.3 ppm and $-GeH_2-$ = 3.0 ppm lower than that of tetramethylsilane. The tetragermanes were identified by their comparative retention times on the column, their comparative abundances, and their mass spectra. The proton magnetic resonance spectrum of n-tetragermane is similar to that of n-butane in that no easily explained pattern is seen. The spectrum of isobutane consists of a series of equally spaced lines, which are presumed to be part of a series of 10, and two much stronger, equally spaced doublets caused by the splitting of the $-CH_3$ protons by the =CH- proton.[5] The spectrum of isotetragermane, which was taken in a very dilute solution of n-hexane, shows a symmetrical doublet. The expected series of ten lines caused by the splitting of the =GeH- hydrogen is presumably too weak to be seen under these circumstances. The spin-spin coupling constant, J_{GeH, GeH_3}, is 4 cps, (whereas J_{CH, CH_3} is 5 cps) at 60 Mc.

The pentagermanes were assigned on the basis of the expected relative retention times of the three isomers on the chromatographic column--i.e. we assumed that they emerge in the order neo-, iso-, and n-pentagermane. The relative yields of these isomers--based on the areas under the peaks--are remarkably close to those predicted on the basis of a statistical build-up of Ge_1, Ge_2, Ge_3, and Ge_4 units.

---

[3] J. E. Drake and W. L. Jolly, Proc. Chem. Soc. 379 (1961).

[4] J. J. Turner, Ph.D. Thesis, Kings College, Cambridge University, 1960.

[5] J. A. Pople, W. G. Schneider, and M. G. Bernstein, High Resolution Nuclear Magnetic Resonance (McGraw-Hill Book Company, New York, 1959), p. 235.

By similar arguments the four peaks of the hexagermanes have been tentatively assigned, but it is not possible to make realistic assignments for the higher germanes.

Typical yields for the hydrides, based on the amount of monogermane that was converted, were as follows: pentagermanes 0.8%, hexagermanes 0.3%, heptagermanes 0.3%, octagermanes 0.05%, and nonagermanes less than 0.01%.

7. INFRARED SPECTRA OF METAL-AMMONIA SOLUTIONS

Marvin Gold and William Jolly

The nature of the species present in moderately concentrated solutions of metals in liquid ammonia has been the subject of considerable controversy for years.[1] Two models for these solutions have been widely discussed: the electron cavity model[2, 3] and the monomer-dimer model.[4] There have been few quantitative investigations of the absorption spectra of metal-ammonia solutions, and it was felt that such a study would provide useful data for the characterization of these solutions.

The spectra were recorded with a Cary Model 14 spectrophotometer and an optical cell having a light path of 0.02 mm. The experimental details are reported elsewhere.[5]

The spectra of lithium, sodium, potassium, cesium, and calcium were recorded from 6000 to 25,000 A at concentrations from about 0.005 to 0.20 M. Up to 0.03 M the band maximum was observed, but above this concentration only the tails of the band were visible.

Concentration and Temperature Dependence of the Absorbance

In the 0.005- to 0.03-M region, the spectra are identical for all the alkali metals, and Beer's Law is obeyed at all wavelengths (see Fig. ID. 7-1a). Above 0.03 M a positive deviation of Beer's Law occurs at the long-wavelength tail of the spectrum (see Fig. ID. 7-1b), but Beer's Law is very nearly obeyed at the short-wavelength tail. Recent work on sodium and potassium solutions up to 0.004 M showed that, at the maximum, sodium obeyed Beer's Law whereas potassium exhibited a negative deviation.[6]

---

[1] W. L. Jolly, Metal Ammonia Solutions, in Progress in Inorganic Chemistry, F. A. Cotton, Editor (Interscience Publishers, Inc., New York 1959) Vol. 1.

[2] S. Freed and N. Sugarman, J. Chem. Phys. 11, 354 (1943).

[3] R. A. Ogg, J. Chem. Phys. 14, 114 (1946).

[4] E. Becker, R. H. Lindquist, and B. J. Alder, J. Chem. Phys. 25, 971 (1956).

[5] Marvin Gold and William L. Jolly, The Spectrophotometry of Metal-Ammonia Solutions at Low Temperatures, UCRL-9887, Dec. 1961.

[6] R. C. Douthit and J. L. Dye, J. Am. Chem. Soc. 82, 4472 (1960).

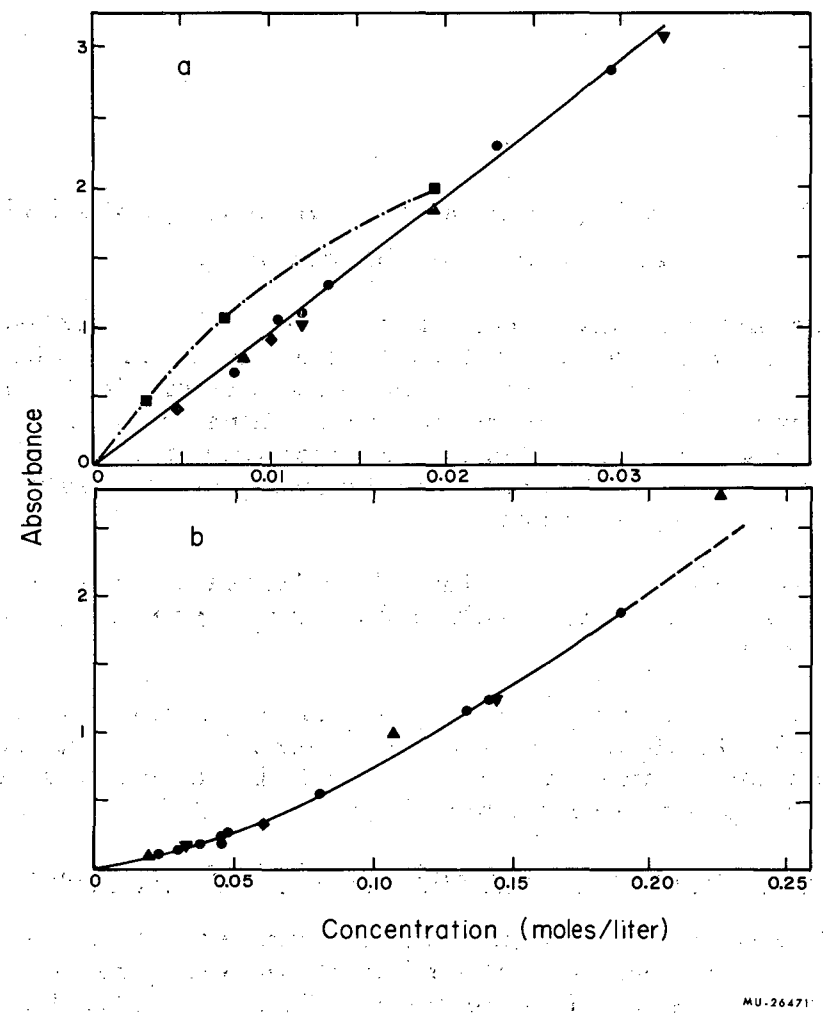

Fig. ID. 7-1. Absorbance vs concentration at (a) 15,250 A (-65°); (b) 24,000 A (-65°).

Na —O— Cs ◇
K △ Ca–·–□–·–
Li ▽

These results for potassium are not in agreement with ours. Calcium shows a different behavior up to 0.02 M. Liquid-liquid phase separation prevented observation of more concentrated calcium solutions. An increase in temperature shifts the peak and long-wavelength side of the peak to longer wavelengths with an increase in the maximum absorbance.

Concentration dependence of the maximum.

From 0.005 to 0.03 M there is a slight shift of the peak to longer wavelengths. This shift is so small, however, that Fig. ID. 7-1a is changed insignificantly if absorbance at the maximum is plotted instead of absorbance at 15,250 A. Although the peak could not be observed above about 0.03 M, the large increase in extinction coefficients at the long-wavelength tail (which is not due to a new band) indicates that the peak may be shifting to longer wavelengths at higher concentrations. In very dilute solutions also the shift is large.[6] These results are shown in Fig. ID. 7-2.

Addition of Sodium Iodide

If metal ions and electrons are in equilibrium with an ion pair, monomer, dimer, or any such associated species, then the addition of excess metal ion should decrease the concentration of electrons and increase the concentration of the associated species. It has been reported[7] that the addition of sodium iodide (0.1 M) to a 5×10^{-4} M sodium solution results in a small shift of the spectrum to shorter wavelengths and the appearance of a new band at 8000 A. In our work, the spectra of solutions that were 0.006 to 0.06 M in sodium and 0.4 to 1.5 M in sodium iodide were shifted to shorter wavelengths with an increase in the maximum absorbance, but no new bands were observed by us in four such runs.

Discussion

Although the spectral investigations straddle the region where electron spins are pairing and where the equivalent conductance is falling off, the relatively unchanging spectrum indicates that the absorbing species retains its basic structural features throughout this whole concentration range. In dilute solutions the absorption is associated with an electronic transition to an excited state within the cavity, and it appears that the cavity remains intact as other species, whose formation satisfactorily account for the conductivity and susceptibility data, are being formed.[2, 8, 9] With regard to spin pairing, it must be concluded that this takes place without a significant effect on the electronic energy levels. The small shift of the peak that occurs as the concentration is increased may be due to the formation of associated species in which the electronic energy levels are only slightly different from those in an unassociated solvated electron. The diamagnetic species is probably a dimer which may be in equilibrium with a monomer,

[7] H. C. Clark, A. Morsfield and M. C. R. Symons, J. Chem. Soc. 2478 (1959).

[8] C. A. Kraus, J. Am. Chem. Soc. 43, 749 (1921).

[9] E. Huster, Ann. Physik 33, 477 (1938).

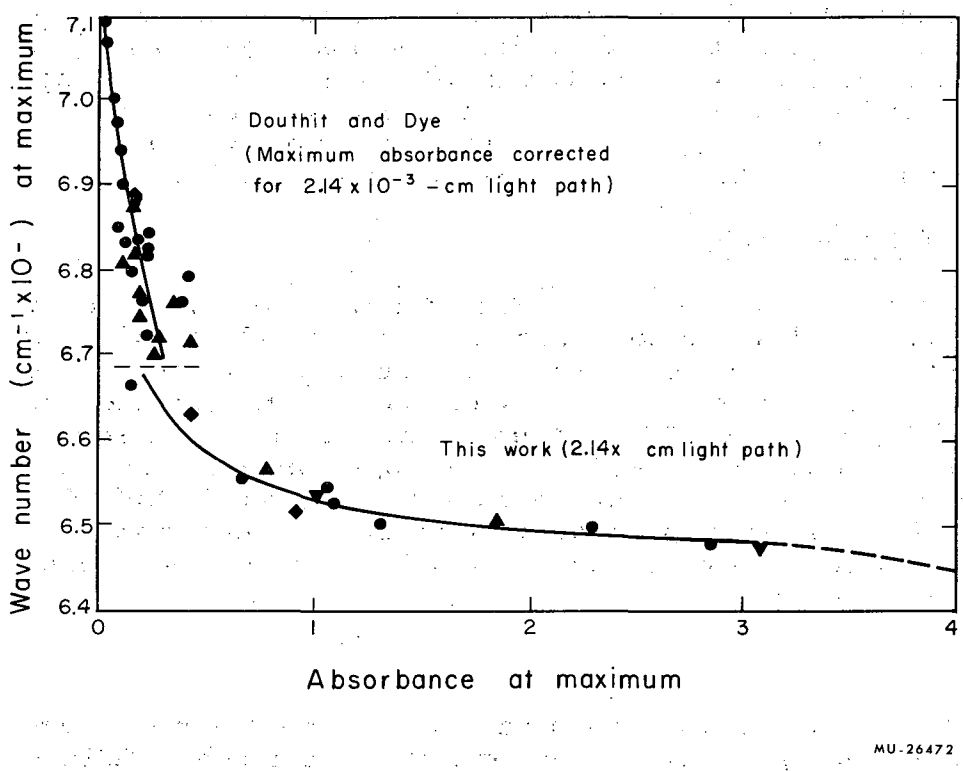

Fig. ID. 7-2. Wave number at maximum vs absorbance at maximum - (65°)

Na	O	Li	▽
K	△	Cs	◇

$$2M = M_2,$$

or with metal ions and electrons,

$$2M^+ + 2\,e^- = M_2.$$

However, it is unlikely that the electron moves in an expanded orbital of the monomer or dimer as has been postulated.[4] The state of such an electron would be quite different from its state in the dilute solution--i. e. in a cavity--and it is hard to understand why two such different species should have practically the same spectrum. Retention of the cavity appears necessary to explain the spectra.

The increase of the extinction coefficients at the long-wavelength tail indicates that one or more new species are being formed when the concentration exceeds about 0.03 M. It is likely that this is due to the formation of higher polymers such as M_3, $M_4, \cdots, M_n$. Such clusters are consistent with the trend toward metallic behavior as evidenced by the large increase in conductivity in this region. If we assume that the absorption is due to the contribution of two unresolved bands, a graphical method can be used to test this assumption. From the equation

$$\epsilon c\ \ell = (\epsilon_a c_a + \epsilon_b c_b)\ \ell$$

one obtains

$$\frac{c_a}{\epsilon c} = \frac{1}{\epsilon_a} - \frac{\epsilon_b}{\epsilon_a}\ \frac{c_b}{\epsilon c}\ ,$$

where ϵ is the measured extinction coefficient, c is the metal concentration, and ϵ_a and ϵ_b are the extinction coefficients for the low- and high-concentration species, respectively, and c_a and c_b are the concentrations of these species. If one knew the true reaction and its equilibrium constant, one would expect a plot of $c_a/\epsilon c$ vs $c_b/\epsilon c$ to yield a straight line of negative slope, the intercepts determining the values of ϵ_a and ϵ_b.

The results of several plots are shown in Fig. ID. 7-3, for which are used assumed equilibria and appropriate values for the corresponding equilibrium constants that give the best straight lines. As can be seen, reasonable plots can be obtained for several equilibria and the correct one could not be chosen solely on the basis of this graphical method. We suggest that polymers are forming at high concentrations, and the plot obtained for the reaction $5Na_2 = Na_{10}$ is at least consistent with this interpretation. The value of K has no real meaning, as there are probably many equilibria operating and many different polymers being formed.

The foregoing discussion is, of course, valid only for the alkali metals. Interpretation of the different behavior of calcium is under consideration.

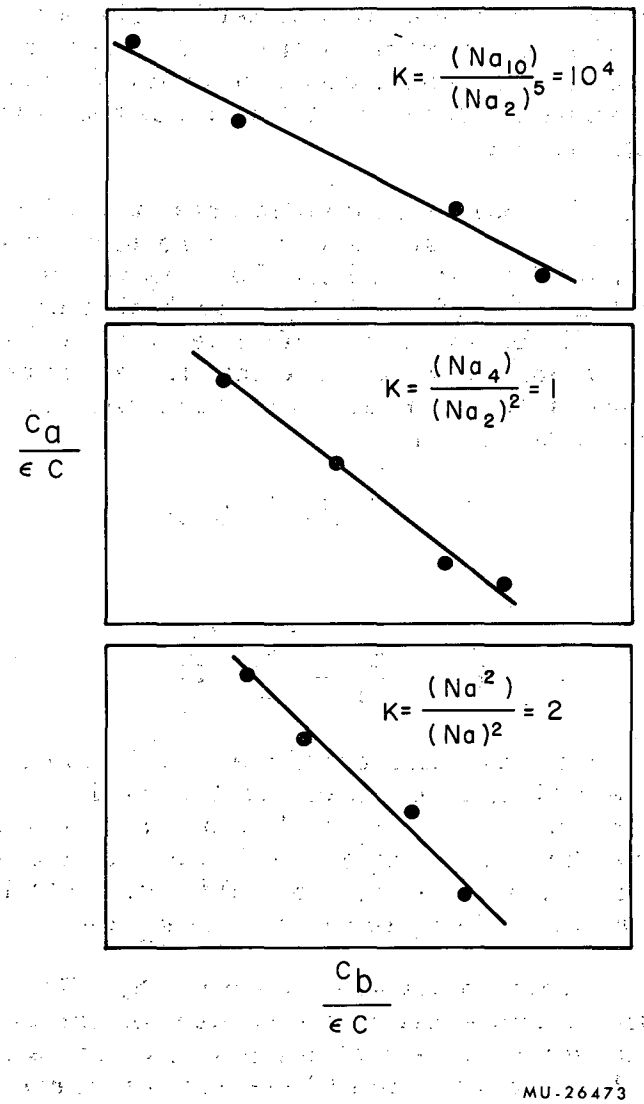

Fig. ID. 7-3. Examples of equilibrium trials using data of the four most concentrated sodium runs at 24,000 A (-65°).

8. DIPHOSPHORUS TETRACHLORIDE

Charles Lindahl and William Jolly

Besson and Fournier[1] in 1910 reported passing a mixture of PCl_3 and H_2 through a silent electric discharge and collecting a small amount of P_2Cl_4 (bp 180; mp -28°) as well as larger amounts of red and yellow nonvolatile solids.[1] Stock and co-workers[2] in 1925 and Finch[3] in 1959 also reported the preparation of small amounts of P_2Cl_4 and red and yellow solids by reaction of PCl_3 with zinc and mercury arcs respectively. Sandoval and Moser have recently reported the preparation of P_2Cl_4 in a discharge over a solution of phosphorus in PCl_3.[4]

We are studying the action of electric discharges on PCl_3 to improve yields of P_2Cl_4. Several early experiments, unsuccessful in the production of P_2Cl_4, as well as successful methods are described. The goal of improved yields of P_2Cl_4 is preliminary to the study of some of its chemistry.

Microwave Discharge Experiments

The success of microwave discharge preparations of B_2Cl_4 from BCl_3[5] and of Ge_2Cl_6 from $GeCl_4$[6] led us to try a microwave discharge. The following observations were made.

a. In our initial experiments we passed PCl_3, at a pressure of 1 to 5 mm Hg, through a microwave discharge; the emerging gas passed through successive cold baths. We found that PCl_5 always condensed in the initial trap when the trap was cooled to -22° and sometimes even when cooled only to +10°. A red material, similar in appearance to red phosphorus, condensed in a second trap at -45°, and a yellow-tan, pyrophoric phosphorus subchloride condensed in a third trap at -63°. Phosphorus trichloride condensed in the -63° trap and subsequent colder traps. The chloride content ranged between 1 and 2% for the red material and between 10 and 25% for the yellow-tan material. These materials are nonvolatile at room temperature, and x-ray patterns show that they are amorphous.

b. When a mixture of the red and yellow materials and PCl_5 was exposed at room temperature to a stream of the gas emerging from the microwave discharge, the red and yellow materials were removed while the PCl_5 remained. No reaction was observed in a stream of ordinary PCl_3.

---

[1] A. Besson and L. Fournier, Compt. rend, 150, 102 (1910).

[2] A. Stock, A. Brandt, and H. Fisher, Ber. deut. chem. Ges. 58, 643 (1925).

[3] A. Finch, Can. J. Chem. 37, 1793 (1959).

[4] A. A. Sandoval and H. C. Moser, New Synthesis of P_2Cl_4, paper to be presented before the Division of Inorganic Chemistry at the Washington meeting of the American Chemical Society, March 1962.

[5] J. W. Frazer and R. T. Holzmann, J. Am. Chem. Soc. 80, 2907 (1958).

[6] D. Shriver and W. L. Jolly, J. Am. Chem. Soc. 80, 6692 (1958).

c. When the gas emerging from the discharge was allowed to pass into an evacuated bulb at room temperature and allowed to stand for 5 min, only PCl_3 was condensed by a -196° trap. However, when the -196° trap was placed about the bulb within a few seconds after the bulb was shut off from the discharge, PCl_5 and the red and yellow materials condensed along with PCl_3. Thus the excited species have a half-life of at least 0.5 sec before they return to normal PCl_3.

d. When H_2 was mixed with PCl_3 in ratios of P_{H_2}/P_{PCl_3} greater than 1, a red material deposited throughout the line beyond the discharge; the thickness of the deposit decreased with increasing distance from the discharge. Phosphorus pentachloride was not formed, but HCl was formed. Qualitative tests on the red material indicated that it contained no Cl, so it is thought to be red phosphorus. This red material could also be removed slowly by reaction with the gas emerging from the discharge zone if the P_{H_2}/P_{PCl_3} ratio were lowered below 1.

e. A plug of copper wool placed in the reaction tube past the discharge zone reacted to form, among other things, a gray material whose x-ray powder pattern showed the presence of CuCl. Traces of red phosphorus formed on the wall of the tube at the plug, and a small amount of P_2Cl_4 condensed in a -45° cold trap. No PCl_5 or red or yellow solids formed in the cold traps. Yields of 10 to 50 mg of P_2Cl_4 were obtained in 1-hr runs. Under optimum conditions 0.4% of the PCl_3 was converted to P_2Cl_4 in 75% yield, assuming the reaction

$$2PCl_3 + 2\ Cu \longrightarrow P_2Cl_4 + 2CuCl.$$

Presumably the remainder went to red phosphorus according to the equation

$$PCl_3 + 3\ Cu \longrightarrow P + 3CuCl.$$

Observations a through d are consistent with the assumption that the vapor leaving the discharge contains PCl_5 and one or more of the reduced species PCl_2, PCl, P_2 or P. Surely copper wool would quantitatively reduce PCl_5 to PCl_3. Hence observation e suggests that copper wool also acts as a catalyst for the dimerization of PCl_2 or the reaction of PCl_3 with one of the other possible reduced species. Future mass-spectrometric studies may help elucidate the nature of the transient discharge products.

60-Cycle Glow Discharges

In an attempt to improve yields, a 60-cycle glow discharge between copper wool plugs is being studied.[7,8] In a series of experiments with a flow of PCl_3, pressure 1 to 4 mm Hg, the best yield was 52 mg of P_2Cl_4 in 24 min. A 12-hr run gave only 240 mg. Other work in progress involves nonflow systems at 35 mm Hg (0° vapor pressure of PCl_3). This method is being developed following a preliminary yield of 75 mg in 15 min.

---

[7] T. Wartik, The Use of Discharge Metals for Inorganic Synthesis, Paper No. 55 presented before the Division of Inorganic Chemistry at the New York meeting of the American Chemical Society, September 1960.

[8] W. L. Jolly, The Use of Electric Discharges in Chemical Syntheses, UCRL-9501, Dec. 1960.

Diphosphorus Tetrachloride

Qualitative studies of decomposition indicated no observable change in 24 hr at 0°, but a trace of yellow appeared in 48 hr. At 110° the liquid turned yellow in an hour and decomposed to an orange solid and a liquid (probably PCl_3) over a 48-hr period. A vapor pressure of about 1 mm Hg was measured at 25°. A mass-spectral analysis gave the fragmentation pattern shown in Table I. The spectrum was recorded by use of a Consolidated Model 21-103A mass spectrometer. Ions found agree with those found by Sandoval and Moser.[4]

Table I. Results of mass-spectral analysis.

m/e	Relative intensities	Ion	m/e	Relative intensities	Ion
31	28.3	P^+	134	1.39	$P_2Cl_2^+$
35	21.8	Cl^+	136	3.63	$P_2Cl_2^+ + PCl_3^+$
36	13.4	HCl^+	138	3.32	PCl_3^+
37	7.31	Cl^+	140	1.51	PCl_3^+
38	4.13	HCl^+	142	1.03	PCl_3^+
62	13.8	P_2^+	144	1.25	?
66	32.2	PCl^+	167	11.5	$P_2Cl_3^+$
68	10.5	PCl^+	169	11.1	$P_2Cl_3^+$
97	8.99	P_2Cl^+	171	3.59	$P_2Cl_3^+$
99	2.15	P_2Cl^+	173	0.40	$P_2Cl_3^+$
101	100.00	PCl_2^+	179	1.12	?
103	64.2	PCl_2^+	183	1.58	?
105	11.8	PCl_2^+	185	1.68	?
107	2.30	?	202	10.3	$P_2Cl_4^+$
109	3.04	?	204	13.3	$P_2Cl_4^+$
111	1.32	?	206	6.41	$P_2Cl_4^+$
124	2.91	P_4^+	208	1.38	$P_2Cl_4^+$
132	2.15	$P_2Cl_2^+$			

9. RESEARCH IN PROGRESS--JOLLY

1. Some of the reactions of P_2Cl_4 are now being studied.

2. A new class of hydrides, the germyl phosphines (e. g., $GePH_5$ and Ge_2PM_7), are being prepared with a view to examining their physical properties.

3. The physical and chemical properties of Ge_2Cl_6 are under investigation.

4. The plasma jet synthesis of sulfur-nitrogen compounds is being investigated.

10. A STUDY OF THE MECHANISM OF ELECTRO-OXIDATION OF CHROMOUS ION IN CHLORIDE MEDIA*

Wayne Mathews and Edwin F. Orlemann

Cyclic oxidation--reduction of chromous and chromic ions at a hanging-mercury-drop electrode--was studied as a function of the rate of change of the potential applied to the electrode. Aquo chromic ion is reduced to chromous ion at a potential of -0.98 v (vs a N. C. E.). Monochlorochromic ion is reduced at -0.70 v. In the presence of chloride ion, in the concentration range from 10^{-3} to 1.0 M, the oxidation of chromous ion at -0.55 v goes through a monochlorochromous ion intermediate. It is not certain whether this intermediate is the normal monochlorochromous ion found in solution or a species characteristic of the electrode solution interface. Apparent equilibrium between this intermediate species and the other chromous ion species in chloride media is attained within 10^{-3} sec. Oxidation of chromous ion through the monochloro intermediate always produces monochlorochromic ion. These results are in agreement with those of Aikens and Ross,[1] who have recently reported a study of this system.

---

*Summary of a paper presented September 1961 at a meeting of the American Chemical Society.

[1] David A. Aikens and J. W. Ross, J. Phys. Chem. 65, 1213 (1961).

11. RESEARCH IN PROGRESS--ORLEMANN

1. Development and general study of a mercury microelectrode having cylindrical symmetry and stable geometry was started during the summer of 1961 by Dr. Peter Linde. This project will be continued upon his return.

2. A study of the reduction of nickel and related 2+ ions of the first-transition-group metals is to continue using techniques particularly designed to characterize unipositive intermediate oxidation states if they exist.

3. Study of the rates of interconversion of oxidizable or reducible ionic species is planned.

12. TEMPERATURE-DEPENDENT CHEMICAL SHIFTS IN THE NMR SPECTRA OF GASES*

Leonidas Petrakis† and Charles H. Sederholm

It is found that the chemical shifts of various gaseous compounds, referred to gaseous methane as a standard, vary with temperature. The slopes of chemical shift versus temperature at 50°C are tabulated for several compounds. This effect is ascribed to excitation of vibrational modes of the molecules, the protons in the excited molecules being differently shielded than the protons in the molecules in the ground vibrational states. The data are interpreted to yield approximate chemical shifts associated with the excitation of various types of modes. NMR isotopic shifts are discussed on the basis of these data.

*Abstract of a paper published in J. Chem. Phys. 35, 1174 (1961).

†Now at National Research Council, Ottawa, Canada.

13. NMR FLUORINE-FLUORINE COUPLING CONSTANTS IN SATURATED ORGANIC COMPOUNDS*

Leonidas Petrakis† and Charles H. Sederholm

The spectra of fluorine-substituted organic compounds have been investigated. It has been found that the nuclear magnetic resonance coupling

*Brief version of a paper published in J. Chem. Phys. 35, 1243 (1961).

†Now at National Research Council, Ottawa, Canada.

constants between 1, 2 fluorine atoms are usually near zero. The coupling constants between 1, 3 fluorine atoms in a free chain are usually between 7 and 10 cps if all the intermediate skeletal atoms are carbon atoms. If one of the intermediate skeletal atoms is a nitrogen atom, these coupling constants increase to between 10 and 17 cps. The coupling constants between 1, 4 fluorine atoms are usually in the range 2 to 7 cps when a nitrogen atom is in the intermediate skeletal chain. Rings usually reduce all coupling constants below the above stated values.

Several exceptions are found to these generalizations. These generalizations with their exceptions lead the authors to believe that in coupling constants between fluorine atoms the main effect is not a through-the-bond effect as has been formerly assumed, but rather a direct-through-space effect. The approximate order of magnitude of this through-space coupling is given by $D > 2.73$ A, $J = 0$ cps; $D < 2.73$ A, $J = (2.73 \text{ A} - D)\ 507$ cps, where J is the coupling constant and D is the distance between the fluorine atoms. It is demonstrated that the restricted rotation about the carbon-carbon bonds has little to do with the near-zero coupling constants, but that these are readily explained on the basis of through-space coupling.

14. NMR INVESTIGATION OF THE POTENTIAL ENERGY FUNCTION IN HALOGEN-SUBSTITUTED ETHANES

Charles H. Sederholm, Douglas Thompson, and Robert Newmark

Recent interest has led to an investigation of potential energy as a function of the angle of rotation in some halogen-substituted ethanes by NMR methods. The only compound that has been treated completely is CFCl Br-CFClBr. The F spectrum at 56.4 Mc of a mixture of the two isomers, a meso form and a d-l form, as a function of temperature from room temperature down to -100°C has been examined. At room temperature, where free rotation is taking place, the two isomers each have only one kind of fluorine atom, and hence the spectrum consists of a pair of lines, with a separation of 48.4 cps. The high-field peak contains 52.8% of the total integrated area.

At -100°C, the spectrum is a superposition of the spectrum of the three rotamers of each of the two isomers:

Ia 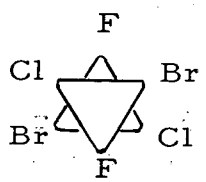

Ib 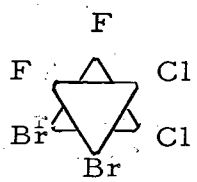

Ic 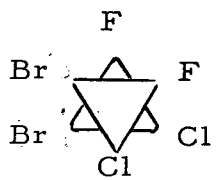

IIa 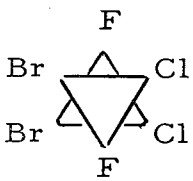

IIb 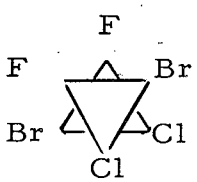

IIc 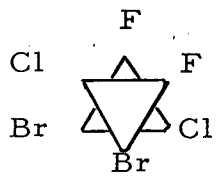

Rotamers Ia, IIa, IIb, and IIc should yield single lines. Rotamers Ib and Ic are mirror images of each other, and hence have identical spectra. They should yield a pair of doublets. This is precisely the spectrum observed at -96°C, as shown in Fig. ID. 14-1. Chemical shifts and integrated areas of the several lines are tabulated below. By fairly straightforward reasoning, it is possible to make the following assignments of the low-temperature peaks.

Line	Chemical shift (cps)	% of total integrated area	Assignment
A	0.0	23.7	IIb
B	94.9 }	10.0	Ib and Ic
C	116.0 }		
D	205.3 }	50.4	Ia
E	214.2 }		IIa
F	264.5 }	9.3	Ib and Ic
G	286.2 }		
H	368.1	6.6	IIc

It is immediately apparent that the coupling constant between the fluorine atoms that are gauche to each other in rotamers Ib and Ic is 21.5 cps.

From the low-temperature areas, the relative energies of the three potential minima can be calculated, and are tabulated below. By use of the Eyring equation for estimating rate constants of interconversion between the three rotamers as a function of barrier heights, an IBM program was written to calculate the observed spectra as a function of temperature from the low-temperature data with various assumed barriers to rotation.

Not all the barrier heights affect the calculated spectra. The calculated spectra depend only upon the following three parameters:

1. The height of the lowest barrier in isomer I.
2. The height of the barrier between configurations IIa and IIb.
3. The height of the lower of the other two barriers in isomer II.

In Figs. ID. 14-2, ID. 14-3, and ID. 14-4 the calculated spectra are compared with the observed. The following values of the above tabulated parameters were chosen as the best-fit values.

Parameter	194°K	207°K	233°K	Best value
1	10.0 kcal	10.0 kcal	10.5 kcal	10.2 kcal
2	9.5 kcal	10.0 kcal	9.5 kcal	9.7 kcal
3	10.0 kcal	10.5 kcal	10.0 kcal	10.2 kcal

Potential energy as a function of rotation configuration.

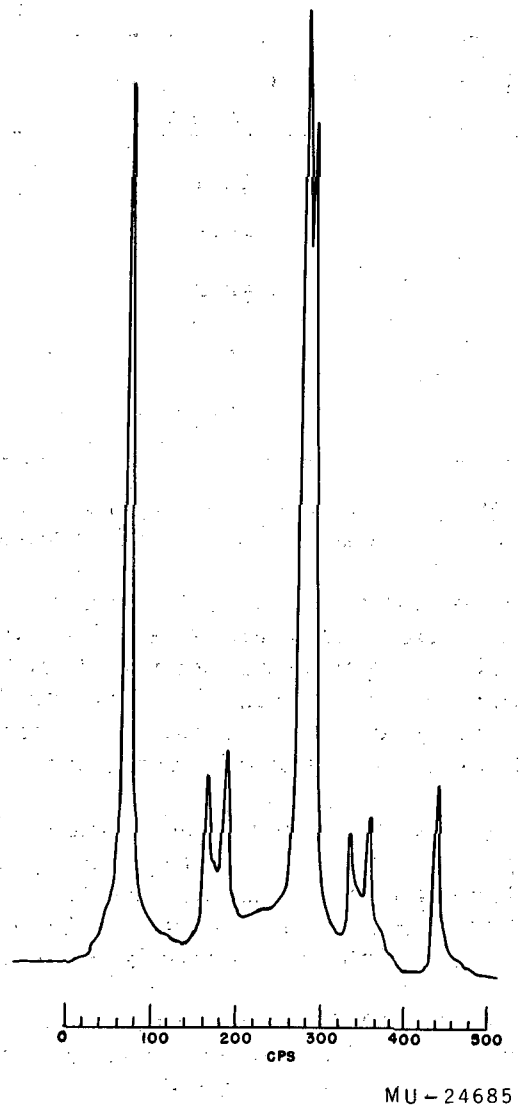

Fig. ID. 14-1. F^{19} spectrum of $(CFCl\ Br)_2$ at 117°K.

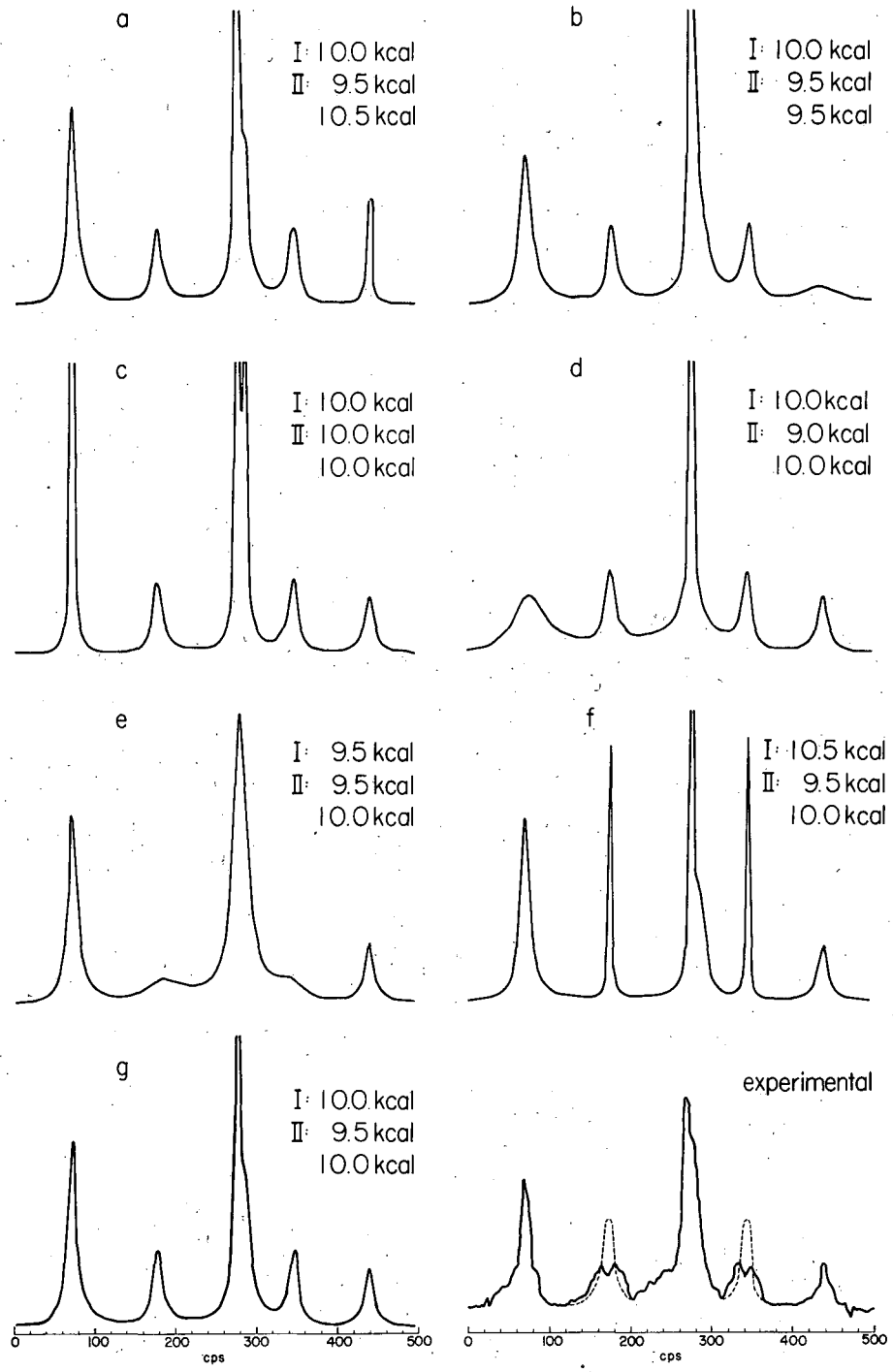

Fig. ID. 14-2. Experimental and calculated spectra of $(CFClBr)_2$ at 194°K.

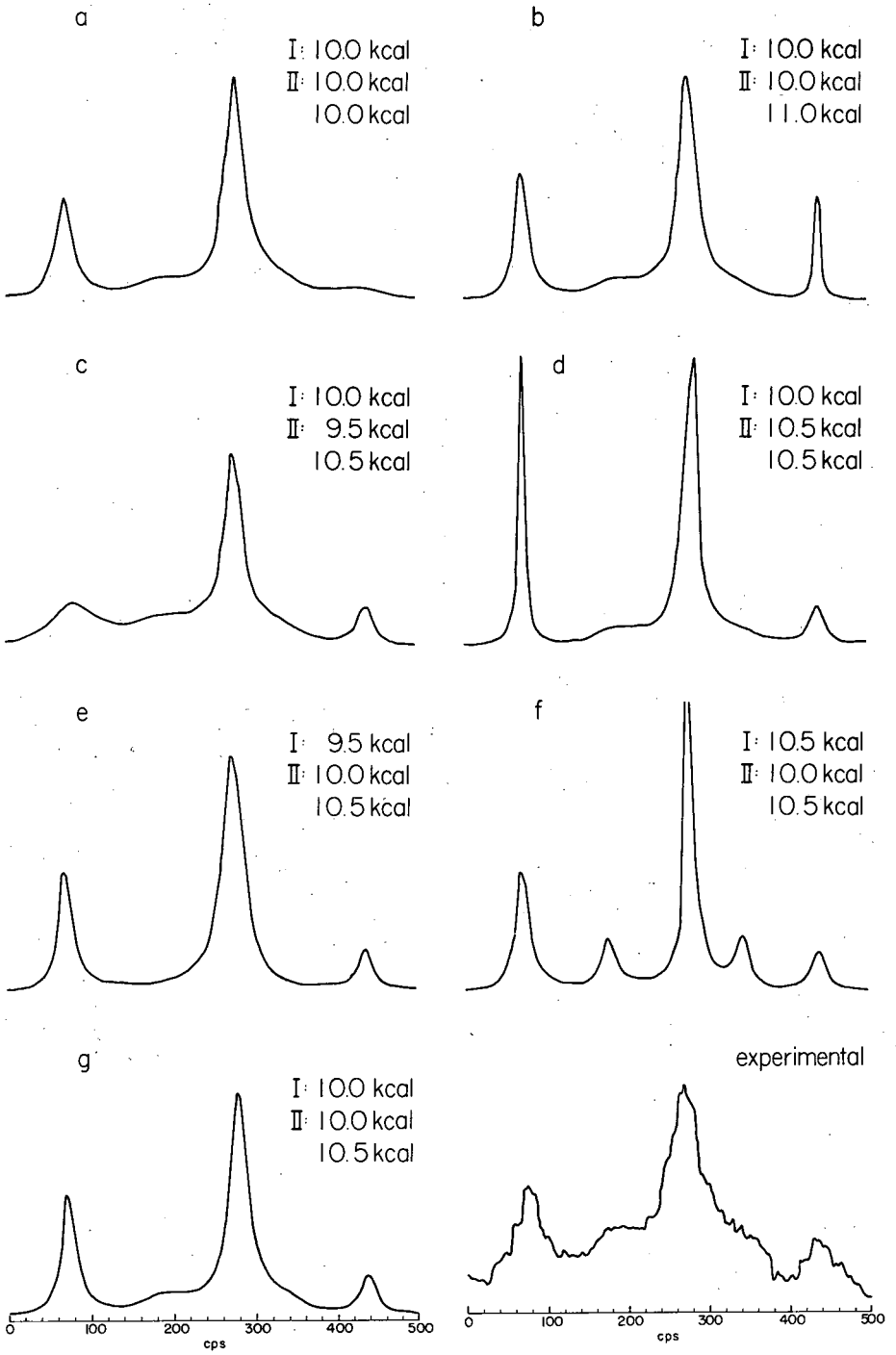

MUB-844

Fig. ID. 14-3. Experimental and calculated spectra of $(CFCl\ Br)_2$ at 207°K.

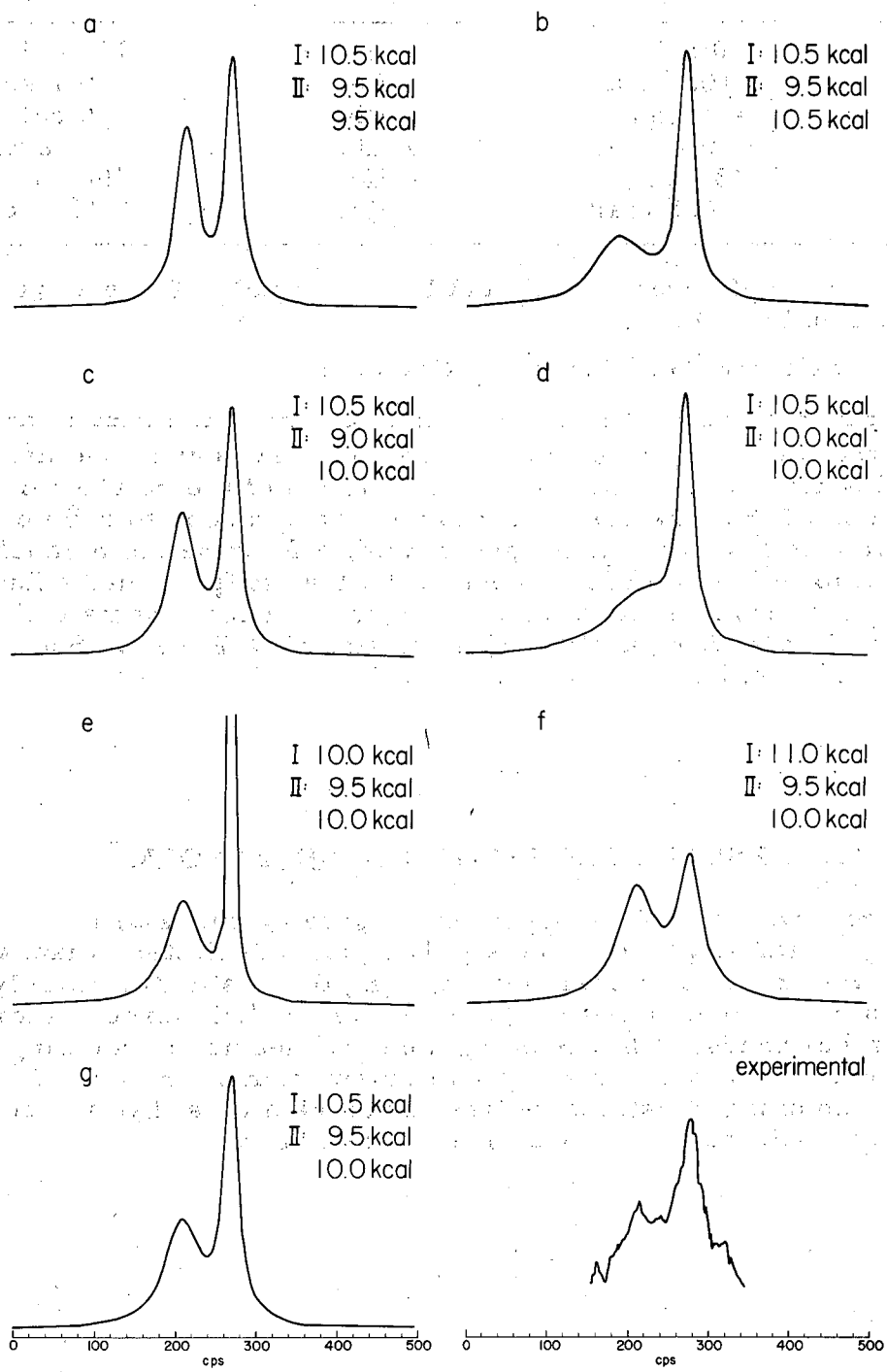

MUB-842

Fig. ID. 14-4. Experimental and calculated spectra of $(CFCl\ Br)_2$ at 233°K.

Isomer I		Isomer II	
Configuration	Energy	Configuration	Energy
Ia	0 cal	IIa	119 cal
Iab	≥ 10.2 kcal[a]	IIab	9.7 kcal
Ib	438 cal	IIb	0 cal
Ibc	≥ 10.2 kcal[a]	IIbc	≥ 10.2 kcal[b]
Ic	438 cal	IIc	450 cal
Ica	≥ 10.2 kcal[a]	IIca	≥ 10.2 kcal[b]

[a]The energies of configurations Iab and Iac are equal. The energy of either Iab or Ibc is equal to 10.2 kcal.

[b]The energy of IIbc or IIac is equal to 10.2 kcal.

From the low-temperature data, one can draw some conclusions about the chemical shift of a fluorine atom as a function of the relative orientation of the other end of the molecule. A fluorine atom gauche to a fluorine and a chlorine atom is subject to the highest field; a fluorine atom gauche to a fluorine and a bromine atom is subject to the lowest field; and a fluorine atom gauche to a bromine and a chlorine atom is at intermediate field. In order of high-field shifting ability, this implies Cl > F > Br. Such an order is somewhat surprising.

15. RESEARCH IN PROGRESS--SEDERHOLM

At present we are continuing to investigate barriers to internal rotation and the relative stability of rotamers in halogen-substituted ethanes by NMR techniques. We are also further investigating the postulate, namely that the nuclear spins of fluorine atoms couple directly through space rather than through chemical bonds. This is being done by measuring coupling constants between fluorine atoms with fixed spatial orientations. In general, we are looking at the coupling constants between fluorine atoms that are separated by many bonds, but are very close together in space.

II. METALLURGY AND CERAMICS

A. INFLUENCE OF MICROSTRUCTURE ON PHYSICAL PROPERTIES

1. THE INFLUENCE OF DISPERSED OXIDE PHASES ON THE MECHANISM OF DEFORMATION OF SILVER

Patrick J. Fetta and Larry Himmel

The presence of dispersed second-phase particles in a ductile metal often gives rise to a substantial increase in the room-temperature strength. Depending on its thermal stability, such a dispersion may also lead to a significant improvement in the creep resistance at elevated temperatures. Existing theories of dispersion hardening are still very rudimentary, mostly because little is known concerning the detailed interactions that occur between matrix dislocations and dispersed phases. Attempts are therefore being made to study dislocation-particle interactions directly by thin-film electron transmission techniques. The materials chosen for this study are internally oxidized Ag-Mg, Ag-Al, and Ag-Cd alloys. After oxidation these alloys consist of dispersions of the respective solute oxides in a matrix of essentially pure (oxygen-saturated) silver.

Techniques have been developed for preparing thin foils of these materials which are suitable for transmission microscopy. Thus far, no distinct second-phase oxide particles have been observed in either Ag-Mg or Ag-Al alloys that have been oxidized in air at temperatures about 800°C. The average size of the oxide particles or solute atom clusters that exist in these materials must therefore be less than about 100 A. By contrast, clearly recognizable particles with idiomorphic shapes are found in the oxidized Ag-Cd alloys. Some of these particles are at least 1000 A in diameter. These differences in the scale of the dispersion between the internally oxidized Ag-Mg and Ag-Cd alloys are believed to be related in part to differences in the thermodynamic stability of the respective oxides.

Observations have also been made on the paths taken by moving dislocations under the influence of thermal stresses. Dislocations in the Ag-Mg and Ag-Al alloys appear to be strongly pinned and move irregularly in jumps across the specimen. On the other hand, the movement of dislocations in the oxidized Ag-Cd alloys does not appear to be strongly influenced by the presence of CdO particles, and the dislocation motions are similar to those observed in pure silver. The number of foils so far examined is not sufficient to determine whether these observations have general validity, although the results are consistent with the observed scale of distribution of the dispersed oxides and with the fact that hardening in the Ag-Mg and Ag-Al alloys is considerably greater than that in Ag-Cd.

Work now in progress is being carried out with specially oriented single crystals deformed in tension at room temperature. Thin foils will be prepared from these crystals and examined by transmission microscopy in order to study the development of the dislocation substructure and to relate these structural changes to the macroscopic stress-strain behavior.

2. DISLOCATION DAMPING PHENOMENA IN HIGH-PURITY SILVER AND DILUTE SILVER ALLOYS

Michael Guinan and Larry Himmel

To study various damping phenomena associated with dislocations in silver and its alloys, an apparatus has been constructed for measuring the internal friction in single crystals over the frequency range from 5 to 100 kc. An electrostatic drive system and FM detection are employed, the specimen being driven in an extensional mode while supported at its midpoint by two parallel knife edges. The internal friction can be measured at strain amplitudes from 10^{-8} to 10^{-4} with a sensitivity or noise level equivalent to a strain amplitude of 10^{-9}. Values of the internal friction, Q^{-1}, ranging from 10^{-6} to 10^{-4} are measured in free decay, while values higher than 10^{-4} are determined from the half width of the specimen resonance.

An important feature of the apparatus is that after being mounted in the supports, the crystal may be annealed in situ at temperatures up to 900°C, either in vacuo (10^{-5} to 10^{-6} mm Hg) or in a purified helium atmosphere. It is hoped that such an annealing operation will minimize the lack of reproducibility resulting from accidental damage during handling and mounting of the crystals. At present, measurements can be made from room temperature to approximately 900°C, but additional modifications, which will permit the measurements to be extended to temperatures as low as 4°K, are nearing completion.

For purposes of calibration of this apparatus, preliminary measurements were carried out on silver single crystals of 99.99% purity which have been grown in a graphite crucible by a Bridgman technique. These preliminary experiments have served equally well in developing the necessary techniques for specimen preparation and handling, and we are gradually approaching the stage at which systematic experiments can be undertaken utilizing crystals of known or controlled purity and perfection. Our initial investigations will be concerned with the strain-amplitude, temperature, and cold-work dependence of the internal friction in ultrahigh-purity (99.9999%) oxygen-free (< 1 ppm) silver.* Special attention will be given to the following problems:

(a) The strain-amplitude dependence of the damping will be studied over the range from 4°K to approximately 900°K, primarily to establish a reference frame for future work with impurity-doped crystals.

(b) The temperature dependence of the background damping will be measured at low strain amplitudes over the range from room temperature to about 600°C. In aluminum[1] and copper,[2] it has been found that the background damping increases exponentially with temperature with an activation energy roughly corresponding to that for self-diffusion. Although various thermally

*Supplied by Consolidated Mining and Smelting Co. of Canada Ltd.

[1] T. S. Kê, J. Appl. Phys. 21, 414 (1950).

[2] H. S. Sack, in Symposium on Plastic Deformation, Pittsburgh, 1950.

activated mechanisms have been proposed to explain the observed effects,[3-8] the process responsible for the high-temperature background damping is still in doubt. We feel that a careful study of the temperature-dependent damping in high-purity silver will contribute significantly to an understanding of this phenomenon as well as its relationship to other relaxation processes such as creep.

(c) The low-temperature Bordoni damping in cold-worked silver will be investigated in order to test the theoretical model recently proposed by Seeger, Donth, and Pfaff.[9] Application of the theory allows the Peierls stress acting on the dislocations to be calculated from the observed activation energy. Although a Bordoni damping peak has previously been found in silver,[10, 11] the characteristics of the damping have not been studied in much detail. It does appear, however, that the Bordoni peak in silver is much broader and less well defined than that in other f. c. c. metals such as copper or aluminum. No explanation has yet been offered for this behavior.

Elaborate precautions are being taken at all stages of the process of crystal growing, cutting, handling, and mounting in order to prevent contamination and to avoid deformation of the crystals. The measurements described above on high-purity silver will eventually be extended to crystals which have been deliberately doped with controlled concentrations of impurities. Both substitutional (i. e., Mg, Al, etc.) and interstitial (i. e., oxygen) impurities will be employed. Thus, a study of the strain-amplitude dependence of the damping in Ag-Mg and Ag-O alloys should make it possible to estimate the relative binding energies between dislocations and substitutional or interstitial solutes. Finally, we intend to study internally oxidized Ag-Mg alloys to determine whether or not the interaction between magnesium and oxygen atoms leads to an anticipated depinning effect.

---

[3] L. A. Kamentsky, Thesis, Cornell University, 1956.

[4] J. Weertman, J. Appl. Phys. 26, 202 (1955).

[5] J. Weertman and E. I. Salkovitz, J. Appl. Phys. 27, 1251 (1956).

[6] A. S. Nowick, Prog. in Metal Phys. 4, 1 (1953).

[7] C. Zener, Elasticity and Anelasticity of Metals (University of Chicago Press, 1949).

[8] J. Weertman, J. Appl. Phys. 28, 193 (1957).

[9] A. Seeger, H. Donth, and F. Pfaff, Discussions Faraday Soc. 23, 19 (1957).

[10] P. G. Bordoni, J. Acoust. Soc. Am. 26, 495 (1954).

[11] P. G. Bordoni, Ricerca Sci. 19, 851 (1949).

3. THE NUCLEATION OF POROSITY DURING DIFFUSION PROCESSES IN METALS

Dennis Maher and Larry Himmel

Porosity is generally observed within the diffusion zone in bimetallic couples.[1] This porosity is believed to result from the condensation of excess vacancies associated with an unequal mass flow of the two diffusing components.[2] The available evidence indicates that the pores are nucleated heterogeneously at internal surfaces such as inclusions or second-phase particles.[3,4] To obtain further information concerning the nature of possible nucleating sites, a study is being made of the influence of dispersed oxides on the amount and distribution of the diffusional porosity in the Cu-Ni and Ag-Au systems. The corresponding Kirkendall shifts are also being measured relative to fixed reference markers (0.001-in. tungsten wires) located well outside the diffusion zone.

The diffusion couples are prepared by welding under pressure in vacuo. Preliminary experiments with Cu-Ni couples have revealed marked differences in the extent and distribution of the porosity on the copper side, depending upon the purity of the copper employed. For example, the total amount of porosity observed in OFHC copper is approximately twice that found in copper of 99.999% purity after diffusion for 240 hr at 900°C. The width of the porous zone in OFHC copper is also substantially greater than that in the "5-9's" materials. Consistent with these observations, the marker shifts indicate that a much smaller contraction has occurred on the copper side of the original weld interface in OFHC copper than in 99.999% copper. Although the precise nature of the nucleating sites has not yet been established, it seems clear that more effective nucleation catalysts exist in OFHC than in 5-9's copper.

Similar experiments are now in progress with copper in which a fine dispersion of Al_2O_3 particles has been introduced by internal oxidation. The average size of these oxide particles is estimated to be of the order of 500 A or less.[5] It remains to be seen whether or not these Al_2O_3 particles are even more potent nuclei for the condensation of vacancies than those which exist in either OFHC or 5-9's copper. Parallel studies have also been initiated with the Ag-Au system, using high-purity (99.999+%) silver as well as internally oxidized silver alloys.

---

[1] A. D. Le Claire, Prog. in Metal Phys. 4, 265 (1953).

[2] R. Seitz, Acta Met. 1, 355 (1953).

[3] R. Resnick and L. L. Seigle, Trans. A. I. M. E. 209, 87 (1957).

[4] R. S. Barnes, Acta Met. 6, 1 (1958).

[5] M. F. Ashby and G. C. Smith, Phil. Mag. 5, 298 (1960).

4. RESEARCH IN PROGRESS -- HIMMEL

1. An inverted torsion pendulum is being assembled in order to study internal friction effects at low frequencies (1 to 10 cps). When this is completed a search will be made for a Zener-type relaxation which may possibly be associated with the stress-induced reorientation of magnesium-oxygen atom pairs in internally oxidized Ag-Mg alloys (with John Papazian).

2. Marked changes in mechanical properties are observed when dilute Ag-Mg alloys are internally oxidized. This behavior appears to be associated with the formation of very small clusters of magnesium and oxygen atoms rather than distinct second-phase oxide particles. The nature of these clusters is being studied primarily by x-ray techniques (with Subash Gupta).

3. The recovery of the strain hardening in cold-worked internally oxidized silver alloys is being followed during annealing by measuring the changes in electrical resistivity, hardness (or yield stress), and x-ray line broadening (with Raymond Bush).

5. INTERNAL STRESSES IN CERAMIC SYSTEMS*

L. A. Jacobson† and Richard M. Fulrath

The strength of a two-phase system is governed by many variables. They are porosity of the system, volume fraction of each phase, particle size of the crystalline phases, particle shape, relative thermal expansion, and reactivity or bonding of the phases. The model system chosen for this study consisted of nickel microspheres dispersed in a continuous glass matrix. Two glasses were used, one of which had a higher thermal expansion coefficient than nickel, and one of which had a lower thermal expansion coefficient. Volume fractions of nickel below 0.5 were used to insure that theoretical density of the system could be realized. Compacts were fabricated by vacuum hot-pressing at temperatures above the glass-softening point, and all compositions tested had zero porosity.

Test specimens of different volume fractions of nickel were broken in four-point cross loading, and for each composition three testing temperatures were used. The nickel particle size was varied at 0.4 volume fraction nickel in order to evaluate the particle size effect on compact strength. For the higher-expansion glass, the dependence of strength on particle size did not follow predicted behavior, whereas the strengths of compacts of the lower-expansion glass followed closely the theoretical size dependence. The strengths of compositions with the lower-expansion glass

*A detailed description of this study is to be submitted for publication in J. Am. Ceram. Soc.

†Now at Wright Air Force Base, Ohio.

and increasing volume fractions of nickel spheres showed lower values than that of the glass alone. The strengths of compacts with the higher-expansion glass increased linearly with increasing nickel content. The slopes of these lines decreased with increasing temperature. From the results of strength determinations and the observation that the nickel did not participate in the fracture, it was possible to arrive at a qualitative demonstration of the role played by internal stresses in determining the strength of a particular two-phase system.

Comparison with other work on two-phase model systems shows agreement with observations on the importance of the interfacial condition between phases. A study on a system with mullite particles dispersed in a glass matrix shows the importance of a chemically bonded interface. The study using nickel spheres and glass shows a parallel necessity for an interface in compression, where chemical bonding is not present. An increase in the strength of the two-phase medium by increasing the volume concentration of the crystalline phase is thereby realized.

(This work was primarily supported under AFOSB49(638)-4 until December 31, 1961. Fundamental research in this area will be continued under the auspices of the U. S. Atomic Energy Commission.

6. MECHANICAL PROPERTIES AND CHEMICAL REACTIVITY IN MULLITE - GLASS SYSTEMS*

Perry L. Studt and Richard M. Fulrath

This study investigated the dependence of strength of two-phase crystal-glass systems on crystal particle size, shape, internal stress, and interfacial boundary reactions, if such should occur. Specimens were formed by vacuum hot-compacting sized mullite crystal particles ($3Al_2O_3 \cdot 2SiO_2$) with known glass compositions. Two types of glass were used--one a soda-borosilicate and the other a soda-aluminosilicate. Several specimen compositions of the first type were prepared and tested. Mechanical strengths were determined by four-point modulus-of-rupture measurements, with results outlined below.

Significant chemical reaction was observed to take place during the hot pressing of mullite with the soda-borosilicate glasses. The reaction led to precipitation of a silica-rich crystalline phase in the glass matrix and to a change in the mullite structure as evidenced in the x-ray diffraction pattern. The precipitated material was tentatively identified as α-cristobalite. Minimum hot-press pressures and temperatures required for the reaction to occur were 2500 psi and 650°C, respectively. Two of the three soda-borosilicate glasses considered reacted in this manner. These contained

*A protion of this study was supported by an Owens-Illinois Glass Company Grant-in-Aid.
Accepted for publication J. Am. Ceram. Society.

12% and 14% by weight B_2O_3, while the nonreactive glass contained 25% by weight B_2O_3. Photomicrographs of the compacts disclosed that the α-cristobalite precipitated primarily from the glass phase and that the precipitation appeared to begin at the mullite-glass interface and then spread throughout the remainder of the glass phase. In one case, on extended heating in air at approx 850°C, the α-cristobalite diffraction lines changed to those of α-tridymite. Glass-mullite wetting studies in air indicated that none of the glasses wet mullite. However, occurrence of the interfacial chemical reaction caused the soda-borosilicate glass to wet mullite.

The effect of interfacial reaction on the mechanical strength of the compacts was to increase the strength for small amounts of precipitate, but ultimately to decrease the strength for large amounts of precipitate. The general dependence of strength on particle size and amount was not changed.

Contrary to previous investigations,[1,2] the correlation of particle size with strength did not follow a grain size to some power law (generally about -1/2). This glass-crystal system followed an exponential relationship. Porosity dependence followed an exponential relationship,

$$\exp(-\text{constant} \times \text{volume fraction porosity}).$$

The constant in this case agrees with values given by other investigators and is of the order of 6.

Internal stress measurements gave strain values of the correct sign as predicted by the difference in thermal expansion coefficients between glass and crystal. The internal stress effect was not quantitatively evaluated, as the stress effect could not be separated from the other variables of the system.

Conclusions that may be drawn from dependence of strength on grain size are (a) compacts with uniformly strong interfaces have a strength proportional to the grain size raised to some power; variable-strength interfaces tend to change the relationship into an exponential;
(b) the grain boundary reaction observed in this system first gives a net increase in strength because many interfaces become stronger, but ultimately the increased internal stress caused by the precipitate decreases the strength;
(c) the effect of particle shape is of secondary importance compared with size and amount;
(d) the mechanical strength of brittle glass-crystal bodies can be represented by an equation of the same form as that for single-phase brittle crystalline bodies.

---

[1] F. P. Knudson, Dependence of Mechanical Strength of Brittle Polycrystalline Specimens on Porosity and Grain Size, J. Am. Ceram. Soc. 42, 376-387 (1959).

[2] L. N. Grossman, Fracture of Model Ceramic Systems (M. S. Thesis), University of California, 1961.

7. STRESS-ENHANCED GASEOUS PERMEABILITY OF CERAMIC MATERIALS

Perry L. Studt and Richard M. Fulrath

This investigation is concerned with (a) demonstrating that stress-enhanced gaseous permeability of ceramic bodies occurs, and (b) relating this enhancement to grain boundary conditions.

Two methods of rapidly stressing prepared ceramic specimens are currently being used. The first is thermal, and the second is mechanical. In the thermal method the radial temperature distribution in the wall of a hollow cylinder is reversed by heating alternately the interior and exterior surfaces. The mechanical method utilizes disks mounted with clamped edges and loaded at their centers.

Both helium pressure loss and flow rate have been used as a measure of the permeability change during the cyclic stressing. Difficulties in simultaneously achieving high thermal stresses and high sensitivity in permeability measurements have led to inconclusive results with the present thermal-stress apparatus.

Primary emphasis is currently on the mechanical stressing method, making use of both permeable and impermeable high-alumina bodies (97.6% to 99.85% by weight Al_2O_3). The change in permeability is determined by the change in helium flow rate (through a thinned section at the outer surface of the disk) as measured with a mass spectrometer.

Stress-enhanced permeability of normally impermeable 97.6% Al_2O_3 bodies has been established. The behavior observed is a sudden large increase in flow rate (on the order of one magnitude or more), which then drops rapidly to the previous background rate. Once the stress enhancement begins, it generally occurs when the stress in the helium-conducting membrane changes from compression to tension, and drops back to the background flow rate on reversal to compression. Removal of the cyclic loading causes the flow rate to rise to an elevated value which then decays exponentially to the previous background rate. During this general exponential decay period the flow rate frequently drops to background levels for short times. Calculated stresses of approx 6,000 psi tension and compression for 1- to 2-min cycles produce the described effects. The thickness of the test section through which flow apparently occurred is approx 1.0 mm. The stress-enhancement process is at least partially reversible.

Behavior of permeable 99.85+% Al_2O_3 disks differs markedly from that in disks of 97.6% purity. Under tension there is a small increase in flow rate, but reversal to compression causes an immediate drop in flow rate of about 50%. There is then a gradual increase in flow rate until a steady-state value is reached which is about 10% higher than the minimum observed. Time required to reach the new steady state under compression is nearly 15 min. No dependence of the minimum and maximum flow rates on cycle time was found until the tension and compression periods were reduced to 15 sec. Higher minimum and lower maximum flow rates were then observed.

A minimum stress level is required before the permeability of either material is changed. This is on the order of 5,200 psi tension or compression for the 97.6% purity Al_2O_3, and 3,200 psi tension or compression for the 99.85% purity Al_2O_3, if porosity is neglected. All experiments were performed at room temperature. As more data become available, a model for the phenomenon will be developed and, if feasible, quantitative correlations evolved relating the details of microstructure and composition to the permeability change.

8. RESEARCH IN PROGRESS--FULRATH

1. Development work on the dynamic differential calorimeter is being continued in order to extend reaction heat measurements to higher temperatures. A new design with reduced contact points and electrical shielding is being evaluated in hopes of reducing electrical leakage at a high temperature.

2. Work has been initiated to consider the mechanism and kinetics of solidification of aluminum oxide, pertinent to the production of ceramic spheres, for studies of sintering and other properties of multiphase systems. The experimental assembly is complete and preliminary tests are in progress.

9. INVESTIGATION OF STRUCTURE AND PROPERTIES OF MARTENSITE

Earl R. Parker

Martensite is the hardest known structure that can be produced in an alloy by heat treatment, but the fundamental properties leading to this hardness and strength are not understood. Studies have shown that martensite can be formed in certain nonferrous alloy systems, yet these nonferrous martensites are not hard. Martensite in steel is strong only when carbon is present, thus it is known that the presence of carbon is essential for high hardness. Just how the carbon contributes to the strength is not understood. Electron microscope studies have not yet revealed the subtle nature of the structure, although efforts along this line are continuing both here and elsewhere. Only when we understand strengthening processes throughly can we hope to develop new ultrahigh-strength materials.

One of the main difficulties encountered in studies of martensite is that individual crystals are too tiny to be examined and tested separately. Single needles of hard martensite, as normally produced, are of micron dimensions. However, with technique development, it may be possible to produce large martensite crystals for examination.

Research on this problem began with the procurement of alloys having martensite transformation temperatures below room temperature. Equipment for zone melting 0.25-in.-diameter bars of these alloys has been set up, and preliminary runs are in progress. The first step is to make single crystals of austenite by the zone-melting technique. No major difficulty is expected in this step--single crystals of austenite have already been made by others using similar techniques. The second step is to transform the single crystals of austenite into single crystals of martensite, or at least into large martensite grains. In the opinions of many investigators working in this field, the chances for successful completion of this second step are small. Nevertheless, it is worth the effort because of the potential value of the knowledge that might be acquired.

To transform the austenite to martensite, the single-crystal bars will be placed in a temperature gradient and the temperature gradually lowered. Martensite will form first at the colder end and grow into the remaining austenite. If this simple procedure does not produce a single crystal, or at least large grains of martensite, the procedure will be repeated with a tensile or shear stress imposed on the austenite crystal. The stress produced as a result of the dimensional changes associated with the austenite-martensite reaction will favor martensite growth in one of the normal growth directions while tending to suppress it in the others.

10. DUCTILE CERAMICS

Earl R. Parker

The ductile ceramics research program was started a number of years ago under the sponsorship of the Air Force Office of Scientific Research and was continued until March 31, 1962 with ARPA financing. A statement concerning this work is included herein because it is expected that a small effort related to the fundamental portion of this research will be continued under this Division.

This program may lead to a new class of structural materials, but the chances for success are not to be exaggerated, because of the inherent nature of the materials involved. However, this program has already led to an understanding of the fundamental nature of a number of the problems involved in the plastic flow and fracture of materials. It is fair to state that through work inspired by the initiation of this project, more has been learned about the fundamental processes leading to fracture than was learned through all of the preceding and concurrent work on metals. In addition, a great deal has been learned about the detailed processes involved in plastic flow, such as strain hardening, creep, and grain boundary effects.

On the technological side, considerable progress has been made. Nonmetallic materials such as LiF are regularly being extruded in polycrystalline form at an elevated temperature. Although single crystals of LiF or MgO can be deformed plastically 10% or more at room temperature, polycrystalline specimens of the same materials are brittle, the elongation being nearly

zero. Experiments under way at present show that impurities and processing techniques play major roles in contributing to brittleness (as they often do in metals). Only recently has it become possible to make fully transparent polycrystalline LiF extrusions, and this relatively pure material exhibits some room-temperature ductility.

11. RESEARCH IN PROGRESS -- PARKER

Grain boundaries play a major role in controlling mechanical behavior of metals. At high temperatures, they provide the vacancies that permit creep; they are so mobile that grains can slide past one another along boundaries, and fractures nucleate and grow along them. At low temperatures, boundaries interfere with slip dislocations and are therefore sources of strength. Evidence available at present indicates that solid-solution strengthening is probably caused by the concentration of foreign atoms at grain boundaries. Very little is known about the atomic configuration in boundaries, the energy of boundaries, or how boundary energy is affected by alloy content and temperature. Prior to the current research program, the only method available for determining grain-boundary energy was the high-temperature process of thermal grooving. As part of the present program on grain-boundary studies, a new method for determining boundary energy has been devised. It is the chemical equivalent of thermal grooving, and consists of placing a polished piece of polycrystalline metal in contact with a solution that is in equilibrium with the metal. Exchange of metal ions produces a groove that assumes an equilibrium shape, providing for the first time a method suitable for yielding information about the effect of temperature and alloy content on grain-boundary energy.

During the past year, the concept has been checked experimentally. Continued work will reveal the advantages and shortcomings of the method. It is hoped that a quantitative relationship can be developed between the increase in strength provided by a solute element and the change in boundary energy produced by the alloying element.

B. INFLUENCE OF SUBMICROSCOPIC STRUCTURE ON PHYSICAL PROPERTIES: ELECTRON MICROSCOPY

1. THE STRUCTURE OF PRECIPITATION-HARDENED ALLOYS*

Gareth Thomas

This paper reviews information obtained, mainly by transmission electron microscopy, on the microstructure and related properties of alloys hardened by precipitation (not involving martensite transformations).

A description is given of age hardening through the various stages: quenching, zone formation, intermediate precipitation, equilibrium precipitation. The nature of the interface for coherent and partially coherent phases is discussed as well as the influence of the dislocation substructure on heterogeneous precipitation. Direct experimental evidence is now available to prove the existence of both coherency strains and dislocation networks at partially coherent interfaces. The importance of using selected area electron diffraction to give information on crystallography and orientation relationships is discussed and examples are given of the anomalous diffraction effects obtained from zones.

A discussion is given of the effects of plastic deformation on precipitation; the discontinuous type of precipitation, the interaction of dislocations and precipitates, the relation between microstructure and stress-corrosion cracking, and, finally, direct observations of precipitation by using high-temperature electron microscopy. With the latter technique a rapid method of obtaining diffusion data is now possible.

*Abstract of a review paper presented at the First Berkeley International Materials Conference, July 1961, to appear in Electron Microscopy and Strength of Crystals, (Eds. G. Thomas and J. Washburn (Interscience Publishers, Inc., New York, 1962).

2. HELICAL DISLOCATIONS IN QUENCHED AND AGED Al-5% Mg

Alf Eikum and Gareth Thomas

Helical dislocations have been observed in binary aluminum alloys (Thomas,[1] Thomas and Whelan,[2] and Smallman et al.[3]), silicon-gold

[1] G. Thomas, Phil. Mag. 4, 1213 (1959).

[2] G. Thomas and M. J. Whelan, Phil. Mag. 5, 511 (1959).

[3] R. E. Smallman, K. H. Westmacott, and J. H. Coiley, J. Inst. Metals 88, 127 (1959).

(Dash[4]), and alkali halides (Bontinck and Amelinckx[5, 6]). Associated with the helices, columns of prismatic loops are often found. The loops and helices always have parallel axes, ⟨110⟩, and many times a single axis appears to be common to both. The purpose of this work is to study the behavior of helical dislocations as a function of isothermal annealing. The Al-5% Mg system was chosen because the β phase does not precipitate during the short annealing times required to appreciably alter helices.

The electron micrograph in Fig. IIB. 2-1 illustrates the nonuniformity found after quenching from 550°C. It should be noted that the specimen is essentially aged at room temperature prior to thinning and observation. Adjacent regions of the specimen include a segment of relatively uniform helix at A, poorly developed helices at B, and columns of loops, C. The variation in structure within a small volume of specimen is common and may well indicate progressive stages of the aging process as equilibrium is approached. Local fluctuations in vacancy supersaturation, magnesium supersaturation, and thermal stresses would explain the heterogeneous as-quenched structure.

Electron micrographs from specimens aged for 60 min at 183°C and 200°C are shown in Figs. IIB. 2-2 and IIB. 2-3. Adjacent segments of the helix in Fig. IIB. 2-2 appear ready to combine at A. In Fig. IIB. 2-3 a loop has formed on the interior of a helix AC, and the parent dislocation has moved away, ABC. In both cases, Figs. IIB. 2-2 and IIB. 2-3a, the apparent loop formation is occurring on the interior of the helices. Also, the helices are not uniform, indicating a relatively large difference in climb within a very short length. Uniform helices adjacent to a uniform column of loops can be seen in Fig. IIB. 2-3b. The loop spacing and pitches of the helices are approximately equal to their respective radii.

A possible mechanism for the degeneration of helices into a column of prismatic loops is schematically illustrated in Fig. IIB. 2-4. The helix is thought to be stable because of solute pinning (Thomas and Whelan[7]); also, the concentration of vacancies trapped with the lattice may be sufficiently large to maintain a supersaturation force on the helix. At the aging temperature, then, one can assume re-solution of magnesium atoms from the helix at A and C, Fig. IIB. 2-4a. The dislocation would become glissile, moving along the defined cylinder, creating loops at each intersection B, Fig. IIB. 2-4b.[8] An alternative case can also be visualized. Mg atoms going

[4] W. C. Dash, J. Appl. Phys. 31, 2275 (1960).

[5] W. Bontinck and S. Amelinckx, Phil. Mag. 2, 94 (1957).

[6] W. Bontinck, Phil. Mag. 2, 561 (1957).

[7] G. Thomas and M. J. Whelan, Phil. Mag. 6, 221 (1961).

[8] This glide mechanism was suggested by Georges Saada (Lawrence Radiation Laboratory), private communication.

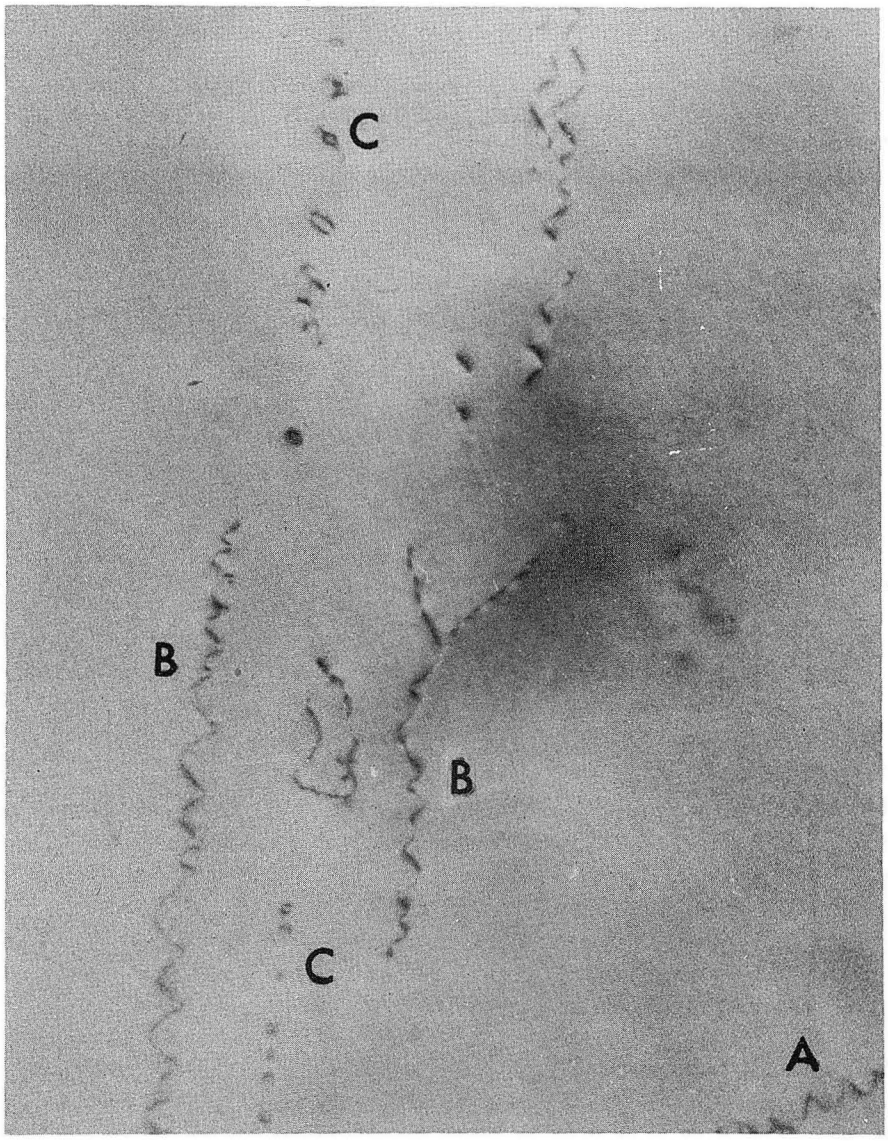

ZN-3077

Fig. IIB. 2-1. Al-5% Mg quenched from 550°C into ice-brine. ×60,000.

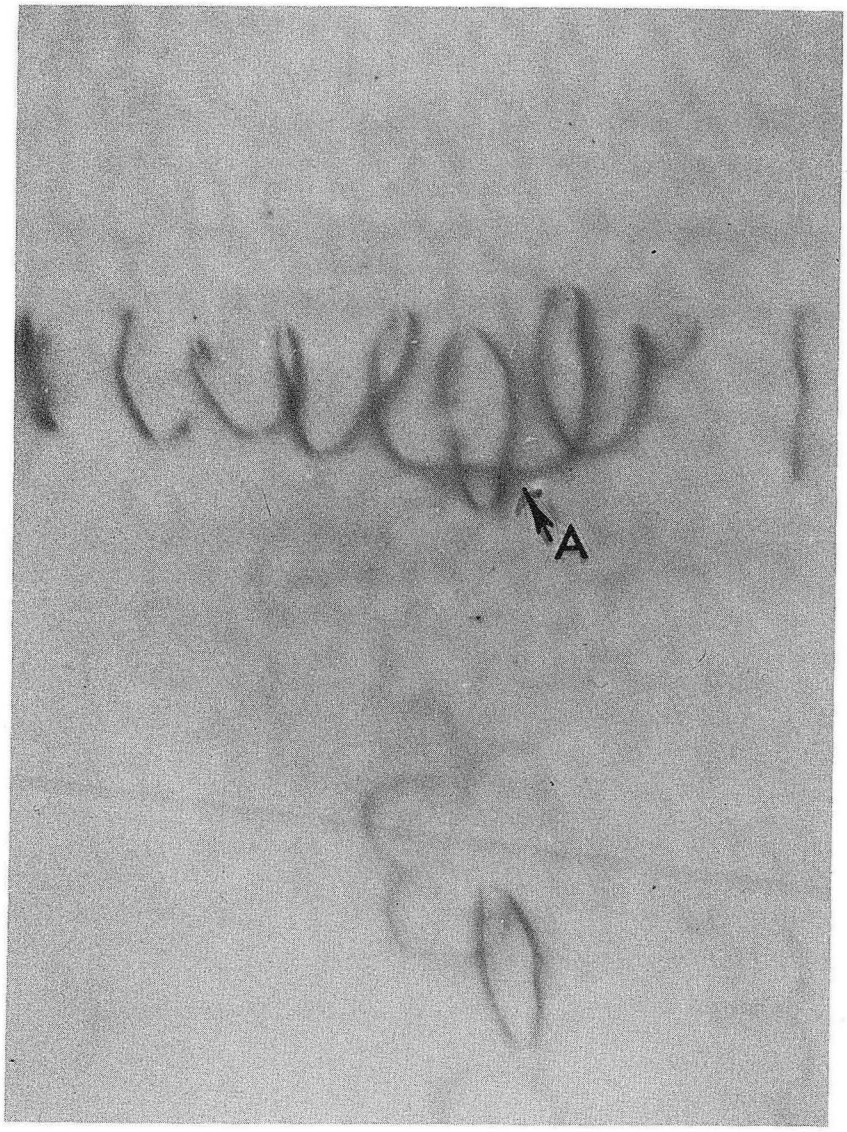

ZN-3078

Fig. IIB. 2-2. Al-5% Mg quenched from 520°C into 78°C water and aged 60 min at 200°C. × 60,000.

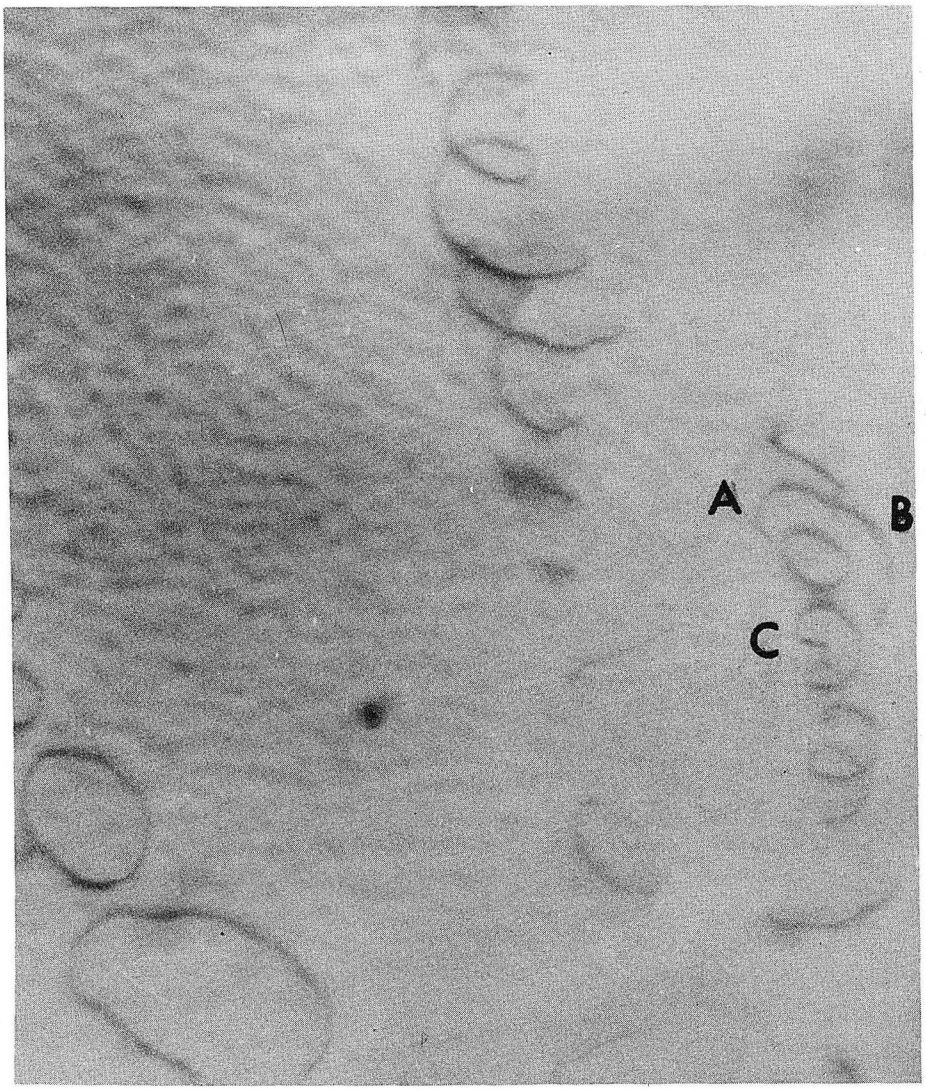

(a)

ZN-3079

Fig. IIB. 2-3(a) Al-5% Mg quenched from 550°C into ice-brine and aged 60 min at 183°C. × 60,000.

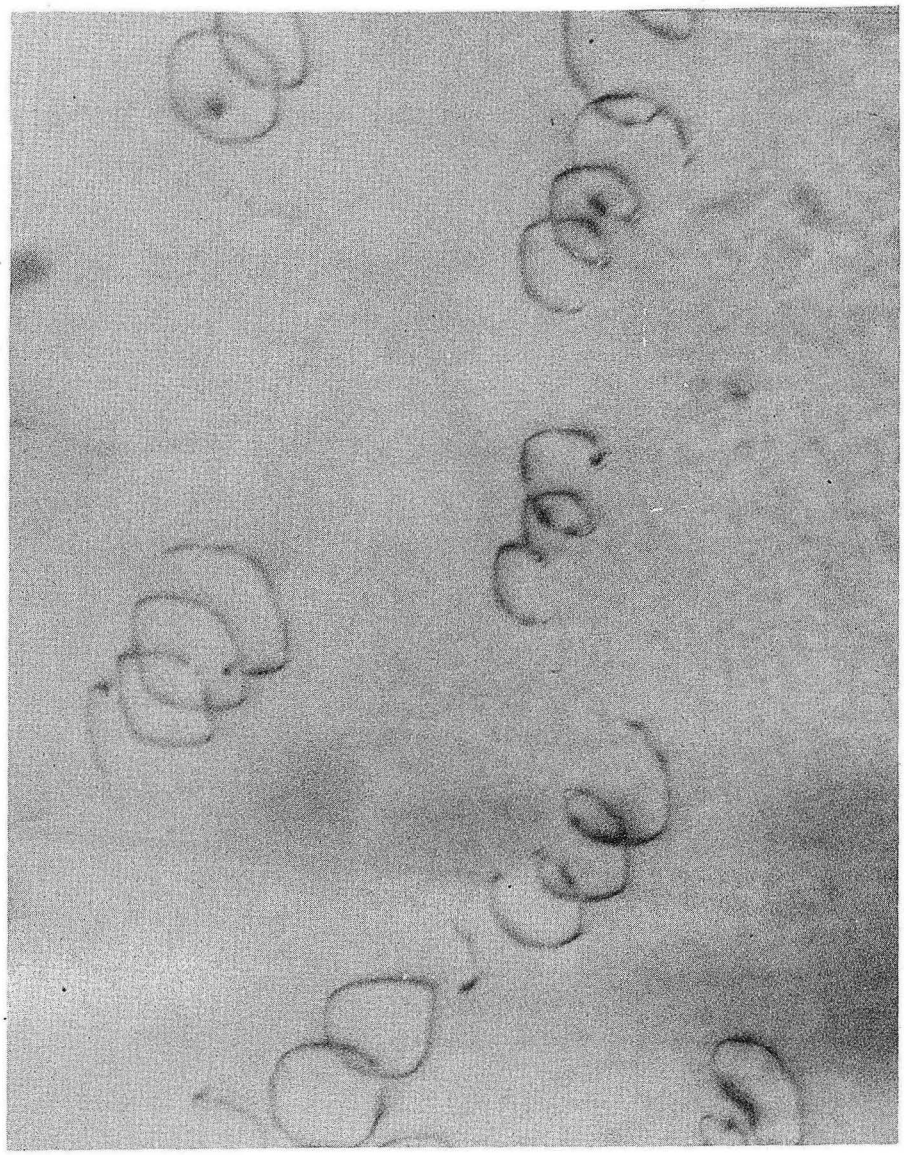

(b) ZN-3080

Fig. IIB. 2-3(b) Al-5% Mg quenched from 550°C into ice-brine and aged 60 min at 183°C. × 60,000.

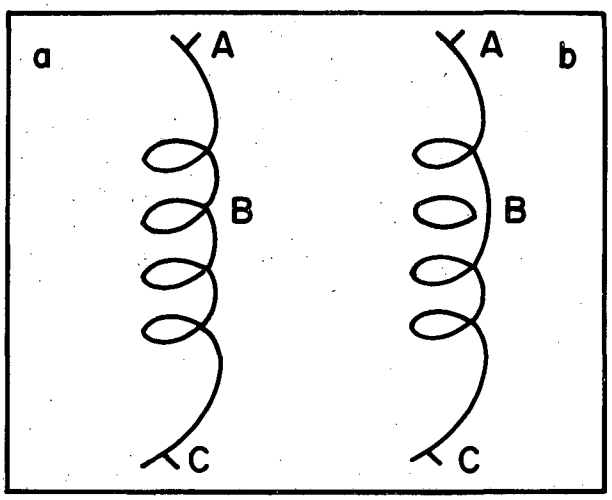

MU-26474

Fig. IIB. 2-4. Schematic illustration of prismatic loop formation from helices.

into solution from the helix may carry with them vacancies. Adjacent line segments, B, would climb together, forming the intersection previously described as having been formed by glide. This mechanism could explain why we have not yet observed precipitation on dislocations and why in other Al alloys helices do not degenerate into loops but become stuck by precipitation.

Helices have not been observed in pure metals. In alloys they exist only where we suspect some binding energy between solute atoms and vacancies, e.g., they are not often seen in Al-Zn alloys. This need not necessarily mean they never form. It is possible, because of lack of impurity pinning on the helix, that helices form and readily degenerate into loops in one continuous process. The more difficult stage of spontaneous loop nucleation is eliminated and replaced by the relatively easy process of "sinking" vacancies at existing dislocations. Resistivity experiments are planned which should give insight into the exact processes occurring. If appreciable solute redistribution takes place, as the tentative mechanism requires, one should see an effect on resistivity as a function of isothermal annealing. We will also measure energies of migration and formation for vacancies in the Al-5% Mg alloy which would enable us to estimate the Mg-vacancy binding energy.

3. THE INTERACTION BETWEEN VACANCIES AND ZONES AND THE KINETICS OF PREPRECIPITATION IN Al-RICH ALLOYS*

Tiziano Federighi† and Gareth Thomas

It is now well known that the very high rates of clustering of solute atoms (i.e., formation of Guinier-Preston zones) in aluminum alloys immediately after quenching from the homogenizing temperature can be explained on the basis of the high concentration of vacancies retained by the quench. This paper discusses the probable reasons for the differences in the clustering processes for various kinds of alloys; for example, the complete time of reaction for Al-10% Zn alloys (a few hours) is the same as that for the elimination of vacancies in pure Al,[1,2,3] whereas for Al-Cu and more complex alloys the reaction proceeds for days or weeks. The initial problem is thus to explain the mechanism by which excess vacancies can be kept in solution for much longer times in alloys than in pure aluminum. We believe that this can be explained by considering the magnitudes of the binding energies between vacancies and zones, which is a natural consequence

*Extract of paper in Phil. Mag. (in press).

†Institute for the Study of Light Metals, Novara, Italy.

[1] C. Panseri and T. Federighi, Acta Met. 8, 217 (1960).

[2] C. Panseri and T. Federighi, Phil. Mag. 3, 1223 (1958).

[3] M. Wintenberger, Compt. rend. 244, 2800 (1957).

of the vacancy-solute atom binding energy. The basic outline of our theory is as follows.

Let the binding energy between vacancies and zones be E_b and consider the following cases:

(a) E_b = zero: vacancies cross zones as if they are of pure solvent and are eliminated at normal sinks (grain boundaries, surfaces, dislocations). From the experimental results (resistivity[1] and electron microscopy[4]) this seems to be the case in Al-Zn alloys.

(b) E_b very large: in this case a vacancy is permanently trapped at zones. This trapping can be understood in terms of relief of elastic strains or in terms of chemical effects. Thus the time for reaction should be very short and the process should occur very rapidly. An example is the Al-5% Mg alloy.

(c) E_b intermediate value: This would represent the general case. A vacancy is trapped for a relatively long (but not infinite) time, and therefore the rate of reaction progressively decreases until equilibrium is attained between vacancies reaching zones and those evaporating from zones. This would indicate an initially fast reaction which is followed by a slow reaction. The experimental evidence shows that Al-Cu and Al-Mg_2Si alloys behave in this way.

In the paper we discuss the properties of the zones which are to be expected from the above hypothesis; there is ample experimental evidence to support our views.

[4] G. Thomas, Phil. Mag. 4, 606 (1959).

4. DIRECT OBSERVATIONS OF SOLID-STATE PHASE TRANSFORMATIONS

John A. Hren† and Gareth Thomas

It was recently demonstrated that phase transformations can be observed directly by using a heating device in the electron microscope, and that it is possible to estimate diffusion coefficients by measuring dissolution rates of precipitates.[1] We have worked on the Al-20% Ag alloy. Direct observations have been made of precipitation and dissolution of the γ phase by recording dynamical changes on ciné film. Figure IIB. 4-1 shows a

† Now at Korntal bei Stüttgart, West Germany.

[1] G. Thomas and M. J. Whelan, Phil. Mag 6, 1103 (1961).

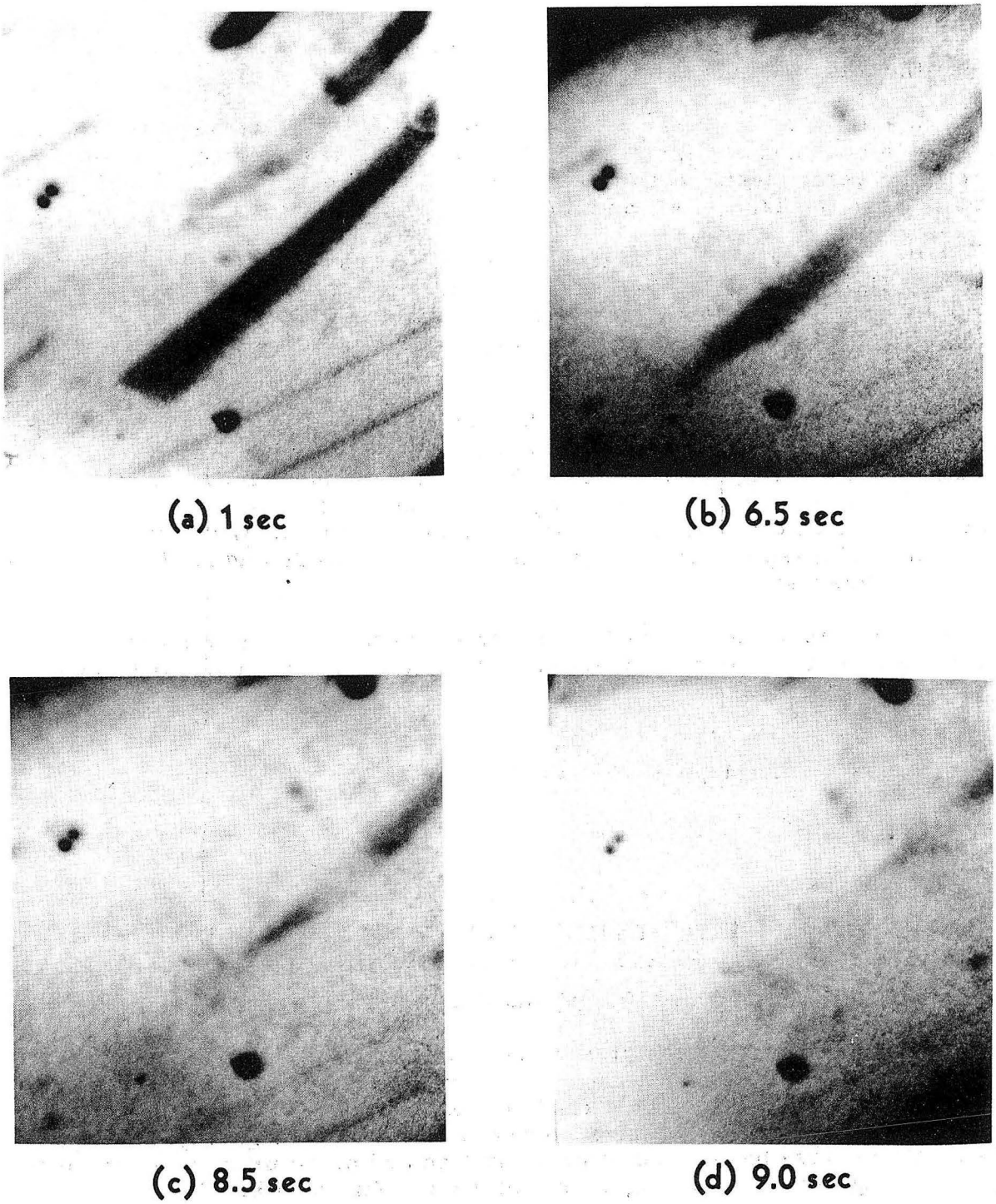

ZN-3058

Fig. IIB. 4-1. Dissolution sequence for γ in Al-20% Ag alloy; temperature approx 480°C. × 80,000.

typical dissolution sequence. From the data we have found that during dissolution of precipitates of length ℓ, the plot of (length)^2 versus time is linear. This result is expected for bulk diffusion in the spherical, cylindrical, or one-dimensional case.[2] Figure IIB. 4-2 shows the results for five determinations at 480°C. In each the diffusion equation from Thomas and Whelan[1] holds:

$$(\ell_1/\ell_0)^2 = kDt \qquad (1)$$

and

$$2(\rho_s - \rho_e)/(\rho_c - \rho_s),$$

where ℓ_1 and ℓ_0 are instantaneous and original lengths, respectively, and ρ_c, ρ_s, and ρ_e are the concentrations of silver inside, at the surface, and at large distances from the precipitate. From the Al-Ag phase diagram at 20 wt% Ag we have $\rho_s \approx 0.06$, $\rho_e \approx 0.0$, and $\rho_s \approx 0.6$, hence k = 0.2. Solving Eq. (1) from Fig. IIB. 4-2, we have

Case (a) $D = 5.4\times10^{-10}$ cm^2/sec,
(b) $D = 1.4\times10^{-9}$ cm^2/sec,
(c) $D = 2.9\times10^{-10}$ cm^2/sec,
(d) $D = 5.6\times10^{-9}$ cm^2/sec,
(e) $D = 1.0\times10^{-10}$ cm^2/sec.

All these values are within the order of magnitude of D reported in the literature.[3]

The observations suggest that the precipitates dissolve layer by layer and that final dissolution is accompanied by the elimination of partial dislocations which form the interface (the precipitates are HCP so that the last layer represents a growth fault; as the layer disappears the fault can be removed by annihilation of the partials). At present the hot stage has to be used with a long focal length objective pole piece which allows only about 100 A resolution, so that the details of the final stages are not very clear. It is hoped that we will have higher resolution facilities shortly and with these we hope to study the details of dissolution more closely and to measure rates of precipitation at dislocations. It is hoped to extend the technique to other alloy systems.

---

[2] F. C. Frank, Proc. Roy. Soc. (London) A 201, 586 (1950).

[3] C. J. Smithells, Metals Reference Book, Vol. 2 (Butterworths, London, 1955).

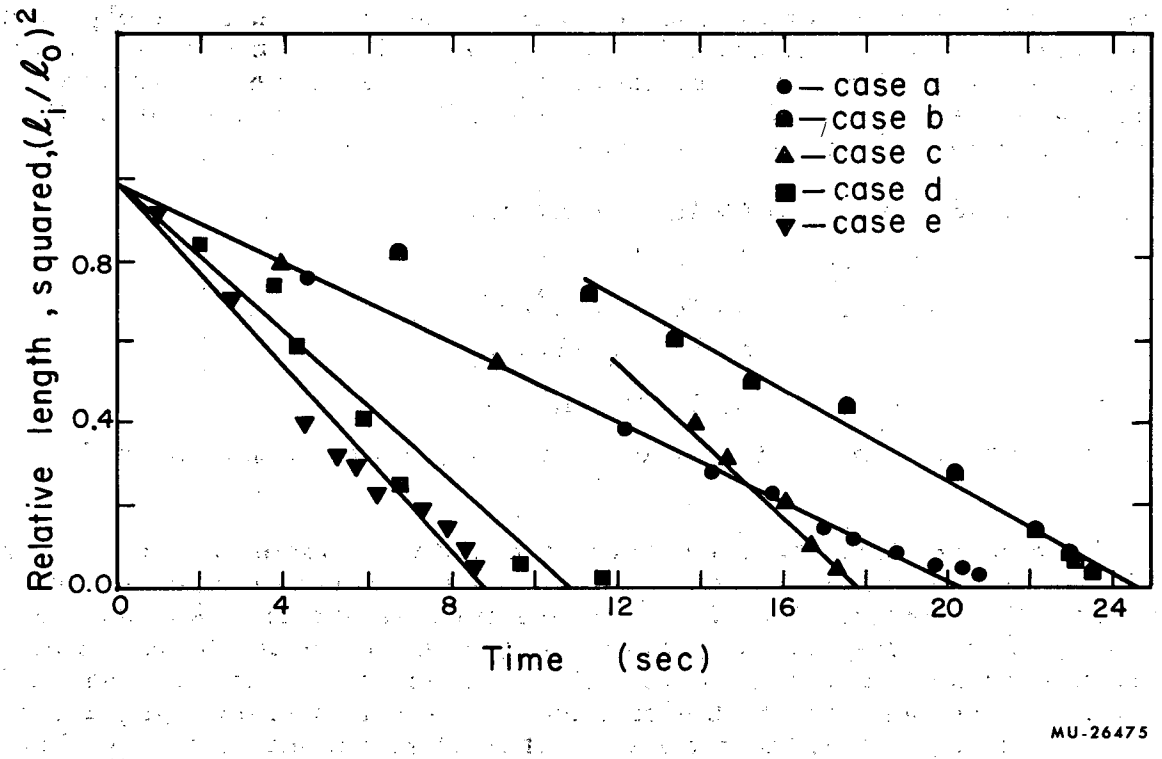

Fig. IIB. 4-2. Plots of square of relative precipitate length versus time for sequences similar to that in Fig. IIB. 4-1.

5. MECHANISM OF YIELDING IN NIOBIUM

Lenon I. Van Torne and Gareth Thomas

This report describes results obtained on the discontinuous-yielding phenomenon in niobium, and is part of a program of work on mechanisms of plastic deformation in BCC materials. Elsewhere research on the mechanical behavior of BCC metals[1-6] has mainly been concerned with analyses of the parameters σ_1 and k in the Petch relationship,[1]

$$\sigma \text{ (tensile stress)} = \sigma_1 + k\, d^{-1/2},$$

without detailed investigations of the dislocation substructures existing in the metal prior to and during yielding.[7] In our experiments, Nb foils 0.005 in. thick, fully recrystallized after 30 min annealing at 1300°C in vacuo, were examined by transmission electron microscopy after various stages of straining in an Instron machine (see Fig. IIB. 5-1).

Figure IIB. 5-2 shows the microstructure of the sample after annealing (grain size ~ 20 μ). In this can be seen large precipitates (approx 600 A diam) spaced approx 0 to 1000 A apart on dislocation lines lying in all possible ⟨111⟩ {the ⟨111⟩ directions project along ⟨112⟩ in foils of (111) orientation}. These will be barriers to all slip systems {111} ⟨110⟩ and {111} ⟨112⟩. Figure IIB. 5-3 shows the structure after 1% plastic strain (end of Luders strain), and here one observes tangling and bowing of dislocations at the pinning points. We have never observed stacking faults in our specimens.

From our results, we suggest that the contribution σ_{uY} must arise from pinning by precipitates. The shear stress τ to unpin a segment of dislocation line over a distance R is Gb/2R, thus with $G = 3.82 \times 10^3$ kg/mm^2 (Reynolds[8]), b = 2.86 A, R = 1000 A, the minimum stress $\tau = 5.5$ kg/mm^2. The measured σ_{uY} is 14.4 kg/mm^2, and if we assume $\tau = (1/2)\sigma$ the agreement is excellent. We thus attribute the upper yield stress to unpinning of dislocations locked by precipitates. The drop in stress to σ_{LY} and the Luders strain can then be explained by the passage of freed dislocations across precipitate-free areas, as suggested by the tangling in Fig. IIB. 5-3 and the high density of dislocations in Fig. IIB. 5-4. If this is correct there should be no visible Luders band during yielding; this is exactly what we have found. Furthermore, we have not been able to resolve slip bands, and

---

[1] N. J. Petch, Phil. Mag. 1, 186 (1956).

[2] H. Conrad, ibid. 5, 745 (1960).

[3] H. Conrad, J. Iron Steel Inst. (London) 198, 364 (1961).

[4] H. Conrad and G. Schoek, Acta Met. 8, 791 (1960).

[5] A. A. Johnson, J. Less-Common Metals 2, 241 (1960).

[6] A. A. Johnson, Phil. Mag. (in press).

[7] However, work is now being carried out in a coordinated program involving five different laboratories (e.g., see B. S. Lement, D. A. Thomas, S. Weissmann, W. S. Owen, and P. B. Hirsch, Substructure and Mechanical Properties of Refractory Metals, WADD TR 61-181, April 1961).

[8] M. B. Reynolds, Trans. Am. Soc. Metals 45, 396 (1953).

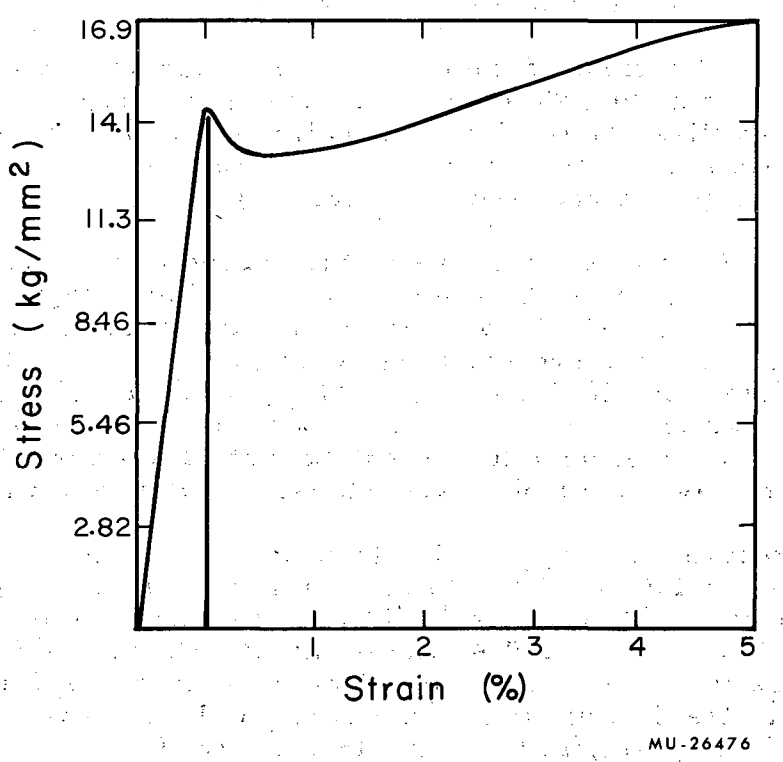

Fig. IIB. 5-1. Average stress-strain curve for polycrystalline niobium tested in tension in an Instron machine at constant strain rate of 3.3×10^{-4} sec^{-1} (room temperature). Analysis: C = 0.003%, O_2 = 0.011%, N_2 = 0.014%; grain size = 20 μ.

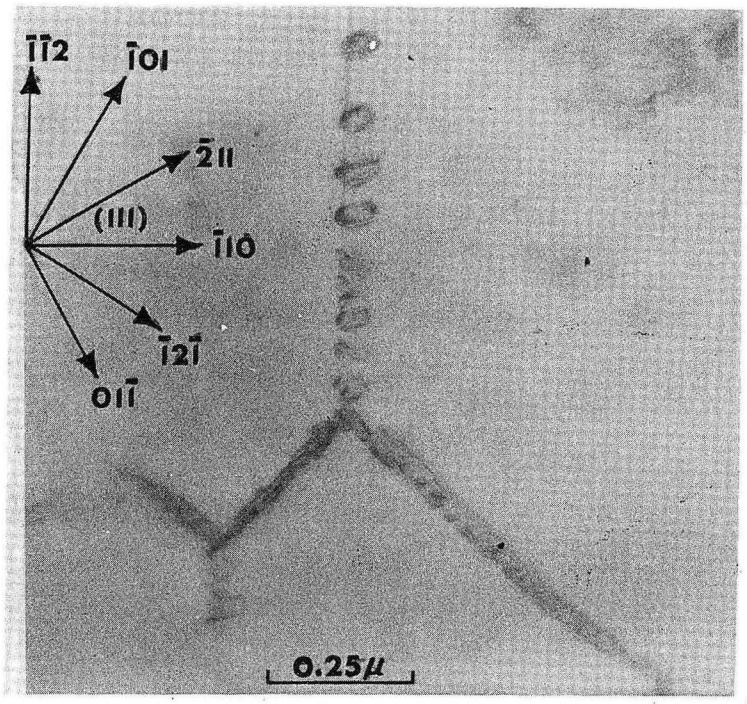

ZN-3059

Fig. IIB. 5-2. Niobium 99.9% pure, (111) foil, annealed and unstrained.

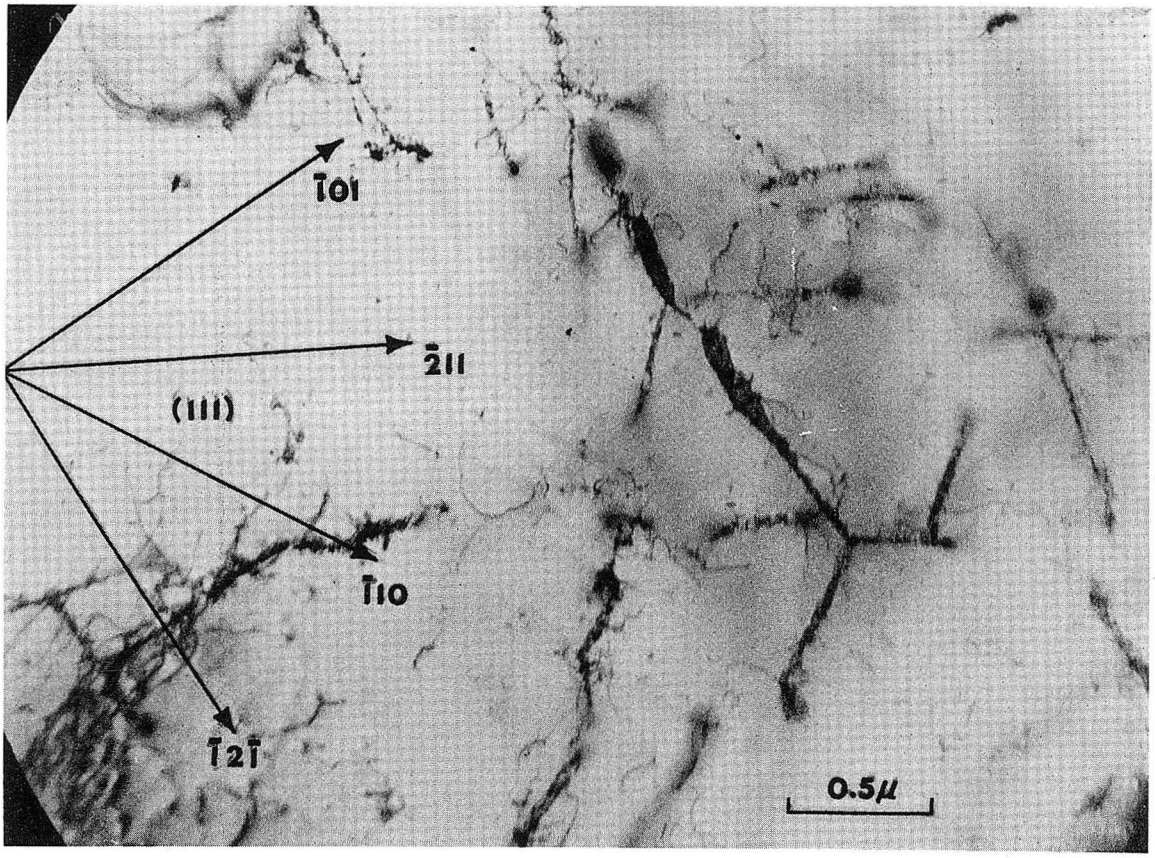

ZN-3060

Fig. IIB. 5-3. Niobium 99.9% pure, (111) foil, after 1% tensile strain.

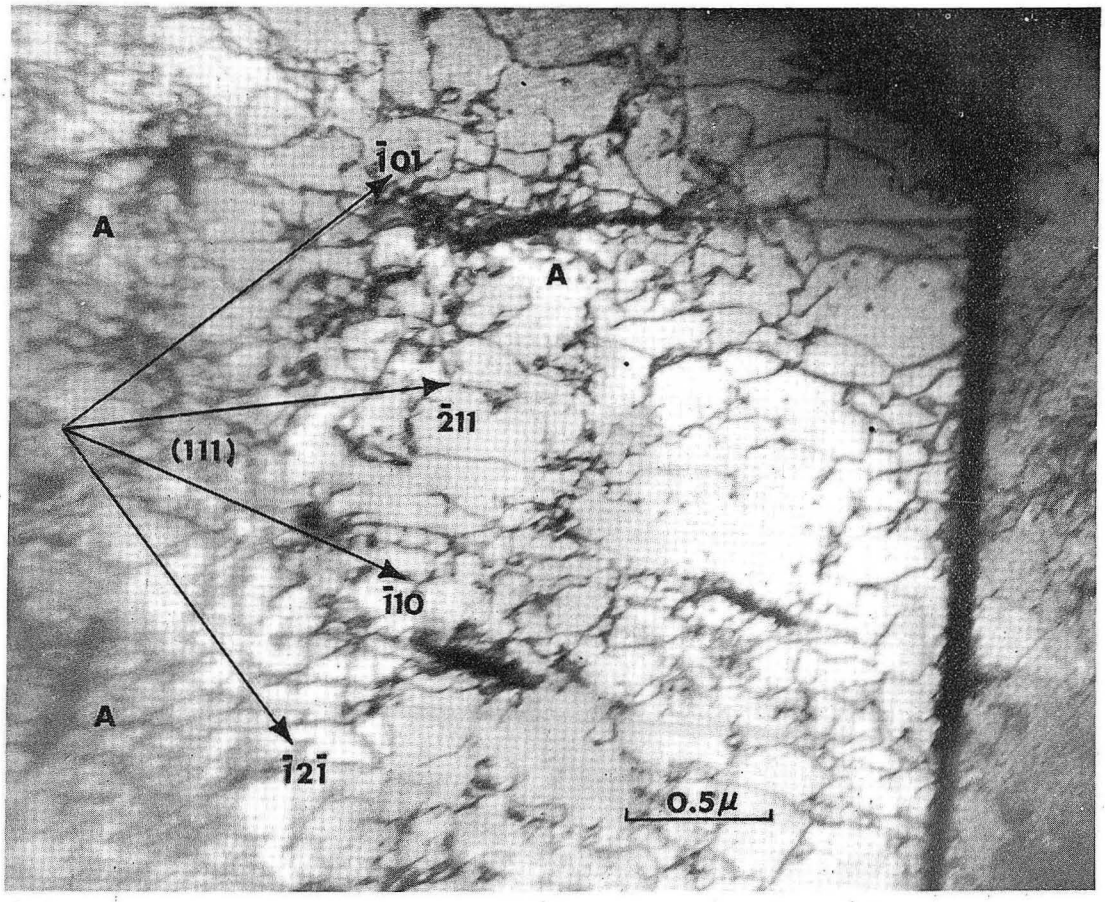

ZN-3061

Fig. IIB. 5-4. Niobium 99.9% pure, strained 5% in tension.

this is to be expected on the above hypothesis, since slip lines should be very short. The temperature dependence of σ_{uY} can now be attributed to thermally activated climb or cross slip around the pinning points, and in favorable circumstances (e.g., short climb distances) precipitates could act as sources in the manner depicted by Hirsch.[9] This also accounts for the stronger temperature dependence of σ_{uY} than of σ_{LY}. Figure IIB. 5-5 is offered as experimental evidence for this mechanism.

More experiments are to be done on the temperature dependence of σ_{uY} and on materials of higher purity; in particular we wish to investigate more closely the effect of nitrogen on dislocation locking.

[9] P. B. Hirsch, J. Inst. Metals 86, 13 (1958).

6. RESEARCH IN PROGRESS -- THOMAS

1. Development of a Thinning Technique for an Electron Microscope Study of the Structure of Pure Aluminum Deformed at Low Temperatures

A specimen of polycrystalline aluminum with a gauge length of 3 in. and cross section of 0.1×0.75 in. was deformed to 5,060 psi and 7.4% true strain. The sample was then

(a) ground and polished to remove surface roughness caused by the deformation,

(b) chemically "milled" in a 10% NaOH solution containing 5% $NaNO_2$ at 120 to 160°F until the sample was about 0.015 in. thick,

(c) electropolished in an ethyl alcohol solution containing 20% $HClO_4$ at 20 volts and a temperature $< -10°C$ until the sample appeared to be of proper thickness (empirical observation),

(d) mounted for observation in the electron microscope.

Examples of dislocation patterns could be observed by this technique. A question has been raised concerning whether the patterns seen are those present in the originally deformed samples. Since all work following step (a) is carried out at approximately room temperature, some recovery takes place in the sample. In addition, the heating by the electron beam may also cause changes in dislocation pattern. In the latter case no such change was observed during inspection of the dislocations with the electron microscope.

In order to detect any recovery effects due to treatments at room temperature, a tensile test was performed which repeated tests performed by Professor Dorn's group at 196°K except that after obtaining a stress of 6,400 psi was obtained and the load was removed the sample was annealed at room temperature for 3 hours. Subsequent application of the load at 196°K revealed that the sample now yielded at 6,080 psi. This load is believed to

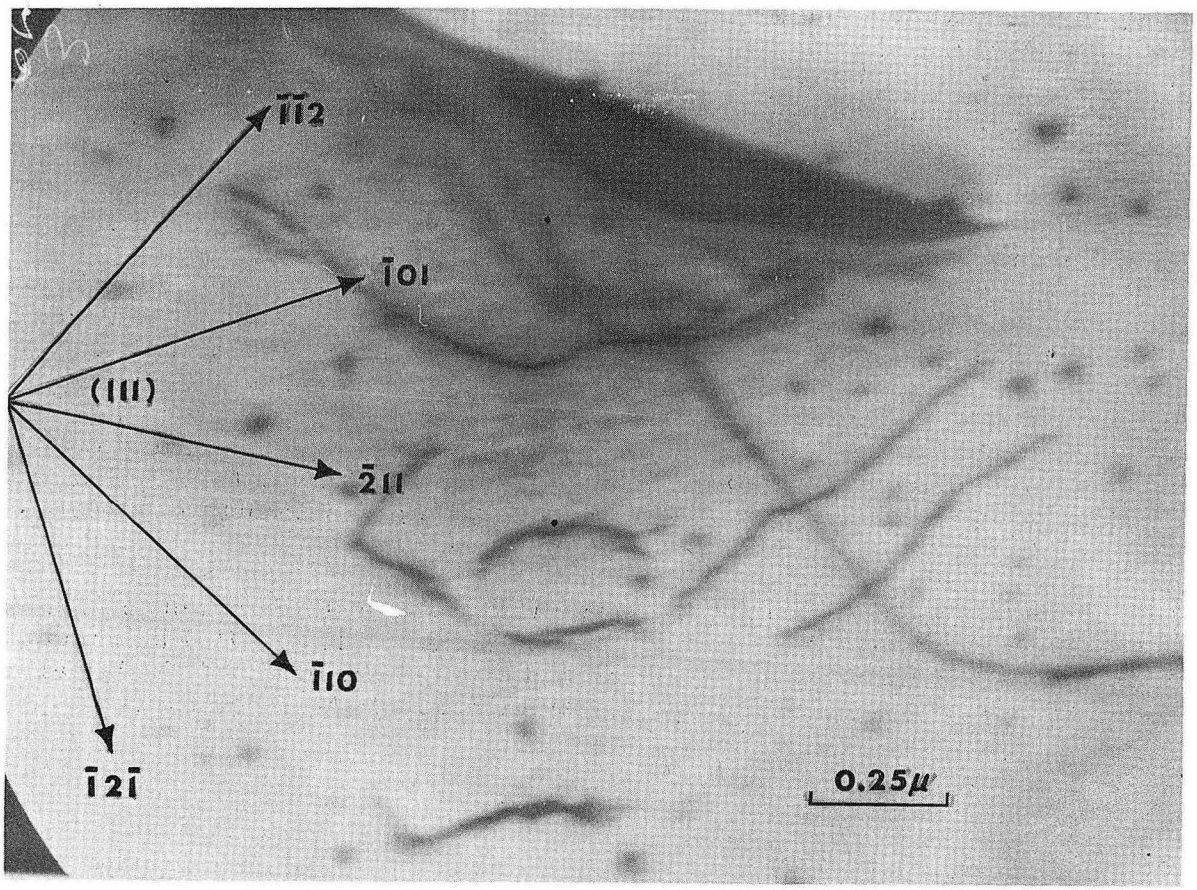

ZN-3062

Fig. IIB. 5-5. Niobium 99.8% pure, showing possible dislocation source; contains four times as much carbon and five times as much oxygen as in Figs. IIB. 5-2 through 4.

have only a minor effect upon the structure. In addition, measurements were made to obtain a stress-related parameter used in Professor Dorn's work. This parameter is

$$\beta = \partial \ln \dot{\gamma} / \partial \tau \ .$$

According to Professor Dorn's theory, this parameter is a good measure of the short-range dislocation structure. In this test the value obtained for β was identical to that obtained in previous tests not utilizing a room-temperature anneal.

It is concluded that the above technique is sufficiently developed that the proposed low-temperature study can be carried out.

2. Study of Explosion-Deformed Nickel

Recently, work has been initiated on a project to study explosively deformed nickel by means of transmission electron microscopy. Samples deformed at the Arthur D. Little Company were obtained and we are at present working on a method by which we can thin the samples for microscopy work. At present, the samples are 1/4-in. thick when received, and we have cut these pieces to half this thickness by means of an acid saw and spark cutting. They are then etched until they are 0.002 in. thick. The usual type of electropolishing may then be used in order to obtain a microscope specimen.

The present work is being carried out on facsimile samples to develop suitable techniques. Initial experiments show that an HNO_3-HCl solution will be suitable for the etching solution and a 23% perchloric–77% glacial acetic acid solution will be suitable for an electropolishing solution.

7. GROWTH FAULTS IN SILICON

Gareth Thomas and Jack Washburn

Origin of Faults

Stacking faults and coherent twins have been identified by optical and electron microscopy in epitaxially deposited silicon grown on silicon substrates. (This research is being carried on as a joint project with R. H. Finch and H. J. Queisser of the Shockley Transistor Co. All preparation of specimens has been carried out at their laboratory.) A brief report of results has been published.[1] This note summarizes the observations made so far relative to the origin of these growth faults.

[1] R. H. Finch, H. J. Queisser, and J. Washburn, J. Appl. Phys. (1962) (in press).

The stacking faults have been observed by transmission electron microscopy on thin foils prepared by chemically polishing away the substrate material and enough of the epitaxial layer to reach a thickness of about 0.5 μ.

Faulting may occur in the epitaxial layer regardless of its crystallographic orientation relative to the plane of the surface. It has been observed for (111), (110), (100), and high-index surface orientations. Figure IIB. 7-1 shows a typical pattern of stacking faults for a (111) surface. The size of the areas enclosed by faults is uniform for a given specimen. Their geometry can be explained by assuming that faults start at points on or near the original surface of the substrate material. They frequently grow out from these points on three {111} planes so as to form an inverted pyramid. However, isolated faults are also observed as well as other defects (e. g., at A, Fig. IIB. 7-2) which have not yet been identified. The following factors seem to be important relative to the frequency with which faults occur.

a. Oxygen

If all traces of oxygen are removed from the interface (e. g., by heating over hydrogen) no faults or only a few are observed regardless of the orientation of the surface. If oxygen is deliberately admitted before growth, the density of faults increases. Of all the growth variables studied, this seems to be the most important.

b. Temperature

The lower the growth temperature, the less perfect is the growth and the greater the stacking-fault density. However, it is difficult to study the effect of deposition temperature independently. Other factors that may be important include rate of deposition, state of perfection of substrate surface, effect of impurities other than oxygen, and a difference in lattice parameter between doped substrate and deposit.

c. Mechanical Damage to Substrate Surface

Scratches were deliberately introduced before growth of the epitaxial layer. They were not found to nucleate stacking faults if other factors were favorable.

Identification of Faults

The stacking-fault ribbons in Fig. IIB. 7-2 show the characteristic fringe contrast. The diffraction contrast conditions can be predicted from theory.[2] Faults and dislocations are visible only when $\bar{g} \cdot \bar{R} \neq 0$, where $\bar{g}$ is the operating reflection and $\bar{R}$ is the displacement vector. Table I gives a summary of these conditions for faults on {111}, considering the important

[2] M. J. Whelan and P. B. Hirsch, Phil Mag 2, 1121, 1303 (1957).

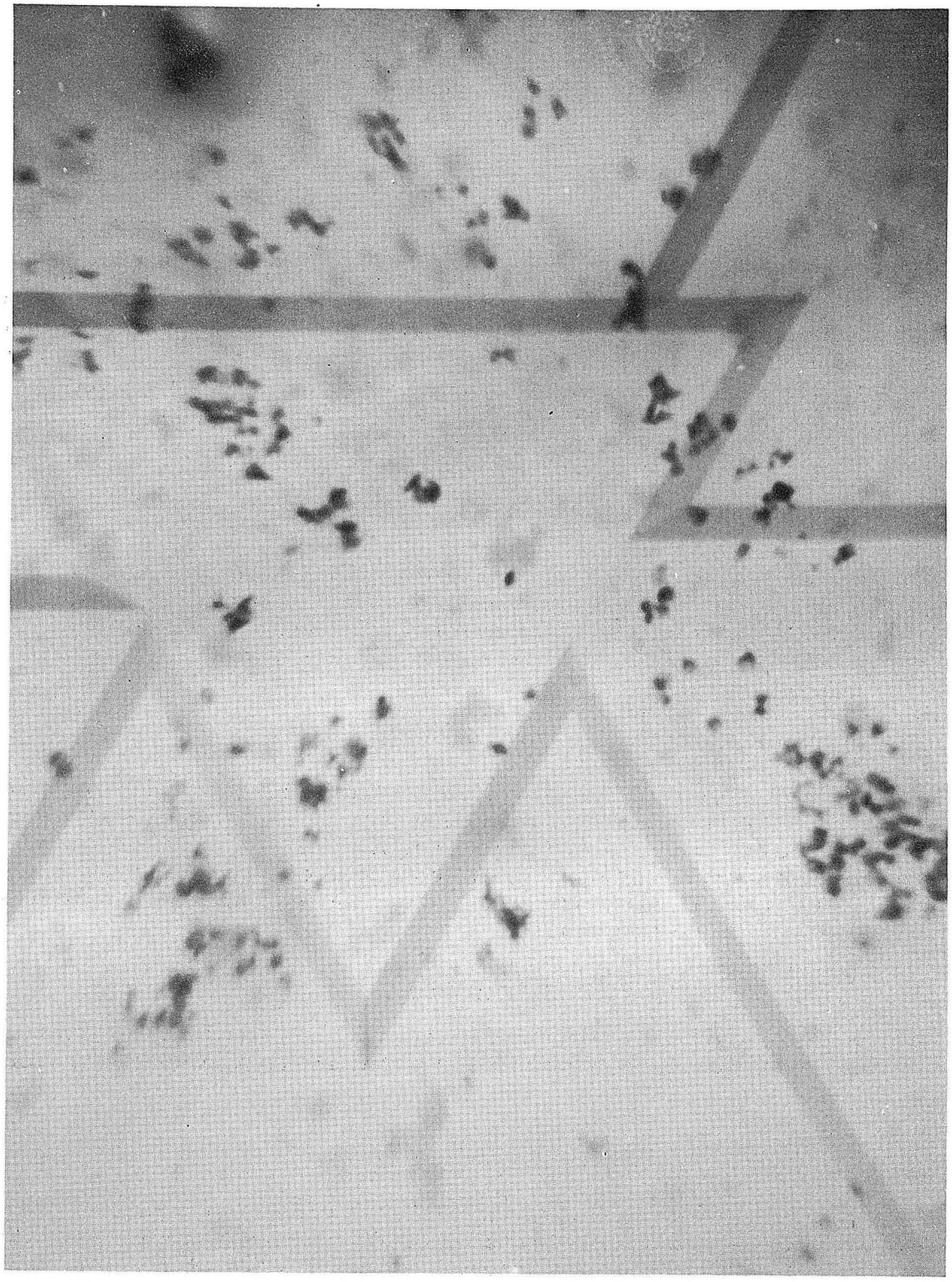

ZN-3063

Fig. IIB.7-1. [111] Si foil showing closed figures of stacking fault. × 60,000.

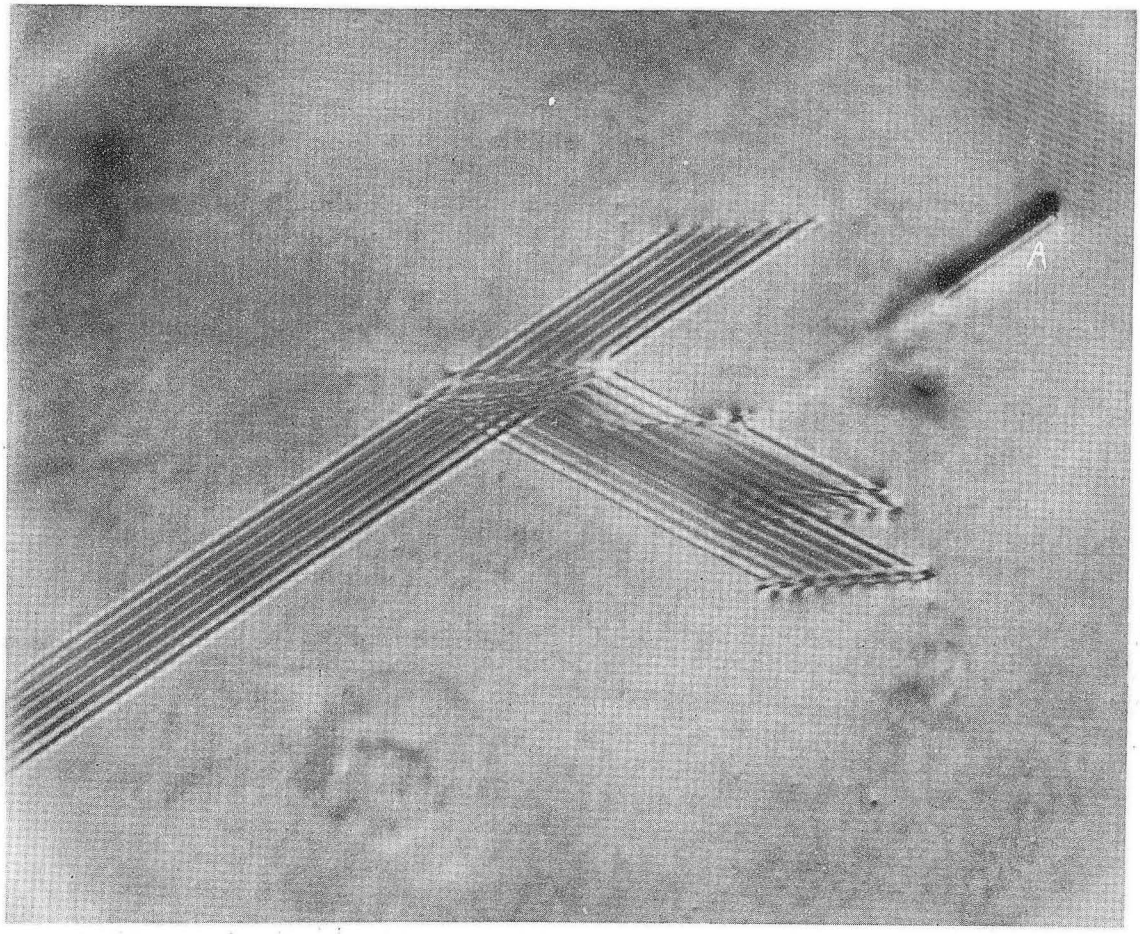

ZN-3064

Fig. IIB.7-2. [111] Si foil showing characteristic fringe contrast and bundles of dislocations at ends of faults. × 80,000.

Table I. Summary of conditions for faults on {111}.

		$\alpha = 2\pi \bar{g} \cdot \bar{R}$						
Fault Plane	$\bar{R}$	$\bar{g}$=400	$0\bar{4}0$	$2\bar{2}0$	111	$1\bar{1}\bar{1}$	$4\bar{2}\bar{2}$	311
(111)	$a/6[\bar{1}\bar{1}2]$	$2\pi/3$	$-2\pi/3$	0	0	$-2\pi/3$	0	$-2\pi/3$
$(11\bar{1})$	$a/6[\bar{1}\bar{2}1]$	$2\pi/3$	$+2\pi/3$	$2\pi/3$	$-2\pi/3$	0	$-2\pi/3$	$2\pi/3$
$(1\bar{1}1)$	$a/6[\bar{2}\bar{1}1]$	$-2\pi/3$	$-2\pi/3$	$-2\pi/3$	$-2\pi/3$	$-2\pi/3$	$-2\pi/3$	0
$(\bar{1}11)$	$a/6[\bar{2}1\bar{1}]$	$-2\pi/3$	$2\pi/3$	0	$-2\pi/3$	$-2\pi/3$	$-2\pi/3$	0

reflections corresponding to the three orientations of foils. Thus, for a [100] foil a fault on (111) should disappear for the $2\bar{2}0$ reflection and appear for the 400 reflection. Figure IIB. 7-3 shows such a fault in contrast (400 reflection operating), whereas in Fig. IIB. 7-4, after tilting to bring in the $2\bar{2}0$ reflection, the fault becomes invisible. This proves that the defects are stacking faults and that they occur on {111}. Similar experiments prove that the closed defects (Fig. IIB. 7-1) are bounded by stair-rod dislocations ($\bar{b} = 1/6a \langle 110 \rangle$), whereas enclosed defects are separated by Shockley partials $\{\bar{b} = 1/6a \langle 112 \rangle\}$. From electron diffraction patterns and contrast experiments we have also proved the existence of coherent twins in $\langle 100 \rangle$ foils. Further information on the nature of the faults can be obtained from the extinction distances corresponding to fringes. For silicon (diamond cubic, eight atoms per unit cell) the structure factor F is 8f for hkl even and $4\sqrt{2}f$ for hkl odd. The extinction distances for λ = 0.037A (100-kv electrons) and the first three reflections are as follows:

Reflection	111	220	311
Extinction distance	460	885	1050

The error in this calculation is approx 10%, since the value of t_0 depends on the deviation of the diffracted beam from the exact Bragg angle; however, measurements of t_0 for {200} and {220} reflections give values much less than the calculated values, which might suggest segregation of impurities at the fault. This point needs further verification.

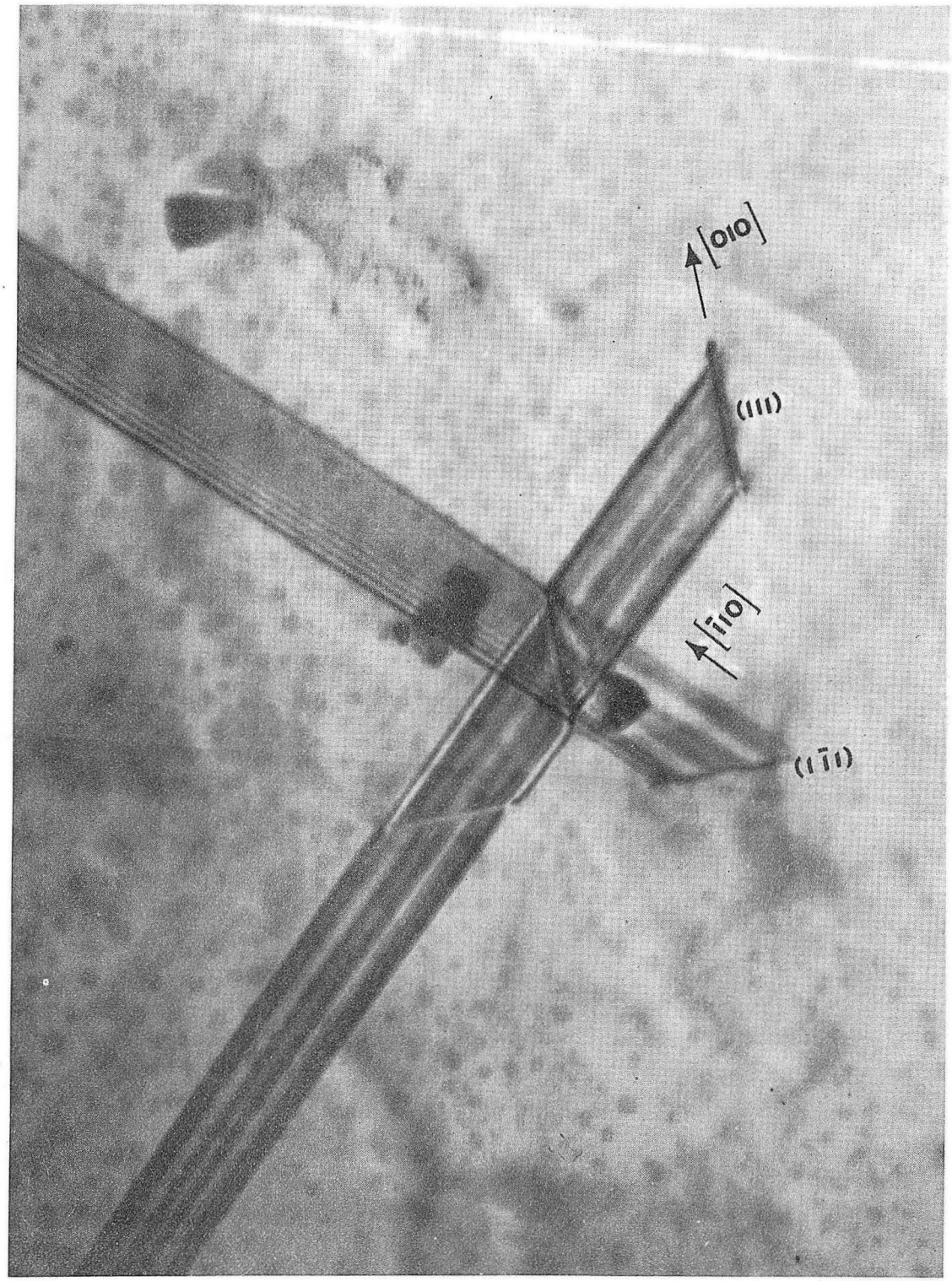

ZN-3065

Fig. IIB. 7-3. [100] Si foil (400) reflection operating.

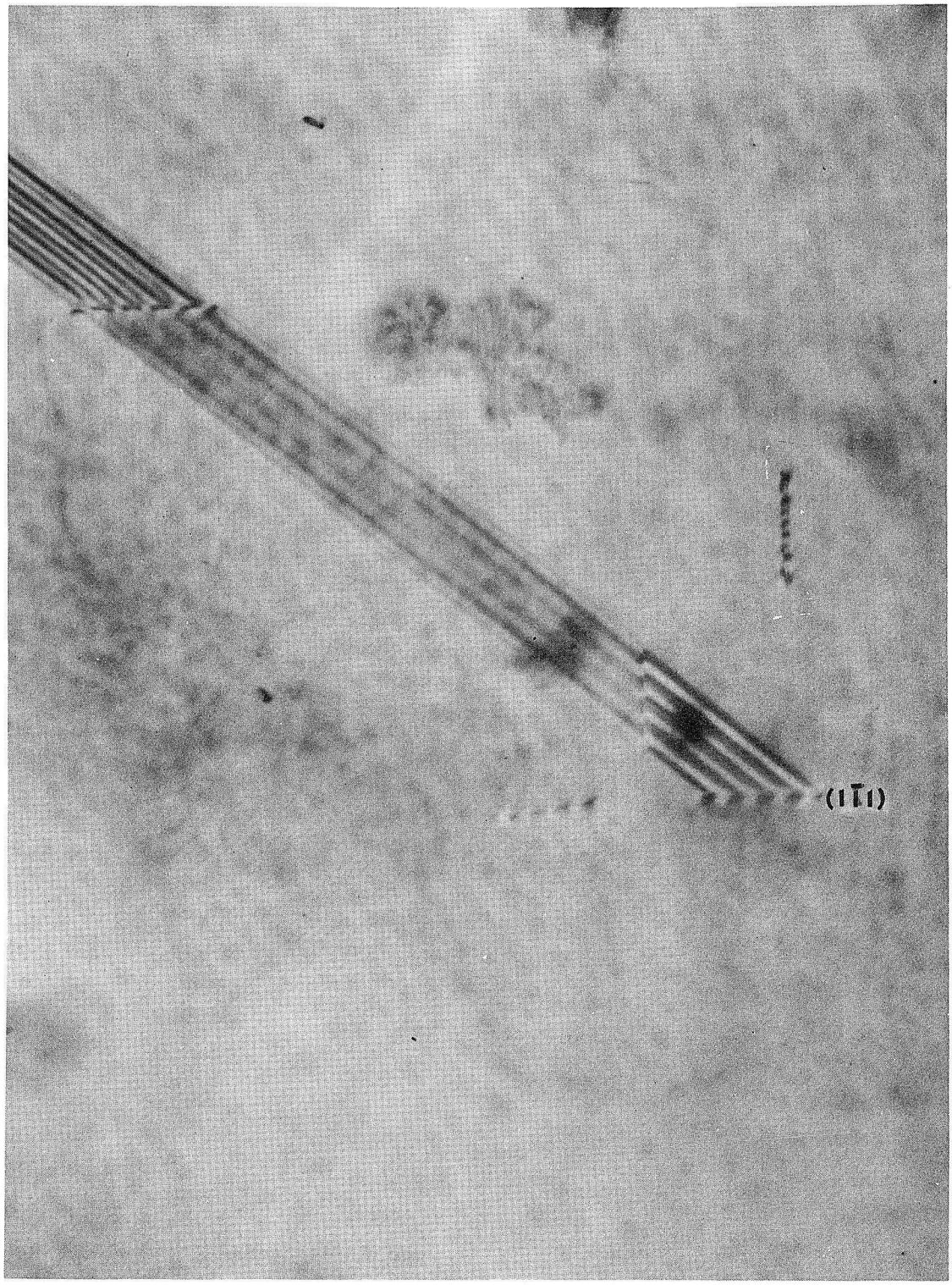

ZN-3066

Fig. IIB. 7-4. As the foil in IIB. 7-3 was tilted to utilize (2$\bar{2}$0) reflection: notice that the fault on (111) has vanished. This micrograph also shows that the (1$\bar{1}$1) faults are actually overlapping bundles.

8. DISLOCATION SUBSTRUCTURES IN DEFORMED AND RECOVERED MOLYBDENUM*

Ray Benson, Gareth Thomas, and Jack Washburn

Polycrystalline Mo specimens of purity 99.9% were deformed in tension and the resulting dislocation substructure examined by thin-film transmission electron microscopy. Other specimens were annealed at various temperatures after 5% plastic strain and examined in the microscope. The results are summarized as follows:

(a) After small amounts of plastic strain (1 to 3%) well-defined networks, mainly hexagonal in shape, and long irregular dislocations were observed. Analyses of the networks proved the existence of a [100] dislocation in addition to a a/2 ⟨111⟩ dislocations. The networks could lie in {111} or {112}, which supports results reported for other BCC metals.[1, 2]

(b) With increasing amounts of plastic strain, the dislocations formed in dense tangles, which developed into a system of subgrain boundaries (Fig. IIB.8-1). The average dislocation density was observed to increase from 1×10^9 to 8×10^9 as the strain was raised to 10%.

(c) The formation of large numbers of closed dislocation loops suggest frequent cross slip and that double cross slip or dislocation-point defect interactions are important mechanisms for spreading of slip from one glide plane to nearby parallel planes.

(d) After the annealing treatments it was found that the dislocation density decreased appreciably only after 3 hours at 900°C (Fig. IIB. 8-2). The very high density of closed loops in the annealed samples suggests that annihilation of close screw dislocation pairs occurs, leaving behind small loops where edge-dislocation jogs exist. This mechanism is illustrated in Fig. IIB. 8-3.

---

*Summary of paper presented at AIME Symposium on Dislocations, St. Louis 1961. In press 1962.

[1] W. Carrington, K. F. Hale, and D. McLean, Proc. Roy. Soc. (London) A259, 203 (1960).

[2] D. Hull, in Proceedings of the First Berkeley Materials Conference (Interscience Publishers, Inc. New York, 1962).

ZN-3067

Fig. IIB. 8-1. Mo deformed 10% in tension. Note bowing out of loops at A. × 47,000.

ZN-3068

Fig. IIB. 8-2. Mo annealed 3 hr at 900°C after 5% tensile strain. Notice large number of closed loops and lower dislocation density than in Fig. 1. × 120,000.

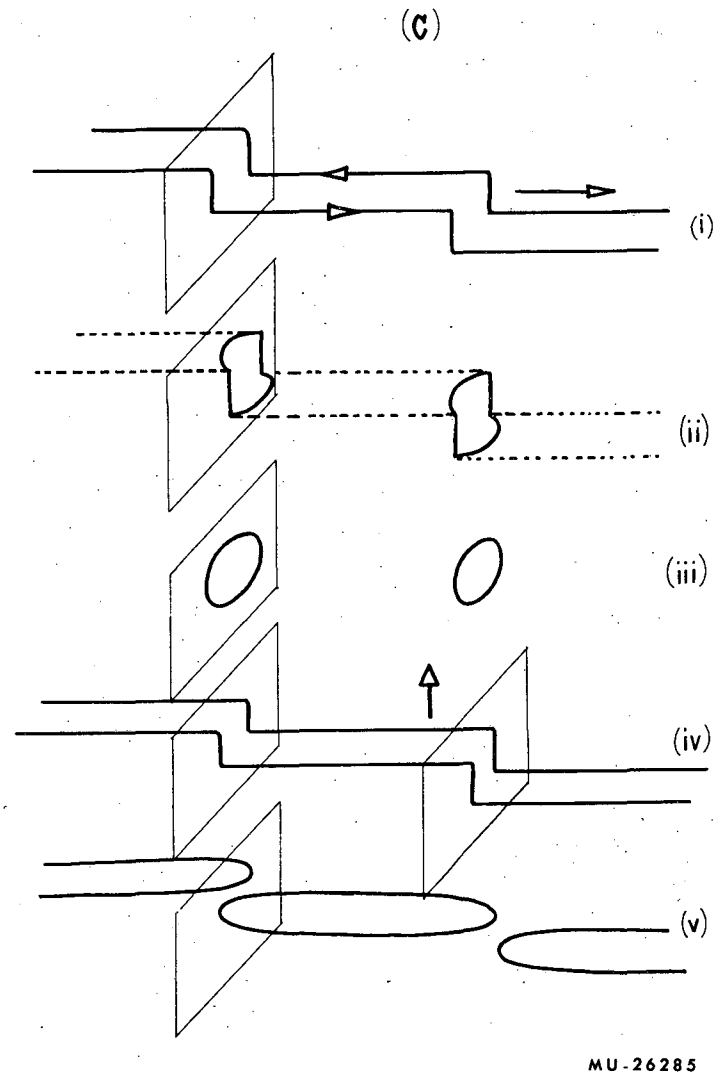

Fig. IIB. 8-3. Schematic illustration of annihilation of dislocations to form closed loops: (i), (ii), (iii), combination of screw dislocations; (iv), (v), combination of edge dislocations.

9. FACTORS AFFECTING THE DISLOCATION SUBSTRUCTURE IN DEFORMED MgO

Walter Elkington,† Jack Washburn, and Gareth Thomas

Direct observations by transmission microscopy of the dislocation substructure in slip bands of deformed MgO have revealed the presence of many elongated dislocation pairs.[1] It has been proposed that such pairs are formed when a moving screw dislocation develops a jog large enough to pin it at a point. When the screw dislocation becomes pinned, a pair of edge dislocations of opposite sign is formed when the unpinned arms on either side of the jog move forward.

This mechanism of pair formation is also capable of explaining dislocation multiplication and slip-band widening which has been observed in LiF[2] and MgO,[3] for if the edge dislocations comprising a pair are on slip planes far enough apart, they can pass each other so that each arm can act as a dislocation source on widely separated planes. For a given shear stress σ, dislocation theory requires that for the dislocations to pass each other, they must be on slip planes separated by a distance greater than $h = Gb/8\pi(1-\gamma)\sigma$, where G is the shear modulus, b is the Burgers vector, and γ is Poisson's ratio.

This paper presents results of recent electron microscope studies of the dislocation substructure in deformed MgO.

Slabs were cleaved from bulk MgO single crystals, polished in hot orthophosphoric acid, and deformed in four-point bending at temperatures from -196°C to 1200°C. Load-deflection curves were obtained for samples tested in the temperature range -190°C to 756°C. Following deformation, thin foils suitable for transmission studies were obtained from the tensile surface of each sample. Observations were made both with a Siemens Elmiskop I and a Hitachi HU-10 electron microscope.

The Effect of Deformation Temperature on Dislocation Substructure

The dislocation substructure in samples deformed at -196°C was very dense and was composed of dislocations which were often quite angular. As the deformation temperature was increased and, consequently, the stress necessary to move dislocations decreased, the substructure became less dense and the dislocations less angular. Increasing the deformation temperature above 750°C seemed to have little effect on the dislocation density, and the dislocations themselves were usually very long and straight.

A large number of dislocation pairs was observed at all deformation temperatures. The separation of the pairs increased with increasing

---

†Now at Lawrence Radiation Laboratory, Livermore.

[1] J. Washburn, G. W. Groves, A. Kelly, and G. K. Williamson, Phil. Mag. 5, 991 (1960).

[2] J. J. Gilman and W. G. Johnston, Dislocations and Mechanical Properties of Crystals (John Wiley and Sons, Inc., New York, 1956), p. 116.

deformation temperature but not to the extent originally expected. If the mechanism of pair formation described earlier was operating as a dislocation source, it would be expected that there would be some pairs whose separation approached the theoretical maximum h_{max}. The largest pair observed in a sample deformed at room temperature at a stress of 7.5 kg/mm^2 had a separation of 140 A. For this flow stress, however, h_{max} would be expected to be 300 A. The comparison of observed to calculated (i. e., h_{max}) separation in other samples showed that the observed separation was always less than expected.

That the values observed did not approach the theoretical values more closely might indicate that the proposed mechanism is not operating. Just as likely, however, it is an indication that only a very few pairs are formed which are large enough to be potential dislocation sources, and since only a small portion of the total sample is actually observed in the electron microscope (at best about 10^{-9} cm^3), these pairs were not observed.

At deformation temperatures of 750°C and above, it was observed that narrow dislocation pairs broke up into rows of small circular prismatic loops. This phenomenon has been observed previously by Washburn et al. in MgO[1] and by Price in zinc[4] and Cd.[5] The driving force for this change in dislocation configuration has been shown to be the associated decrease in elastic energy. Since the transformation to loops occurs at temperatures at which thermally generated vacancies are present only in small concentrations, the mechanism appears to be one of local diffusion along dislocations. In this study it was observed that the loops were formed by pinching off from the end of the pair. This is to be expected, since there is an additional climb force here due to the sharp dislocation curvature at the end of the pair.

The Effect of Grown-In Dislocations on Pair Formation

For a dislocation pair to be formed it appears that a screw dislocation must become jogged. Jogs may be formed in MgO by any one of the following mechanisms: (a) cross slip on a {100} slip plane, (b) intersection with other dislocations having the proper Burgers vector, and (c) by nonuniform collection of point defects.

Only in two special cases, however, does it seem possible that these mechanisms can lead to a jog sufficiently large to form a pair that can act as a dislocation source. The first case is one in which a screw dislocation intersects a subgrain boundary and develops many jogs of the same sign. The second case is one in which a screw dislocation cuts through a slip band that contains an excess of dislocations of one sign and therefore develops many jogs of the same sign.

---

[3] J. Washburn and A. Gorum, Rev. Met. 57, 67 (1960).

[4] P. B. Price, Phil. Mag. 5, 873 (1960).

[5] P. B. Price, J. Appl. Phys. 32, 1746 (1961).

Etch pit studies have shown, however, that dislocation multiplication does not depend upon dislocations passing through either slip bands or subgrain boundaries. The question, then, is how large jogs are formed.

Electron microscope observations of sample areas where glide dislocations had intersected grown-in dislocations have suggested a mechanism that may cause large pairs to form. In these areas, it was found that many edge dislocation pairs were present. It is most likely that these pairs were formed when a moving screw dislocation containing jogs intersected a grown-in dislocation and became pinned. A schematic diagram of this process is shown in Fig. IIB. 9-1. Figure IIB. 9-2 is an electron micrograph showing numerous pairs in a slip band of a sample deformed at room temperature. It can be seen that two of the pairs have formed at a grown-in dislocation.

In view of the large number of pairs that have been observed to form at grown-in dislocations, it is possible that two pairs may be formed, each having one dislocation on a mutual slip plane. If the jogs that led to the pinning of these dislocations were of the same sign, the edge dislocations on the mutual slip plane would be opposite in sign and could move together and be annihilated. A schematic diagram of this process is shown in Fig. IIB. 9-3.

It is not necessary, however, that the two dislocations lie on the same plane. Even if they were several Burgers vectors away, they would still reduce their stress fields appreciably when they move together and would essentially leave one larger pair. By this mechanism, it would be possible for a number of small pairs to join and form a large pair which could act as a dislocation source.

10. PLASTIC BEHAVIOR AT LARGE STRAIN

Gollapudi Murty and Jack Washburn

Evidence has been obtained for the importance of stacking-fault energy as one of the factors that control the maximum flow stress to which a face-centered cubic metal can be work-hardened. By deforming 1-cm cubes in compression successively along each of the three orthogonol axes, very large total plastic strains were achieved while the shape of the specimen was kept almost invariant.

In all cases a maximum flow stress was approached after an initial period of hardening. This maximum hardness depended on the temperature, and represented an equilibrium dislocation substructure in the metal. This could be shown by deforming first at 78°K until the maximum corresponding to this deformation temperature had been reached, and then continuing the deformation at 300°K. Softening then took place, the flow stress approaching the same maximum as would have been obtained by deforming from the start at the higher temperature.

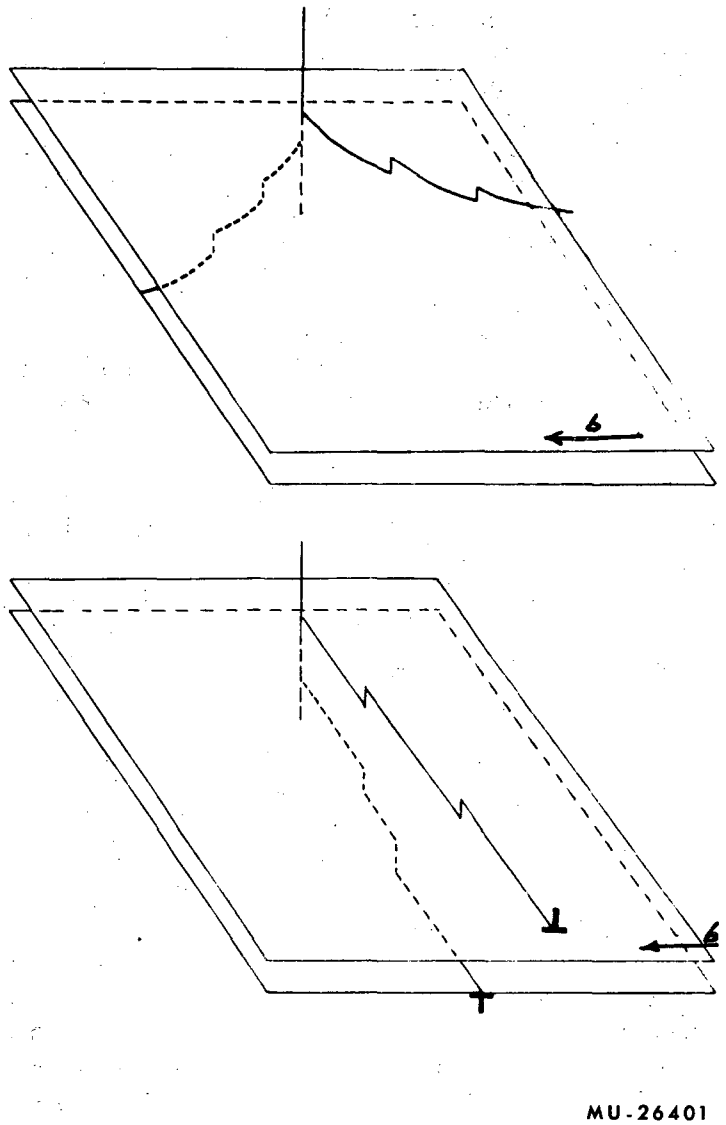

Fig. IIB. 9-1. Schematic illustration showing how plus-minus pairs of dislocation can form when a screw dislocation containing jogs cuts a grown-in dislocation.

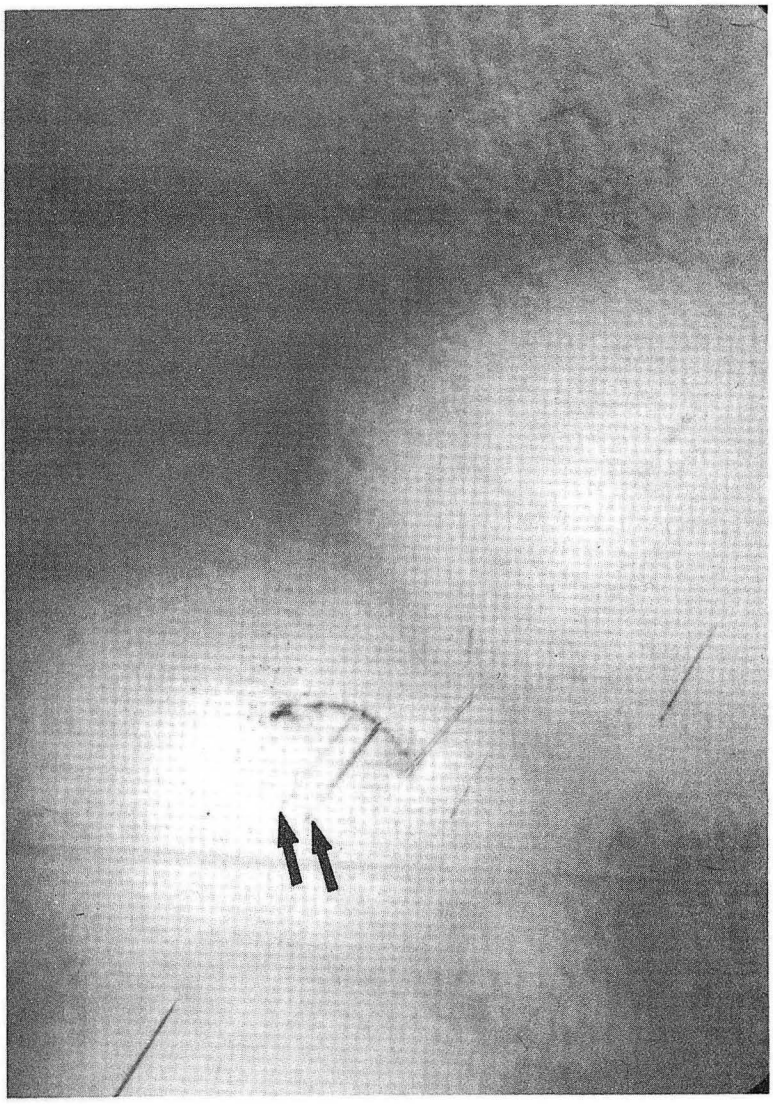

ZN-3081

Fig. IIB. 9-2. Edge-dislocation pairs in slip band of MgO sample deformed at room temperature. Arrows locate pairs formed at a grown-in dislocation.

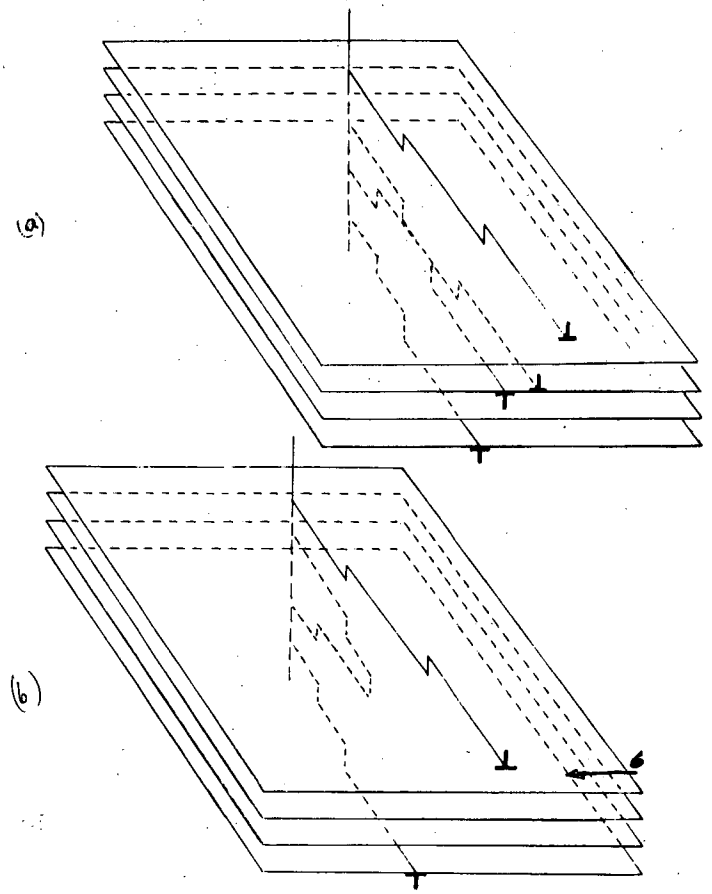

Fig. IIB. 9-3. Schematic illustration showing (a) two plus-minus pairs forming, each with one dislocation on a mutual slip plane. If these are of opposite sign they will move together and annihilate (b).

The dependence of maximum flow stress on stacking-fault energy was demonstrated by comparing the maximum flow stress for a series of CuAl alloys for which the estimated stacking-fault energy varied from 37 ergs/cm^2 to 20 ergs/cm^2. Stacking-fault energies and the corresponding maximum flow stress are summarized in the table.

Composition	γ (ergs/cm^2)	σ_{max} (20°C) (psi)
Cu	37	55400
Cu - 0.55% Al	33	56400
Cu - 1.17% Al	28	64000
Cu - 2.33% Al	20	74400

A factor that was found not to be important was the presence of grain boundaries. Single-crystal specimens and polycrystalline specimens of the same composition approached almost the same maximum flow stress.

11. DEFORMATION SUBSTRUCTURES IN COPPER

William L. Price† and Jack Washburn

New information on the nature of the complex dislocation network in deformed copper has been obtained by transmission electron microscopy of specially oriented single-crystal specimens. Flat tensile specimens having a (110) surface were pulled along the $[1\bar{1}1]$ direction. For this tensile direction three slip planes are active. Two of these are inclined at 35° to the (110) surface and the third is at 90° to the surface. The inactive slip plane is also at 90° to the surface. The curve of resolved shear stress vs resolved shear strain for this orientation is shown as Fig. IIB. 11-1. Strains at which transmission electron microscopy observations were made are indicated. Figure IIB. 11-2 shows a typical substructure.

Because of the special orientation of the {111} planes relative to the surface of the electron microscope foil, it was possible to show the following.

(a) Lomer-Cottrell dislocations were not important for the development of tangles.

(b) The subgrain boundaries that developed from the dislocation tangles did not tend to lie on active glide planes.

(c) Individual segments of dislocation line, within the tangles, did not show a noticeable preference for the {111} planes. Even at small strains the dislocations in the tangles were heavily jogged.

†Now with Lockheed Corporation Space and Missile Division, Palo Alto, Calif.

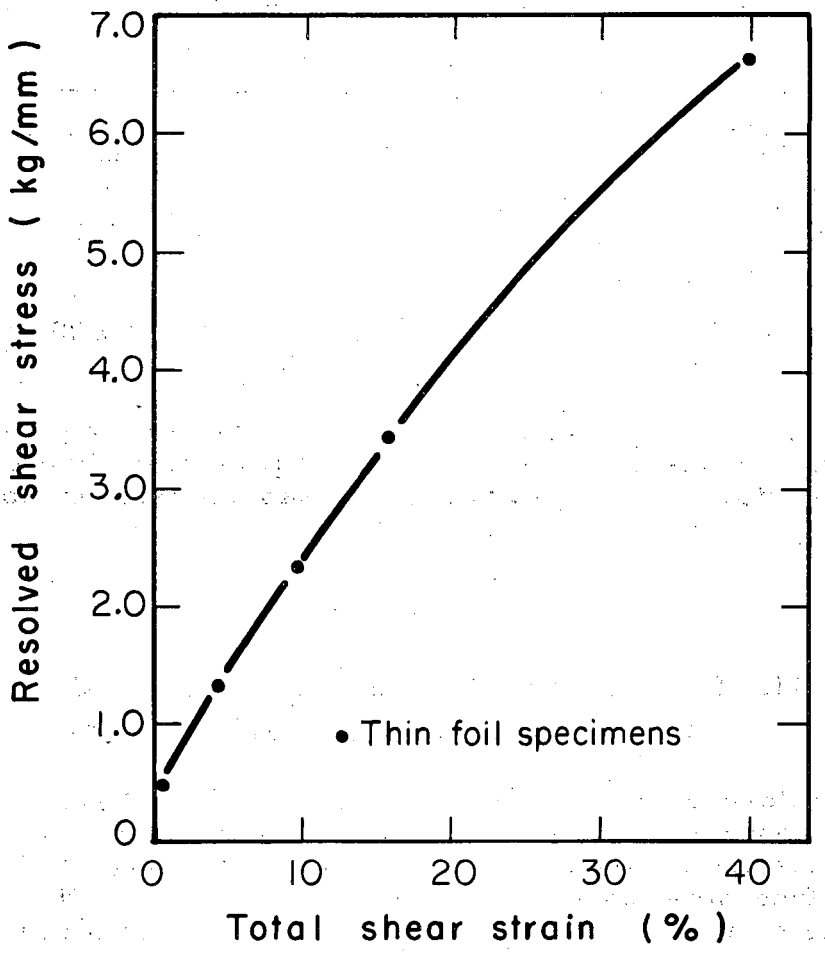

MU-26286

Fig. IIB. 11-1. Curve of resolved shear stress vs resolved shear strain for copper crystal with [111] tensile axis. Dots show strains at which transmission electron microscope observations were made.

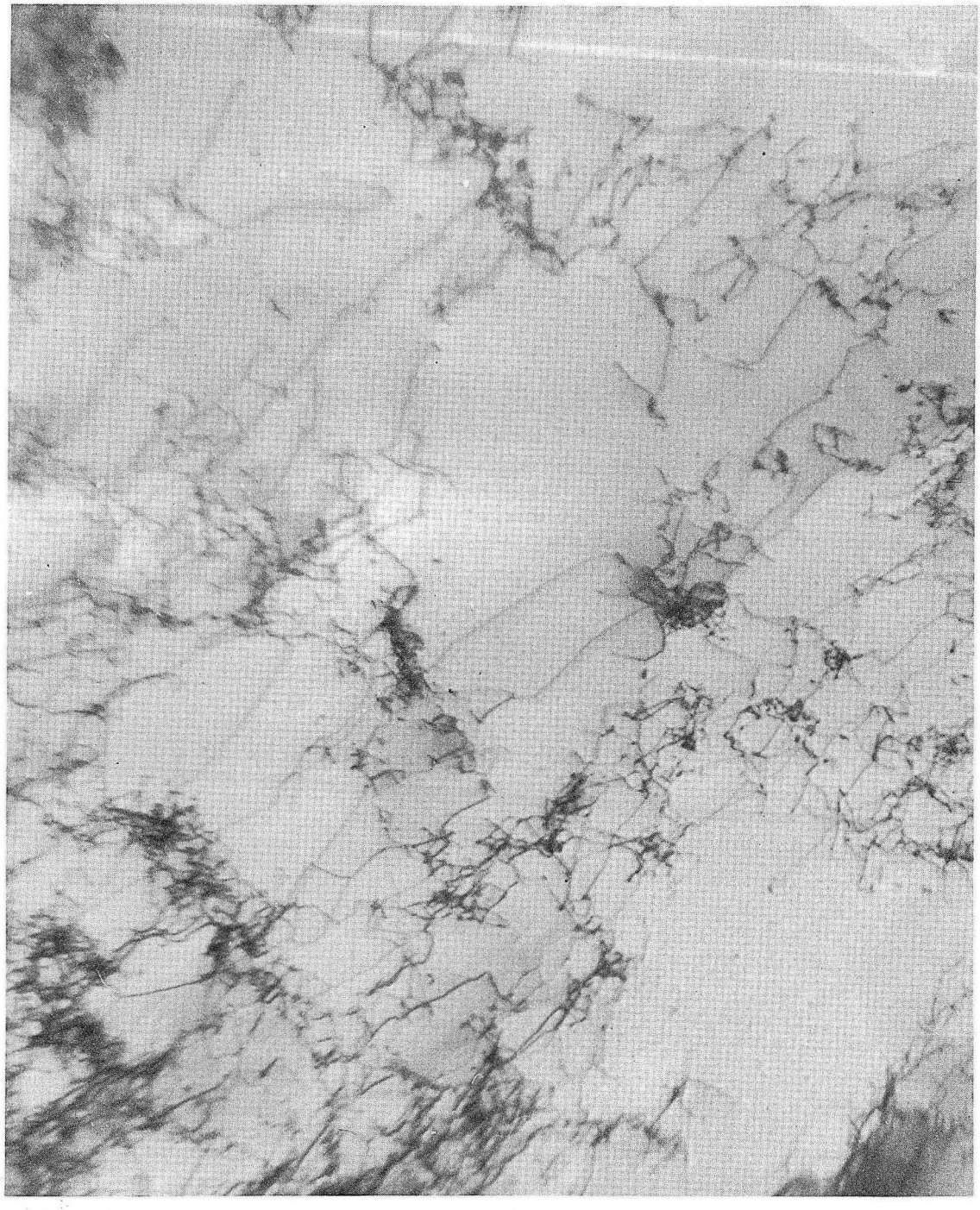

ZN-3069

Fig. IIB.11-2. Transmission electron micrograph showing dislocation substructure in deformed copper crystal after 10% total shear strain. × 40,000.

(d) The average length of individual segments of dislocation between nodes decreased with increasing strain.

(e) The average size of the relatively perfect volumes of crystal between tangles was established at small strains and did not change much over the strain range studied.

(f) The subgrains varied in size from about 0.2 μ to 2 μ.

12. FATIGUE DAMAGE IN MgO

Karatholuvu N. Subramanian† and Jack Washburn

The nature of the damage produced by fatigue in magnesium oxide has been studied by correlated optical-etch pit and transmission electron microscopy observations. Specimens were deformed in cantilever bending up to more than 10^6/cycles. Assuming elastic behavior, the calculated maximum stress (alternately compression and tension) at the outer surface was just below the yield stress as measured in a tension test.

The experiments have given new information concerning the mechanism of slip-band growth and the formation of dislocation dipoles during deformation. Study of slip-band intersections has given further support to the idea that at any instant during deformation all the moving dislocations are at the interfaces of widening slip bands. The same observations also confirm the idea that jogs formed when intersecting screw dislocations cut through each other can start the formation of plus-minus edge-dislocation pairs.

Figure IIB. 12-1 shows an example of a slip-band intersection. Slip planes for the horizontal and vertical bands lie at 90° to the surface and their slip directions are parallel to the surface. If moving dislocations exist only at the interfaces of the bands, then moving screw dislocations on the two systems cut through each other only along four lines that end on the external surface at the four corner points marked "A" on the photograph. As the two bands grow wider, the positions of these lines change. The fact that etching reveals successive positions of these lines of intersection as a deep groove is strong evidence for an abnormally high density of plus-minus edge dislocation pairs or dipoles along the surfaces that are generated.

The variable width of slip bands that can be seen in Fig. IIB. 12-1 is possible in fatigue because a severe stress concentration does not build up when the width of a band changes. The net strain within bands formed during fatigue is probably close to zero. Therefore, intersecting bands are much more effective barriers than in unidirectional deformation.

Dislocation substructure within the slip bands was similar to that found for unidirectional deformation. Figure IIB. 12-2 is a typical example showing long plus-minus edge dislocation pairs.

---

†Now at Michigan State University, East Lansing, Michigan.

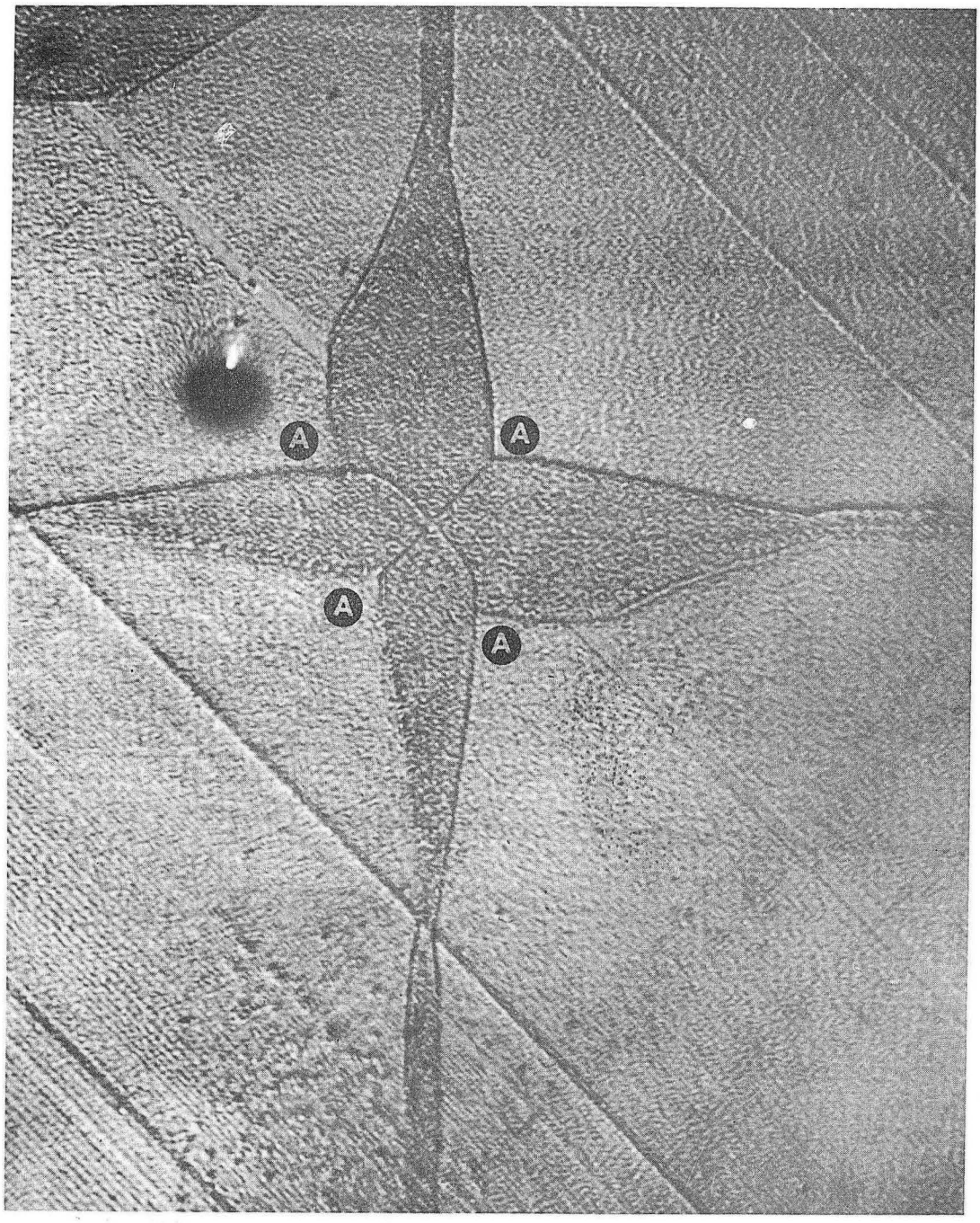

ZN-3082

Fig. IIB. 12-1. Slip bands on the surface of a magnesium oxide fatigue specimen as revealed by dislocation etch pits. × 500.

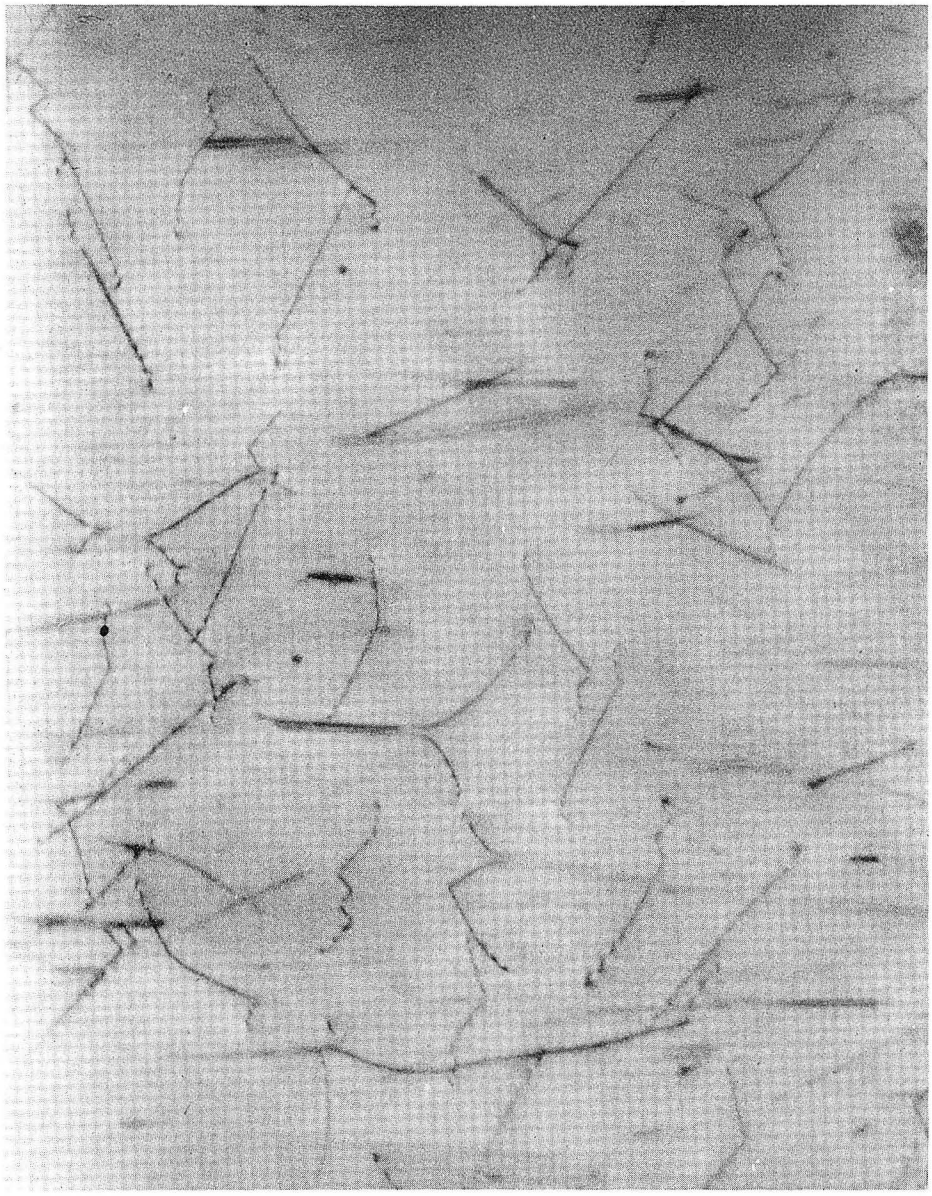

ZN-3070

Fig. IIB. 12-2. Transmission electron micrograph showing dislocation substructure within a deformed region after 10^6 cycles of fatigue. $\times$ 60,000.

13. RESEARCH IN PROGRESS -- WASHBURN

Active research is being carried out at present in these areas:

1. A theoretical study of the migration and clustering of vacant lattice sites during cooling of a crystal from high temperature.

2. The interaction between moving dislocations and prismatic loops and helical dislocations, being investigated both from the theoretical point of view and by experiments using transmission electron microscopy.

3. An experimental study of quench hardening in copper and gold, making use of coordinated small-angle x-ray scattering, electrical conductivity, length change, and mechanical measurements.

4. The mechanical behavior of materials at very large plastic strains; variables being considered are crystal structure, stacking-fault energy, mode of deformation, and temperature of deformation.

C. KINETICS OF DISLOCATION MECHANISMS

1. DETERMINATION OF THE SHORT-RANGE ORDER IN THE INTERMETALLIC COMPOUND Ag_2Al

John E. Dorn and Joachim Neumann

Because investigations of the mechanical properties of the hexagonal Ag-Al intermetallic phase indicated the presence of short-range order,[1] an investigation of the degree of short-range ordering by means of x-ray analysis was started.

The order in a binary alloy of components A and B can be expressed by the short-range order coefficients $\alpha_{\ell mn}$, which are defined by

$$\alpha_{\ell mn} \equiv 1 - P_{\ell mn}/2x_A x_B .$$

$P_{\ell mn}$ is the probability of finding an A-B pair separated by the vector $\vec{r}_{\ell mn}$, where ℓ, m, and n are the vector components along the axes a_1, a_2, and c_1 of the hexagonal crystal; x_A and x_B are the atomic fractions of A and B.

The short-range-order coefficients are determined by measuring the background intensity over a unit cell in reciprocal space, using a single crystal and monochromatic radiation. The intensity distribution can be expressed by a Fourier series, with the α's being the Fourier coefficients.

To obtain strictly monochromatic radiation, an asymmetrical Guinier-type monochromator for molybdenum K-α radiation was built (Fig. IIC. 1-1). The α_1 and α_2 radiations are separated by a platinum slit. Corrections will be made for contributions to the intensity due to incoherent and thermal scattering. The former is determined from tables, the latter by measuring the intensity as function of temperature. A chamber has been built which allows measurements of single crystals (3/4 in. diam, 1/4 in. thick) in vacuum (to eliminate air scattering) between room temperature and liquid nitrogen temperature. Figure IIC. 1-2 shows an assembly of the chamber with the beryllium window to the left and the vacuum connection to the right. The upper part of the chamber with the specimen holder is shown in Fig. IIC. 1-3; in Fig. IIC. 1-4 can be seen the gear mechanism which permits a rotation and a tilt of the specimen about two horizontal axes perpendicular to each other. The equipment is now completed and attempts are being made to grow rather perfect single alloy crystals.

---

[1] J. D. Mote, K. Tanaka, and J. E. Dorn, Trans. Am. Inst. Mining Pet Engrs. (AIME) 221, 858 (1961).

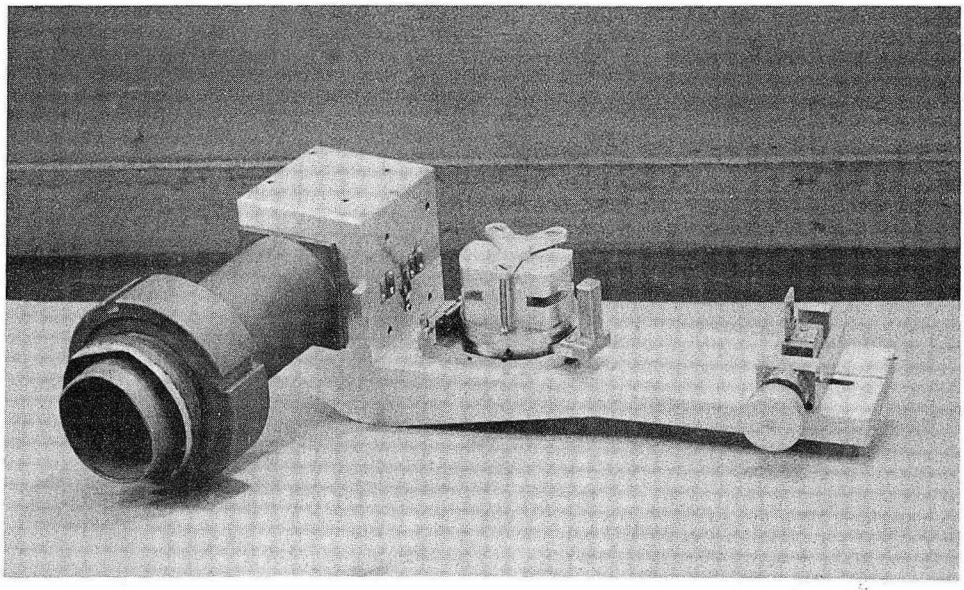

ZN-3071

Fig. IIC. 1-1. Monochromator (attached to x-ray tube).

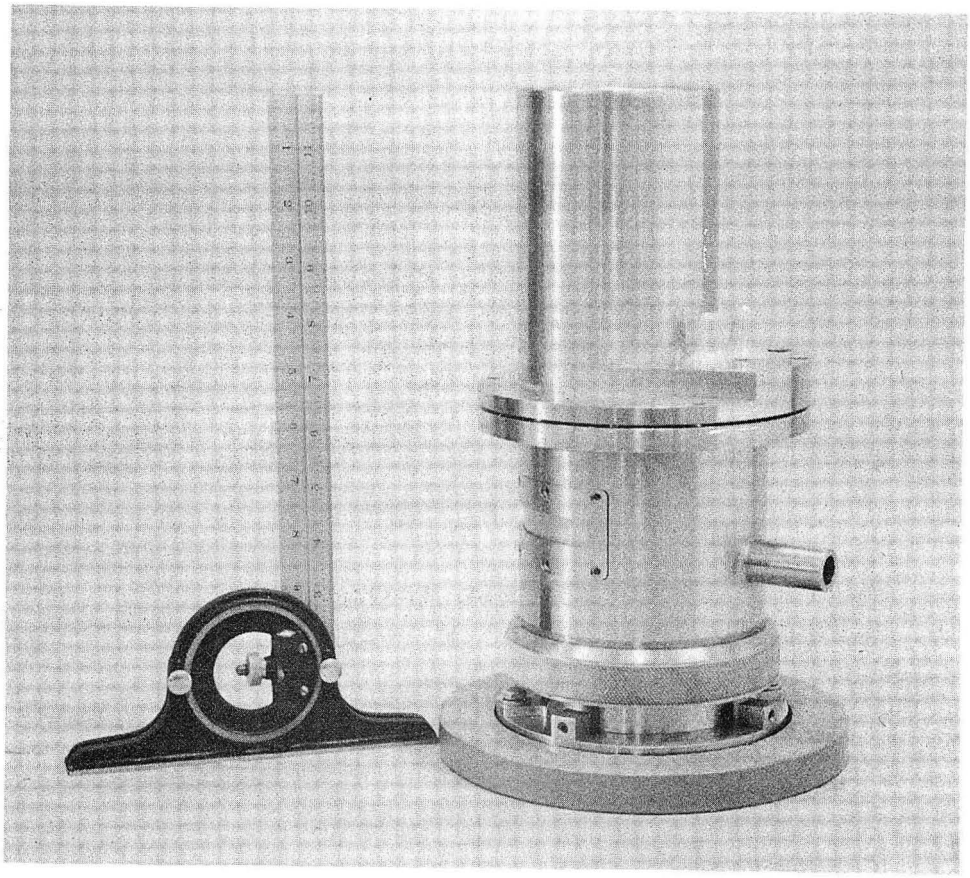

ZN-3072

Fig. IIC. 1-2. Assembly of low-temperature vacuum chamber.

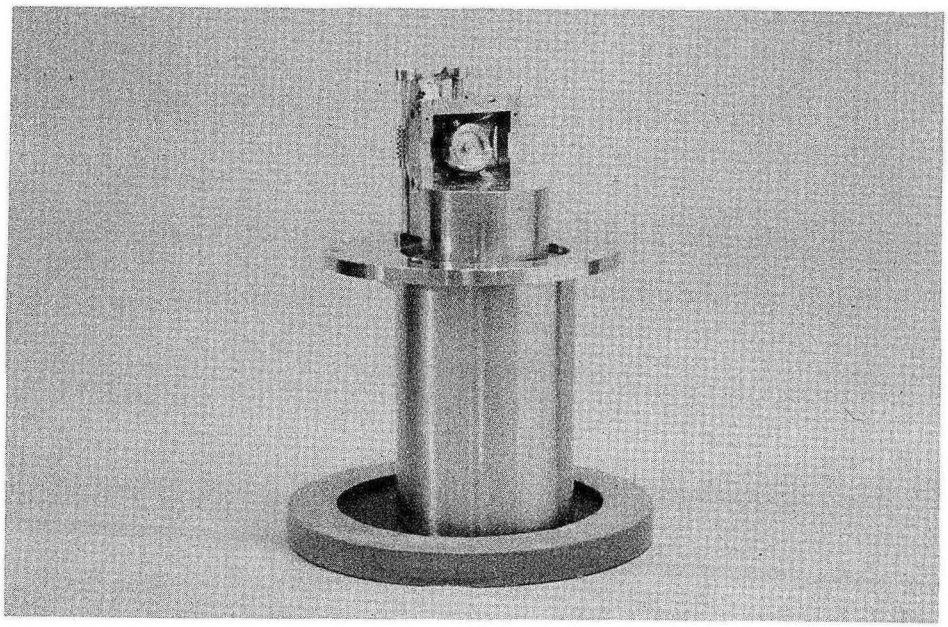

ZN-3073

Fig. IIC. 1-3. Upper part of chamber: specimen holder.

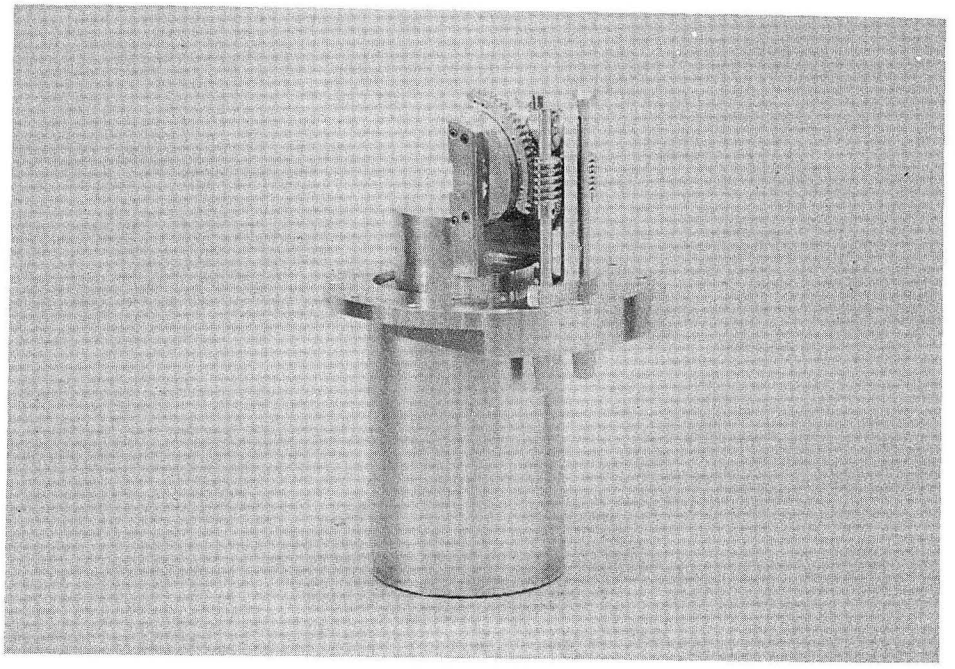

ZN-3074

Fig. IIC. 1-4. Upper part of chamber: gear mechanism.

2. ON THE NATURE OF DISPERSED-PARTICLE STRENGTHENING AT LOW TEMPERATURES

John E. Dorn and Jack B. Mitchell

This investigation concerns the rationalization of the effect of dispersed hard phases on the plastic behavior of alloys. By use of techniques previously developed to study the strain-rate dependence on the stress and temperature,[1,2] it will be possible to determine the activation energy, activation volume, density of forest dislocations, and back stresses. Data now available on a fine and a coarse dispersion of $CuAl_2$ in Al reveal that the low-temperature strain-rate-controlling mechanism is that of intersection of dislocations.

Experiments are now in progress to determine the nature of particle-dislocation interactions that contribute to the strain hardening. Analysis of low-temperature flow stress measurements will permit a determination of the nature of the change in long-range temperature-independent strengthening contributions resulting from dislocation pile-up on particles acting as barriers to dislocation glide.

The analysis will also reveal the increase in dislocation density with strain and the resulting short-range temperature-dependent strengthening contribution.

Measurements and analysis are now in progress to determine the relative magnitudes of these strengthening contributions for various particle sizes and distributions. The results of this analysis together with electron-microscopic observations of the dislocation distributions in these materials should disclose the mechanisms of strengthening due to dispersions of second-phase particles.

---

[1] S. K. Mitra, P. W. Osborne, and J. E. Dorn, Trans. AIME 221, 1206 (1961).

[2] S. K. Mitra and J. E. Dorn, On the Nature of Strain Hardening in Face-Centered Cubic Metals, Trans. AIME (to be published).

3. ON THE RATE-CONTROLLING MECHANISM OF DEFORMATION IN ALUMINUM-MAGNESIUM ALLOYS

John E. Dorn and Sandip K. Mitra

The major objective of this investigation is to uncover the rate-controlling dislocation mechanisms that are operative in polycrystalline aluminum-magnesium alloys.

Polycrystalline specimens of aluminum 0.79, -0.97, and 2.82 wt.% magnesium were deformed over a range of temperatures down to 4°K.

During deformation in tension at a given strain rate and temperature--viz, 1×10^{-4} per second at 90°K--the strain rate was reduced occasionally to one-tenth of the initial value, and the quantity

$$\beta = \frac{\partial \ln \gamma}{\partial \tau} \approx 2 \frac{\Delta \ln \gamma}{\Delta \sigma}$$

was obtained, where γ = the strain rate, τ = the shear stress, and σ = the uniaxial tension. Another set of experiments was performed by rapidly changing the temperature while keeping the strain rate constant at a predetermined strained state. At a given state for an alloy, the values of β and flow stress at different temperatures were thus obtained. From the values of βkT at 4°K for different states of the alloys, and assuming the activation distance for this temperature equal to the Burger's vectors, the average distance between dislocations, L, was estimated. By comparing the values of β at other strains with that for the above state for a given temperature, viz 90°K, the values of L at various strained states were obtained. The dislocation density ρ was found to increase for about 10% deformation from 5×10^{11} to 7×10^{11} cm/cm^3.

The force-distance curves for the three alloys were found almost the same as that obtained for the Al single crystal.[1] The nature of the force-distance curve depends upon the stacking-fault energy, thus the similarity of the force-distance curve indicates that the dilute alloying of Al with Mg does not affect the stacking-fault energy very much.

The flow stresses for the alloys were found much higher than that for Al single crystals. The back stresses for the alloys, therefore, were found much larger. With the force due to short-range elastic interactions among the intersecting dislocations taken to be the same as that for single crystals, the opposing force due to long-range intersection was computed. The long-range back stress in these alloys was found at least twice as large as the short-range back stress.

[1] S. K. Mitra, P. W. Osborne, and J. E. Dorn, Trans. AIME 221, 1206 (1961).

4. THEORY OF CREEP BASED ON FLUCTUATIONS OF SHORT-RANGE ORDER

John E. Dorn and Sandip K. Mitra

The degree of short-range order in an α-solid solution influences the yield stress for plastic deformation to a considerable extent. When a dislocation passes through a region of certain short-range order in a crystal it displaces atoms on either side of the slip plane, thereby changing some of the nearest atom neighbors. The free energy to disorder the atoms must be supplied mechanically by the applied stress. Consequently, a higher stress is necessary for a more ordered alloy.

With decrease of temperature, the absolute value of degree of order of an alloy increases. As cooling is continued below one-half the melting temperature the atomic exchanges becomes so infrequent that any particular degree of order becomes frozen in. Consequently, the yield stress for the alloys annealed below half the melting temperature is found to be almost constant. Therefore, at moderate temperature the process is found to be athermal, whereas at low temperatures either the Peierls' or the intersection mechanism becomes more difficult than the disordering process and so the yield stress is observed to increase with decrease in temperature. On the other hand, in the high-temperature region the atomic exchange can occur at a reasonable rate. As a result, fluctuations in composition and short-range order from the equilibrium value may occur, and plastic deformation may be initiated at a stress less than that necessary for the equilibrium degree of order.

Analyses along these lines to obtain a theory of deformation at high temperatures for α-solid solutions is in progress. Other factors such as Suzuki and Cottrell locking will be neglected in this analysis in order to obtain a theory for creep arising exclusively from effect of the short-range order.

5. ON THE LOW-TEMPERATURE RATE-CONTROLLING MECHANISM OF DEFORMATION FOR PRISMATIC SLIP IN SINGLE CRYSTALS OF THE HEXAGONAL Ag-Al INTERMETALLIC PHASE

John E. Dorn and Jim D. Mote

A preliminary investigation of the deformation mechanisms in single crystals of the hexagonal Ag-Al intermetallic phase[1] revealed that over the temperature range 4 to 150°K prismatic slip occurs according to the dictates of the Peierls' mechanism as formulated by Lothe and Hirth.[2] However, the data are insufficient at present to clarify all the details of this process. The current investigation was initiated to elucidate these details.

Single crystals of Ag-33 at. % Al have been grown. The effect of a change in temperature on the flow stress at constant strain rate will be determined. Additional experiments to determine the effect of a change in strain rate on the flow stress at constant temperature will also be carried out. The results of these experiments will be analyzed in terms of the above-mentioned theory.

---

[1] J. D. Mote, K. Tanaka, and J. E. Dorn, Trans. AIME 221, 858 (1961).

[2] J. Lothe and J. P. Hirth, Phys. Rev. 115, 543-550 (1959).

6. DEFORMATION MECHANISMS OF Mg-Li ALLOYS

John E. Dorn, Jim D. Mote, and Aziz Ahmadieh

Whereas polycrystalline Mg is brittle over a wide range of low temperatures, alloys containing several at. % Li are ductile. Previous investigations have shown that the increased ductility was associated with a decrease in the axial ratio and the introduction, upon alloying, of prismatic as well as basal slip.[1] The present investigation is directed to a study of why Li additions induce easy prismatic slip in Mg. For this purpose an investigation was initiated to ascertain what dislocation mechanisms control prismatic slip in single crystals and what role Li additions play in modifying the mechanism.

Previously encountered difficulties in growing nearly perfect single crystals of Li α-solid solutions in Mg oriented for prismatic slip have now been solved, and many good crystals have been grown and tested. The experimental phases of an investigation on the mechanism of deformation for prismatic slip in specially oriented single crystals of 12.5 at. % Li in Mg over a range of temperature between 4.2°K and 298°K has been completed.

The data obtained revealed that the alloy specimens oriented for prismatic slip have a critical resolved shear stress, τ_c, of about 75% that of pure Mg oriented for the same slip,[1] and that τ_c decreases linearly with the absolute temperature. All crystals fractured on the prismatic planes upon initiation of duplex slip, and showed about 40% resolved shear strain; no plastic deformation was observed in pure Mg below 450°K for prismatic slip. A few tests were made to determine the apparent activation energy; it increases almost linearly with temperature.

Neither Friedel's theory for cross-slip, the dislocation intersection mechanism, nor the thermally activated motion of jogged screw dislocations was found to agree with the experimental data. The observations, however, strongly indicate that the Peierls' mechanism may be rate-controlling. Detailed analyses are now in progress; studies are also being made of prismatic slip in single crystals of 6 and 3 at. % Li in Mg.

Previous investigations reveal that Friedel's theory for cross-slip is the rate-controlling process in pure Mg above 450°K;[2] therefore, attempts will be made to identify the range of Li content for which the change in the mechanism takes place. The Peierls' stress on the slip plane may be so high in pure Mg that below 450°K the fracture stress is reached before slip can be induced. This stress is lowered by the addition of Li. The cause of this effect is being studied.

---

[1] Frank E. Hauser, Philip R. Landon, and John E. Dorn, Trans. AIME 8, 1 (1956).

[2] P. W. Flynn, J. D. Mote, and J. E. Dorn, Trans. AIME 221, 1148 (1961).

7. MECHANISM OF HIGH-TEMPERATURE DEFORMATION IN Ag-Al-Zn ALLOYS

John E. Dorn, Jim D. Mote, and Eugenia Howard

Previous investigations suggested that the thermally activated creep of Ag-Al and Ag-Al-Zn alloys might arise from fluctuations in short-range order.[1,2] It was therefore considered desirable to ascertain the effect of stress, temperature, and strain on the creep rate of these alloys in order to acquire the essential data to check the theory which is being developed concurrently. Both activation energies and the effect of stress on the creep rate have been measured over a range of temperatures and stresses. The activation energy for creep is about 36,800 cal/mole, and remains independent of the temperature.

The effect of stress on the strain rate was obtained over the temperature range 481°K to 649°K for single crystals of the same alloy. Log-log plots of strain rate vs. stress yield straight lines which are shown in Fig. IIC. 7-1. The slopes are approximately equal, the lines being merely displaced from one another owing to the temperature differences in the tests. These data do not correspond to theories of creep based on the thermally activated motion of jogs or on the dislocation-climb mechanism. They will be used for comparisons with the theory, now under study, of creep arising from fluctuations in short-range order.

---

[1] J. D. Mote, K. Tanaka, and J. E. Dorn, Trans. AIME 221, 858 (1961).

[2] William L. Barmore, Activation Energies for Prismatic Slip in Single Ag-Al-Zn Crystals at Intermediate Temperatures (M. S. Thesis), University of California, Berkeley, September 1960.

8. THE EFFECT OF TEMPERATURE ON THE YIELD STRENGTH OF THE POLYCRYSTALLINE HEXAGONAL Ag-Al INTERMETALLIC PHASE*

Kichinosuke Tanaka,† Jim D. Mote, and John E. Dorn

The effect of temperature on the yield strength of the polycrystalline hexagonal Ag-Al intermetallic phase was investigated over the temperature range 77° to 775°K. It was found that the curve for yield stress vs. temperature, both for polycrystalline Ag-33 at. % Al specimens that were heavily cold-worked prior to deformation and for specimens that were recrystallized prior to deformation, was parallel to that for prismatic slip in simple crystals.[1]

---

*Abstract of a report issued as UCRL-9992, Dec. 1961.

†Now at the University of Kyoto, Kyoto, Japan.

[1] J. D. Mote, K. T. Tanaka, and J. E. Dorn, Trans. AIME 221, 858 (1961).

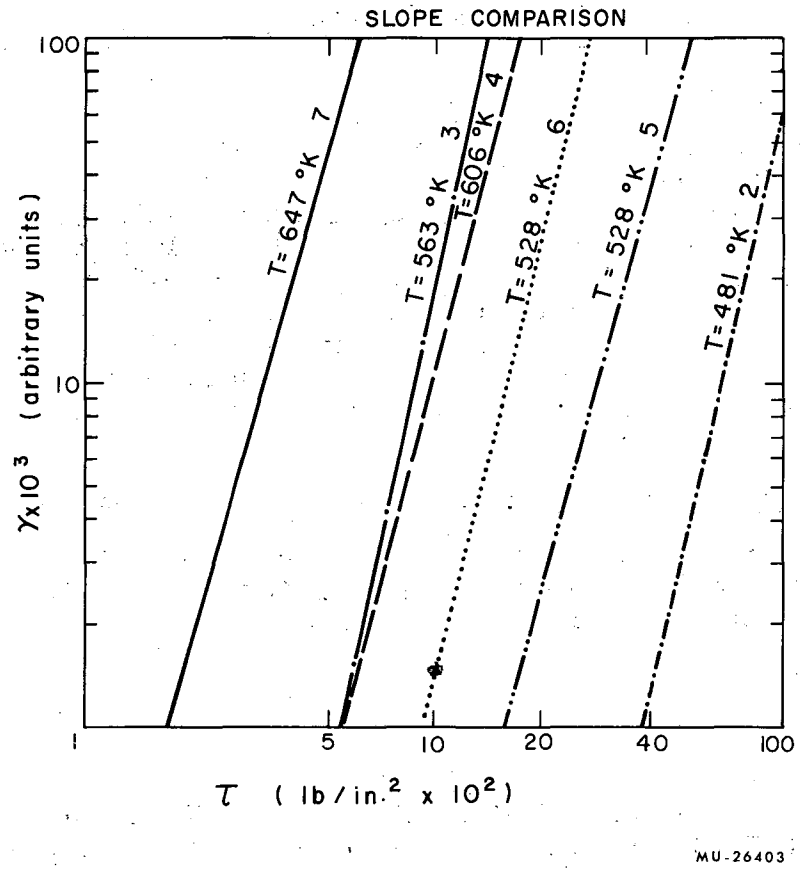

Fig. IB. 7-1. Total heat capacity, C(mj/mol deg), of MnF_2 and CoF_2 shown as CT^2 versus T^5.

Increase of the percentage of Al in the specimens resulted in an abrupt decrease in the ductility at a composition of about 37 at. % Al. This decrease in ductility was attributed to precipitates in the grain boundaries.

9. THE EFFECT OF STRAIN RATE ON DIFFUSION

John E. Dorn, Jim D. Mote, and Ahmed R. Wazzan

Experiments to determine the effect of plastic deformation on self-diffusion in nickel single crystals have been completed. The major objective was to determine the effect of strain rate on the concentration of vacancies in metals at elevated temperatures.

The experimental procedure was as follows: single crystals of high-purity Ni were produced by a modified Bridgman technique. The crystals were carefully machined to the approximate dimensions 0.1 in. thick, 1/2 in. wide, and 4 in. long. These tensile specimens were electroplated with radioactive Ni^{63}. The surface activity of the specimen was determined by means of a flow counter, the specimen was given a static anneal, and the surface activity was again determined. This procedure was repeated until the static diffusivity was determined. The same procedure was followed with specimens strained at a constant rate.

The data thus obtained revealed that the coefficient of self-diffusion, D_u, for nickel single crystals in the unstrained state is a function of temperature, represented by the expression

$$D_u = 1.9 \exp\left(-\frac{668{,}000}{RT}\right) \text{ cm}^2/\text{sec} .$$

The coefficient of self-diffusion of nickel single crystals undergoing plastic tensile deformation was measured for strain rates ranging from 0.0085 to 0.55 hr^{-1} at three temperatures, namely, $948 \pm 1.5\,^{o}K$, $1021 \pm 1.5\,^{o}K$, and $973 \pm 1.5\,^{o}K$. It was found that the coefficient of self-diffusion increased with an increase in strain rate at a constant temperature, and decreased with an increase in temperature at constant strain rate.

These results are being analyzed in terms of various mechanisms that have been proposed for the production of vacancies during plastic deformation.

Experiments are also being carried out to determine the effect of pre-strain on self-diffusion in polycrystalline nickel. Polycrystalline nickel specimens are prestrained by various amounts at room temperature and then the diffusivity is determined at elevated temperatures. Experiments in this area are continuing.

10. MECHANISMS OF DEFORMATION IN PURE POLYCRYSTALLINE ALUMINUM

John E. Dorn and Phillip W. Osborne

The purpose of this investigation is to uncover the reasons for the well-known differences in the plastic behavior of single crystals and polycrystalline aggregates. For this purpose an attempt was made to determine the activation energy, the activation volume, the force-displacement diagram for the significant thermally activated dislocation process, and the back stress. The experimental techniques employed were analogous to those previously used to identify the same quantities in single crystals.[1] Because dislocations pile up at the grain boundaries of polycrystals, the stresses are known to be sufficiently high to induce cross-slip. It was therefore thought that this mechanism might be operative in the polycrystals, whereas, as previously shown, the dislocation intersection mechanism controls the deformation rate of single Al crystals over the easy-glide and linear-hardening ranges. Preliminary analyses of the data on polycrystals, however, reveal that here, too, the intersection mechanism is operative. The major distinction between single and polycrystals concerns the back-stress field; the force-displacement diagram, the activation volume, and the activation energy for polycrystals coincide with those for intersection in single crystals. This unexpected result, however, can be rationalized because each time a dislocation cross-slips to contribute to the strain, it must also undertake intersection. Thus, the strain rate in this region is not only that demanded by cross-slip but it is also equal to that required for intersection. This is accomplished by the relief of the back stresses on intersecting dislocations by the cross-slip mechanism. The details of this mechanism are now being examined.

[1] S. K. Mitra, P. W. Osborne, and J. E. Dorn, Trans. AIME 221, 1206 (1961).

11. GEOMETRIC FOUNDATIONS OF CONTINUUM MECHANICS*

John A. Simmons and John E. Dorn

This investigation was concerned with the foundations of the geometry of a continuum approximation to the deformation of a crystalline solid.

A method of formulating the infinitesimal deformation of a system of particles based on an averaging process was developed. This formulation was based on the construction of a "polyhedral mesh" valid for any system of particles whether or not they lie in a lattice configuration. However, for particles lying in a perfect lattice, the mesh was shown to yield the familiar definition of dislocation motion. The averaging process was then extended to include deformations at grain boundaries.

*Abstract of a report issued as UCRL-9922, Oct. 1961.

By use of these results, the concept of infinitesimal plastic transformation was formulated, and it was shown that if the initial state of the material was assumed to be described by a spatial lattice affine connection, the entire dynamic description of the material deformation was then given by a four-dimensional space-time affine connection whose invariants together with the integrated strain define the state of the material. Equations of continuity for plastic as well as for ordinary elastic deformation were derived. The exterior calculus of E. Cartan was utilized in this section to simplify the computations.

12. RESEARCH IN PROGRESS -- DORN

A substantial effort is being made to extend our knowledge of deformation in metals and alloys with particular emphasis in the following areas:

Short-range order and its relation to creep.
Dispersed-particle strengthening mechanisms.
Specific deformation mechanisms for various alloys.

D. HIGH-TEMPERATURE REACTIONS

1. GLASS-METAL INTERACTIONS: NATURE OF WETTING AND ADHERENCE*

Joseph A. Pask and Richard M. Fulrath

The sessile-drop method is used for evaluation of wetting. For wetting, as indicated by acute angles, the driving force is a lower solid-liquid interfacial energy relative to the solid-gas interfacial energy. Contact angles of approximately 35° and less obtained under appropriate conditions appear to be associated with interfacial conditions that lead to the development of a chemical bond (an interchange or sharing of electrons). In vacuum $Na_2Si_2O_5$ molten glass wets and adheres chemically to platinum and oxidized iron, and wets and adheres physically to gold and iron.

A modified Dupré's equation to take into account a strain factor and a contact coefficient is developed; normally the equation takes into account only interfacial energies. The principal condition for the achievement of good adherence is the realization of chemical bonding at the interface. A theory is proposed whereby the development of such bonding is dependent upon a balance of bond energies across the metal-glass interface. An unbalance of bond energies results in a van der Waals type of bond. A lowering of the internal energy of the glass by saturating it with an oxide to the point of precipitation of a crystalline phase within the glass leads to a balance of bond energies at the interface.

Such a balance is also achieved when the bonding within the metal is stronger than the bonding between the metal atom and oxygen, as for platinum.

*Abstract of paper submitted to J. Am. Ceram. Soc.

2. WETTABILITY OF IRON BY MOLTEN SODIUM DISILICATE*

Robert W. Cline, Richard M. Fulrath, and Joseph A. Pask

An experimental unit was developed to allow application of the glass specimen onto the metal surface at elevated temperatures and under controlled atmospheric conditions. Sodium disilicate glass on Armco iron had a contact angle of 55 ± 2 deg at 900° to 1000°C in vacuum and poor adherence; on magnetite, 2 ± 1 deg and excellent adherence. Behavior on oxidized iron was affected by the ability of the glass to dissolve large quantities of oxide rapidly. Glass when dropped onto a lightly oxidized surface spread toward lower angles and retracted essentially to the 55-deg angle on solution of the

*J. Am. Ceramic Soc. 44, 423-428 (1961).

oxide; adherence, in this case, correspondingly ranged from good to poor. When the glass dissolved a sufficient amount of iron oxide and etching of the metal occurred, resulting in the appearance of fayalite, the contact angle was in the range 15 to 35 deg and the best adherence was obtained. Vaporization of iron in vacuum at 1000°C did not seem to be retarded by thin oxide films.

3. EFFECT OF COMPOSITION ON THE GLASS-IRON INTERFACE*

Frances Gaidos† and Joseph A. Pask

Development of good wetting and adherence is dependent on the formation of a strong chemical bond across the glass-metal interface. A theory has been suggested that such a bond can be formed by adjusting the glass composition so that a balance of bond energies occurs at the interface. King and co-workers have found that better adherence can be obtained by saturating the glass with an oxide of the metal. This paper presents and discusses experiments designed to verify the proposed theories.

Adjusting the oxygen-silicon ratio by solution of an oxide on the surface of the metal to the point at which the glass becomes saturated and a second phase appears is accompanied by a lowering of the internal energy of the glass. Such a condition should lead to a balance of bond energies with the metal and to the development of a chemical bond, and also to a lowering of the interfacial energy, which would produce better wetting and adherence. Five compositions in the soda-silica system and five compositions in the soda-borate system in contact with iron were investigated with regard to this point. Saturation of the glass can also be achieved by incorporating an oxide of the metal in the glass composition. A $Na_2O \cdot 2SiO_2$ glass was thus saturated with ferrous oxide and ferric oxide, respectively, to determine the effect on the glass-iron interface. The presence of ferric ions causes a redox type of reaction with the metal, leading to an irregular interface; use of the glass with ferrous ions should avoid such a reaction. These two glasses should thus permit the evaluation of the effect of an irregular interface on adherence. To still further determine the effect of the type of network-modifying cation, $Na_2O \cdot 2SiO_2$ was modified by replacing Na by Fe while maintaining a constant oxygen-silicon ratio.

---

*Abstract of paper to be presented at the VI International Glass Congress in Washington, D. C., in July 1962, and to be published in the Proceedings of the Congress.

†Now at American Glass Research, Butler, Pa.

4. THE VAPOR PRESSURE OF MAGNESIUM FLUORIDE*

Reuben R. Hammer† and Joseph A. Pask

The purpose of this study was to measure the vapor pressure of condensed-state magnesium fluoride, to determine the average molecular weight of the vapor above the solid or liquid, and to calculate the heat of sublimation of the solid at 298°K.

In the first part of the investigation, the vapor pressure of magnesium fluoride was determined by the Knudsen Effusion Method. A high-temperature recording balance for operation in vacuum was designed and constructed for this purpose. Weight-loss rates were determined at ten different temperatures, ranging from 1178 to 1340 °C. Assuming a monomeric vapor of $MgF_{2(g)}$, vapor pressures were calculated from these data.

The second part of this research consisted of vapor-pressure measurements of magnesium fluoride by the torsion-effusion method. A torsion-cell apparatus was constructed, in which the torque due to the effusing vapor is balanced by an electromagnetic torque. Vapor pressures were measured at twenty-three different temperatures, ranging from 1140 to 1341 °C.

Results of Knudsen and torsion experiments were combined to give an average molecular weight of the vapor. In the range of experimental temperatures, the vapor of magnesium fluoride was found to be essentially monomeric $MgF_{2(g)}$. Calculations to evaluate the heat of vaporization of solid magnesium fluoride at 298°K by the Third-Law method gave a mean value of 88.0 kcal/mole.

*Abstract of a paper prepared for publication in J. Am. Ceram. Soc.
This work has been primarily supported by O. N. R. and by Gen. Edward Orton, Jr., Ceramic Foundation.

†Now in Haifa, Israel.

5. THE EFFECT OF CRYSTAL ORIENTATION ON THE PLASTIC FLOW OF MAGNESIUM OXIDE*‡

Charles O. Hulse, S. M. Copley, and Joseph A. Pask

Since the original demonstration by Parker et al.[1] that single crystals of MgO could be deformed at room temperature, much attention has been

*Summary of a paper being prepared for publication in J. Appl. Phys.

‡This work was primarily supported by the N. A. S. A., but represents the type of study to be continued under A. E. C. sponsorship.

[1]E. R. Parker, J. A. Pask, J. Washburn, A. E. Gorum, and W. Luhman, J. Metals 10, 351-353 (1958).

given to the factors affecting their mechanical behavior. A major reason for this interest has been the hope that a detailed understanding of the single crystals would reveal the factors that determine the mechanical behavior of polycrystalline MgO.

Polycrystalline MgO is known to be brittle at room temperature.[2] Little is known of its mechanical behavior at other temperatures. Wygant has observed polycrystalline MgO to creep when tested in torsion at 1100°C.[3] Wachtman and Lam have observed polycrystalline MgO to deform plastically at 1000°C and attributed the observed flow to grain boundary shear controlled by diffusion processes.[4]

In this paper are presented stress-strain curves for polycrystalline MgO tested in compression at temperatures ranging from 25 to 1200°C. Strains of as much as 2% were obtained at temperatures greater than 600°C.

Stress-strain curves for single crystals of MgO, tested in compression with ⟨111⟩ and ⟨110⟩ loading axis, are presented for the same temperature range as the polycrystals.

Single crystals with a ⟨111⟩ loading axis were observed to deform plastically at temperatures greater than 350°C. Strains of 6% were observed at 1200°C. In this orientation, the critical resolved shear stress on the {110} ⟨110⟩, which is the easiest slip system for MgO, vanishes. Thus the observed plastic deformation must be caused by flow on another slip system. Figure IID. 5-1 shows dislocation band structures as revealed by etching (100) faces in a ⟨111⟩ specimen just yielded at about 650°C and air-quenched. The vertical line in the middle of the figure marks an edge between two {100} faces, and the bands are therefore traveling along {100} planes. The lowest-energy Burger's vector in the {100} planes is the (a)/2, ⟨110⟩, and it is concluded that these bands must be caused by flow of the {100} ⟨110⟩ slip system.

The difference between the observed deformation of single crystals with a ⟨110⟩ loading axis and the previously reported mechanical behavior of single crystals loaded in compression with a ⟨100⟩ loading axis[5] can be accounted for by using Schmidt's law.

On geometrical grounds, it is shown that the {100} ⟨110⟩ slip system can contribute to the deformation of polycrystalline MgO at elevated temperatures. A comparison of the temperature dependence of the yield stress for single crystals of MgO to that for the polycrystalline samples, and the microstructures of polycrystalline samples deformed at various temperatures, suggest that activation of the {100} ⟨110⟩ slip system is necessary for polycrystalline ductility.

---

[2] Charles E. May, Hurbert H. Grimes, and Robert A. Lad, Ductile Ceramics. II. Introductory Study of Ductility in Polycrystalline Sodium Chloride and Magnesium Oxide, NASA Technical Note D-76, Oct. 1959.

[3] J. F. Wygart, J. Am. Ceram. Soc. 34, 234-260 (1959).

[4] J. B. Wachtman and D. G. Lam, J. Am. Ceram. Soc. 42, 234-260 (1959).

[5] C. O. Hulse and J. A. Pask, J. Am. Ceram. Soc. 43, 373 (1960).

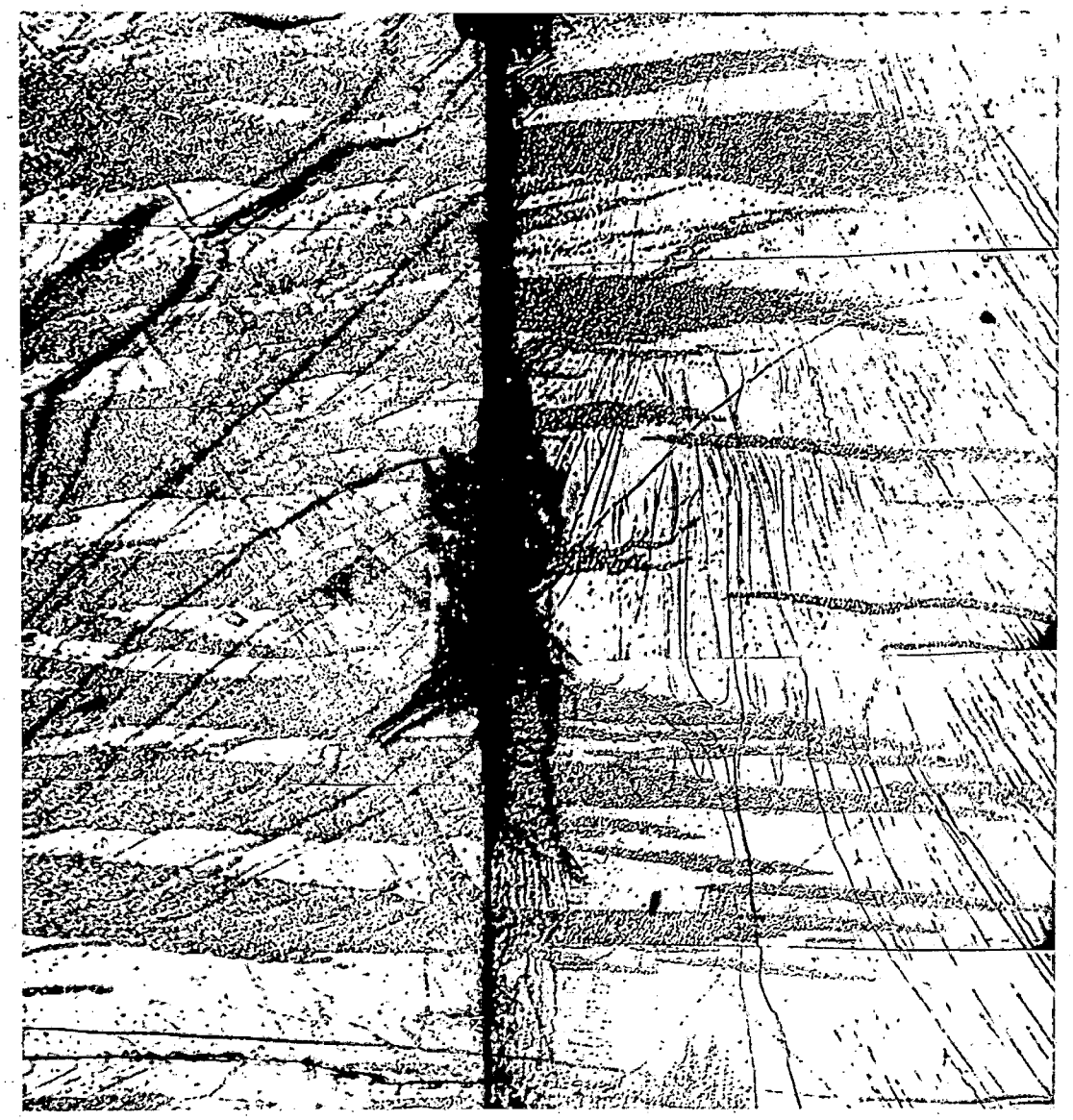

ZN-3075

Fig. IID. 5-1. Etched slip bands of the $\{100\}\langle 110\rangle$ slip system in MgO.

6. KINETICS OF THE OXIDATION OF MAGNESIUM FLUORIDE*

Donald R. Messier and Joseph A. Pask

The kinetics of the reaction between MgF_2 and water vapor were studied in the temperature range from 950 to 1100°C. Determinations on powdered, sintered polycrystalline, and single-crystal specimens yielded different activation energies. The differences were attributed to differences in microstructure among the several specimen types.

Reaction rates were determined by measuring weight loss with a silica helix and cathetometer. The reaction was carried out in an atmosphere of flowing argon which had a known partial pressure of water vapor.

With all sample types, the reaction was interface-controlled. After the attainment of steady-state conditions, a 2/3-order rate law was followed.

Activation energies of 25, 56.1 ± 6, and 42.3 ± kcal/mole were obtained for the powdered, sintered polycrystalline, and single-crystal specimens, respectively. The single-crystal value agreed with the heat of reaction of 43.8 kcal/mole, indicating that the rate-controlling step was the chemical reaction itself. The low value for the powdered specimens was a result of area changes caused by sintering. The structure of the product layer on the presintered polycrystalline specimens was such that it provided a greater impedance to gas flow than the single-crystal product layer, and this increased the reaction-rate temperature coefficient and the activation energy.

*Abstract of M. S. Thesis of Donald R. Messier, University of California, August 1961.

7. PURIFICATION OF MgF_2 AND GROWTH OF SINGLE CRYSTALS*

William D. Scott† and Joseph Pask

A modified Bridgman-Stockbarger method was used to grow single crystals of MgF_2 weighing about 200 g. The purity of the charge material was critical. Purification was achieved by first drying technical grade MgF_2 and then vaporizing in vacuum. Spectral transmission of the single crystals was measured: in comparison with CaF_2, it was slightly less transparent in the ir region and of about the same transparency in the uv region. Modulus-of-rupture values were also obtained in several orientations. No plastic flow was observed.

*Abstract of a paper prepared for publication in J. Am. Ceram. Soc.

†Now at Houldsworth School of Applied Science, University of Leeds, Leeds, England.

8. DEFORMATION AND FRACTURE OF POLYCRYSTALLINE LITHIUM FLUORIDE*

William D. Scott† and Joseph A. Pask

Techniques for the formation of large-grain polycrystalline LiF from the melt and for the fabrication of polycrystalline test specimens were developed. Grain size control was found to be difficult because of easy grain growth during annealing. Specimens were tested in four-point bending. The marked influence of crystal orientation on the shape of the macroscopic stress-strain curve was demonstrated with single crystals; the shape of the curves was also found to depend on sample preparation as well as crystal orientation. At room temperature, there was always some plastic deformation of the polycrystalline specimens before fracture; the outer fiber strain (elastic and plastic) ranged from 0.076 to 0.798% at fracture. Their plastic flow, however, was much less than that for single crystals.

An etch was developed which revealed dislocations on all crystallographic faces of LiF; it was used to investigate the deformation of polycrystalline LiF. Orientations of a number of different grains in a polycrystalline specimen were determined to show that the orientation of the aggregates is truly random, and that the etch does act on all planes.

Deformation was inhomogeneous among the grains of a polycrystalline specimen because of the differences in orientation with respect to the applied stress. Favorably oriented grains deformed first under the applied stress, but their deformation was hindered by unfavorably oriented neighbors which were not deforming as easily. Grain boundaries were generally barriers to slip in the sense that adjoining grains were unfavorably oriented for transmission of slip. Stresses resulting from slip in one grain, however, were transmitted to neighboring grains; boundary contact was thus maintained by local deformation near the boundary or by long-range slip in the neighboring grains. The resulting secondary fine boundary slip orientation was determined in a number of grains and was found to be of the type (100)[110]. The principal slip system, as in all NaCl crystal structure types, is of the (110) [110] type. This behavior indicates that the grain boundaries were not inherently weak, and that they were often able to accommodate large amounts of plastic flow.

Three-grain junctions were points of high residual stresses, especially if local boundary deformation occurred along boundaries near the junction. Because of these high stresses, fractures originated at boundaries close to or at three-grain junctions and traveled in the boundary before moving into a favorable cleavage plane; fractures thus were mixed transgranular and intergranular. It is postulated that the fractures occurred at grain boundaries where stresses arising from deformation were not sufficiently relieved by plastic flow because LiF has a limited number of slip systems available for plastic flow at room temperature.

---

*Summary of a paper being prepared for J. Am. Ceramic Soc.

†Now at Houldsworth School of Applied Science, University of Leeds, Leeds, England.

9. KINETICS OF THE OXIDATION OF MAGNESIUM FLUORIDE

Donald R. Messier and Joseph A. Pask

The study on the oxidation of MgF_2 has been extended in order to obtain further insight into the nature of the mechanism of this reaction.

It was reported that the powder specimens showed considerable sintering during reaction. Such a process causes changes in the surface area of a specimen, thus modifying the reaction kinetics. Furthermore, since sintering is temperature-dependent, its relative effect varies according to the reaction temperature. Therefore, sintering experiments were carried out on MgF_2 powder at 950 and 1100°C. Sintering is so extensive at 1100°C that, unless the resulting area change is taken into account, the experimentally determined reaction rates do not accurately reflect the true reaction rates.

Work was continued on the determination of the microstructure of the MgO product layer. The highly porous nature of the MgO leads to difficulties in fabricating suitable replicas. However, some replicas revealed the presence of blocky, irregular particles about 0.2 to 0.5 μ in diameter.

An infrared transmission spectrum was run on a slightly reacted single-crystal MgF_2 plate. It was hoped that the presence of combined OH^- could be detected, thus giving information concerning the reaction mechanism. No OH^- peak was found, but this area seems promising for future experiments.

In the course of this study it has become evident that there is a considerable number of factors that can influence the reaction rate. The effects of change in sample area and resistance of the product layer have proved especially difficult to account for. It is felt that there difficulties could be circumvented by making further runs at low reaction rates and determining the weight loss with a more sensitive balance. In this way the kinetics of the very early stages of the reaction could be followed. Such measurements would also allow the extrapolation of the rates to zero time, thus eliminating product-layer resistance and area-change effects.

In addition, it appears that a study of the variation of the reaction rate with changes in water vapor partial pressure would yield significant information concerning the reaction mechanism. Therefore work is in progress to rebuild and improve the original apparatus so that it will be possible to make very precise determinations of weight change in a controlled atmosphere or under vacuum.

10. THE ANATASE-RUTILE TRANSFORMATION

Robert D. Shannon and Joseph A. Pask

The purpose of this investigation has been to study the mechanism of the crystallographic phase transformation-anatase to rutile (TiO_2). Rao et al. in 1957 determined the kinetics of the transformation of pure titania.[1] They found an activation energy of 80 kcal/mole, but were not able to interpret the data in terms of a molecular mechanism. The kinetics of transformation of commercial and more impure titania were determined in 1958 by Cole and Sullivan,[2] who found a somewhat higher activation energy, 110 kcal/mole. It was therefore proposed to study (a) the transformation of single crystals of anatase and (b) the effect of impurities on the kinetics of transformation of commercial polycrystalline materials.

During precipitation of anatase both sulfate and phosphate impurities are present. It has been shown that the presence of large concentrations of these impurities stabilizes the anatase form and can raise the transformation temperature from between 600 and 700°C to the range 1000 to 1100°C. It seems reasonable that these impurities could be incorporated into the lattice, although there is no evident change in the lattice constants of anatase. An x-ray spectrographic analysis showed 0.007% sulfur. Such small quantities of impurity would not change the lattice constants appreciably, although they could exert a large influence on the transformation temperature and kinetics.

In order to determine the effect of sulfate impurities, it was proposed to follow the loss of sulfur trioxide from various commercial varieties of anatase. Preliminary work included construction of an atmosphere furnace in which the anatase could be transformed and the sulfur trioxide given off could be analyzed. The first attempts were by precipitation of $BaSO_4$ from a saturated solution of $BaCl_2$. This resulted in identification of SO_3 as the $BaSO_4$ precipitate, but the kinetics of the precipitation were too slow to give a sensitive identification. Further work will include the use of a more sensitive reagent for identifying the SO_3.

To clarify the mechanism of transformation, single crystals of anatase of octahedral habit have been obtained from several suppliers. These single crystals have been subjected to heat-treating temperatures from 800 to 950°C in order to partially transform them to rutile. Laue patterns made on the habit faces of the original anatase crystals showed gradual breakup of the original crystal into smaller fragments, most of which remain in the same orientation as the untreated crystal. These fragments then transform to rutile crystals which are oriented in preferred directions. Analysis of this orientation has been carried out by means of Laue, rotating-crystal, and oscillation patterns.

---

[1] A. W. Czandema, C. N. R. Rao, and J. M. Honig, Trans. Faraday Soc. 54, 1069 (1958).

[2] S. S. Cole and W. F. Sullivan, J. Am. Ceram. Soc. 42, 127-32 (1959).

The Laue patterns showed nonuniform distribution around the diffraction rings formed from transformed rutile crystals. Because orientation equipment for use with the Laue apparatus was not available, it was decided to utilize oscillation and rotation patterns. The preliminary work shows two possible orientations which, when repeated by the symmetry of the anatase crystal, result in 16 possible orientations of the rutile crystals. In the first orientation the [001] rutile corresponds to the [102] anatase direction with a rotation of [001] rutile in the (102) anatase plane. The other orientation has not yet been completely specified.

There is a scatter of $\pm 10^{\circ}$ about the above directions. This scatter is to be expected, since the anatase crystals during the transformation are considerably strained and, as mentioned earlier, are known to break up into smaller fragments. This strain occurs because of the 19% shrinkage involved in transition. Despite this shrinkage, the external form of the anatase single crystal is remarkably well preserved, allowing good but distorted reflections from the crystal faces.

There is some indication that the transformation is nucleated either at the centers of faces or in [hko] directions. These possibilities will be studied further.

11. RESEARCH IN PROGRESS--PASK

Previous work on mechanical behavior of single crystal and polycrystalline MgO is being extended to temperatures ranging from 1000 to $1650^{\circ}C$.

The mechanical behavior of thin plates of single-crystal MgO approximately 0.001 in. thick is being studied. It is hoped that these studies will lead to a better understanding of dislocation multiplication in this material.

The fabrication of high-density polycrystalline MgO with the use of LiF additives is being studied in an effort to obtain better samples of this material for mechanical behavior studies.

Mechanical behavior studies are being made on polycrystalline LiF at temperatures up to its melting point.

Plastic deformation studies are being made on single-crystal and polycrystalline specimens of CsBr.

12. TERMINATION OF ONR-ARPA CONTRACT

Alan W. Searcy

A contract with the Office of Naval Research and ARPA was terminated in August 1961. Several papers reporting work performed under this contract were submitted for publication during the first half of 1961:

A. G. Tharp, The Structures of the Lanthanum Family Silicides, J. Phys. Chem. (in press).

L. N. Finnie, Structures of the Silicides of Ruthenium, Osmium, Rhodium, and Iridium, J. Less Common Metals (in press).

A. W. Searcy and L. N. Finnie, Stabilities of Solid Phases in the Ternary Systems of Silicon and Carbon with Rhenium and the Six Platinum Metals, J. Am. Ceram. Soc. (in press).

A. W. Searcy, High-Temperature Inorganic Chemistry, Vol. 3 of Progress in Inorganic Chemistry (Interscience Publishers, Inc., New York, 1962).

Publication of a study of the vaporization of In_2S_3 which was completed under ONR-ARPA sponsorship, is being delayed to allow identification of the vapor species with the high-temperature mass spectrometer. This work will continue under AEC sponsorship.

13. THE COMPOSITION AND PROPERTIES OF THE SOLID PRODUCED BY REACTION OF THORIUM WITH HYDROCHLORIC ACID*

Ray S. Newbury† and Alan W. Searcy

A zinc blende modification of thorium monoxide has been reported by Katzin to be an insoluble product of the reaction of thorium metal with hydrochloric acid.[1] The original purpose of this research was to investigate this material and the reactions it might undergo on heating.

Once the experiments were under way, it became obvious that the black material formed when thorium metal was treated with concentrated HCl was not ThO but something more complex; it was designated I for convenience. The research objectives then became to identify and to characterize this reaction product.

*Submitted for publication in J. Inorg. Chem.

†Lawrence Radiation Laboratory, Livermore.

[1] L. J. Katzin, J. Am. Chem. Soc. 80, 5908 (1958).

I had the same x-ray pattern as reported by Katzin. It is concluded here, from evidence presented below, that the pattern is of oxygen-deficient ThO_2. When vacuum-dried samples of I were heated under vacuum, large quantities of hydrogen gas were evolved. It was found that the gas came off in two stages--a part came off at temperatures below 300°C with a heat of activation of about 2.6 kcal per mole of H_2, and the rest at high temperatures with a heat of activation of 25 kcal per mole. I had sufficient surface, as measured by the B. E. T. method, to adsorb about 1/10 of the total hydrogen initially present. At least for temperatures of 300°C and lower, the evolution of H_2 appeared to be reversible.

After hydrogen evolution had ceased, some of the material remaining, designated II, was heated to 800°C, at which point a white sublimate was formed on the adjacent cool parts of the vacuum line and a black residue, designated III, remained. Analysis of this white material showed it to be $ThCl_4$. III yielded a weak but clear pattern of thorium metal in addition to a sharpened pattern of the oxygen-deficient ThO_2.

Oxygen was introduced into the line to react with III. III reacted so strongly that it glowed white hot. The white powder formed as the product was identified as ThO_2 by x-ray diffraction. On this basis, III would have the composition $(ThO_{1.57\pm.01}$. The composition of II can be calculated from the known weight of $ThCl_4$ sublimed from III. Its composition is $ThO_{1.3(\pm0.2)}Cl_{.67(\pm0.02)}$. Finally, from the measured volume of hydrogen evolved, the composition of I can be calculated:

$$\text{I: } ThO_{1.31(\pm0.2)}Cl_{.67(\pm0.02)}H_{1.28(\pm0.05)}.$$

Katzin's identification of I as ThO cannot be correct because of the large quantities of H_2 and $ThCl_4$ that I releases on heating. Karabash, in an independent investigation, identified I as a thorium oxide-hydride-hydroxide phase.[2] Our more complete experimental results are generally consistent with his, but demonstrate that chlorine is an integral component of I. Furthermore, the diffraction pattern of I persists with unchanged spacings when the hydrogen is nearly all evolved and even, as demonstrated by Karabash, after I is converted to a peroxide-hydride-oxide. We interpret this as evidence that the observed pattern is that of a surface coating of oxygen-deficient ThO_2, not of the bulk material as believed by Karabash.

I, then, is a mixture of at least two phases, oxygen-deficient ThO_2 and a phase of approximate composition $ThO_{0.8}H_{1.2}Cl_{0.8}(OH)_{0.4}$ designated IV. The evolution of hydrogen in two stages can be explained as the result of the slow internal reaction, $H^- + OH^- \rightarrow O^= + H_2$. The H_2 formed by this reaction is held as adsorbed hydrogen which is readily and reversibly desorbed. The remaining IV decomposes on heating to give off additional H_2.

If the reasonable assumption is made that only the ThO_2 phase in I is present in a reasonably developed crystalline form, then this also explains why only the lines corresponding to this phase can be recognized in the original material, why these lines should persist unchanged on heating in vacuum, and why weak thorium metal lines should finally appear after prolonged heating has driven off the hydrogen and thorium tetrachloride.

[2] A. G. Karabash, Zhur. Neorg. Khim. 3, 986 (1958), AEC-TR-3533.

14. EFFECT OF CHANNEL LENGTH ON THE FORCE EXERTED BY EFFUSING VAPORS*

David A. Schulz† and Alan W. Searcy

For molecular streaming conditions, Clausing has calculated values of the ratio K of the number of molecules that escape through an orifice of finite length ℓ to the number that escape through an orifice of infinitesimal length but the same radius r.[1] Provided that the cosine distribution law is valid, the method is exact and yields values of K that can be calculated to any desired limits of uncertainty.[2]

Clausing has provided an alternative derivation which yields approximate values of the ratio K'.[3] From this approximate equation, Freeman and Searcy have calculated the fraction of molecules that escape through various solid angles made with the orifice axis.[4] By a simple modification, they were also able to calculate the ratio f of the force of molecule that escape through an orifice of finite ℓ/r to the force for the same r but for $\ell = 0$.[5]

Because of the tediousness of the numerical integrations, Freeman and Searcy used angular increments of 15 deg in evaluation of K' and f. The practical validities of Clausing's approximate equation and of the numerical integration were demonstrated for values of ℓ/r between 0 and 2 by agreement to within 0.5% in the calculated values of K' with Clausing's K values.

In the work reported here, the calculations of K' and of f were extentended to $\ell/r = 10.0$. The calculations were performed on an IBM 704 computer with 0.1-deg intervals in the Simpson method integration, thus bringing the above-mentioned agreement to within 0.1% over the range ℓ/r from 0 to 4. A further decrease in summation interval by a factor of 10 produced no change in sample ℓ/r calculations.

Detkov has recently declared[6] that a molecular-distribution equation by Vlasov[7] yields better number and force corrections for short orifices than are obtainable from Clausing's approximate equation.

---

*Brief version of a note in J. Chem. Phys. (in press).

†Now at National Carbon Corp., Lawrenceburg, Tennessee.

[1] P. Clausing, Ann. Physik 12, 961 (1932).

[2] W. C. DeMarcus and E. H. Hopper, J. Chem. Phys. 23, 1344 (1955).

[3] P. Clausing, Z. Physik 66, 471 (1930).

[4] R. D. Freeman and A. W. Searcy, J. Chem. Phys. 22, 1137 (1954).

[5] Ibid. 22, 762 (1954).

[6] S. P. Detkov, Zhur. Fiz. Khim. 34, 1634 (1960).

[7] O. Ye. Vlasov, Izvest. Vsesoyuz. Teplotekh. Inst. im Feliksa Dzerzhinskogo 44, 1 (1929).

DeMarcus has obtained refined values of K from Clausing's exact equation.[8] A plot was made showing how Detkov's values, K_d, and our refined values, K', calculated from the approximate Clausing equation, deviated (in percent) from the exact K values. Both approximations showed maximum deviations of 0.12 in the range of ℓ/r values up to 2.9. From $\ell/r = 2.9$ to the limit of Detkov's calculations, $\ell/r = 4$, our approximation gave markedly better agreement.

Values of K' and f and, for comparison, Detkov's values f_d were tabulated. At $\ell/r = 4.0$, where our K' and Detkov's K_d differ by 1.16%, the values of f and f_d differ by less than 0.1% because the force equations are insensitive to the assumed behavior of molecules that travel at high angles to the orifice axis. Deviations of K' from the exact equation value K reaches -1.14% at $\ell/r = 7.0$, and -2.32 at $\ell/r = 10.0$. These deviations are within the confidence limits of present effusion measurements, and the force corrections should be closer to the true values than are the corresponding values of K'.

[8] W. C. DeMarcus, The Problem of Knudsen Flow. III. Solutions for One-Dimensional Systems, Oak Ridge Gaseous Diffusion Plant Report K-1302, March 1957.

15. THE VAPOR PRESSURE AND HEAT OF SUBLIMATION OF CALCIUM FLUORIDE*

David A. Schulz† and Alan W. Searcy

The vapor pressure of CaF_2 was measured in order to check the reported pressures[1] and in order to obtain a value for the heat of sublimation at 298°K from data that required less extrapolation. The torsion effusion method was employed.[2, 3]

In the application of the torsion-effusion method, a graphite block containing an effusion cell was suspended in a vacuum furnace by a 2-mil tungsten wire. Upon heating, vapor escaped through the eccentrically placed orifices in the cell, thereby exerting a torsional force on the wire. The angle through which the cell turned was measured, and from this angle the vapor pressure could be calculated by means of the formula

$$P = 2\phi D/(\Sigma qaf),$$

where P is the vapor pressure, D is the torsion constant of the wire, q is the perpendicular distance from the cell center to the axis of the effusion [illegible] is the area of the [illegible]

*Short version of a paper to be submitted to J. Phys. Chem.

†Now at National Carbon Corp., Lawrenceburg, Tennessee.

[1] O. Ruff and L. Le Boucher, Z. anorg. algem. Chem. 219, 376 (1934).

[2] H. Mayer, Z. Physik 67, 240 (1931).

[3] M. Vollmer, Z. Physik. Chem., Bodenstein Festband, 863, (1931).

hole, a is the area of the orifice, f is the force-reduction factor[4] due to finite orifice channel length, and ϕ is the angle through which the cell has rotated.

Studies on low-pressure gas flow have demonstrated that the molecular flow equations become inapplicable when the mean free path, λ, of the vapor approximately equals the diameter d of the effusion orifice. Therefore, for each pressure and temperature the approximate mean free path to orifice ratio λ/d was tabulated. These ratios were calculated by the hard-sphere approximation. The numerical values of λ/d calculated by this approximation are satisfactory for internal comparisons.

When the larger orifice was used, molecular flow prevailed to just the temperature for which λ/d is calculated to be unity. When the smaller orifice was used, molecular flow prevailed to a temperature for which λ/d is about 0.3. These results substantiate the conclusion in a previous paper[5] that the pressure limit of effusion studies depend on orifice length as well as orifice diameter.

For the high-temperature modification, β-CaF_2, the vapor pressure, in atmospheres, is given by the expression $\log P = 19{,}973/T + 7.8717$.

The heat of sublimation of α-CaF_2, the low-temperature modification, at 298°K was calculated from the lower temperature data for each orifice by both the second law method and the third law method.

The least squares second law calculation yields $\Delta H^o_I/T + I = (111{,}615)/T - 133.27$, from which $\Delta H^o_I = 111{,}615$; and $\Delta H^o_{1543} = 91.50$ kcal. This corresponds to $\Delta H^o_{1543} = 91.39$, calculated from the assumption that $\Delta C_p = 0$ in the experimental range. ΔH^o_{298} for sublimation of α-CaF_2 is calculated to be 101.44 kcal.

For the third law calculations, free energy functions were combined with the individual pressure values in the equation

$$\Delta H^o_{298} = -RT \ln P - T \frac{(\Delta F^o_T - \Delta H^o_{298})}{(\quad T \quad)}$$

to yield ΔH_{298} values. The average ΔH_{298} is 101.17 ± 0.06 kcal. Taking all estimated errors into account, a gross uncertainty of 1 kcal is estimated for the heat of sublimation at 298°K. The data extrapolated over 300° from below the melting point yield pressure values higher than those of Ruff and Le Boucher by less than 10%.

The excellent agreement between heats of sublimation calculated by the second and third law methods and the excellent agreement between our extrapolated pressures and the measured pressures of Ruff and Le Boucher lend confidence to the conclusion that the principal vapor species is monomeric CaF_2.

---

[4] R. D. Freeman and A. W. Searcy, J. Chem. Phys. 22, 762 (1954).

[5] A. W. Searcy and D. A. Schulz, Effect of Channel Length on the Force Exerted by Effusing Vapors, J. Chem. Phys. (in press).

16. AN EXPERIMENTAL EVALUATION OF THE TORSION-EFFUSION METHOD FOR DETERMINATION OF VAPOR PRESSURES WITH TIN, GERMANIUM, AND SILVER

David A. Schulz and Alan W. Searcy

The research presented here was undertaken to delineate in the torsion-effusion method for determination of vapor pressures the pressure range of applicability, the consistency of measurements made with various torsion wire diameters, and the reliability of theoretical corrections for the influence of effusion orifice geometries.

Tin was chosen as the principal experimental material because previous investigation indicated that it evaporates predominantly as atoms and with an evaporation coefficient near unity. Additional studies were made with germanium because its vapor pressure had been previously measured in our Laboratory by both the torsion-effusion method and the Knudsen method. Silver was studied because early torsion-effusion measurements on silver had yielded results in disagreement with results obtained by other methods.

Apparatus and Experimental Techniques

A vacuum furnace with a 3-in.-diameter tantalum resistance element was used. The furnace was capable of a maximum temperature of 2020°C and a vacuum while in high-temperature operation of less than 5×10^{-5} mm. This procedure appears to yield temperatures within ±10° of the correct values.

Tungsten torsion filaments of 1-, 2-, and 5-mil diameters are used. Each filament is approximately 17 in. long.

The graphite effusion cell assembly consists of four parts: (a) cell block, (b) crucibles, (c) crucible lids, and (d) lid-retaining caps. The cell block is 1.5 in square in horizontal cross section by 3/4 in. high. Four holes extend, two each on opposing faces, into the side of the block. Crucibles 1/2 in. in diameter fit in these holes. Graphite lids and retaining caps fit snugly onto the crucibles. The holes on each of the drilled faces are opposed in torque contribution, and only one chamber on each face is used during a vapor pressure experiment. The other chambers are used for evaluation of the effect of direction of twist on the experimental results.

Experimental Method

None of the torsion wires exceeds its elastic limit on twisting through angles of 100°. Since the lowest angle practicably measurable is about 0.1 deg, pressures can be measured over three orders of magnitude with a single experimental assembly.

The most serious limitation to accuracy in measurements with this apparatus is imposed by a residual deflection of the suspension system. This deflection results from the interaction of the electromagnetic field of the

furnace with the suspension assembly. The tungsten torsion wires were demonstrated to be slightly anisotropic and to twist under action of a critical force.

Vapor pressure runs were carried out so that the sequence of temperature and the time spent at each temperature closely approximated those of runs with empty cells. The residual deflections obtained with empty cells were accurately reproducible. Vapor pressures were corrected, therefore, either by subtraction of deflections obtained in blank runs, or by averaging vapor pressure curves obtained from two runs which differed in effusion hole orientation but were otherwise identical.

Results obtained with one set of effusion orifices and 1-, 2-, and 5-mil torsion wires were in excellent agreement.

Orifice areas used for measurements in the range 10^{-6} to 10^{-5} atm were varied by a factor of 17 with ℓ/r held constant. No dependence of apparent pressures on orifice dimensions was found.

Experimental Verification of the Force-Correction Factor f

The effect of finite effusion hole lengths on the number of escaping molecules K (Clausing correction) and the effect on the force of the escaping molecules, f,[1,2] both depend on assumption of the cosine distribution law for re-emission of molecules after they strike a surface. But metal vapors can perhaps diffuse for significant distances on a surface before being re-vaporized. Either diffusion of atoms along the walls of an orifice or specular reflection from the walls could invalidate the values calculated for K and f. An experiment was designed, therefore, to test the validity of the theoretical values of f for tin vapor in a carbon orifice.

Two pairs of orifices were designed such that the effective areas a if were approximately equal. For one pair of orifices, however, f was made 0.413, while for the other pair f was made 0.741. Thus, if the f factor is correct, the two different sets of orifices should give identical deflections, while if the f correction were not applicable the apparent pressures might differ by as much as a factor of 0.74/0.41 = 1.8.

Agreement between data collected with the two sets of orifices is excellent at temperatures near 10^{-5}. At pressures of 10^{-4} atm or higher, the two curves deviate by a factor of 0.8 rather than 1.8; i.e., the duration is in the wrong direction to be explained as arising from unrecognized specular reflection or wall diffusion. This deviation is believed to arise from departure from pure molecular streaming conditions.

---

[1] R. D. Freeman and A. W. Searcy, J. Chem. Phys. 22, 762 (1954).

[2] D. A. Schulz and A. W. Searcy, Effect of Channel Length on the Force Exerted by Effusing Vapors, J. Chem. Phys. (in press).

Transition to Viscous Flow

The limit to pure molecular streaming has been reported to be variously the pressure above which the mean free path becomes less than three times the diameter of the orifice,[3] or becomes as little as 0.002 times the diameter of the orifice.[4]

Measurements were deliberately extended to far higher temperatures than are normally investigated in Knudsen effusion or torsion-effusion studies in order to obtain information concerning not only the initial pressures at which Knudsen flow conditions break down but also about the extent of deviation of the apparent pressure curve from the equilibrium pressure curve (Fig. IID. 16-1).

The scatter in data obtained above pressures of 10^{-4} atm is largely due to the systematic deviations that became apparent in the high-pressure range. With some orifices, deviations of apparent pressures from true pressures became evident at pressures as low as 2×10^{-5} atm. All orifices gave data that deviated upward from the pressures obtained by extrapolating the low-pressure data when pressures as high as 10^{-3} atm were investigated. The highest points for apparent pressure may be in error by as much as a factor of 2, but the general trend of the results is clear and certain. At the temperature for which the true vapor pressure becomes 10^{-2} atm the apparent vapor pressure is higher by a factor of from 4 to 9 than the true pressure.

A qualitative explanation of a deviation of this order can be given.

Viscous flow through a very thin orifice should raise the apparent pressure as calculated by the torsion-effusion equation by a factor of two. If the orifice channel is of finite length, the channel becomes a region of viscous flow at sufficiently high pressures so that the outer face of the channel becomes the source of vapor, and apparent pressures are in error by as much as 2/f. In this research 2/f had values from 3 to 9 for orifices used in the high-pressure studies.

Data obtained in this research do not prove the hypothesis of a limit at 2/f, but are consistent with the hypothesis to within estimated errors.

The maximum pressure for which pure molecular streaming conditions prevail with a given orifice can best be established by analysis of the trends in calculated values of ΔH_{298}. These values remain constant over a long range of temperatures for a given run to within ± 0.2 kcal, but deviate systematically toward lower values when the range of pure molecular streaming is exceeded.

An examination of ΔH_{298} values measured at high pressures demonstrates that the limit to the molecular streaming range is not simply dependent on the ratio of the mean free path, λ, of the vapor to the orifice diameter d

[3] F. Knauer and O. Stern, Z. Physik 39, 764 (1926).

[4] T. H. Johnson, Phys. Rev. 31, 102 (1928).

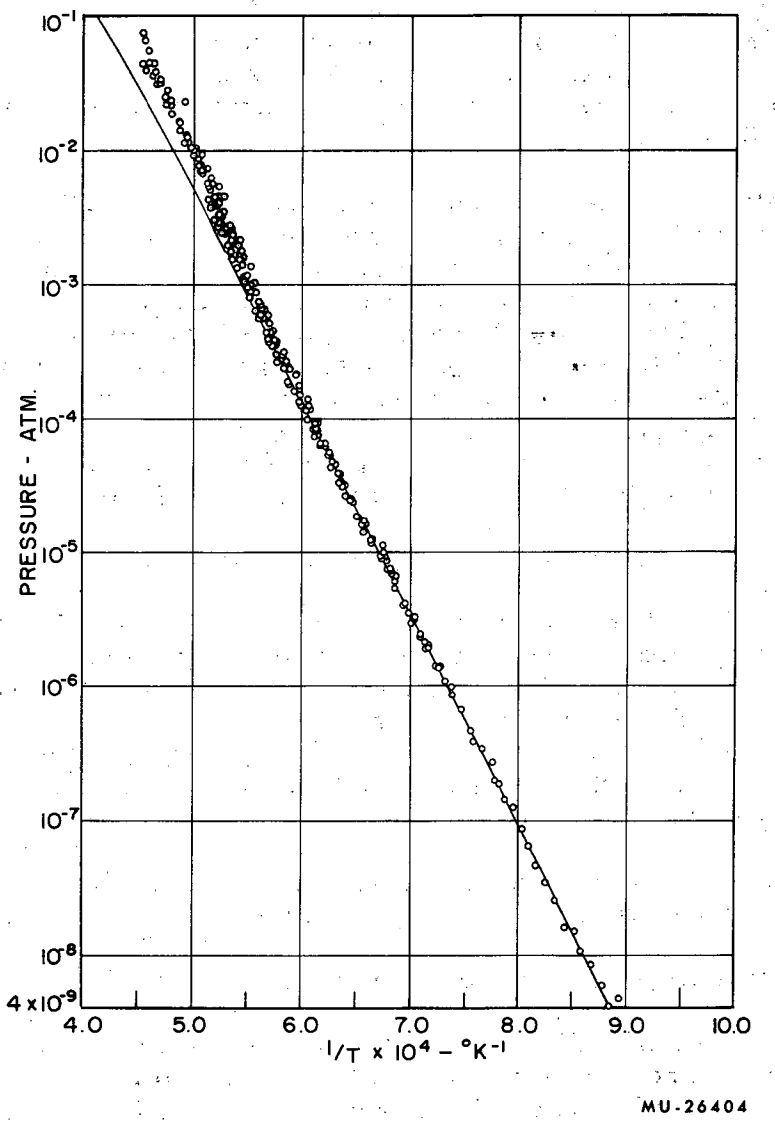

Fig. IID. 16-1. The vapor pressure of tin: composite plot.

as usually stated, but also is dependent on the orifice channel length. For the shortest channels investigated the molecular flow equations gave good heat data only below 2×10^{-5} atm, but with a long channel the equations could be used to pressures as high as 6×10^{-4} atm.

The λ/d ratio appears to be less important than the channel length in fixing the limit to molecular streaming. This observation and the difficulty in calculating a meaningful value for λ explain why the conditions for deviation from molecular streaming equations have been so poorly understood.

The important conclusion is drawn that molecular streaming conditions do not prevail to as high pressures for thin orifices as previously believed. The anomolous data on vaporization of uranium dioxide undoubtedly can be explained as arising from breakdown of molecular streaming.

Heats of Sublimation

Heats of sublimation were calculated for tin, germanium, and silver by both the third-law and second-law methods. The third-law methods are in each case considered the more reliable. The third-law values are: for tin, ΔH_{298} = 71.7 kcal, for germanium, ΔH_{298} = 89.8 kcal, and for silver, ΔH_{298} = 67.7 kcal. Each value agrees within 0.5 kcal of the selected value accepted in recent compilations. For tin and germanium the new values are believed to be somewhat more reliable than the older values.

17. RESEARCH IN PROGRESS -- SEARCY

1. The experimental portion of a study of the reactions of O_2, N_2, and NO at pressures of 10^{-5} to 10^{-6} atm with tungsten at 2000 to 2800°K has been completed. Analysis of the data is in progress (with Harlan U. Anderson). (This work was initiated under ONR and ARPA sponsorship).

2. Experimental data for a short paper on use of a mass spectrometer for pressure-gauge calibration have been collected (with Harlan U. Anderson).

3. A paper on the vaporization of magnesium oxide and the dissociation energy of MgO gas is in preparation (with Robert L. Altman).

4. Studies of the kinetics of evaporation of several oxides are continuing (with Donald F. Anthrop and Clarence L. Hoenig).

5. The vapor pressure of GaN and the nature of the gas molecules in equilibrium with solid GaN is under investigation (with Zuhair A. Munir).

6. A theoretical study of the partial molal thermodynamic properties of the metal atoms and of hydrogen in UH_3 and in zirconium-hydrogen solid phases is in progress. An abstract of a paper on this topic has been submitted for presentation at the International Atomic Energy Commission meeting on thermodynamics of nuclear materials to be held in Vienna this Spring (with David J. Meschi).

7. A study of the dissociation pressure of $AlPO_4$ is in progress (with Lies N. Finnie).

8. An attempt to correlate the activation energy for self-diffusion in metals with fundamental structural and thermodynamic properties has met some success and is being continued (with Louis Toth).

9. Apparatus for a study of the thermal accommodation coefficient for cold gases on a hot tungsten surface has been designed and will be used for study of several gases during the coming year (with David J. Meschi and Gerald DePoorter).

III. REACTOR MATERIALS ENGINEERING

1. LIQUID METAL EXTRACTION

Donald R. Olander

This work is a study of mass-transfer phenomena in liquid metal systems at high temperatures.

The system selected (one of interest in the reprocessing of uranium fuels for use in nuclear reactors) consists of a typical rare earth fission product transferring from a molten uranium-chromium-eutectic phase to a molten metal-extractant phase.

The planned experiment is to drop a sphere of U-Cr containing the fission product through a column of the liquid extractant metal. At the bottom of the column, the sphere falls into a fused salt (alkali halide) which is more stable than the corresponding solute halide. The extraction is stopped in this manner. By maintaining a temperature gradient in the fused salt, the U-Cr sphere is solidified before contacting the bottom of the column, thus avoiding the corrosive effects of liquid uranium and the resulting contamination of the sample.

Cerium^{144} has been selected as a typical radioactive rare earth fission product. Magnesium has been selected from those metals immiscible with uranium as the extractant because its low density makes possible the use of a fused salt at the bottom of the column and because there is a fair amount of equilibrium data available for the system consisting of cerium equilibrated between a uranium-chromium eutectic and magnesium. The eutectic melts at about 860°C, corresponding to a magnesium vapor pressure of about 60 mm Hg. The use of the eutectic will offer a considerable experimental advantage over pure uranium, which melts at 1132°C, corresponding to a magnesium vapor pressure of about 1000 mm Hg.

Calcium chloride (or possibly a mixture of alkali halides) meets the density, melting point, and relative stability requirements of the fused salt.

The U-Cr spheres will be formed in a separate operation by a needle-valve dropper. Most liquid metals wet solid surfaces (thus promoting drop formation), especially if there is any reaction at all between the liquid and solid. There is some reaction between molten uranium and even as corrosion-resistant a metal as tantalum. Drawings for the dropper have been completed, and it will be constructed of tantalum metal.

2. KINETICS OF THE CHLORINATION OF UCl_4 IN UCl_4-LiCl-KCl MELTS WITH ELEMENTAL CHLORINE

Donald R. Olander

The kinetics of the chlorination of UCl_4-LiCl-KCl melts with elemental chlorine will be studied both experimentally and theoretically. The kinetics of this system should resemble those of the analogous F_2-UF_4-UF_6 system. The over-all process involves the classical combination of diffusional transport of the reactants to the phase boundary, chemical reaction, and the removal of the reaction product. The over-all kinetics will depend upon the relative rates of the diffusion and reaction steps. The latter may involve intermediate compounds.

The final choice of the chlorine system over the fluorine reaction was based largely on the less corrosive and toxic nature of the former. Furthermore, the lower melting point of the LiCl-KCl eutectic (59 and 41 mole %, respectively; m. p. 315°C) will allow investigations at lower temperatures (400 to 500°C). This will make possible a closer study of the chemical reaction step.

The absorption kinetics will be investigated by the laminar-jet technique: A rodlike laminar jet of the molten salt will flow through an orifice or capillary at the bottom of a constant-head tank into a reaction chamber containing pure chlorine gas or a diluted mixture with helium, at 1 atm and at the melt temperature. After passing through a fixed length of reaction chamber, the jet will enter another slightly larger orifice at the bottom of the chamber and be collected in a receiving tank. The rate of conversion of the tetrachloride and the rate of production of gaseous UCl_6 (or UCl_5) can be determined by measurement of the total uranium and its average valence state in the exit salt or by the rate of evolution of the volatile higher chlorides.

A preliminary run using water and an all-glass apparatus will be undertaken to acquire a basic familiarity with the laminar-jet technique and to test the feasibility of its use in the kinetic studies of the uranium-chlorine system.

3. DIFFUSION OF FISSION GASES IN CERAMIC FUEL BODIES

Thomas H. Pigford, Donald R. Olander, Raphael Jaffe, Firroz Rufeh, and Hagai Shaked

Work is under way to study the mechanism of diffusion of fission gases in uranium dioxide and uranium carbide.

In the first experiment helium gas is dissolved in the fuel body at high temperature (1000 to 2000°C) and high pressure (100 atm). After equilibrium is attained, the hot fuel body is exposed to vacuum, and the amount of helium released as a funtion of time is observed. In this way, uncertainties due to release of fission gases by recoil and knockout mechanisms as well as irradiation effects upon the lattice structure are avoided. Single crystals will be used when available.

A small furnace capable of operating in a helium environment at 2000°C and 100 atm has been constructed and operated. Modifications to the heater assembly are under way. The necessary vacuum system, controls, and helium mass spectrometer have been assembled.

In a second experiment, lightly irradiated fuel bodies are heated in the temperature range of 1000° to 2000°C. Xe^{133} fission gas is measured. An induction heater has been procured, and the necessary vacuum, adsorption, and counting systems have been assembled, as shown in Fig. III. 3-1. Samples of arc-melted uranium carbide have been obtained for the first experiments. Single crystals of uranium carbide are being procured.

4. PARTICLE-VOLTAIC EFFECT IN SEMICONDUCTORS

Thomas H. Pigford and Lawrence Posey

The conversion of kinetic energy of heavy charged particles to electrical energy by interaction with semiconductor junction diodes is under investigation. Effects to be determined are the ratio of net electrical energy to incident kinetic energy of the incident particle, and the extent and nature of damage to the crystalline structure. The conversion efficiency is related to the ratio ϵ of the average energy for production of an electron-hole pair to the energy gap of the semiconductor. Work is under way to develop an analytical approach for predicting ϵ from known material properties. Apparatus is being assembled for the measurement of ϵ for various semiconductor materials having large energy gaps.

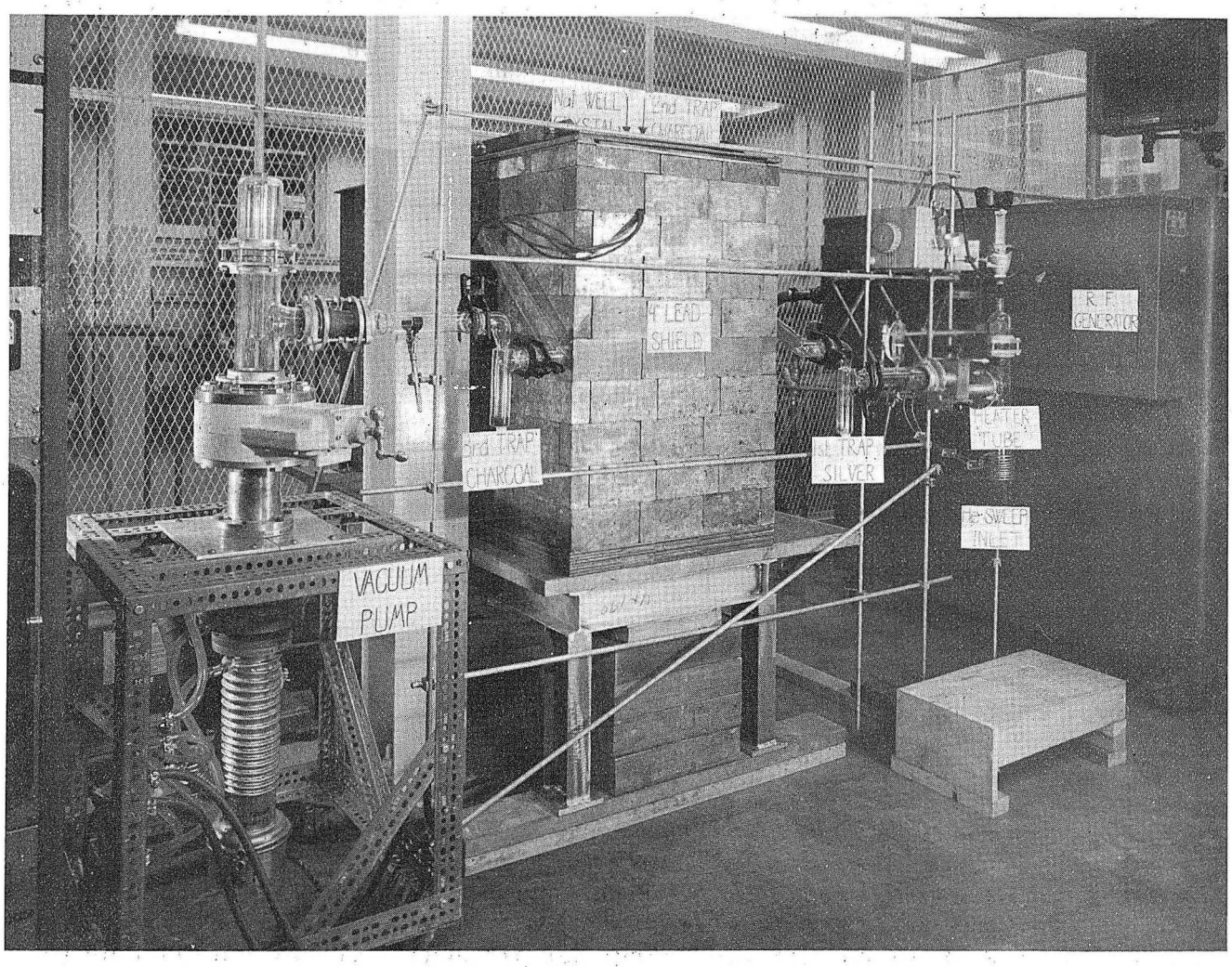

ZN-3076

Fig. III. 3-1. Fission-gas release apparatus.

5. THERMIONIC EMISSION BY REFRACTORY MATERIALS

Thomas H. Pigford, Donald Koenig, and Ronald Wichner

Equipment for the study of the thermionic emission properties of refractory metals and ceramics has been assembled. Measurements are under way for simple wire-type emitters, and these results will be compared with emission for planar geometries which are now being fabricated.

IV. MISCELLANEOUS

1. THE TIDES: A DYNAMIC EXPLANATION*

Ira P. Pratt, Jr.

This "off-the-subject" tract is the result of an informal discussion which brought out several difficulties in relating the conventional tide theory of Laplace and Darwin [1-5] to the empirical data.

A model, consisting of unit mass acting as a free point on the rotating earth's surface, is proposed to explain certain situations such as: (a) The Antarctic circumpolar current, which slightly exceeds the earth's surface velocity, (b) the anomalously small semidiurnal tides at coast lines parallel to the equator, (c) the 180° phase difference in tides on either side of narrow North-South land barriers, and the predominance of small tide ranges to be found at the smaller islands (Saipan, Midway, Oahu, Tahiti, etc.).

The approach here is to consider a free point, P, moving with the earth's surface from an essentially neutral plane into a field gradient which is predominantly gravitational on the side facing the moon, and predominantly centrifugal in the classical sense. The simplified model is diagrammed and explained in Fig. IV. 1-1. The lunar orbit is eccentric, owing in part to solar "tidal" forces expanding the orbit twice during each lunar rotation.

The effect is that the free point on the rotating surface facing the moon sees a predominantly gravitational force directed toward the moon, and the surface away from the moon sees a predominantly centrifugal force directed away from the moon. As a consequence, we have the two tides each lunar day -- this is, of course, modified by a similar, although smaller, pair of tides each solar day due to the interaction between the sun and earth.

In Fig. IV. 1-1, the earth is rotating around its axis E so as to carry a fluid at P_1 away from the neutral-plane intersection and into an increasing force field. We have a situation analogous to an unbalanced rotating wheel with the heavier portion being carried over the upper neutral center and starting to gain velocity. The result is that a fluid gains a velocity faster

---

*Shortened version of UCRL-10008, Jan. 1962.

[1] H. A. Marmer, The Tide (Appleton and Co., New York, 1926). Chapter Two presents a brief historical development of the subject.

[2] A. Defant, Ebb and Flow (University of Michigan Press, Ann Arbor, 1958).

[3] W. H. Munk and G. J. F. McDonald, The Rotation of the Earth (Cambridge University Press, 1960).

[4] J. Proudman, Dynamical Oceanography (John Wiley & Sons, Inc., New York, 1953).

[5] P. Schureman, Manual of Harmonic Analysis and Prediction of Tides (U. S. Department of Commerce, Coast and Geodetic Survey, Washington, D. C., 1941).

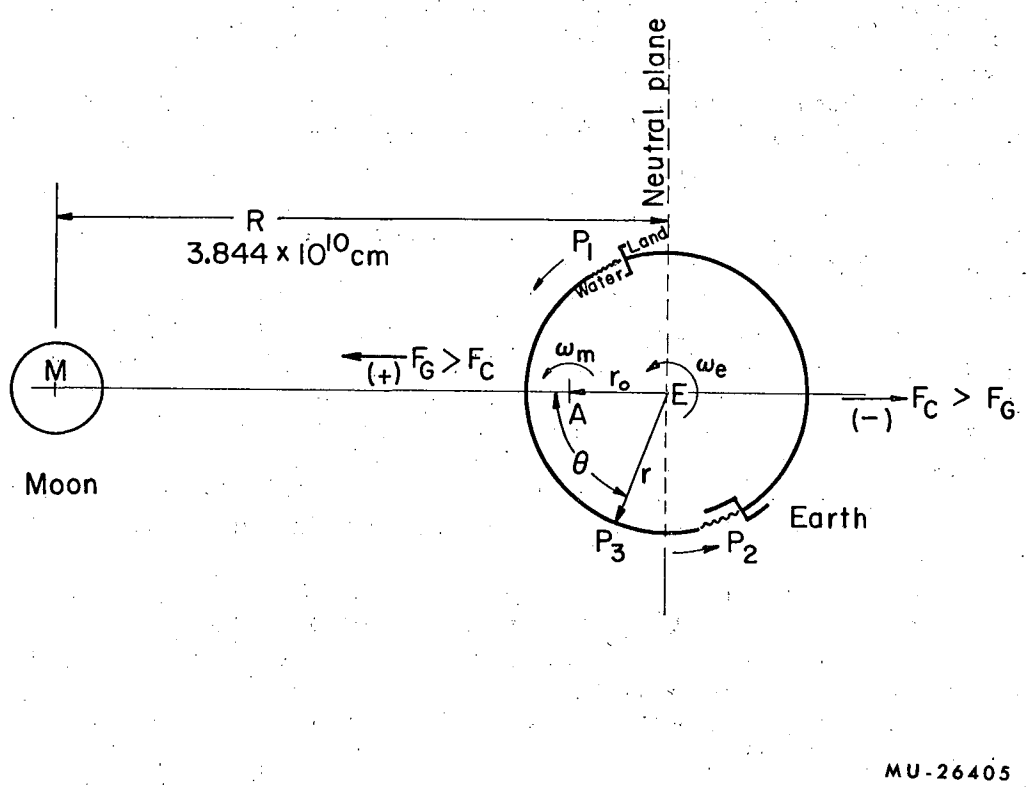

Fig. IV. 1-1. The rotating earth-moon system. A plane intersecting the earth at its center E, and perpendicular to line ME, may be considered a neutral plane with respect to the earth-moon system. F_C is the centrifugal force owing to earth-moon rotation ω_m around A, and F_G is the gravitational interaction with moon M of a unit mass on the earth's surface. The centrifugal force resulting from rotation around A is essentially balanced at the neutral-plane intersection by gravitational attraction between the moon and earth. A fluid at P_1 (east of barrier) tends to flow away from the coastline, and a fluid at P_2 (west of barrier) tends to flow toward the coastline, as the earth rotates from the indicated position. A high tide is displayed by P_2 each time it crosses the line through M and E. A low tide is displayed by P_1 at these same intersections.

than that of the earth's surface as it leaves the area of the neutral plane. At P_2 we have a similar situation, but with a fluid following rather than preceding a barrier -- fluid accumulates against the barrier, rather than flowing away from it. With this viewpoint, we immediately see two consequences: (1) A narrow north-south line barrier with a rising tide on one side should have an ebbing tide on the other, and (2) a barrier (coast line) along the equator would have essentially no tide at all if the planes of the equator, the ecliptic, and the lunar orbit were all coincident. Experimental data[6] for regions such as the Florida Cape and vicinity are consistent with these predictions. Other stations of the same approximate latitude show a similar correlation. However, allowance for different zenith times must be considered with wider land masses.

It would appear that in an ideal sense, coastal tide actions due to the moon and sun are simple sine-line vector functions which are multiplied by sineβ, where β is the coastal direction angle (zero to 360°) in reference to the equator. The amplitude of the sine-like function is determined by the kinetic energy gained as the fluid falls in the force fields and interacts with local bottom features. Considering an ideal Poisson ratio such that a radial force would produce an equivalent lateral hydraulic force toward the point of lowest potential, we may calculate a velocity amplitude due to the sine-like forces resulting from interaction with the moon in an ideal circular orbit system with the ecliptic, equatorial, and lunar orbit planes coincident.

We are interested in the velocity of this unit mass, as the energy available for producing coastal tides must be derived from the kinetic energy associated with the current (velocity) gained as the unit mass "falls" into the force field. Referring to Fig. IV. 1-1, we may set up the following equations for "free point" velocity due to lunar effect:

$$dv = \Sigma \frac{F}{m}\, dt = \left[\frac{GM_m}{(R - r\cos\theta)^2} - (r_0 - r\cos\theta)\omega_m^2 \right] dt\,; \qquad (1)$$

quadrature component, normal to the line ME,

$$dv^* = \Sigma \frac{F^*}{m}\, dt = \left[\frac{r\sin\theta}{r} \frac{GM_m}{(R - r\cos\theta)^2} - (r\sin\theta)\omega_m^2 \right] dt. \qquad (2)$$

The resultant amplitude V of the velocity function would be the difference between the quadrature velocities for the rotation carrying a point P from the "neutral" plane to intersect line ME:

$$V = \int_{\theta = (3/2)\pi}^{\theta = 2\pi} dv - \int_{\theta = (3/2)\pi}^{\theta = 2\pi} dv^* .$$

Solving these equations gives a value for V of approximately 2.4 cm/sec greater than, and in the same direction as, the earth's surface movement due to axial rotations. This current is not large, but is in the same direction for each tide. The result is, effectively, an alternating-current component superimposed upon the continuous west-to-east current inherent in this model.

[6] U. S. Department of Commerce, Coast and Geodetic Survey, Tide Tables, 1961.

To account for observed tidal currents, we must consider the lower water depths as more or less confined, and invoke Bernoulli's equation, which energetically predicts an increased velocity in the areas of less restricted motion -- near the surface.

2. RESEARCH IN PROGRESS -- PRATT

Current responsibilities are primarily administrative, but a program has been initiated to develop an intense ultraviolet source for study of fluorescence resulting from optical excitation of the 11- and 13-ev absorption bands in single-crystal MgO.

V. PUBLICATIONS, 1961

Papers and reports by members of Inorganic Materials Research Division
(including certain publications supported by agencies other than the U. S. Atomic Energy Commission)

Papers are grouped under the name of the principal investigator.

Brewer, Leo, "Non-Stoichiometry in Non-Metallic Compounds," J. Chem. Educ. 38, 90 (1961).

——, "Thermodynamic Properties of Alkali Halides," UCRL-9952, Nov. 1961.

——, with Pitzer, Kenneth S., Eds. revised edition of Lewis and Randall's Thermodynamics (McGraw-Hill Book Co., Inc., New York, N. Y., 1961).

——, and Brackett, Elizabeth, "The Dissociation Energies of Gaseous Alkali Halides," Chem. Revs. 61, 425 (1961).

——, and Rosenblatt, G. M., "Dissociation Energies of Gaseous Metal Dioxides," Chem. Revs. 61, 257 (1961).

——, Simonson, T. R., and Tong, L. K. J., "A Vapor-Phase Equilibrator for Activity Coefficient Determinations," J. Phys. Chem. 65, 420 (1961).

——, Margrave, J. L., Porter, R. F., and Wieland, K., "The Heat Formation of CF_2," J. Phys. Chem. 65, 1913 (1961).

——, Brackett, E., and Somayajulu, G., "Thermodynamic Properties of Gaseous Metal Dihalides," UCRL-9840, Sept. 1961.

Somayajulu, G. R., "Orbital Radii Bond Length and Resonance," UCRL-9568, Feb. 1961.

Somayajulu, G. R., "Bond Energies. Valence-State Energies and Resonance," UCRL-9590, Feb. 1961.

Trajmar, Sandor, "Study of the Near-Ultraviolet Spectrum of Magnesium Oxide" (Ph. D. Thesis) UCRL-9773, July 1961.

Connick, Robert, "Kinetics and Mechanisms of Reactions of Coordination Compounds." Advances in the Chemistry of the Coordination Compounds. Proc. 6th Internat. Conf. on Coordination Chemistry, Detroit, August 1961 (MacMillan Co., New York, 1961), p. 15.

——, and Paul, A. D., "The Fluoride Complexes of Silver and Stannous Ions in Aqueous Solution," J. Phys. Chem. 65, 1216 (1961).

——, and Fine, D. A., "The Identification of Neutral Ruthenium (III) Chloride Complexes: Equilibria Involving Neutral and Cationic Species," J. Am. Chem. Soc. 83, 3414 (1961).

Genser, E. E., "Studies of Fast Exchange Reactions by the Use of Nuclear Magnetic Resonance" (Thesis), UCRL-9846, Sept. 1961.

Dorn, J., Mitra, S. K., and Osborne, P. W., "On the Intersection Mechanism of Plastic Deformation in Aluminum Single Crystals," AIME Trans., 221, 1206 (1961).

——, Flynn, P. W., and Mote, J., "On the Thermally Activated Mechanism of Prismatic Slip in Magnesium Single Crystals," AIME, Trans., Dec., 221, 1148 (1961).

——, Wazzan, A. R., and Mote, J., "The Effect of Plastic Deformation on Self-Diffusion in Nickel," OSR 3rd Tech. Report, Apr. 1961.

Simmons, J. A., "Geometric Foundations of Continuum Mechanics," UCRL-9922, 1961.

Tanaka, K., and Mote, J., "The Effect of Temperature on the Yield Strength of the Polycrystalline Hexagonal Ag-Al Intermetallic Phase," UCRL-9992, Dec. 1961.

Fulrath, R. M., "Model Polyphase Ceramic Systems and Resultant Stress Systems," In Proceedings of Conference on Mechanical Properties of Engineering Ceramics, edited by W. W. Kriegel and H. Palmour, III (Interscience Publishers, Inc., New York, 1961), pp. 549-573.

——, with R. W. Cline and J. A. Pask, "Fundamentals of Glass-to-Metal Bonding: V. Wettability of Iron by Molten Sodium Disilicate," J. Am. Ceram. Soc. 44, 423-428 (1961).

——, and Grossman, L. N., "X-Ray Strain Measurement Techniques for Ceramic Bodies," J. Am. Ceram. Soc. 44, 567-571 (1961).

Herschbach, D. R., "Chemical Reactions in Crossed Molecular Beams," Vortex (Am. Chem. Soc., California Section, Summary) 22, 348 (1961).

——, and Kinsey, J. L., "Angular Distribution of Products in Chemical Reactions," Bull. Am. Phys. Soc. 6, 339 (1961).

——, and Brooks, P. R., "The Kingdon Cage as a Molecular Beam Detector," Bull. Am. Phys. Soc. 6, 513 (1961).

——, Norris, J. A., Kwei, G. H., and Kinsey, J. L., "Reactive Scattering in Crossed Molecular Beams: Asymmetry of Angular Distributions," Bull. Am. Phys. Soc. 6, 339 (1961).

——, and Laurie, V. W., "Anharmonic Potential Constants and Their Dependence Upon Bond Length," J. Chem. Phys. 35, 458 (1961).

——, Kwei, G., and Norris, J., "Reactive Scattering in Crossed Molecular Beams. K Atoms with CH_3I and C_2H_5I." J. Chem. Phys. 34, 1842 (1961).

——, Datz, S., and Taylor, E. H., "Chemical Reactions in Crossed Maxwellian Molecular Beams," J. Chem. Phys. 35, 1549 (1961).

Howe, J. A., and Muirhead, J. S., "The Near-Ultraviolet Absorption Spectrum of Tetrolaldehyde," UCRL-9896, Oct. 1961.

——, Muirhead, J. S., and Goldstein, J., "Simple Molecular Orbital Theory of the Dichloroethylenes," UCRL-9817, Aug. 1961.

——, and Flygare, W. H., "Strong-Field Stark Effect," UCRL-9794, July 1961.

——, and Flygare, W. H., "Microwave Spectrum and Quadrupole Interaction in Cis-1, 2-Dichloroethylene, UCRL-9786, July 1961.

Jolly, W. L., "The Preparation of the Volatile Hydrides of Groups IV-A and V-A by Means of Aqueous Hydroborate," J. Am. Chem. Soc. 83, 335 (1961).

——, "Some Physical Properties of the Volatile Hydrides," UCRL-9630, April 1961.

——, and Mesmer, R., "Exchange of Hydrogen Between Water and the Hydroborate Ion," J. Am. Chem. Soc. 83, 4470 (1961).

——, and Drake, J. E., "The Preparation and Identification of Volatile Germanes," Proc. Chem. Soc. 1961, 379.

——, and Drake, J. E., "Hydrides of Germanium, Tin, Arsenic, and Antimony," UCRL-9615, May 1961.

——, and Gold, M., "The Spectrophotometry of Metal Ammonia Solutions at Low Temperatures," UCRL-9887, Oct. 1961.

Mesmer, Robert, "Hydroborate Chemistry" (Thesis), UCRL-9842, Sept. 1961.

Drake, J. E., "The Preparation of Some Germanium Hydrides," UCRL-9709, May 1961.

Jura, G., Harris, W., Vaisnys, E., and Stromberg, H., "Resistance and Thermal Gap Measurements to 400,000 Atmospheres," in Progress in Very High Pressure Research, edited by Bundy, Hibbard and Strong (John Wiley and Sons, Inc., New York 1961), p. 165.

——, Montgomery, P., and Stromberg, H., "Calibration of Bridgman Anvils," UCRL-9807, Aug. 1961.

——, McWhan, D., Montgomery, P., and Stromberg, H., "Pressure Temperature Resistance Properties," UCRL-9808, Aug. 1961.

——, Montgomery, P., and Stromberg, H., "Sintering of Refractory Materials at Room Temperature by High Pressure," in Advances in Chemistry 33, (American Chemical Society, Washington, D. C., 1961).

Mahan, B., and Doering, B., "Photolysis of Nitrous Oxide. I. 1236 A," J. Chem. Phys. 34, 1617 (1961).

Myers, R. J., Jr., and Hayes, R., "Line Widths in the Paramagnetic Resonance of Mn^{++} in Aqueous Solution," Bull. Am. Phys. Soc. 6, 141 (1961).

——, and Meyer, R., "Dipole Moment of the OH Radical from the Stark Effect of Its Microwave Spectrum," J. Chem. Phys. 34, 1074 (1961).

——, Harmony, M., Schoen, L., Lide, D., and Mahn, D., "Infrared Spectrum and Structure of the NF_2 Radical," J. Chem. Phys. 35, 1129 (1961).

Hayes, Robert, "Electron Spin Resonance Linewidths" (Thesis) UCRL-9873, Aug. 1961.

Olander, D. R., "The Distribution of Nitric Acid Between Water and Tributyl Phosphate-Hexane Solvents," AIChE Journal 7, 152 (1961).

——, "Design of Direct-Contact Cooler-Condensers," Ind. Eng. Chem. 53, 121 (1961).

——, "Tributyl Phosphate Solvent Extraction Column Design," Ind. Eng. Chem. 53, 1 (1961).

——, "The Diffusivity of Water in Organic Solvents," AIChE Journal 7, 175 (1961).

——, "Mass Transfer," Ind. Eng. Chem. 53, 925 (1961).

Parker, E. R., "Fatigue," Mechanical Behavior of Materials at Elevated Temperatures (McGraw-Hill Book Co., New York, 1961).

Pask, J. A., "Effect of Interfacial Reactions in the Densification of Crystal-Glass Systems," in Transactions of the VIIth International Ceramic Congress (British Ceramic Society, London, 1961).

——, "Mechanical Properties of Ceramic Materials," Chapter 11, in Mechanical Behavior of Materials at Elevated Temperatures, edited by J. E. Dorn (McGraw-Hill Book Co., New York, 1961), pp. 288-318.

——, with Cline, R. W., and Fulrath, R. M., "Fundamentals of Glass-to-Metal Bonding: V. Wettability of Iron by Molten Sodium Disilicate," J. Am. Ceram. Soc. 44, 423-428 (1961).

——, and Adams, R. B., "Fundamentals of Glass-to-Metal Bonding: VII. Wettability of Iron by Molten Sodium Silicate Containing Iron Oxide," J. Am. Ceram. Soc. 44, 430-433 (1961).

——, McCartney, E. R., and Templeton, L. K., "The Solid-State Reaction Between Barium Metatitanate and Barium Carbonate to Form Barium Orthotitanate," in Reactivity of Solids, edited by J. H. DeBoer et al. (Elsevier Publishing Company, Amsterdam, 1961).

——, and Scott, W. D., "Nucleation and Growth of Sodium Disilicate Crystals in Sodium Disilicate Glass," J. Am. Ceram. Soc. 44, 181-187 (1961).

——, Hulse, C. O., "Formation and Strength of Magnesia Whiskers," J. Am. Ceram. Soc. 44, 572-575 (1961).

Phillips, N. E., and Matthias, P. "Heat Capacity of Ferromagnetic Superconductors," Phys. Rev. 121, 105 (1961).

——, and Lien, W., "Heat Capacity Anomaly in Solid Air," J. Chem. Phys. 34, 1073 (1961).

——, and Petersen, E., "Heat Capacity of Antiferromagnetic $CuCl_2 \cdot 2H_2O$ in the Spin Wave Region," J. Chem. Phys. 34, 1463 (1961).

——, and Lien, W. H., "The Electronic Heat Capacity of Potassium, Rubidium, and Cesium," in Proceedings of the VIIth International Conference on Low-Temperature Physics (University of Toronto Press, 1961).

——, and Douglas, R. L., "Heat Capacity of Gallium and Mercury at Temperatures Below 1°K," in Proceedings of the VIIth International Conference on Low-Temperature Physics (University of Toronto Press, 1961).

Pitzer, K. S., "Thermodynamics of Thermocells with Fused or Solid Electrolytes," J. Phys. Chem. 65, 147 (1961).

——, "Irreversible Thermodynamics," Pure and Applied Chemistry 2, 207-210 (1961).

——, and Brewer, L., Eds. revised edition of Lewis and Randall's Thermodynamics (McGraw-Hill Book Co., New York, 1961).

——, Gerkin, R. E., Gregor, L. V. and Rao, C. N. R., "Transitions and Therman Anomalies in Silver Oxide," Pure and Applied Chemistry 2, 211-214 (1961).

——, and Beckman, T. A., "The Infrared Spectra of Marginally Metallic Systems: Sodium-Ammonia Solutions," J. Phys. Chem. 65, 1527 (1961).

Ortung, W., "Thermal Properties of Solid Hydrogen Under Pressure" (Thesis); UCRL-9388, Feb. 1961.

Acrivos, J., "Analysis of the $A_3(X_3)_3$ Nuclear Spin System π-Electrons Coupled Hyperfine Splitting Constants in Aromatic Hydrocarbons," UCRL-9531, May 1961.

Gregor, L., "The Heat Capacity of Silver Oxide at Low Temperatures" (Thesis), UCRL-9723, May 1961.

Acrivos, J., "Electron Spin Resonance," UCRL-9998, Dec. 1961.

Brown, J., "Magnetic Resonance of Metals and Paramagnetic Ions in Solution" (Thesis), UCRL-9944, Dec. 1961.

Sinanoglu, O., and Mortensen, E. M., "Core Polarization in Li_2," J. Chem. Phys. 34, 1078 (1961).

Searcy, A. W., Davis, S. G., and Anthrop, D. F., "Vapor Pressure of Silicon and the Dissociation Pressure of Silicon Carbide," J. Chem. Phys. 34, 659-664 (1961).

Sederholm, C. H., and Petrakis, L., "Temperature-Dependent Chemical Shifts in the NMR Spectra of Gases," J. Chem. Phys. 35, 1174 (1961).

——, and Petrakis, L., "NMR Fluorine-Fluorine Coupling Constants in Organic Compounds," J. Chem. Phys. 35, 1243 (1961).

Petrakis, L., "Nuclear Magnetic Resonance Studies" (Thesis), UCRL-9733, June 1961.

Thomas, G., "The Aging Characteristics of Al-Mg-Si Alloys," J. Inst. Metals 90, 57 (1961).

——, "The Improvement of Stress Corrosion in Al-Mg-Zn Alloys," J. Inst. Metals 89, 287 (1961).

——, and Huffstutter, M. C., "Specimen Tilting Device for the H. U. -10 Electron Microscope," Rev. Sci. Instr. 32, 86 (1961).

——, and Huffstutter, M. C., "Structure of Cu-12% Al Alloy," (A letter), Acta Cryst. 14, 693 (1961).

——, and Whelan, M. J., "Direct Observations of Precipitation in Thin Foils of Al-4% Cu Alloy," Phil. Mag. 6, 1103 (1961).

——, Sandler, N. P., and Cornet, I., "Studies of Fatigue by Reflection Electron Microscopy" (A technical note), J. Inst. Metals 89, 253 (1961).

——, Frank, G. R., and Robinson, D. L., "Influence of Dislocation Substructure on Precipitation," J. Appl. Phys. 32, 1763 (1961).

——, and Whelan, M. J., "Precipitation in Al-4% Cu Alloy," in Proceedings of Delft (Holland) Conference on Electron Microscopy (De Nederlandes Vereniging poor Electronenmicroscopie, Delft, 1961), p. 452.

——, Nadeau, D. J., and Benson, R., "Preliminary Observations of Dislocations in Mo and Mg," in Proceedings of Delft (Holland) Conference on Electron Microscopy (De Nederlandes Vereniging poor Electronenmicroscopie, Delft, 1961), p. 447.

Information Division
sa

This report was prepared as an account of Government sponsored work. Neither the United States, nor the Commission, nor any person acting on behalf of the Commission:

A. Makes any warranty or representation, expressed or implied, with respect to the accuracy, completeness, or usefulness of the information contained in this report, or that the use of any information, apparatus, method, or process disclosed in this report may not infringe privately owned rights; or

B. Assumes any liabilities with respect to the use of, or for damages resulting from the use of any information, apparatus, method, or process disclosed in this report.

As used in the above, "person acting on behalf of the Commission" includes any employee or contractor of the Commission, or employee of such contractor, to the extent that such employee or contractor of the Commission, or employee of such contractor prepares, disseminates, or provides access to, any information pursuant to his employment or contract with the Commission, or his employment with such contractor.